ISSN 0386-4049

TECHNICAL REPORTS OF THE METEOROLOGICAL RESEARCH INSTITUTE No.65

International Research for Prevention and Mitigation of Meteorological Disasters in Southeast Asia

BY

Kazuo Saito, Tohru Kuroda, Syugo Hayashi, Hiromu Seko,
Masaru Kunii, Yoshinori Shoji, Mitsuru Ueno, Takuya Kawabata,
Shigeo Yoden, Shigenori Otsuka,
Nurjanna Joko Trilaksono, Tieh-Yong Koh, Syunya Koseki,
Le Duc, Kieu Thi Xin, Wai-Kin Wong and Krushna Chandra Gouda

気象研究所技術報告

第 65 号

東南アジア地域の気象災害軽減国際共同研究

斉藤和雄、黒田徹、林修吾、瀬古弘
國井勝、小司禎教、上野充、川畑拓矢
余田成男、大塚成徳
Nurjanna Joko Trilaksono, 許智揚、古関俊也
Le Duc, Kieu Thi Xin, 黄偉健、Krushna Chandra Gouda

気象研究所

METEOROLOGICAL RESEARCH INSTITUTE, JAPAN

December 2011

The *Technical Reports of the Meteorological Research Institute* has been issued at irregular intervals by the Meteorological Research Institute (MRI) since 1978 as a medium for the publication of technical report including methods, data and results of research, or comprehensive report compiled from published papers. The works described in the *Technical Reports of the MRI* have been performed as part of the research programs of MRI.

TECHNICAL REPORTS OF THE METEOROLOGICAL RESEARCH INSTITUTE No. 65

International Research for Prevention and Mitigation of Meteorological Disasters in Southeast Asia

BY

**Kazuo Saito, Tohru Kuroda, Syugo Hayashi, Hiromu Seko,
Masaru Kunii, Yoshinori Shoji, Mitsuru Ueno, Takuya Kawabata,
Shigeo Yoden, Shigenori Otsuka,
Nurjanna Joko Trilaksono, Tieh-Yong Koh, Syunya Koseki,
Le Duc, Kieu Thi Xin, Wai-Kin Wong and Krushna Chandra Gouda**

気象研究所技術報告

第 65 号

東南アジア地域の気象災害軽減国際共同研究

**斉藤和雄、黒田徹、林修吾、瀬古弘、
國井勝、小司禎教、上野充、川畑拓矢
余田成男、大塚成徳
Nurjanna Joko Trilaksono, 許智揚、古関俊也
Le Duc, Kieu Thi Xin, 黄偉健、Krushna Chandra Gouda**

気 象 研 究 所

METEOROLOGICAL RESEARCH INSTITUTE, JAPAN

International Research for Prevention and Mitigation of Meteorological Disasters in Southeast Asia

by

Kazuo Saito, Tohru Kuroda, Syugo Hayashi, Hiromu Seko, Masaru Kunii, Yoshinori Shoji, Mitsuru Ueno and Takuya Kawabata
Meteorological Research Institute, Japan Meteorological Agency

Shigeo Yoden and Shigenori Otsuka
Kyoto University

Nurjanna Joko Trilaksono
Institut Teknologi Bandung, Indonesia

Tieh-Yong Koh and Shunya Koseki
Nanyang Technological University, Singapore

Duc Le[1] and Kieu Thi Xin[2]
[1]National Center for Hydro-Meteorological Forecasting, Vietnam
[2]Vietnam National University of Hanoi

Wai-Kin Wong
Hong Kong Observatory

Krushna Chandra Gouda
CSIR Centre for Mathematical Modelling and Computer Simulation, India

Contents

序

東南アジアはインドシナ半島を中心とするアジア大陸南東部と、海洋大陸と呼ばれるインド洋と太平洋の間に広がる領域からなり、12 カ国に EU を上回る約 6 億人が生活している。ASEAN として近年目ざましい経済成長を遂げており、地理的に近いこともあり日本にとってその重要性が大きくなっている。その一方で、台風・洪水・地震・津波などさまざまな自然災害にも見舞われる地域であり、死者 20 万人以上といわれる 2004 年のスマトラ沖地震や死者 14 万人といわれる 2008 年のサイクロン・ナルギスなどは、近年における最大規模の自然災害として記憶に新しい。

文部科学省は、2006 年 3 月に閣議決定された第 3 期科学技術基本計画においてアジア地域共通の課題への取り組みの重要性が指摘されたことを受け、アジア諸国との間での対等なパートナーシップによる共同研究を推進していくことを目標に、平成 19 年度科学技術振興調整費研究の 5 分野の一つに、「アジア科学技術協力の戦略的推進」を設けた。自然災害、感染症対策、エネルギー技術、先端技術の 4 つのテーマに対して 128 件の応募があり、最終的に 11 件が採択された。その中の一つが、京都大学の余田成男教授を研究代表者とする「東南アジア気象災害軽減国際共同研究」であり、東南アジア地域の気象災害軽減に資するための国際共同研究推進ネットワークを立上げることと、数値天気予報に基づく気象災害軽減のための判断支援システムのプロトタイプを構築することを主な目的とした。気象研究所は、国内参画機関としてサブ課題「実用モデル開発・応用実験」を担当するとともに、京都大学やこの国際共同研究に参加した東南アジア研究者と共同で、気象庁非静力学メソモデルを用いた数値天気予報実験などを行った。

東南アジアの大部分は熱帯に属し、そこで発生する気象現象とそのメカニズムは、日本など中緯度でのそれらと大きく異なっている。気象現象を支配する基本的な物理法則は地球上のどこでも同じであるが、大気の傾圧性や地球回転の影響の大きさ、太陽放射の強さの違いなどが、熱帯の気象を特有なものにしている。その一方で、これまでの数値天気予報では、数値モデルに用いられているパラメタリゼーションや変分法初期値解析手法の中で、必ずしも熱帯への適用を前提としない手法が用いられてきている。また、海洋大陸は地球の'boiler box'として、その大きな水蒸気潜熱の解放が地球全体のハドレー循環やウォーカー循環を支配する主要な熱源となっている。この地域での数値モデルの予測特性を改善することは、災害につながる気象現象の短期的な予測にとって直接的に重要であるばかりでなく、気候モデルの改良にも大きな意味を持っている。

本技術報告では、「東南アジア気象災害軽減国際共同研究プロジェクト」への参加を通じて行われた、気象研究所が関わったさまざまな活動についての記述が行われている。この中には、現業数値予報モデルを熱帯に適用した場合の振る舞いやその統計的検証、熱帯に適したデータ同化手法の研究、高潮のアンサンブル予測を含むサイクロン・ナルギスの予報実験など、学問的に興味深い研究成果が多く得られている。本プロジェクトは平成 21 年度に終了したが、平成 23 年度においても、京都大学に留学中のバンドン工科大学からのインドネシア政府給費生の気象研究所への滞在研究が行われるなど、さまざまな形で技術交流が継続している。本プロジェクトで培われた東南アジア研究者との研究ネットワークは、気象研究所の今後の研究活動にとっても大きな財産となったといえる。

予報研究部長
露木　義

東南アジア地域の気象災害軽減国際共同研究

斉藤和雄[1]、黒田徹[2]、林修吾[1]、瀬古弘[1]、
國井勝[3]、小司禎教[1]、上野充[4]、川畑拓矢[1]
余田成男[5]、大塚成徳[5]
Nurjanna Joko Trilaksono[6], 許智揚[7]、古関俊也[7]
Le Duc[8], Xin Kieu Thi[9], 黄偉健[10]、Krushna Chandra Gouda[11]

近年、地球規模の気候変動や経済活動高度化に伴う社会の脆弱化によって、東南アジア域においても、熱帯低気圧やスコールラインなどに伴う暴風雨災害が増加しつつあり、社会的経済的に影響の大きい気象災害の予測・低減が急務となっている。気象研究所では、京都大学と連携して、平成 19 年度から科学技術振興調整費研究「東南アジア地域の気象災害軽減国際共同研究」を実施し、数値モデルによる予測による気象災害軽減のための国際共同研究を推進した。この技術報告は、上記科学技術振興調整費研究に関連して気象研究所が京都大学や東南アジア研究者と連携して行った研究活動について記述した。

「東南アジア地域の気象災害軽減国際共同研究」は、文部科学省科学技術振興調整費研究の「アジア科学技術協力の戦略的推進」分野における「地域共通課題解決型国際共同研究」としての一課題で、京都大学の余田成男教授を研究代表者として、平成 19 年度に採択された。東南アジア諸国における大気科学研究の協力・連携を強化し、この地域の気象災害軽減に資するための「東南アジア地域気象災害軽減国際共同研究推進ネットワーク」を立上げることと、東南アジア地域での数値天気予報実験を国際的連携の下に実施して、気象災害の軽減判断支援システムを構築すること、などを主な目的とした。研究実施体制は、京都大学が代表機関となり、「基礎実験・システム開発」と国際研究集会の開催などを行い、気象研究所は国内参画機関として、サブ課題「実用モデル開発・応用実験」を担当した。また準リアルタイム実用化実験を、インドネシアバンドン工科大学(ITB)を中心とする国外参画機関が行った。

この科振費研究において、京都大学は、代表機関として「基礎実験・システム開発」を担当し、観測・予報データの統合データベース化やホームページの作成(G-4)、国際研究集会の開催(G-1)とニュースレターの発行(G-2, I-1)、災害対策判断支援システムの試作(F-1)、インドネシア政府給費生の長期滞在などを実施した。統合データベースは京都大学のサーバーにアーカイブされ、東南アジアの共同研究者がアクセスできる仕組みを構築した。国際研究集会は、2008 年３月に京都大学で、2009 年３月にインドネシアの ITB で、2010 年３月には大分県の立命館アジア太平洋大学で、それぞれ開催された。ニュースレターは年２回のペースで発行され、国際ワークショップの報告のほか、気象研究所の活動もほぼ毎号紹介された。災害対策判断支援システムでは、D-3 で記述した気象研究所でのアンサンブル予報の結果を入力データに用いた試作が行われた。

国外参画機関としては、ITB が気象庁非静力学モデル(NHM)を用いた準リアルタイム実用

1 気象研究所予報研究部
2 気象研究所予報研究部/海洋研究開発機構
3 気象研究所台風研究部
4 気象研究所物理気象研究部
5 京都大学
6 インドネシアバンドン工科大学
7 シンガポール南洋理工大学
8 ベトナム水文気象センター
9 ベトナム国立大学ハノイ校
10 香港天文台
11 インド科学産業研究機構

化実験や東南アジアを対象とするダウンスケール実験（C-7）を行った。そのほか、シンガポール南洋理工大学(NTU)、ベトナム国立大学ハノイ校(VNU)、インド科学産業機構数値モデリングシミュレーションセンター(CSIR C-MMACS)などが本科振費研究に関連して、NHM の利用申請を行い、研究を実施した(C-5, C-6, C-8)。また、香港天文台は、現業気象機関として気象庁と数値予報に関連した国際業務提携を行っており、NHM の数値予報への適用例について寄稿を頂いた(D-9, E-2)。

気象研究所は、国内参画機関として京都大学と連携して「実用モデル開発・応用実験」を担当した。このサブ課題では、

①気象庁メソモデルの精緻化と検証、熱帯域メソアンサンブル予報技術の開発

②メソモデル国際共同研究のための環境整備と熱帯数値予報に関する技術情報の共有

③メソモデル用データ同化システムを用いた熱帯域同化実験

の３つのテーマを実施した。

①では、NHM を東南アジア地域の災害気象予測に用いるため、熱帯域ダウンスケール予報によるケーススタディ（C-3, C-4）と統計的検証(C-1, C-2）に基づくモデルの問題点の把握を行った。また後述するように NHM を用いた熱帯域メソアンサンブル予報技術を開発した。

②では、NHM を用いた熱帯域数値実験のための環境整備として、気象庁の全球解析や全球モデル予報値、気象庁週間アンサンブル予報などから NHM による再現・予報実験を行うツールの整備を行った(E-3)。また国外研究者がそれらを研究利用するにあたって使用方法をまとめたチュートリアルを気象研究所本研究ホームページ (G-5)にアップした。また研究参加機関への相互訪問を実施し、モデル利用の説明や情報交換などを行った(G-3)。

2008 年 5 月にミャンマーを襲ったサイクロン Nargis は、ヤンゴンをはじめとする同国南部に死者 10 万人とも言われる未曾有の高潮被害をもたらした。本研究では、この事例を東南アジアでの最大級の気象災害として、数値モデルによる研究に取り組んだ。まず気象庁全球解析を初期値とし、全球予報を境界値とする 10km 解像度の NHM によって、サイクロン Nargis の移動と発達が、上陸の２日前にある程度予測可能であったことを示すとともに、プリンストン海洋モデル(POM)を用いた高潮の予報実験を行った（D-1）。次に気象庁全球アンサンブル予報の初期値・予報値からの摂動を用いて、NHM による熱帯域メソアンサンブル予報システムを開発し、Nargis の進路予報の誤差も加味した高潮予測を示した(D-3) 。このアンサンブル予測結果は前述の京都大学での判断支援システム試作の入力データとしても用いられている。

③に関連して、D-4 と D-5 では、気象庁メソ４次元変分法解析を熱帯域に適用できるように改良を加え、熱帯域ボーガス手法を開発するとともにベンガル湾周辺の地上 GPS 観測点から得られる可降水量などのデータ同化予報実験を行い、初期値の変更によって Nargis の進路・強度予報の改善が可能であることを示した。Nargis のデータ同化実験については、局所アンサンブル変換カルマンフィルタを用いた衛星搭載マイクロ波散乱計によるベンガル湾海上風の同化にも取り組んだ(D-2)。D-6, D-7 では、台風ボーガスの開発に関連する台風構造についての調査を載せている。日本における最大級の気象災害として 1959 年の伊勢湾台風による高潮災害があり、非静力学４次元変分法による再解析再予報実験が行われている。この実験は、気象庁の「伊勢湾台風再現実験プロジェクト（ReVera）」の一環として行われたものであるが、気象庁再解析データと NHM、およびその同化システムを用いた台風と高潮の再現研究として D-8 にその概要を載せた。

E 章には、東南アジア域での観測ネットワークに関するレビューについての紹介(E-1)と、前述した香港天文台の数値予報についてのレビューと東南アジア域で NHM を動かす場合のデータやツールの一覧を載せた。そのいくつかは本プロジェクトで整備されたでものある。G 章には、国際パートナーシップとしての活動を載せた。また I 章には付録として、ニュースレターと災害対策判断支援システムの基になっているウェブベースの数値予報結果表示ツール Gfdnavi の解説資料(京都大学 21 世紀 COE プログラム 2009 年サマースクールでの資料)、本報告に関する発表済み論文・報告へのリンク一覧を載せた。

本プロジェクトを遂行するにあたり、多くの方々の協力・助力を頂いた。科学技術振興機構(JST)の西垣隆プログラムオフィサーと小川茂樹主任調査員には、プロジェクトの遂行にご理解とご尽力を頂いた。京都大学の古谷富美子氏には、プロジェクト全般にわたり様々なお世話になるとともに、本報告 G-1, G-2 の執筆に関しても直接のご協力を頂いた。また ITB の T. Hadi 准教授、淡路敏之副学長、津田敏隆教授、里村雄彦教授、石川裕彦教授、竹見哲也准教授をはじめとする京都大学の先生方にも、プロジェクトを通じて様々なご教示とご助力を頂いた。

本報告に関し、気象庁の高野洋雄氏には、(D-1, D-3, D-8)での POM を用いた高潮シミュレーションについて協力頂いた。気象庁の別所康太郎、本田有機、世界気象機関の中澤哲夫、気象大学校の澤田謙の各位は D-8 の、香港天文台の S.T. Lai 博士とタイ気象局の S. Sumdin 博士、インド CSIR の P. Goswami 博士とシンガポール南洋理工大学の C.-K. Teo 博士は、それぞれ D-9, C-8, E-1 の共著者である。また本報告の原稿について、気象研究所の村崎万代、露木義、山田芳則の各位とシンガポール南洋理工大学の C.F. Lo 博士より、閲読の上、コメントを頂いた。これらの方々に深く感謝するものである。なお、本報告は、科学技術振興調整費研究「東南アジア地域の気象災害軽減国際共同研究」のうち気象研究所が行った活動に関連する研究をまとめたものであり、プロジェクト全体についてのレビューは日本気象学会誌「天気」に掲載されており(余田ほか、2008)、また研究成果の全体は、別途アジア科学技術協力の戦略的推進地域共通課題解決型国際共同研究の事後評価報告書として、評価結果とともに公開されている(I-3 参照)。

本報告は、B-1, G-1, G-2 を主に余田が、D-1, D-2 を主に黒田が、C-1, C-2, E-3 を主に林が、C-3, C-4 を主に瀬古が、D-4 を主に國井が、D-5 を主に小司が、D-6, D-7 を主に上野が、D-8 を主に川畑が、D-9 と E-2 を主に黄が、F-1, G-3, I-2 を主に大塚が、C-5 を主に古関が、C-6 を主に Duc と Xin が、C-7 を主に Trilaksono が、C-8 を主に Gouda が、E-1 を主に許が、それ以外を主に斉藤が書いた。

A. Preface

This technical report describes activities by the Meteorological Research Institute (MRI) for the research project "International Research for Prevention and Mitigation of Meteorological Disasters in Southeast Asia", conducted in cooperation with Kyoto University and research institutions in Southeast Asia. This project was proposed by Professor Shigeo Yoden of Kyoto University, and was endorsed in 2007 by the Ministry of Education, Culture, Sports, Science and Technology (MEXT) as one of the research projects in the Asia S & T Strategic Cooperation Program, supported by the Special Coordination Funds for Promoting Science and Technology from fiscal years 2007 to 2009. The main purposes of the project were to strengthen collaboration in atmospheric science research in Southeast Asia and to show the feasibility of disaster mitigation by numerical weather prediction (NWP) through development of a unified data base and a decision support system.

As described in Section B-1, the three main participants of this project were Kyoto University, MRI, and Institut Technologi Bandung (ITB) in Indonesia. MRI also collaborated with Nanyang Technological University (NTU) of Singapore, Vietnam National University of Hanoi (VNU), the Council of Scientific & Industrial Research Centre for Mathematical Modelling and Computer Simulation (CSIR C-MMACS) of India, and the Hong Kong Observatory (HKO). As a major participating institution in Japan, MRI conducted operational model development, described in Section B-2.

We thank many people for their help in making possible our participation in the project. In particular, we are grateful to Dr. T. Nishigaki and Mr. S. Ogawa of Japan Science and Technology Agency (JST), whose help was indispensable. We appreciate Ms. F. Furutani of Kyoto University for her assistance in the project and preparation of manuscripts for this technical report. We also thank Associate Prof. T. Hadi of ITB, and Prof. T. Awaji, Prof. T. Tsuda, Prof. T. Satomura, Prof. H. Ishikawa and Associate Prof. T. Takemi of Kyoto University for their suggestions and help throughout this research project. Mr. N. Kohno contributed to the storm surge simulations described in Sections D-1, D-3, and D-8. We also thank coauthors, Mr. K. Bessho and Mr. Y. Honda of JMA, Dr. T. Nakazawa of the World Meteorological Organization (WMO), and Mr. K. Sawada of the Meteorological College for Section D-8, Mr. S.T. Lai of HKO and Mr. S. Sumdin of the Thai Meteorological Department for Section D-9, Dr. P. Goswami of CSIR for Section C-9, and Dr. C.-K. Teo of NTU for Section E-1. We extend thanks to Ms. M. Murazaki, Dr. T. Tsuyuki and Dr. Y. Yamada of MRI, and Dr. C.F. Lo of NTU, for their review comments on the manuscript.

This report describes only a part of the activities relating to MRI's participation in this research project. A review paper on the project has been published in *Tenki*, the Bulletin of the Meteorological Society of Japan (Yoden et al., 2008), and a detailed achievement report in Japanese on the activities of the project has been uploaded on the JST website (see Section I-3).

The report is organized as follows. Section B presents an overview of the project. Section C reports downscaling numerical experiments in Southeast Asia and verifications. Section D presents numerical experiments for tropical cyclones, including forecast/data assimilation experiments for cyclone Nargis, which hit southern Myanmar in May 2008. Section E covers observations and NWP in Southeast Asia. Section F presents the experimental development of a decision support system for prevention and mitigation of meteorological disasters based on ensemble NWP data. Section G

discusses the international partnerships in the project. Section I, the appendix, includes newsletters, users' guide to the decision support tool, and links to related published papers.

Sections B-1, G-1 and G-2-1 were written mainly by Yoden; Sections D-1 and D-2 by Kuroda; Sections C-1, C-2 and E-3 by Hayashi; Sections C-3 and C4 by Seko; Section D-4 by Kunii; Section D-5 by Shoji; Sections D-6 and D-7 by Ueno; Section D-8 by Kawabata; Sections D-9 and E-2 by Wong; Sections F-1, G-3 and I-2 by Otsuka; Section C-5 by Koseki; Section C-6 by Duc and Xin; Section C-7 by Trilaksono; Section C-8 by Gouda; and Section E-1 by Koh. Other sections were written mainly by Saito.

B. Overview

B-1. Overview of the project[1]

The potential risk of high-impact weather in Southeast Asia is increasing because of economic development and urbanization. Global warming and other types of climate change may become another factor that increases the risk. The change in the research environment due to the rapid growth of computer power and Internet infrastructure has enabled us to start an international research project for prevention and mitigation of meteorological disasters in Southeast Asia. Regional mesoscale models now can be run on personal computers to perform downscaling numerical weather prediction (NWP). Data transfer on the Internet has become fast enough to perform near-real-time NWPs. Making use of the probability information obtained by ensemble NWPs is a challenge for the development of decision support tools, and assessments of the impact of new observational data on the improvement of NWPs with advanced data assimilation schemes are also an important topic.

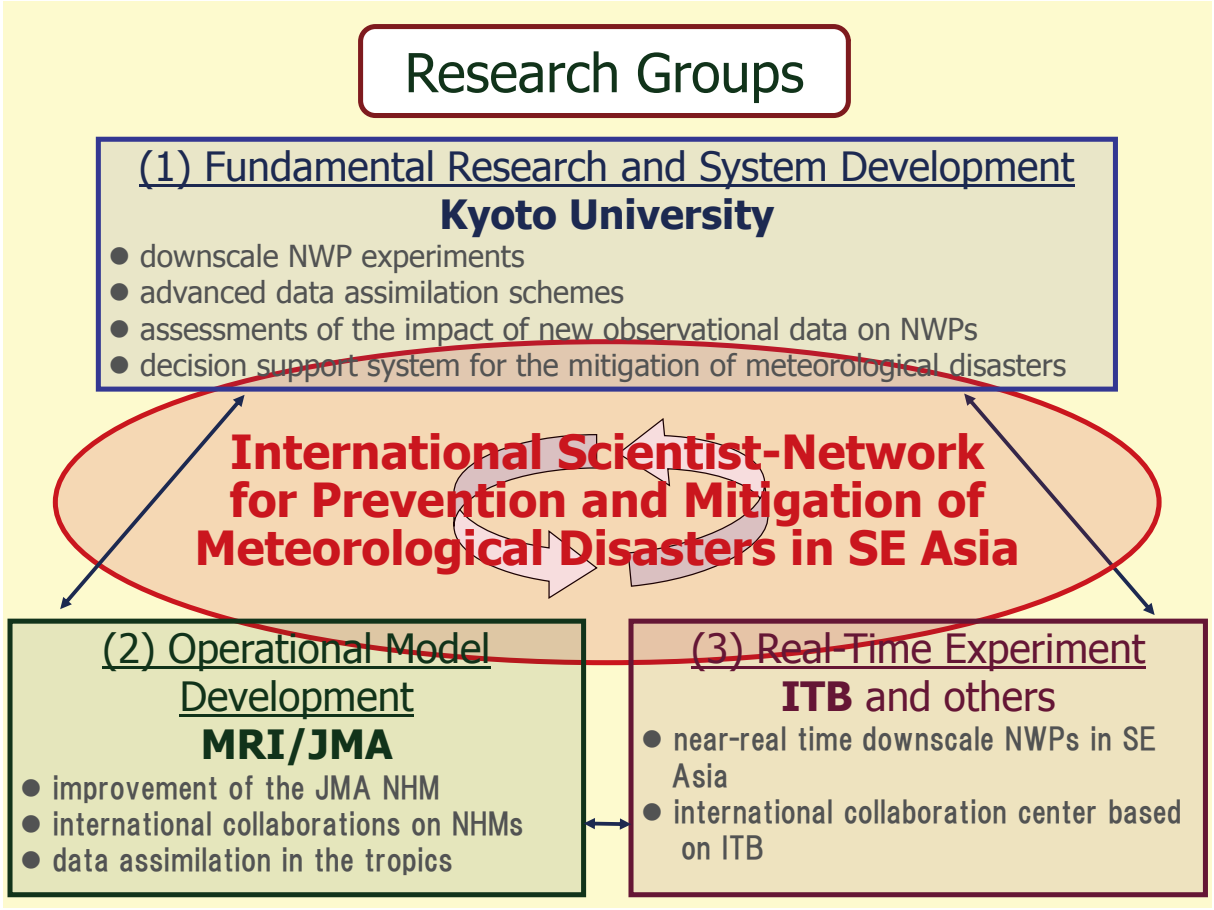

Fig. B-1-1. Three institutes and their roles in the IRPMMDSA project.

In 2007, we started the project "International Research for Prevention and Mitigation of Meteorological Disasters in Southeast Asia (IRPMMDSA)" under the Ministry of Education, Culture, Sports, Science and Technology (MEXT) Special Coordination Funds for Promoting Science and Technology, supported for fiscal years 2007-2009 by the Asia S & T Strategic Cooperation Program (http://www-mete. kugi.kyoto-u.ac.jp/project/MEXT/). This project addressed three main subjects:

[1] S. Yoden and S. Otsuka

(1) Experimental downscale NWP in the tropics with regional mesoscale models

(2) Assessments of the impact of new observational data on NWPs with advanced data assimilation schemes

(3) Development of a unified database and decision support system for prevention and mitigation of meteorological disasters

The three main participants in this international research project were Kyoto University, Meteorological Research Institute (MRI) of the Japan Meteorological Agency (JMA), and Institut Technologi Bandung (ITB) in Indonesia. Figure B-1-1 shows the roles of the participants of this project. Fundamental research and system development was conducted at Kyoto University, and operational model development was conducted at MRI/JMA. Real-time experiments were performed at ITB and other institutes in Hong Kong, India, Singapore, and Vietnam. Our main purpose was to establish the international scientist-network for prevention and mitigation of meteorological disasters in Southeast Asia through research and development of downscaling NWP systems and by holding annual international workshops.

B-2. Overview of MRI's contribution[1]

As a major participating institution in Japan, MRI was responsible for NWP model development and application. This task consisted of three components:

(1) Refinement of the JMA nonhydrostatic model (NHM) and development of mesoscale ensemble prediction techniques for tropical areas

(2) Preparation of tools for numerical experimentations using NHM and collaborative studies to share information on tropical NWP

(3) Development of data assimilation systems in tropical areas and refinement of initialization schemes for tropical cyclones

In the first component, to apply NHM to research on prediction of disastrous meteorological phenomena in the tropics, case studies were conducted with downscale prediction (Sections C-3 and C-4) and statistical verifications of forecast accuracy including intercomparison of NHM and the Weather Research Forecasting (WRF) model (Sections C-1 and C-2). A mesoscale ensemble prediction technique for tropical cyclones also was developed.

In the second component, tools were prepared for numerical experimentations with NHM using the JMA global analysis, the global model forecast, and the JMA one-week global ensemble forecast (Section E-3). An English tutorial on the use of NHM tools was uploaded on the MRI's project website (Section G-5). Exchanges of information and mutual visits of researchers (Section G-3) were conducted in addition to participation in international workshops (Section G-1) organized by Kyoto University.

In May 2008, cyclone Nargis hit southern Myanmar and claimed more than 100,000 lives there in one of the largest meteorological disasters in Southeast Asia, mainly due to the storm surge. We conducted numerical modeling studies of this event. First, we conducted a downscale forecast experiment using NHM with a horizontal resolution of 10 km, employing the JMA global analysis and the global model forecast as the initial and boundary conditions. The track and the rapid development of Nargis were predicted, and the predictability of Nargis' storm surge with a lead time of two days was demonstrated (Section D-1). Next, we developed a mesoscale ensemble prediction system using NHM in the tropics that employs perturbations from the JMA one-week global ensemble forecast, and conducted ensemble predictions of the storm surge considering uncertainty in the forecast of Nargis' track and intensity (Section D-3). Results of this ensemble forecast were used as input data for the decision support system developed by Kyoto University (Section F-1).

In the third component, we conducted data assimilation experiments by modifying the JMA Meso 4D-VAR system to apply to tropical areas. A tropical cyclone (TC) bogus procedure was developed for the Bay of Bengal, and the impact on TC forecasts was investigated (Section D-4). Near real time analysis of precipitable water vapor using the international ground based GPS network around the Bay of Bengal was performed to show its positive impact on the Nargis forecast (Section D-5). A trial of assimilation of QuikSCAT Sea Winds data by the local ensemble transform Kalman filter was also

[1] K. Saito

conducted (Section D-2). Sections D-6 and D-7 describe studies on structures of TC relating to bogus techniques. Similar to the Nargis case, the largest meteorological disaster in Japan resulted from the storm surge of Typhoon Vera in 1959. A reanalysis experiment on Vera using a nonhydrostatic mesoscale 4D-VAR system, conducted in a special research project of JMA (ReVera), is described in Section D-8 for reference.

The researchers' network is a valuable achievement of our project. Collaborations among MRI, Kyoto University and institutions in Southeast Asia are continuing after the project period.

C-1. Statistical verification of short range forecasts by NHM and WRF-ARW with coarse resolution[1]

C-1-1. Introduction

In Southeast Asian countries, meteorological disasters (e.g. heavy rainfall, floods, windstorms) frequently occur, causing severe damages. To reduce such meteorological disasters, NHM is used as a community model in the NWP system for predicting the occurrence of severe meteorological phenomena. To apply NHM to NWP in Southeast Asia, the verification of its forecast accuracy in the tropics is important. We selected 20 km as the horizontal resolution to reduce the lateral boundary nesting gap for the global data (about 100km resolution). In addition, verifications with WRF-ARW (Skamarock et al. 2005; hereafter WRF) were conducted using the same conditions and domains in order to check the performance of NHM relative to WRF.

In this section, the coarse resolution (20 km) results are documented. The fine resolution (5 km) results with 1-way nesting from 20 km results are described in the next section (C-2).

C-1-2. Model description and design of experiments

The same domain size, the same horizontal resolution, the same model top height and the same time step are used to ensure a fair comparison. Initial and boundary conditions are taken from the global forecast system of the National Centers for Environmental Prediction (NCEP-GFS) every 3 hours.

The model specifications and parameters settings in the experiments use the recommended (default) values without tuning (Tab. C-1-1). The same settings in each model are applied to two regions, Japan and Southeast Asia.

Table C-1-1. Model descriptions. After Hayashi et al. (2008)

		NHM ver.2008-Aug-20	WRF-ARW ver.2.2.1
Domain size and forecast hour		150 x 150 grid in horizontal and 40 layer in vertical 20km in horizontal resolution model top height = 22km (about 45 hPa) (vertical coordinate: NHM = z-star, WRF = η) forecast hour = 36hour (dt = 75sec, 1728 steps)	
Initial / Boundary conditions		NCEP-GFS forecast 00UTC, 0-36 hr. (every 3 hr.), 1 x 1 degree horizontal resolution	
Experimental settings	cloud microphysics	6-class bulk microphysics	3-class with simple ice
	cumulus parameterization	Kain-Fritsch scheme (not exactly the same)	
	radiation	GSM0412 scheme	RRTM for longwave Dudhia for shortwave
	boundary layer	Improved Mellor-Yamada Lv. 3	YSU scheme
	land surface	Thermal diffusion scheme (4-layer)	Thermal diffusion scheme (5-layer)
	lateral(L) and upper(U) boundary	L: Rayleigh damping (200km) U: Rayleigh damping (7km)	L: specified boundary(100km) U: no damping
	full formulations	Saito et al. (2007)	Skamarock et al. (2005)
	parameter file for whole settings in the experiments	Nhm/Ss/RF20km/fcst.sh	WRFV2/test/em_real/ namelist.input
		Using these recommended namelists without tuning	

Two simulation periods are selected. One is 15 days from 1 to 15 July 2007, which is the rainy season in Japan and the dry season in Java Island, Indonesia. Another period is 15 days from 1 to 15 January 2008, which is the winter heavy snow season in Japan and the rainy season in Java Island. Simulations for 1.5-day (36 hours) forecasts are conducted from 00 UTC for 15 days and latter 24 hours results are verified.

C-1-3. Statistical verification results

Figures C-1-1a~c indicate the continuous 15 day accumulated precipitation around Japan in July 2007. The observed precipitation area by passive microwave satellites (Fig. C-1-1a), corresponding to

[1] S. Hayashi

the Baiu-front in south Japan, is well reproduced by the models (Figs. C-1-1b and c). In contrast, the precipitation over the western part of Japan and the Sea of Japan are overestimated in the models.

Figures C-1-1d~f are the same as Figs. C-1-1a~c except for January 2008. In this period, the heavy snowfall was retrieved over northwestern coast of the main Island of Japan. CMORPH (Fig. C-1-1d), however, does not yield an exact snowfall precipitation amount for Japan's main island, because snow and ice on a surface cannot be distinguished from frozen hydrometeors by the present precipitation estimation algorithm of CMORPH. Compared with surface observation (AMeDAS), the heavy snow fall was found to be well reproduced (figure not shown).

Figures C-1-1g~i are the same as Figs. C-1-1a~c, but for July 2007 over the maritime continent. This period correspond to the dry season in the Java Island. Both models reproduce the dry climate on Java Island well (Figs. C-1-1h and i). However, the predicted precipitation is overestimated in the northern part of the domain, especially near the north boundary of the WRF result (the edge regions of 300 km width are excluded from the statistical verification).

Figures C-1-1j~l are the same as Figs. C-1-1d~f except for Southeast Asia. The accumulated precipitation over the sea is overestimated in both models (Figs. C-1-1k and l). In addition, WRF results in excessive precipitation over the Borneo Island.

Figures C-1-2a~d show the threat scores for 3-hour precipitation against CMORPH or AMeDAS. A 40 km verification grid size were used in order to avoid the differences between the map projections of CMORPH and the models. The threat scores for both models in July over Japan are 0.27 at 1 mm / 3 hours for CMORPH (Fig. C-1-2a). This value is not far from that of JMA's operational mesoscale model (MSM; the horizontal resolution is 5km). Figure C-1-2b shows the threat score for the wintertime in Japan. The threat scores for two models against CMORPH are less than half of those for July 2007 over Japan. Meanwhile, the deteriorations in the threat scores for the models against AMeDAS were smaller than those against CMORPH. Therefore, the decreasing scores against CMORPH are not caused by the models but by snow on a land surface. The threat scores for both models over Southeast Asia are 0.12-0.14 at 1 mm / 3-hours (Figs. C-1-2c,d), which are about half of the scores in July 2007 over Japan.

In our results, the accuracy of both forecast models around Southeast Asia was worse than that of the forecast for the rainy season in Japan. One of the reasons is that precipitation in the rainy season in Japan is caused by a mid-latitude synoptic disturbance, while tropical precipitation is mainly caused by convection. Other causes may be in the initial and boundary conditions and / or the physical processes of the two models. The accuracy of current global models of coarser grid resolutions may be insufficient for forecasting precipitation in the tropics. In addition, both of the mesoscale models may have some problems or unsuitable settings for forecasting tropical precipitation. We need to obtain more accurate statistical verification of the models.

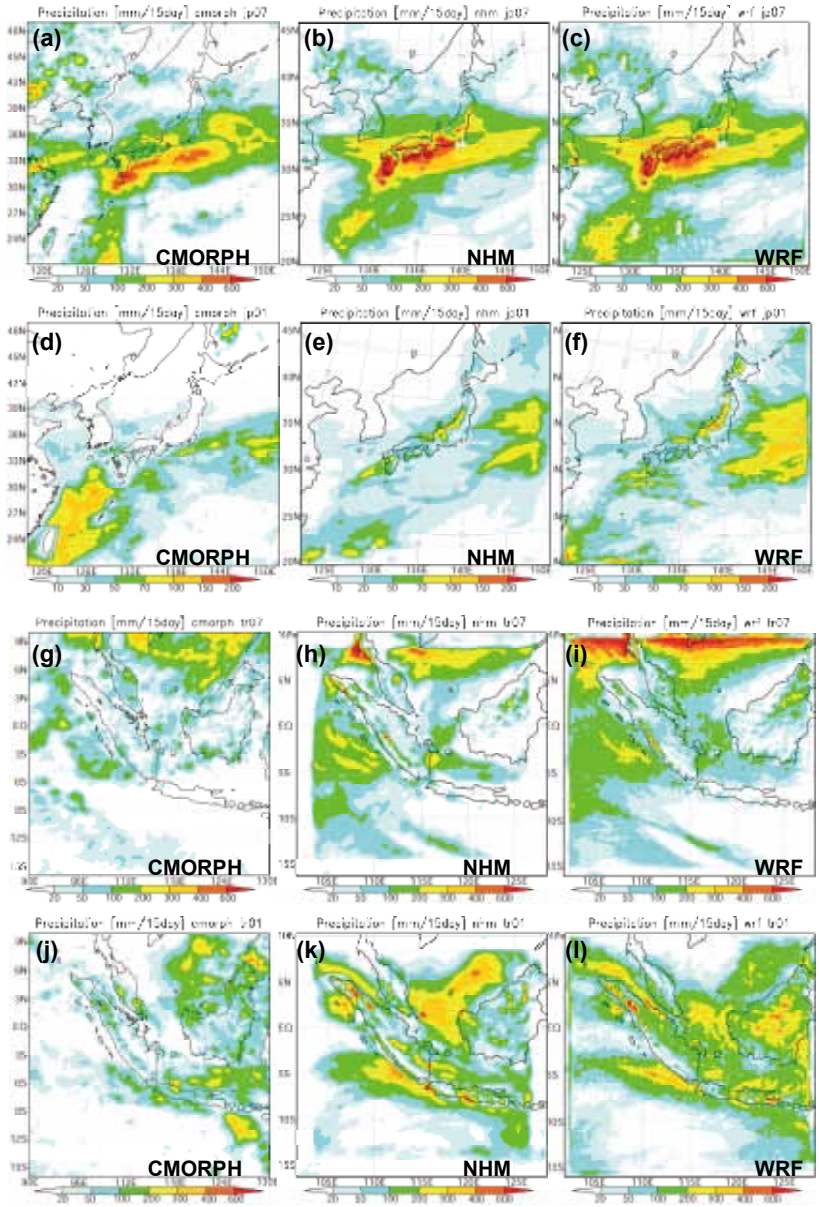

Fig. C-1-1.
(a, b, c,): 15 days accumulated precipitation from 1 to 15 July 2007 around Japan. (a) CMORPH, (b) NHM, (c) WRF,

(d, e, f): Same as (a, b, c,) except from 1 to 15 January 2008,

(g, h, i): Same as (a, b, c) except around Southeast Asia,

(j, k, l): Same as (g, h, i) except from 1 to 15 January 2008,

After Hayashi et al. (2008).

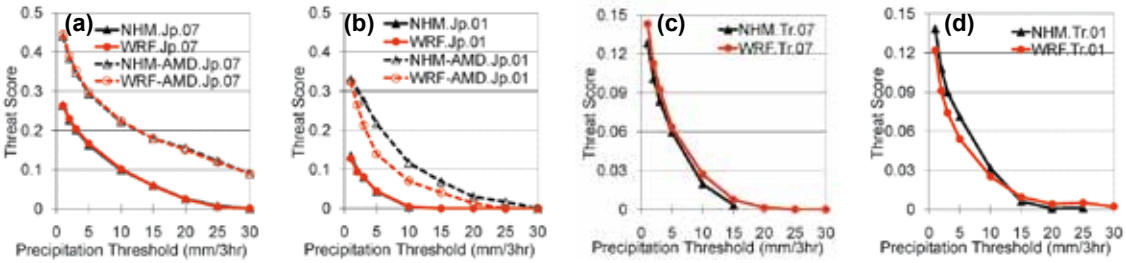

Fig. C-1-2. 3-hour precipitation threat scores, (a) from 1 to 15 July 2007 (b) from 1 to 15 January 2008 around Japan, and (c, d) same as (a, b) except around Southeast Asia. Solid lines show scores against CMORPH and dashed lines show scores against AMeDAS in (a) and (b). After Hayashi et al. (2008).

C-2. Statistical verification of short-range forecasts by the NHM and WRF-ARW models with fine resolution[1]

C-2-1. Introduction

As described in Section C-1, the NWP accuracy over Southeast Asia by models of 20-km horizontal resolution (JMA's nonhydrostatic model NHM and Weather Research Forecasting model WRF-ARW) was worse than that over Japan. We conducted fine-resolution experiments to investigate how forecast accuracy improves by using 5-km horizontal resolution.

C-2-2. Model description and design of experiments

Almost the same settings as listed in Table C-1-1 were used (Table C-2-1). The domain size of the 20-km models was slightly expanded from that in section C-1 to avoid the influence of the lateral boundaries on the 5-km model. We updated both models to their latest versions (NHM ver. 3.1 and WRF-ARW ver. 3.1.1) and updated their default settings (details are described in Section C-2-5). It is notable that NHM's default parameter settings employ a six-class bulk cloud microphysics scheme that predicts number concentrations of cloud ice.

For the Southeast Asia region, 30-hour forecasts from 0600 UTC on each of 31 days in January 2008 were conducted with a 5-km horizontal resolution nested into the 20-km model forecasts with initial times of 0000 UTC. For the Japan region, similar 24-hour forecasts were conducted for July 2007 and analyzed at both resolutions.

C-2-3. Statistical verification results

Figures C-2-1 presents the horizontal distribution of the 31 days of accumulated precipitation in July 2007 in the Japan region from CMORPH satellite precipitation observations and models. Compared with the satellite observations (Fig. C-2-2a), the forecasts from the 20-km horizontal resolution models (Figs. C-2-2b and c) well reproduced the location and precipitation of the Baiu-front. So did the 5-km models (Figs. C-2-2e and f), however, the precipitation amounts were overestimated on the south side of the Japanese Islands compared with CMORPH observations.

Table C-2-1. Model descriptions.

	NHM v3.1 (release candidate)	WRF-ARW v3.1.1
Domain size and forecast period	160x160 grids for 20km resolution in horizontal 301x301 grids for 5km resolution in horizontal 40 layers in vertical, model top 22km (about 45 hPa) (vertical coordinate; NHM = z-star, WRF = η) forecast hour = 36 hour for 20km, 30 hour for 5km in every 31days	
Initial / Boundary	NCEP-GFS forecast at 00UTC for initial and every 3hr forecast for boundary 1x1 degree horizontal resolution, 24 P-levels	
model configurations	Nhm/Ss/RF20km/fcst.sh (for 20km) RFnest/fcst.sh(for 5km)	WRFV3/test/em_real/ namelist.input
	Using these configurations without tuning	
cloud microphysics	6-class bulk with number of ice	3-class bulk with simple ice
cumulus parameterization	Modified Kain-Fritsch scheme	Kain-Fritsch scheme
radiation	GSM0412 scheme	RRM for longwave, Dudhia for shortwave
boundary layer	Improved MYNN3	YSU scheme
Lateral and Upper boundary	damping for lateral and upper boundary	no damping for upper boundary, only for lateral
others	almost the same configurations as JMA operational 5km model (MSM)	

Both 5-km models represented detailed precipitation distributions. Figure C-2-1d shows the 1-km grid radar precipitation amounts calibrated by surface rain gauges (called Radar-AMeDAS, hereafter

[1] S. Hayashi

R-A). The R-A precipitation data have better resolution and more accurate amounts for the Japanese Islands than the CMORPH data. The topographic influence on precipitations was clearly indicated in the R-A data, especially on the south side of Kyushu and Shikoku islands, and the Kii Peninsula. Both the 5-km models well reproduced these details (Fig. C-2-2e and f). Over the San-in area, however, both models overestimated the precipitation. The horizontal spread of the precipitation distribution from WRF was larger than that of observations, and the results of NHM.

Figures C-2-2 depicts the horizontal distribution of the accumulated precipitation for January 2008 over Southeast Asia from observations and models. Compared with the satellite observation (Fig. C-2-2a), all the models overestimated precipitation amounts over the almost all domains (Figs. C-2-2b~e). In particular, WRF-20km over-predicted precipitation over Borneo and Sumatra. Both 5-km models produced the details of the precipitation distribution, especially the orographic precipitation in Sumatra by NHM-5km. It is difficult to verify the detailed precipitation distributions because the resolution of CMORPH data is insufficient to model this fine structure.

To compare CMORPH data against the precipitation models, the equitable threat scores (ETSs) for the 3-hour precipitation in each 40-km verification grid, in order to avoid the differences from the map projections and horizontal resolution between CMORPH and the models, are shown in Figures C-2-3a for Japan C-2-3c for Southeast Asia, and Figure C-2-3b shows the ETS of 3-hour precipitation against AMeDAS rain gauges for Japan. The ETSs against CMORPH for Japan were the same for both the 5-km and the 20-km models (Fig. C-2-3a). The ETSs of the 5-km models against AMeDAS, however, were better than those of the 20-km models (Fig. C-2-3b). In particular, the ETSs of NHM-5km were clearly superior for moderate and strong (10 mm and 40 mm) 3-hour precipitations to those of NHM-20km. The ETSs of the 5-km models for Southeast Asia were slightly better than those of the 20-km models. However, their values were much lower than those for Japan (Fig. C-2-3a).

In addition, we conducted some sensitivity experiments for both Japan and Southeast Asia. First, NHM-5km and WRF-5km without cumulus parameterization reproduced almost the same precipitation distribution as the models with cumulus parameterization (figures not shown). Second, WRF-5km with the parameter settings by the Developmental Testbed Center (http://www.dtcenter.org/) also yielded similar results (figures are not shown). Third, both models were run with a 1.25-km horizontal resolution, but they did not improve upon the 5-km models (figures are not shown). We intend to future subject to investigate ways to improve forecasts in the tropics.

C-2-4. Summary

We found that models with 5-km resolution produced better forecast than models with 20-km resolution. The difference was greater for Japan than for Southeast Asia region, and the scores for Southeast Asia were worse than those for Japan. The accuracy of NHM was better than that of WRF in these experiments. Better verifications methods using finer scale observations are needed to investigate ways to improve forecasts in tropics.

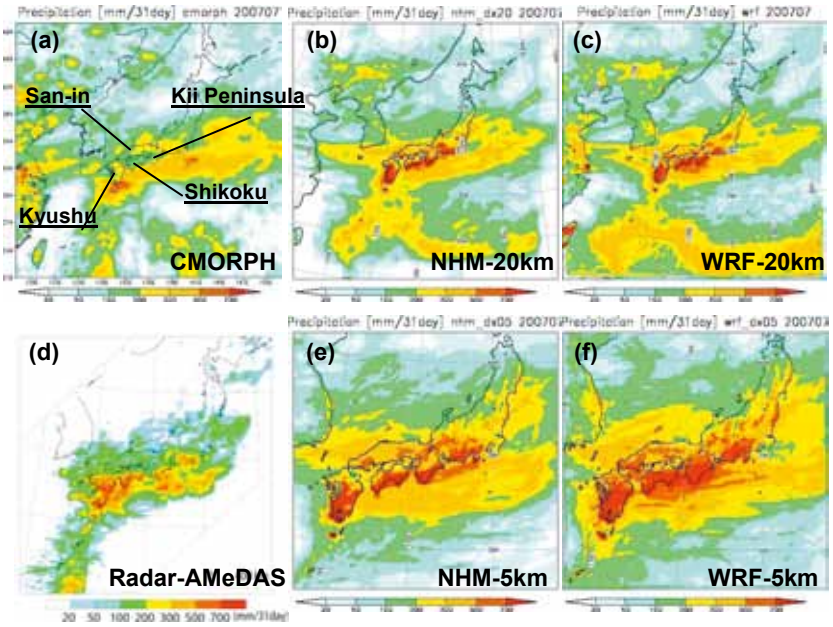

Fig. C-2-1.
(a, b, c, d, e, f): 31 days Accumulated Precipitation from 1 to 31 July 2007 around Japan.
(a) CMORPH, (b) NHM-20km, (c) WRF-20km, (d) Radar-AMeDAS, (e) NHM-5km, (f) WRF-5km

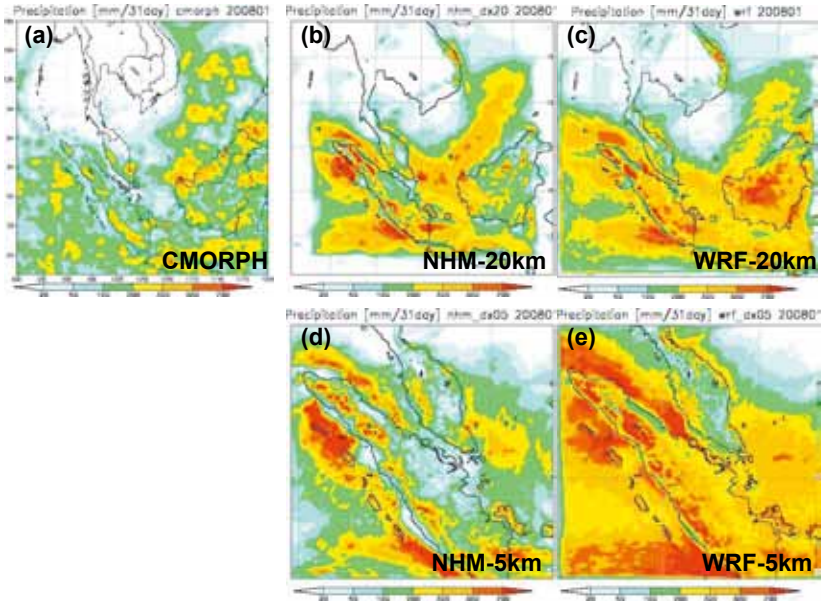

Fig. C-2-2.
(a, b, c, d, e): 31 days Accumulated Precipitation from 1 to 31 January 2008 around Southeast Asia.
(a) CMORPH, (b) NHM-20km, (c) WRF-20km, (d) NHM-5km, (e) WRF-5km

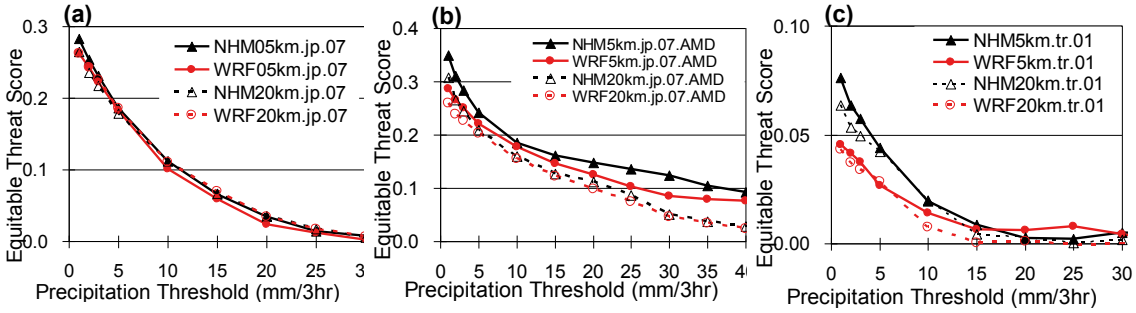

Fig. C-2-3. 3-hour precipitation equitable threat scores, (a) against CMORPH for July 2007 in Japan, (b) against AMeDAS for July 2007 in Japan, (c) against CMORPH for January 2008 in Southeast Asia. Black lines represent NHM, red lines represent WRF, solid lines are for 5-km models and dashed lines for 20-km models.

C-2-5. Supplement on updates in both the models

In this research, NHM was updated from ver. 2.00-MSM0808 (Section C-1) to ver. 3.1 (release-candidate), and WRF-ARW was updated from ver. 2.2.1 (Section C-1) to ver. 3.1.1. Updated points are listed below.

a. NHM updates from ver. 2.00-MSM0808 to ver. 3.1

- Cloud microphysics scheme was changed from a six-class one-moment scheme to six-class one-moment with cloud-ice two-moment scheme.
- Radiation scheme was updated to implement aerosol monthly climatological value, effective radius of cloud ice, and emissivity correction for cloud fraction.
- Nonlinear diffusion coefficient was changed. The test of double nested NHM-5km in the tropics, produced undesirable overestimation of the amount of upper-level clouds (hereafter CH). Simulated CH from NHM-5km was almost 100 % cloud-amount over the whole model domain (Fig. C-2-4a). This overestimation led to underestimation of diurnal change of surface soil/air temperatures through the shortage of short-wave solar radiation.

  Sensitivity tests revealed that the overestimation of CH was caused by inappropriate application of the nonlinear computational diffusion to the number concentration of cloud ice (hereafter QNCI) (Fig. C-2-4b). In NHM, a third-order nonlinear damping and a fourth-order linear damping (Eqs. G4-1 and G4-2 in Saito et al. 2001) were employed as the computational diffusion. The magnitude of the third-order nonlinear damping was set in the NAMELIST parameter 'DIFNL'. For two-grid noises of amplitude -a-, the nonlinear damping gives the equivalent 1/e-folding time DIFNL*Δt/a when DIFNL > 0, and |DIFNL|/a when DIFNL < 0. Because QNCI sometimes takes a very large value (on the order of 10^6), QNCI is diffused excessively by application of the nonlinear computational diffusion, yielding overextension of CH. In the experiment in Section C-2-3, we changed DIFNL from -600 to -2400 to weaken this nonlinear diffusion.

  After NHM ver. 3.2, the nonlinear diffusion is no longer applied to cloud microphysical quantities except for the mixing ratios of water vapor, cloud water, and cloud ice.
- Some trivial bugs were fixed.

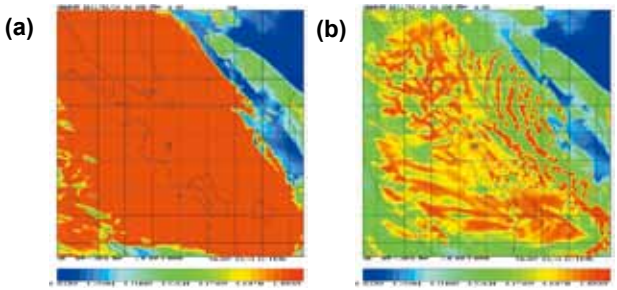

Fig. C-2-4. (a) Simulated upper-level cloud amount (CH) at FT=6-hour when nonlinear diffusion is applied to QNCI. (b) Simulated CH at FT=6-hour nonlinear diffusion is not applied to QNCI.

b. WRF-ARW update from ver. 2.2.1 to ver. 3.1.1

- Land surface scheme was changed from thermal diffusion scheme to Noah-LSM
- Upper-level damping coefficient was changed from 0.01 to 0.2.
- A positive definite advection scheme for moist and scalar variables was applied.
- Some trivial bugs were fixed.

C-3. Structure of the regional heavy rainfall system that occurred in Mumbai, India on 26 July 2005[1]

Heavy rainfalls frequently occur not only in Japan, but also in other countries, especially in southeastern or southern Asian countries. According to the Asian Disaster Reduction Center (ADRC)-Natural Disasters Data Book-2006 (ADRC 2007), the most frequent disasters in member countries (India, Indonesia, Viet Nam, and 22 other countries) are windstorms and floods. These phenomena account for 80% of the disasters affecting the population in the Asian and ADRC member countries.

In this study, the heavy rainfall that occurred at Santa Cruz, a suburb of Mumbai, on 26 July 2005 was investigated. Due to this heavy rainfall, the 24 hour rainfall amount at Santa Cruz reached 944.2 mm (Bohra et al. 2005). The rainfall amount recorded in this event was about a half of the annual rainfall. Because the heavy rainfall was caused by a regional convective system, we reproduced the heavy rainfall by the downscale experiments using a non-hydrostatic model with a fine horizontal grid interval (JMA-NHM; Saito et al. 2006). Probability and formation factors of the heavy rainfall were also investigated by ensemble forecasts.

C-3-1. Observed features of the heavy rainfall

According to Bohra et al. (2005), the rainfall at Santa Cruz started at 0600 UTC (11.5 India Standard Time (IST)) on 26 July 2005, and continued for 18 hours (Fig. C-3-1a). The rainfall region observed by the Tropical Rainfall Measuring Mission (TRMM) satellite revealed that the horizontal scale of this rainfall event was several tens of kilometers (Fig. C-3-1b). These observed results indicated that the rainfall system had a long-lasting structure that brought a large quantity of rainfall to a small region. Figure C-3-1c illustrates the precipitable water vapor (PWV) observed by the Special Sensor Microwave/ Imager (SSM/I). When the heavy rainfall occurred, a region of large PWV over 60 mm existed just north of the heavy rainfall system. This distribution of PWV suggested that the heavy rainfall might have occurred when this humid air was supplied to the rainfall system.

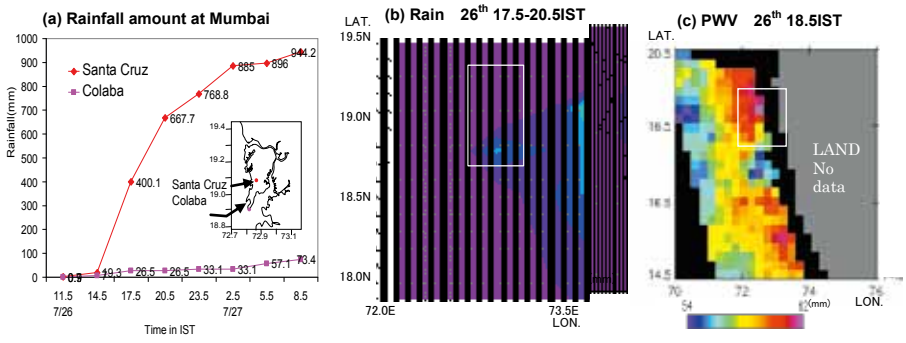

Fig. C-3-1. (a) Time series of observed rainfall amount on 26 and 27 July at Santa Cruz and Colaba (After Fig. 1 of Bohra et al. 2005). (b) Three hour rainfall amount estimated by TRMM satellite (After Fig. 2 of Bohra et al. 2005). (c) PWV distribution observed by SSM/I. White rectangles in (b) and (c) indicate the regions of figs. (a) and (b), respectively. After Seko et al. (2008).

[1] H. Seko, S. Hayashi, M.Kunii, and K. Saito

C-3-2. Design of the downscale experiment

This study used JMA-NHM with triple-nested grids (20 km, 5 km and 1 km). Hereafter, experiments with 20 km will be labeled 20km-NHM (horizontal grid number 200 ×200); those with 5 km will be labeled 5km-NHM (horizontal grid number 400×400); and those with 1 km will be labeled 1km-NHM (horizontal grid number 300×300). Vertically, 40 stretched terrain-following layers were commonly employed in all experiments. The lowest level of the model was located at 20 m, and the top of the model was located at 22.7 km. Initial and boundary conditions of 20km-NHM were obtained from the global analysis data of JMA. Outputs of 20km-NHM and 5km-NHM provided the initial and boundary conditions of 5km-NHM and 1km-NHM. The initial data of 5km-NHM and 1km-NHM were given by the outputs at the forecast time (FT) of 6 hours. Specifically, the initial time of 5km-NHM and 1km-NHM were 11.5 IST and 17.5 IST of 25 July. The forecast period of 20km-NHM, was 36 hours; that of 5km-NHM was 30 hours; and that of 1km-NHM was 9 hours.

C-3-3. Heavy rainfall reproduced by the downscale experiment

Figure C-3-2a depicts the rainfall distributions from FT = 3 to 27 (hours) produced by 5km-NHM. The rainfall regions were generated along the mountain range near the western coast of India by FT = 3 (14.5 IST). An intense rainfall system was organized near Mumbai by FT = 6 (17.5 IST). The system began to split into several rainfall cells along the mountain range at FT = 18 (5.5 IST, 26 July), and then the intense rainfall was terminated at FT = 23 (10.5 IST, 26 July). The rainfall amount in 17 hours from FT = 6 to FT = 23 caused by the system reached 1,149 mm. The rainfall amount and duration indicated that the heavy rainfall was quantitatively well-simulated.

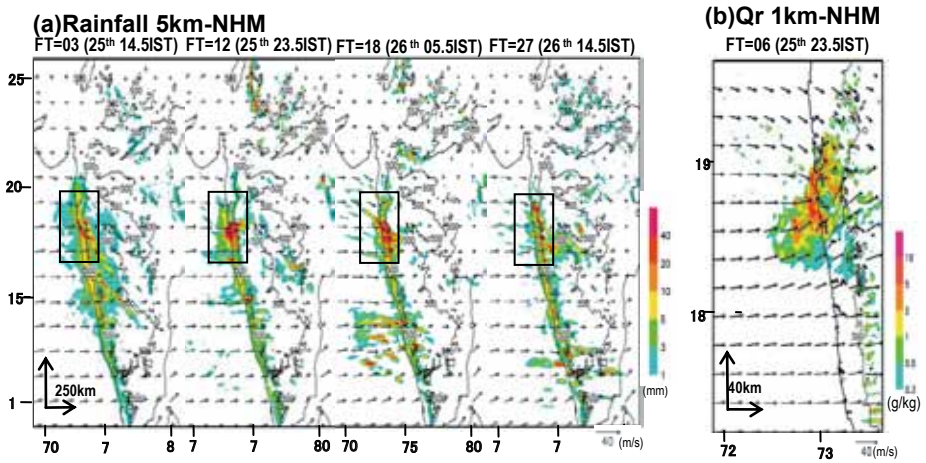

Fig. C-3-2. (a) Rainfall distributions from FT=3 to 27 hour by 5km-NHM and (b) horizontal wind and rainwater mixing ratio (Qr) at z=0.53 km at FT=6 by 1km-NHM. Rectangles in (a) indicate the domain of (b). Large arrows in (a) and (b) indicate the horizontal scale of 250 km and 40 km, respectively. After Seko et al. (2008).

Figure C-3-2b depicts the rainwater mixing ratio of the regional rainfall system reproduced by 1km-NHM. The intense rainfall system had already been organized by FT = 6 (23.5 IST) 100 km south of Mumbai. The horizontal scale of regional heavy rainfall was several tens of kilometers. The good agreement of the simulated position and the horizontal scale with observation indicated that

1km-NHM effectively reproduced the regional heavy rainfall. The structure of this intense rainfall system and the factors that produced intense rain were reported by Seko et al. (2008).

C-3-4. Heavy rainfall reproduced using LETKF

The factors that caused the heavy rainfall were also investigated by the outputs of the ensemble forecast. In this study, a Local Ensemble Transform Kalman Filter (LETKF) for JMA-NHM (Miyoshi and Aranami 2006) was used. As the forecast models, JMA-NHM with a grid interval of 20 km was used. Size of ensemble member was 20. Initial seed was given by the global analysis of JMA at 00 UTC from 5 to 24 July. The conventional data, such as surface and upper sounding data were assimilated with 6-hours assimilation windows.

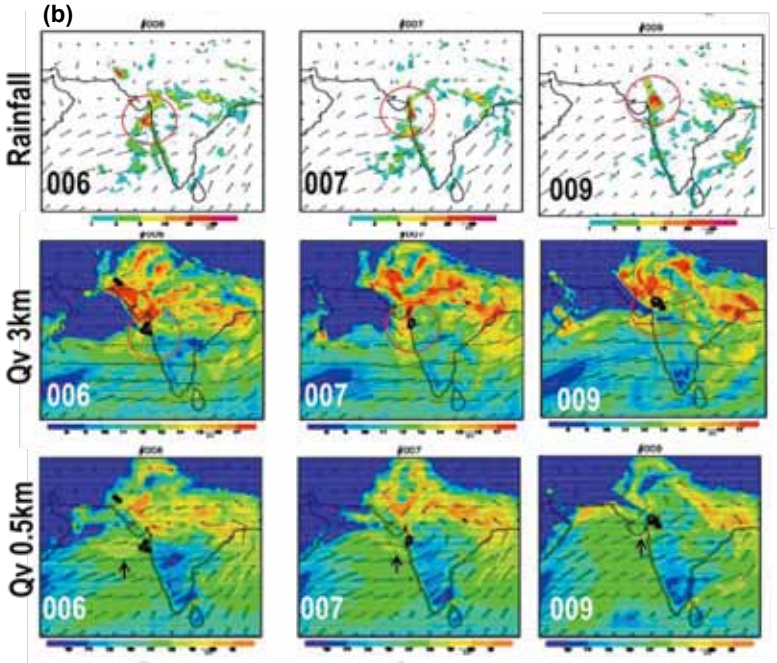

Fig. C-3-3. Rainfall and water vapor mixing ratio distributions at the height of 3 km and 0.5 km. Red circles and thick arrows indicate the heavy rainfalls and the low-level airflows that supplies humid air.

Figure C-3-3 shows that rainfall region and water vapor distributions at the heights of 0.5 km and 3 km by the ensemble forecast. Heavy rainfalls near the western coast of India were reproduced in three ensemble members of #006, #007 and #009 among 20 members. Namely, the probability of heavy rainfalls is 15 %.

Outputs of ensemble members were compared, and then the following features were pointed out as the factors that influence the formation of the heavy rainfall.

(1) Intense rainfalls were generated at the southern tip of the moist region at the height of 3 km.
(2) Northerly flows existed in the moist region on the north of intense rainfall.
(3) Moist air also supplied by the low level westerly flow.
(4) The humid region at the height of 3 km exists in the inland area in #009. Thus, the orographic effect that produces the thick humid northerly flow was not the indispensable condition for the heavy rainfall formation.

These features indicate that the thick humid airflow from the north and the low-level humid westerly flows are the indispensable factors for the heavy rainfalls. This result is consistent with the observed PWV distribution (Fig. C-3-1c) and the sensitivity experiment's results shown in Seko et al. (2008).

C-4. Generation mechanisms of convection cells in the tropical region[1]

Because weather systems that cause heavy rainfall are characterized by intense convection cells, generation and development mechanisms of intense convection cells should be understood for disaster mitigation. In mid-latitudes, large-scale convergences such as the Baiu front, meso-scale convergences induced by cold pools, or thermodynamical low-pressure systems have been reported as causes of heavy rainfalls (e.g., Seko et al. 2005; Kawabata et al. 2007). However, convection cells in tropical regions are not as well studied. Because typical atmospheric profiles in tropical regions differ from those in mid-latitudes, some mechanisms, such as gravity waves, might more strongly affect convection cells in tropical regions.

Tropical convection cells were simulated by a high-resolution 2-dimensional nonhydrostatic model by Yamasaki and Seko (1992; abbreviated to YS92 hereafter) to investigate their generation and development mechanisms. They found that convection cells were generated and developed when updrafts resulting from intersecting gravity waves overlapped, or when gravity waves propagated into the humid region. However, YS92 used a 2-dimensional model in which the influence of gravity waves is overestimated when the gravity waves propagate to all directions. To refine the YS92 results, we conducted a reproduction experiment of tropical convection cells using a high-resolution 3-dimensional model. The JMA Climate Data Assimilation System (JCDAS) was used as the realistic initial fields.

C-4-1. Ideal experiment with a 2-dimensional model (YS92)

YS92 used a 2-dimensional anelastic model (Yamasaki 1984) with a horizontal grid interval of 1 km. Vertical profiles of temperature and humidity used as the basic fields were those typical of the tropical region (see Table 1 in Yamasaki (1983)). For horizontal winds, a vertical profile with a linear vertical shear of 2 m/km below the height of 3 km was used. The horizontal domain size was set as large as 5000 km, so that factors other than gravity waves (e.g., cold outflow) would not affect the generation of the convection cells. Initial disturbances consisted of two sets of four thermal

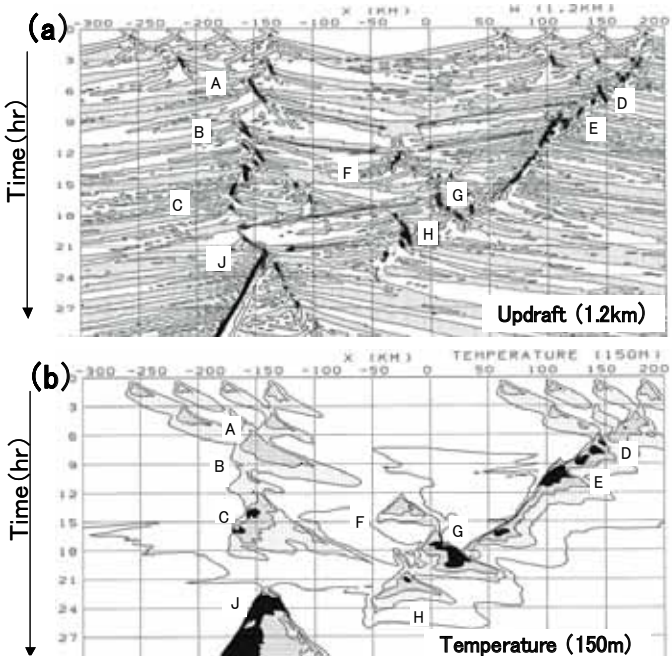

Fig. C-4-1. Hovmöller diagrams of (a) updrafts at 1.2km height and (b) temperature at 150 m height. Shaded and dark regions in (a) indicate updrafts and clouds. Arrows indicate the propagations of gravity waves that generate or develop the convection cells F and J. The shaded and dark regions indicate the cold pools produced by the convection cells. After Yamasaki and Seko (1992).

[1] H. Seko, S. Hayashi and K. Saito

bubbles near the center of the model domain. When the numerical integration was conducted, cold outflows and gravity waves that were produced by the initial bubbles triggered successive convection cells.

Figure C-4-1 shows Hovmöller diagrams of updrafts at 1.2 km height and temperature at 150 m height. Updrafts of gravity waves were generated among groups of convection cells and propagated to both directions (Fig. C-4-1a). When updrafts propagated from convection cells A and D, a new convection F was generated between these convection cells, then developed when gravity waves arrived from convection cells B and E. Convection J was generated when gravity waves arrived from convection G and was developed when gravity waves arrived from convection H. We studied the generation and development mechanisms of these convection cells by the vertical distributions of the deviations from their horizontal averages. When gravity waves approached, temperature decreased and relative humidity increased in the updraft region (not shown). Updrafts and these changes caused by gravity waves constituted favorable conditions for the generation and development of new convection cells. There was no cold pool where convection cells F and J were generated (Fig. C-4-1b), which indicates that gravity waves alone can generate and intensify convection cells.

C-4-2. Design of experiments

This study reproduced convection cells near Sumatra in the monsoon season. Triple one-way nested downscale experiments were performed so that the horizontal grid interval of the innermost model can produce individual convection cells. The grid intervals of the nested models were 20 km, 5 km, and 1 km, respectively. Initial and boundary conditions of the outer model (20km-NHM) were given by JCDAS (global analysis data by JMA and the Central Research Institute of Electric Power Industry). Thermal bubbles were not replaced in the initial fields. The initial time for the 20km-NHM model was 1200 UTC 28 January 2008, during monsoon season in Southeast Asia. A 6-h forecast of 20km-NHM was used as the initial condition for the second model (5km-NHM), which is enough time for spin-up because convection cells were generated during the first 6 h from the initial time of 5km-NHM. A

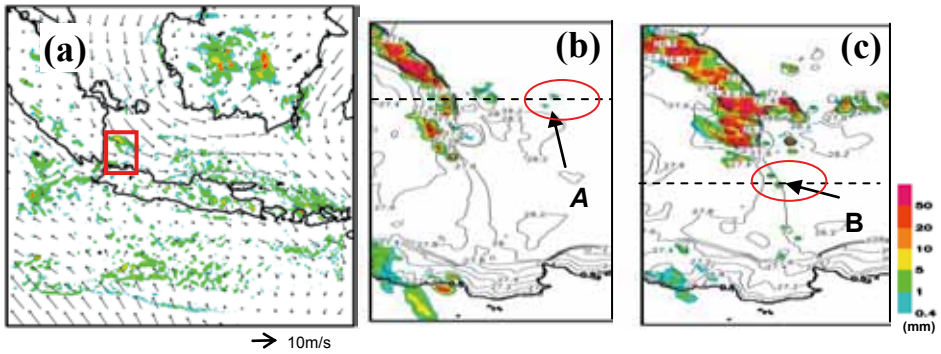

Fig. C-4-2. (a) Rainfall regions at 2100 UTC 29 January 2008 reproduced by 5 km-NHM, and at (b) 2230 UTC on 29 and (c) 2320 UTC on 29 reproduced by 1 km-NHM. Initial time of 5km-NHM and 1km-NHM are 1800 UTC 28 and 1500 UTC 29, respectively. Contours in (b) and (c) indicate the temperature at 1000 hPa. Red rectangular in （a） indicates the regions of (b) and (c).

21-h forecast of 5km-NHM was used as the initial condition for 1km-NHM. The time lag between the initial times of 5km-NHM and 1km-NHM (21 h) was determined by the generation time of convection cells, not by the spin-up time. The Kain-Fritsch convective parameterization scheme was adopted in 20km-NHM and 5km-NHM. The bulk method which predicts cloud water, rainwater, cloud ice, snow, and graupel was adopted as the microphysical process for 1km-NHM.

C-4-3. Generation mechanisms of convection cells by gravity waves

Figure C-4-2a shows the 1-h rainfall and surface horizontal wind distribution at 2100 UTC on 29 January 2008 reproduced by 5km-NHM. On the eastern side of Sumatra, west-northwesterly and northwesterly flow converged and a rainfall region was generated there.

Figures C-4-2b and c show the 1-h rainfall and surface temperature distributions reproduced by 1km-NHM. The intense rainfall band extending southeastward on the eastern side of Sumatra corresponds to the rainfall region in Fig. C-4-2a. Small convection cells A and B were generated on the eastern side of the convective band at 2230 UTC and on the southern side at 2320 UTC. Contours near the convection cells A and B in Figures C-4-2b and c show that an intense cold pool did not exist around them. We chose these two events as the targets of this study because they were not generated by an intense cold pool.

(a) Convection cells generated along the convergence zone

Convection cells A were generated where the temperature gradient was weak. Figure C-4-3 shows Hovmöller diagrams of updrafts at two levels as well as rainfall, temperature, and dew-point deficits (T – Td) across convection cells A. Convection cells were generated repeatedly after the propagation of the weak updraft region at 925 hPa from the west (indicated by arrows in Fig. C-4-3c). These weak updrafts were produced by the convergence of the west-northwesterly and northwesterly flow, shown in Figure C-4-2a. Convection cells A were generated far from other convection cells when the updrafts at 925 hPa (Fig. C-4-3c) and 850 hPa, which propagated from the east (arrow in Fig. C-4-3a), overlapped. The contours of temperature and dew-point deficit at 850 hPa show

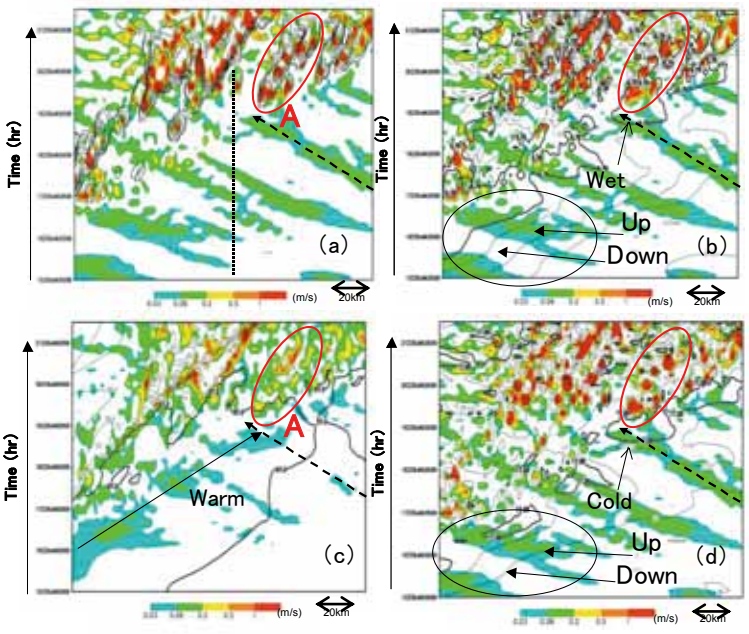

Fig. C-4-3. Hovmöller diagrams of updrafts (colored region) at (a~b, d) P=850hPa and (c) 925 hPa along the broken line in Fig. C-4-2(b). Contours in (a)~(d) indicate (a) rainfall, (b) dew-point deficit at P=850hPa, (c) temperature at P=1000hPa and (d) temperature at P=850hPa, respectively.

that both parameters decreased rapidly as the updrafts passed (Figs. C-4-3d and b). These variations show that the updrafts were induced by gravity waves. Before the generation of convection A, the temperature became lower and the dew-point deficit became smaller than before the arrival of the gravity waves (Figs. C-4-3d and b). These changes favored the generation and development of convection cells, and they are common to convection cells created in the 2-dimensional model of YS92. Temperature at 1000 hPa in Figure C-4-3c shows that a cold pool did not exist and could not have generated the convection cells.

Figure C-4-4 is a time-height diagram of the updraft and deviation of temperature from the temporal average. Temperature below 800 hPa decreased with time, caused by the convergence of west-northwesterly and northwesterly flows. The updrafts below 700 hPa appeared at 30–60 min intervals. As shown in Figure C-4-3, temperature rapidly decreased when the updraft passed. The extent of these variations was limited below 700 hPa, which we attribute to the large vertical gradients of potential temperature (5.5 K/km) at the height of 2–3 km at the initial time of the 1km-NHM model over the Java Sea. Low-equivalent potential temperature air at the middle level (500 hPa) has been reported as the factor causing heavy rainfalls in middle latitudes (e.g., Kato and Aranami 2005). However, the height at which this factor was effective in the generation and development of convection cells in this study was 800–900 hPa. The origin of the gravity waves that propagated to A, investigated by tracing back the pattern of horizontal distribution of vertical velocities at 850 hPa, was around the weak rainfall regions that were developed in the Java Sea from 0200 to 0700 UTC 29 January.

(b) Convection cells generated along the edge of the weak cold pool

On the southern side of the convective band east of Sumatra, a weak cold region moved eastward (Fig. C-4-2c). The drop of temperature was as small as 0.2 °C. Convection cells B were generated at the leading edge of this cold pool.

Figure C-4-5 shows Hovmöller diagrams across convection B. Figure C-4-5c shows that the cold pool (colder than 27.0 °C) extended eastward and that the weak updraft was produced at its leading edge. At 950 hPa, above the extent of the updraft caused by the cold pool, another updraft propagated from the west (indicated by the dashed arrow in Fig. C-4-5a). The propagation speed of this updraft was much greater than the speed of expansion of the cold pool, indicating that the updraft was induced by gravity waves. When the gravity waves propagating from the west reached the leading

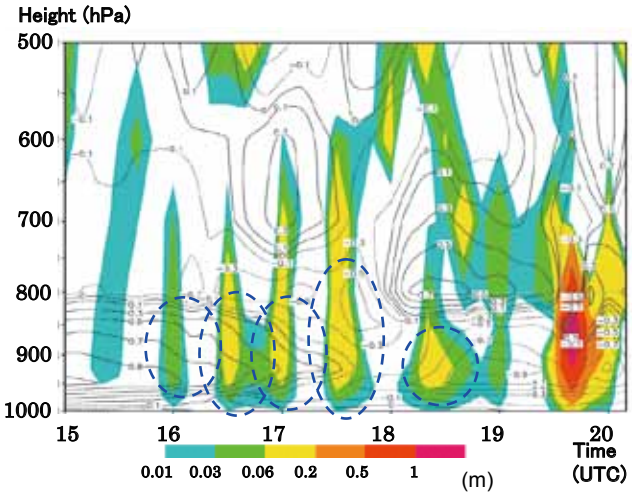

Fig. C-4-4. Time-height diagram of updraft (colored region) and deviation of temperature from temporal average (contours) along the dotted line of Fig. C-4-3(a).

edge of the cold pool, the temperature decreased and the dew-point deficit became smaller (Figs. C-4-5a and d) and convection cells B were then generated. This sequence of events was similar to, but slower than, the events in the case of convection cells A.

C-4-4. Summary

We used convection cells reproduced from the analyzed fields by the high-resolution 3-dimensional nonhydrostatic model to investigate the generation and development mechanisms of convection cells in the tropical region. The results are summarized as follows:

(1) Updrafts from low-level gravity waves made the lower atmosphere cooler and moister and may trigger the generation of convection cells.

(2) When updrafts from low-level gravity waves overlapped with other weak updrafts caused by large-scale convergence or weak cold pools, convection cells were generated. Low-level gravity waves can generate or develop new convection cells if other weak updrafts exist. This result means that the origin and timing of convection cells are influenced by gravity waves.

(3) These results are consistent with those of YS92.

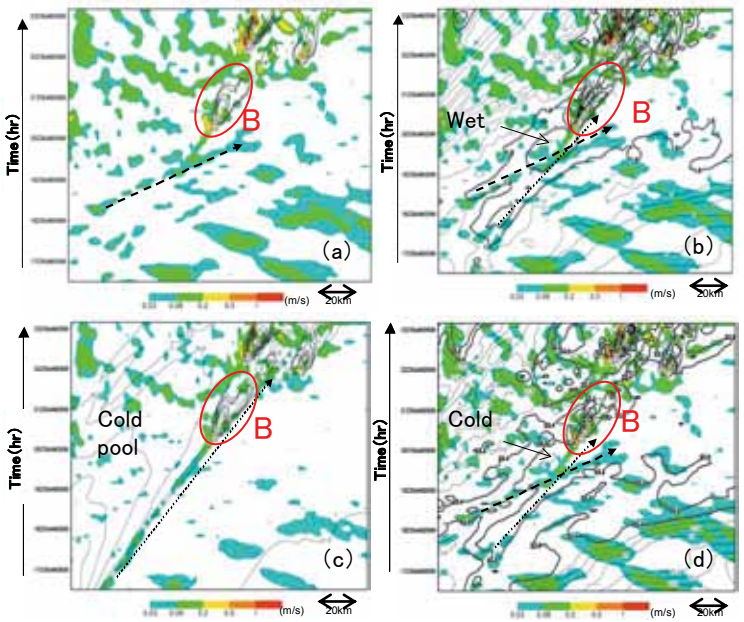

Fig. C-4-5. Hovmöller diagrams of updrafts (colored region) at (a,b and d) P=950 hPa and (c) 975hPa along the broken line in Fig. C-4-2(c), (a) rainfall (b) dew-point deficit at P=950hPa, (c) temperature at P=1000hPa and (d) temperature at P=950hPa.

C-5. Tests of cumulus schemes in JMA-NHM over Southeast Asia[1]

The JMA nonhydrostatic model (NHM) was implemented in Southeast Asia in short-term forecasts of up to 18 h over one year with 25 km horizontal resolution. Three cumulus schemes were tested in the model: Kain-Fritsch, Grell and Arakawa-Schubert. Diagnosis of bias and correlation coefficients of rainfall shows that the Grell scheme performed the best and Arakawa-Schubert performed the worst.

C-5-1. Introduction

NHM (Saito et al. 2006) is an operational weather forecast model developed originally for applications in Japan. To adapt it to weather forecasting in Southeast Asia, we first need to verify its performance in tropical regions. We conducted experiments using three cumulus schemes (Kain-Fritsch, Grell, and Arakawa-Schubert) in NHM to identify which scheme is more suitable to forecast weather in Southeast Asia.

C-5-2. Experimental Design

We integrated JMA-NHM version 2010-May-10 for one year from 0000 UTC 1 January to 2300 UTC 31 December 2004. Because neither El Ninõ nor La Ninã occurred in this year, modeling errors associated with these inter-annual anomalies should be small in the experimental period. We conducted three experiments in which the cumulus scheme was respectively Kain-Fritsch (tuned for Japan region, Saito et al. 2006), Grell, and Arakawa-Shubert. Because neither data assimilation nor Spectral Boundary Coupling (SBC, e.g., Kida et al. 1991) were used, we only examined experiments initialized at 0000 and 1200 UTC with short-term forecasts (e.g., Hayashi et al. 2008) of 18 h where the first 6 h were discarded as model spin-up.

The model resolutions were 25 km horizontally and 40 layers vertically and the grid size is 160×120 points with the domain center at lat 4°N, long 110°E. The time step is set to be 75 s. We used Japan 25-year Re-Analysis data (JRA25) as initial and boundary conditions.

C-5-3. Results

To verify the results of the NHM simulations, we compared rainfall amounts from the model with satellite-derived data from Tropical Rainfall Measurement Mission (TRMM) version 3B42. This was because the conventional weather observation network in Southeast Asia is too sparse to capture mesoscale convective systems at time-scales of hours (Koh and Teo 2009).

Statistical verification was carried out based on measures such as bias and correlation. Use of root-mean-square error (RMSE) was avoided as it depends more on the ambient variability of the weather rather than on the model error itself (Koh and Ng 2009).

Figure C-5-1 shows the annual mean rainfall of TRMM satellite data and the bias in rainfall (NHM minus TRMM) under the three cumulus schemes. The distribution of rainfall in TRMM data shows that rainfall concentrated over land areas such as Borneo, the Malay Peninsula, and Sumatra. NHM

[1] S. Koseki and T-.Y. Koh

underestimated precipitation over land with all three schemes. In particular, underestimation of rainfall was greatest around the northwestern coast of Borneo (lat 2°N to 4°N, long 110°E to 114°E). Although the performances of Kain-Fritsch and Grell were identical over land, the Grell scheme showed the best bias performance of the three schemes, because its underestimation of rainfall was relatively small, especially over the sea. The Arakawa-Schubert scheme was worse than the other two schemes. In contrast, NHM overestimated precipitation in inland Borneo, along the southern coast of Sumatra, and over Sulawesi. These overestimations arose partly from a strong sensitivity of rainfall to model topography, as seen in other models (Teo et al. 2011). Another reason is that the diurnal cycle in the study area may not be reproduced sufficiently. Rainfall here is manifested basically in features of the diurnal cycle, such as sea/land breeze circulation.

Figure C-5-2 shows diagrams of monthly correlation coefficients between NHM (N) and TRMM (T), $r = \frac{\mathrm{cov}(N,T)}{\sqrt{\mathrm{var}(N) * \mathrm{var}(T)}}$ for the area-averaged rainfall in six regions: the Malay Peninsula, inland Borneo, coastal Borneo, southern Sumatra, the South China Sea, and the Java Sea. Note that there is some uncertainty in the correlation values associated with comparing 3-hourly time series snap-shots of rainfall in RMM and NHM accumulated rainfall. The Kain-Fritsch and Grell schemes generally showed better performance than the Arakawa-Shubert scheme in all six areas. As the weather patterns in this region tend to be dominated by a strong diurnal cycle of land-sea breeze circulation (Joseph et al. 2008), the correlation coefficients are indicative of how well the model captures the underlying mesoscale dynamics.

C-5-4. Summary

We conducted test experiments of three cumulus schemes in NHM for Southeast Asia. The Grell scheme showed the best performance in short-term forecasts because its bias was smaller than those of the other two schemes. The correlation coefficient for the Grell scheme was comparable to that of the Kain-Fritsch scheme but better than that of the Arakawa-Shubert schemes, which was the worst of three.

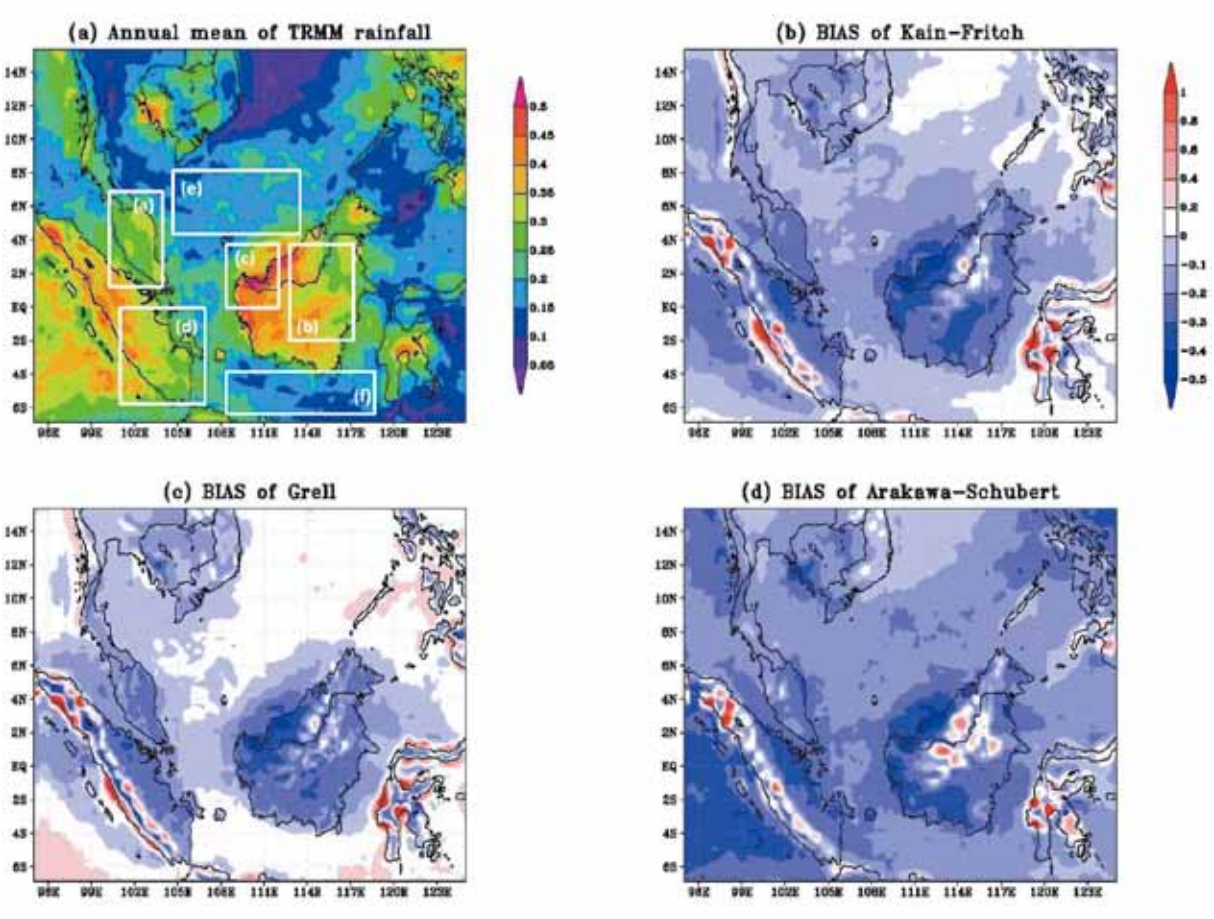

Fig. C-5-1. (a) Annual mean of TRMM rainfall (mm/hr) in 2004. Rectangles are areas where rainfall is averaged in Figure C-5-2. (b)-(d) NHM minus TRMM annual mean rainfall (mm/hr) with the Kain-Fritsch (b), Grell (c), and Arakawa-Schubert scheme (d).

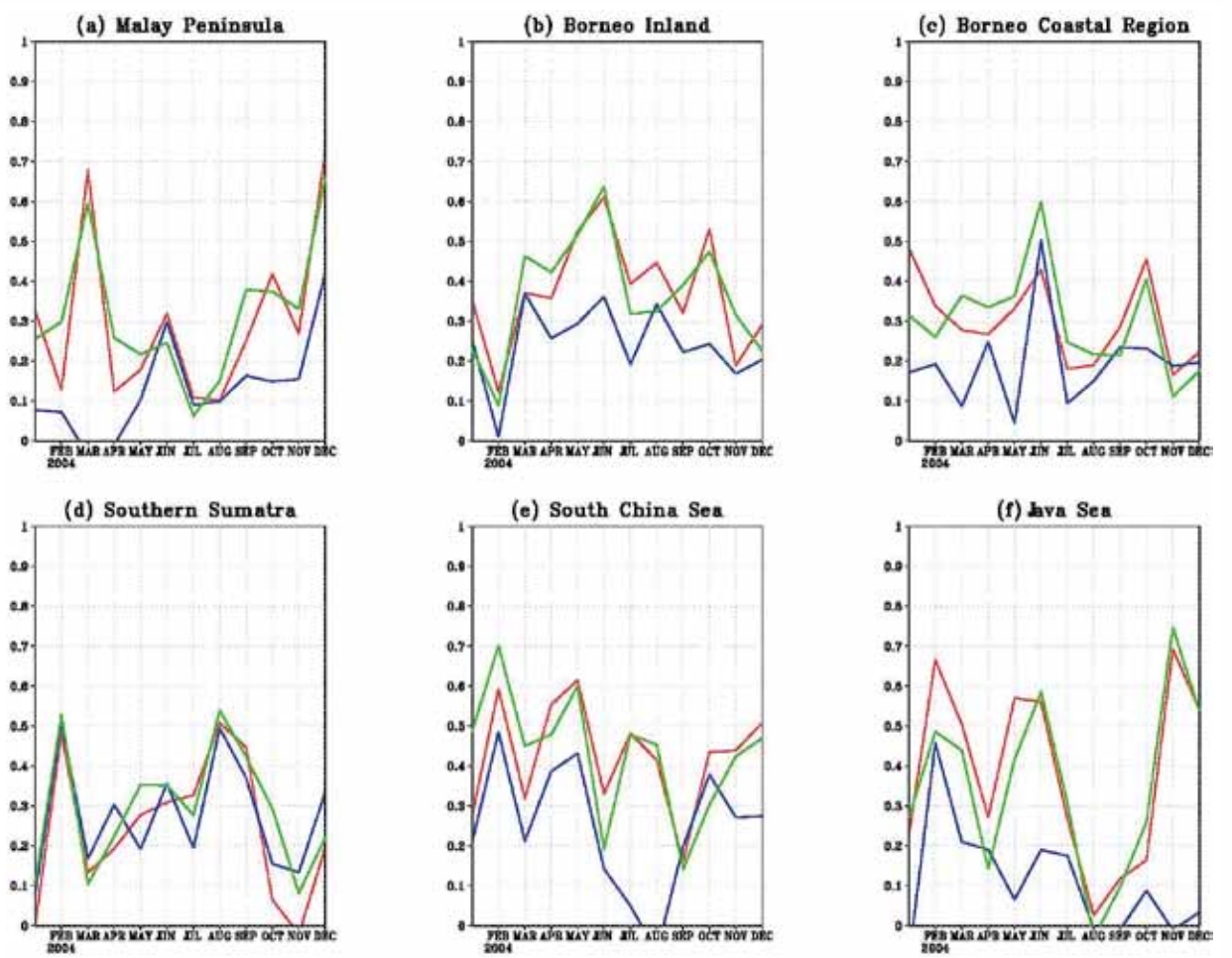

Fig. C-5-2. Monthly correlation coefficients of 3-hourly rainfall between NHM with three schemes and TRMM averaged over the rectangular areas in Figure C-5-1. Red denotes Kain-Fritsch, green denotes Grell and blue denotes Arakawa-Schubert scheme.

C-6. Model verification of HRM, NHM, WRF-ARW, and WRF-NMM in predicting precipitation[1]

C-6-1. Introduction

Numerical weather predictions have been conducted at Vietnam National University of Hanoi (VNU) since 2000 with a mesoscale hydrostatic model named HRM (Majewski, 2009), the former operational limited-area model of the German Weather Service (DWD) that is run at VNU with DWD's permission. With the general shift to nonhydrostatic models, in 2004 VNU started deploying the MM5 model, then the WRF models WRF-ARW (Skamarock et al. 2008) and WRF-NMM (Janjic et al. 2010). When VNU joined the research project "International Research for Prevention and Mitigation of Meteorological Disasters in Southeast Asia," the Meteorological Research Institute of Japan (MRI) provided VNU with a research license for NHM (Saito et al. 2007).

In Vietnam, tropical cyclones and heavy rainfall are the two most severe meteorological disasters. Although VNU uses many models in research, only HRM was applied in forecasting these two events after it was verified for more than two years. Other models were used only for case studies. WRF has shown better performance than HRM in some of these cases, but not in others. To apply a new model for forecasting severe weather phenomena, we need to document its superior skill through a formal comparison (e.g., Hayashi et al. 2008; Chan et al. 2010) with HRM forecasts.

This report documents a performance intercomparison among the four models HRM, NHM, WRF-ARW, and WRF-NMM. Of these models, only HRM is hydrostatic, although the others support hydrostatic options. Our study target was the precipitation forecast for Vietnam in September 2009. This effort was part of a verification project that assesses the performance of all models running in research institutes and operational centers in Vietnam.

C-6-2. Data and method

Because the four models differ in dynamics, physics, and numerical features, it was impossible to use identical configurations for all models. However, we used the same settings for initial and boundary conditions, domains, and resolutions.

First, all models used the same initial and boundary conditions from the Global Forecast System (GFS) analyses and forecasts with a resolution of 0.5°. The boundary condition update interval was 3 h. The sea-surface temperature fields were also taken from the GFS analyses. The constant fields such as topography, land use, and vegetation fraction were derived from the United States Geological Survey (USGS) dataset.

Second, the domain and resolution were nearly the same for all models. NHM and WRF-ARW use Mercator projection, HRM uses regular latitude/longitude projection, and WRF-NMM uses rotated latitude/longitude projection. Figure C-6-1 shows the HRM domain with 201 × 161 grid points; the other models also included this domain but were not limited to it. The resolution of this domain is 0.15°. NHM and WRF-ARW set that resolution to 17 km, which is identical to 0.15° at the equator. Because of its special grid type (Arakawa E), the WRF-NMM resolution was set to 0.11°, which is

[1] L. Duc and K. T. Xin

nearly 0.15° when multiplied by √2. All models had 30 vertical layers.

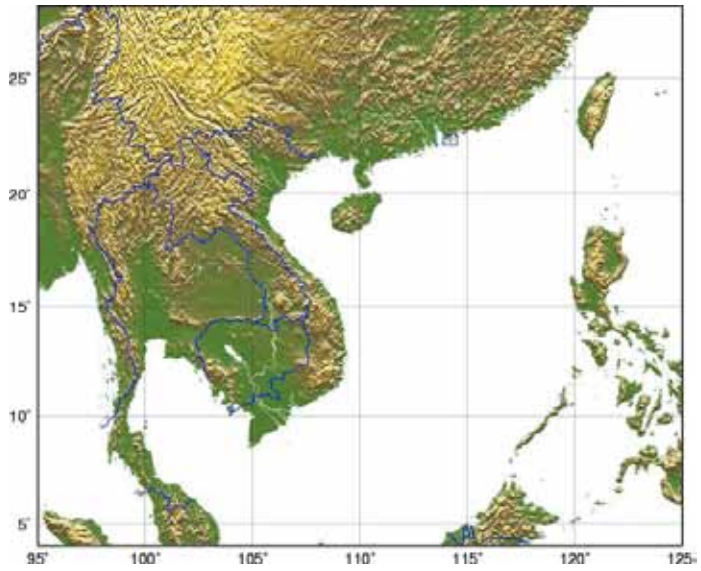

Fig. C-6-1. HRM domain.

The models were targeted to the period September 2009. In this period, tropical cyclones Mujigae and Ketsana hit coastal areas of Vietnam and tropical cyclone Koppu affected all of Vietnam. All models were run out to 48 h. Although the spatial resolutions were nearly the same, the time steps were different. The time steps and other different features are listed in Table C-6-1.

Table C-6-1. Model configurations.

Model	HRM	NHM	WRF-ARW	WRF-NMM
Version	2.4	2008	3.0.1	3.0.1
Time step	90s	40s	90s	40s
Radiation	Ritter and Geleyn scheme	GSM0412	RRTM + Duhia	GFDL
Cumulus parameterization	Tiedtke	Modified Kain-Fritsch	Kain-Fritsch	Betts-Miller-Janjic
Microphysics	Doms and Schattler scheme	6-class	WSM 3-class scheme	Ferrier scheme
Boundary layer	Mellor-Yamada Level 2	Improved Mellor-Yamada Level 3	Yonsei University scheme	Mellor-Yamada-Janjic TKE
Soil model	Heise and Schrodin 7- layer scheme	Thermal diffusion 4-layer scheme	4-layer Noah LSM	4-layer NMM LSM

Precipitation verifications were conducted using ground observations. There are about 400 rain gauges yielding an average resolution of 28 km over Vietnam. As Cherubini et al. (2002) pointed out, for matching spatial scales, upscaled observations should be used instead of point observations such as SYNOP stations; thus, verification on the model space was adopted. The three-pass Barnes scheme (Achtemeier, 1989) was used to upscale rain gauge data into a regular latitude/longitude grid that is a subdomain of the HRM domain covering Vietnam. Precipitation forecasts from the four models were mapped to the observation grid using interpolation to the nearest grid point. Because all models have nearly similar domains and resolutions, this strategy did not distort rainfall patterns or spread out rain fields.

C-6-3. Results

The total accumulated 24-h (first day) rainfall forecasts in September 2009 are shown in Figure C-6-2 along with rainfall observations. The rainfall pattern was well forecasted by HRM. NHM and WRF-NMM also represented this pattern, but these two models underestimated the rainfall amount. WRF-ARW showed a false alarm area south of the rainfall peak in central Vietnam.

The bias and equitable threat scores (ETS) against rainfall thresholds (Fig. C-6-3) show that WRF-ARW overestimated and HRM and NHM underestimated precipitation at all thresholds. NHM bias scores were higher than those for HRM. The WRF-NMM bias score decreased rapidly with rainfall thresholds, indicating that the model predicted more light rain and less heavy rain than observations. In terms of ETSs, WRF-NMM is the worst model and HRM is the best one. However, for thresholds less than 20 mm/day, HRM, NHM, and WRF-ARW have the same performance. HRM only beats other models for heavy rains with thresholds exceeding 25 mm/day.

Figures C-6-4 and C-6-5 show results for forecasts in the range of 24–48 h (second day). Second-day forecasts were much like those for the first-day forecasts, with some minor differences. HRM is still the best model and WRF-NMM the worst, although ETS values were less than those for the first-day forecasts. The underestimation of HRM and NHM was the same; however, the HRM bias was closer to 1 than the NHM bias, the reverse of the situation for the first-day forecasts.

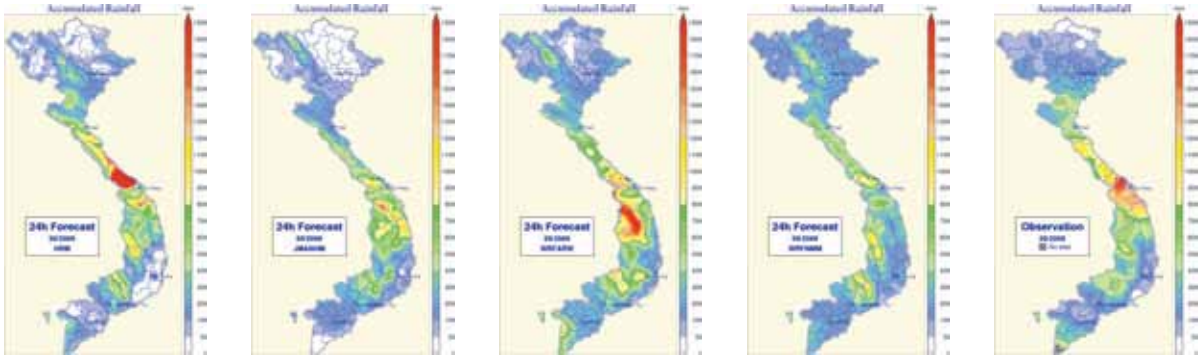

(a) (b) (c) (d) (e)

Fig. C-6-2. Total accumulated rainfalls in 09/2009 as forecasted by (a) HRM, (b) NHM, (c) WRF-ARW and (d) WRF-NMM for the first day and (e) observation.

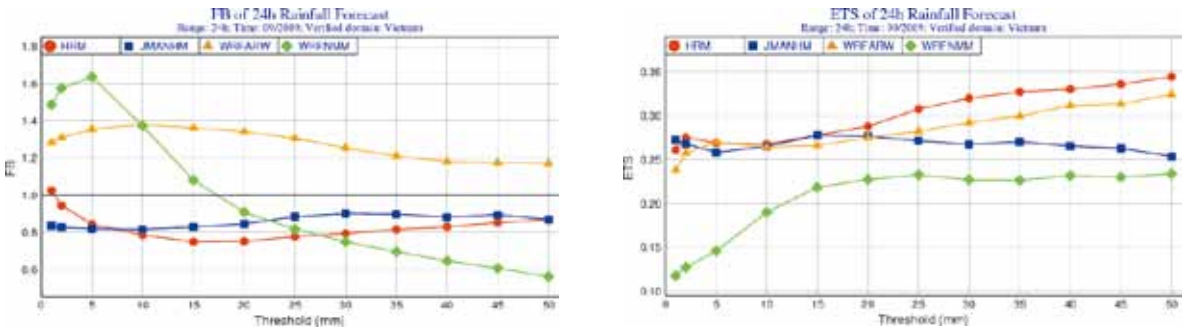

Fig. C-6-3. Bias and equitable threat scores for the first day rainfall forecasts from HRM, NHM, WRF-ARW and WRF-NMM.

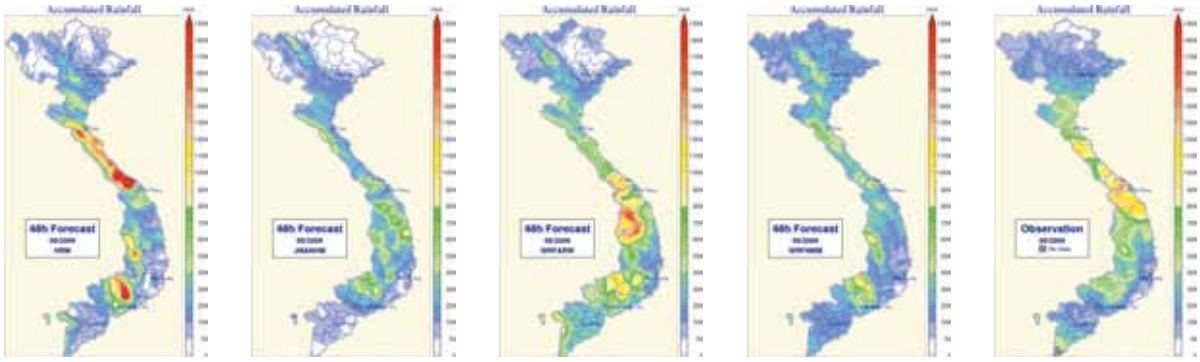

(a) (b) (c) (d) (e)

Fig. C-6-4. The same as Fig. C-6-2 except for the second day forecasts.

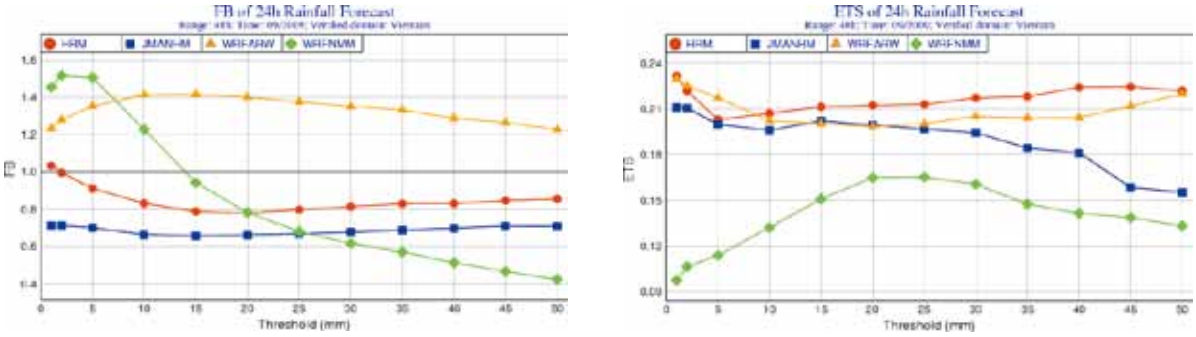

Fig. C-6-5. The same as Fig. C-6-3 except for the second day forecasts.

C-6-4. Conclusion

We compared the performance in precipitation forecasts from the four models HRM, NHM, WRF-ARW, and WRF-NMM using GFS analyses and forecasts as initial and boundary conditions, respectively. The resolutions were almost the same, approximately 0.15°. Differing model projections made the domains for each model different, but domains were chosen to minimize the impact of different domains on forecasts. The period of September 2009 was selected, when three tropical cyclones affected Vietnam.

The forecasts were verified against rain gauge data over Vietnam. In the first step, all observations were mapped to an analysis grid covering Vietnam at a resolution of 0.15° by the three-pass Barnes

scheme. For the next step, rainfall forecasts were interpolated to the analysis grid by the nearest point method. Then, verification was done on the analysis grid.

The results highlighted HRM as the best model and WRF-NMM as the worst. HRM tended to underestimate precipitation, as did NHM. WRF-ARW overestimated precipitation for the whole range of rainfall thresholds. Models HRM, NHM, and WRF-ARW exhibited similar performances for light and moderate rains. HRM was the best at predicting heavy rainfall.

The most interesting result is that the performance of a hydrostatic model (HRM) was better than those of nonhydrostatic models. However, at 0.15° resolution, the difference was small. To have a fair comparison, a higher resolution experiment (0.04° or 0.05°) should be conducted. As a hydrostatic model, HRM is only adequate for resolutions lower than 7 km. In this case, HRM must be excluded from the comparison. In a tropical region like Vietnam, convective processes have an important role in generating precipitation. Using high-resolution models will improve forecasts for convective rains.

We note that none of the models in this experiment was adapted for tropical regions; they were all developed and first applied in extratropical countries. NHM underestimated the diurnal change of surface temperatures, which we attribute to the inappropriate application of the nonlinear computational diffusion to the number concentration of cloud ice (see Section C-2-5).

C-7. A Numerical Experiment on the Heavy Precipitation during the Jakarta Flood Event in January-February 2007[1]

C-7-1. Introduction

A devastated flood event had occurred at Jakarta on February 2007, which was mainly due to heavy rainfall for several times from 31 January to 2 February. According to the Indonesian Meteorological, Climatological, and Geophysical Agency (BMKG) report, the highest daily rainfall was 340 mm, which was measured on 2 February at Pondok Betung Station (6.2°S, 106.6°E). Torrential rains that repeatedly occurred over West Java coincided with a strong and persistent trans-equatorial monsoon surge from the Northern Hemisphere (Wu et al. 2007). The strong monsoon flow near the surface and the upper southeasterly wind over it produced a low-level vertical shear of winds. The shear with wet lower and dry middle layers allowed the severe moist convections to develop repeatedly.

In this study, a time-lagged ensemble forecast (e.g., Branković et al. 1990) is performed for the two-month period including the Jakarta Flood event with a regional model which consists of a single domain with a relatively coarse resolution. Based on the ensemble forecast data, we investigate the temporal modulation of precipitation and three-dimensional synoptic fields in the periods before, during, and after the heavy rainfall in Jakarta in 2007.

C-7-2. Numerical Experimental design

The numerical model used in this study is Japan Meteorological Agency - non-hydrostatic model (NHM; Saito et al. 2006, 2007). We set up a single computational domain with a 20-km horizontal resolution. The domain has 103 × 115 grid points centered at 5°S, 110°E on a Mercator projection. The topography of the domain is presented in Fig. C-7-1. The subgrid scale parameterization schemes and parameter settings that we employ are the same as those of Hayashi et al. (2008) with their recommended values tuned for the 20-km horizontal resolution. The cumulus parameterization scheme is a modified Kain-Fritsch. The cloud microphysics scheme is a 6-class bulk microphysics with prediction of number concentration of ice particles. The GSM0412 radiation scheme (Yabu et al. 2005) and an improved Mellor-Yamada Level 3 planetary boundary layer scheme (Nakanishi and Niino 2004, 2006) are used. The National Centers for Environmental Prediction Global Tropospheric Analyses (final analyses) with the horizontal resolution of 1° × 1° and the time interval of six hours are used for the model input.

To run the time-lagged ensemble forecast, we follow the same procedure and method used by Mittermaier (2007), except for the length of individual forecast. We perform 72-hour forecasts every 6 hours, and exclude the initial 18 hours for analysis to avoid the effect of unrealistic convections in the spinup processes. Thus, the number of ensemble members becomes nine. We analyze the two-month period (twelve pentads) from 0000 UTC 1 January to 2300 UTC 1 March 2007. We use Tropical

[1] N.J. Trilaksono, S. Otsuka, and S. Yoden

Rainfall Measuring Mission (TRMM) 3B42 (Huffman et al. 2007) as comparison data with the model output.

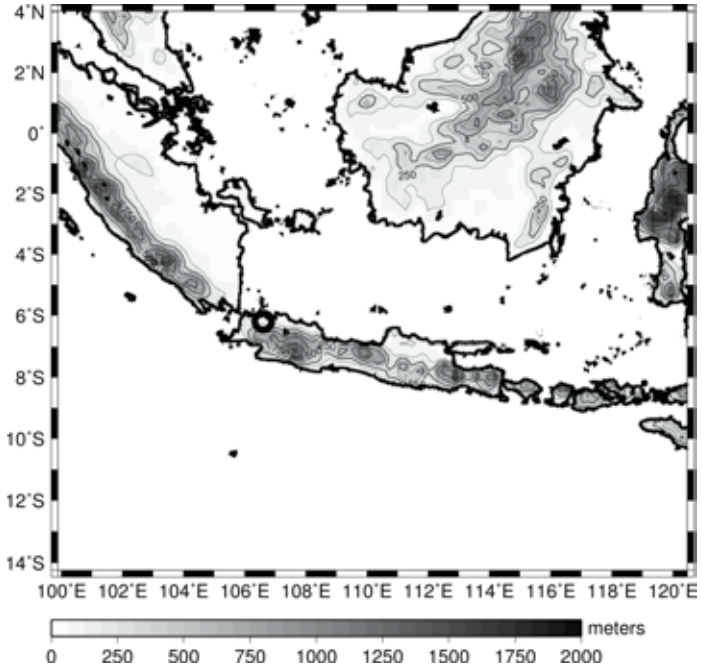

Fig. C-7-1. The model domain of computation. Shading and contours show topography (m) of the domain. The open circle denotes the location of Pondok Betung Station. 'After Trilaksono et al. (2011)' with some modifications.

C-7-3. Results of the experiment

Figure C-7-2 shows the time series of (a) the TRMM estimated rainfall, (b) the model simulated precipitation rate of the nine ensemble members, and (c) their ensemble mean in the unit of mm hr^{-1} at the nearest data point to the Pondok Betung Station for the two-month period. The location of Pondok Betung is denoted by the open circle in Fig. C-7-1. The characteristic time scale of the precipitation rate is generally small (less than one day) suggesting a convective origin, as shown by the TRMM data (Fig. C-7-2a). This feature of convective precipitation is well reproduced in the model. Some ensemble members show heavy precipitation (> 10 mm hr^{-1}) during or just after the period of Jakarta Flood event (Fig. C-7-2b). Such enhancement of precipitation is also discernible in ensemble average (Fig. C-7-2c), although the magnitude is much smaller. Both the TRMM data and the model results show modulation of precipitation rate in the two-month period. There is little rainfall observed during the first half of January, whereas rainfall occurs frequently afterward.

Figure C-7-3 shows the time-latitude cross sections of (a) the TRMM estimated rainfall data and (b) the ensemble mean of the model simulated precipitation rate averaged between 105.5°E - 108.5°E. The horizontal lines in Figs. C-7-3a and b denote the latitude of 6.2°S, which is the latitude of Pondok Betung Station in the northern part of Java Island. The TRMM data (Fig. C-7-3a) shows that in the first half of January, continual precipitation exists between 2°S and 5°S, whereas intermittent rainfall with an interval of about one week exists to the north of 2°S.

There is little rain to the south of 5°S during the period. The meridional extent of heavy rainfall occurrence varies after around 17 January. Before the Jakarta Flood event, a signal of heavy rainfall propagates from 4°N around 25 January to 6°S around 30 January. After the signal reaches the

northern part of Java Island, it does not propagate any farther. The meridional extent of rainfall concentrates in the latitude between 5°S and 8°S from around 30 January to 15 February. Right after 15 February, it becomes larger with higher rain rate to the south of 6°S.

The ensemble mean of the model output precipitation rates (Fig. C-7-3b) resembles that of the TRMM data. The north-south contrast of precipitation before around 17 January is reproduced well in the model. Propagation of a signal of heavy rainfall just before the Jakarta Flood event is also reproduced well. The meridional extent of precipitation is somewhat larger in the ensemble mean from 31 January to 8 February. Modulation of intermittent precipitation to the south of 6°S in the second half of February is also reproduced well.

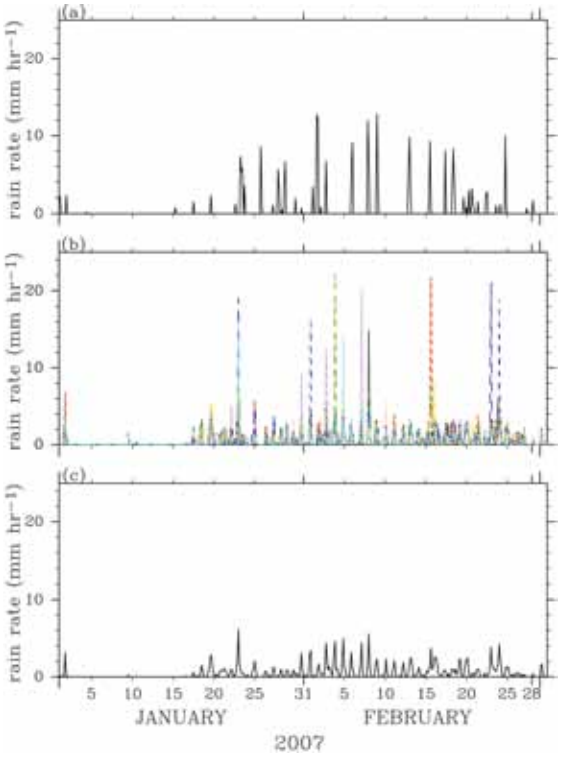

Fig. C-7-2. Time series of (a) the TRMM estimated rainfall, (b) the model simulated precipitation rate of the nine ensemble members, and (c) their ensemble mean in the unit of mm hr^{-1} at the nearest points to the Pondok Betung Station for the two-month period from 0000 UTC 1 January to 2300 UTC 1 March 2007. The location of Pondok Betung station is denoted by the open circle in Fig. C-7-1. 'After Trilaksono et al. (2011).'

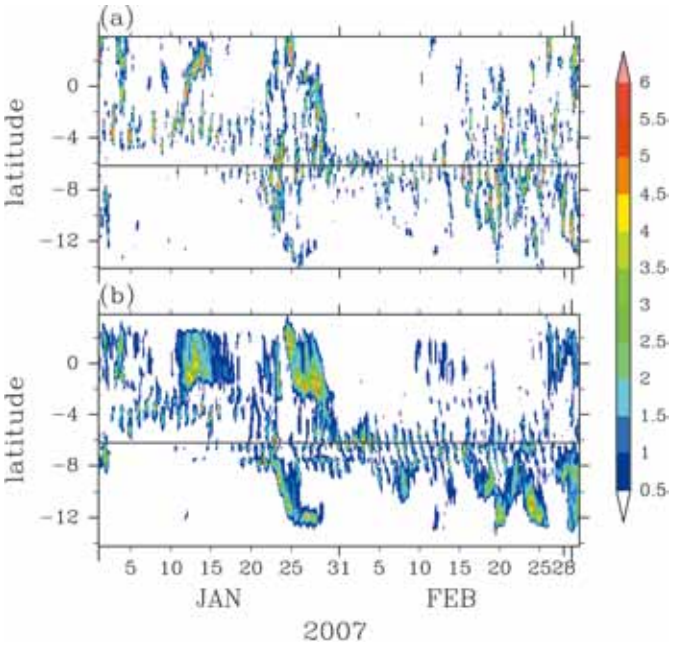

Fig. C-7-3. Time-latitude cross sections of (a) the TRMM data and (b) the ensemble mean of the model simulated precipitation rate averaged between 105.5°E – 108.5°E. The horizontal lines in (a) and (b) denote the latitude of 6.2°S which is the latitude of Pondok Betung station. 'After Trilaksono et al. (2011).'

Figure C-7-4a shows the time-latitude cross section of the ensemble mean of the model simulated meridional wind anomaly. It shows that there is positive (northward) wind anomaly in most of the latitudes in the first 20 days of January. Propagation of a signal of negative anomaly of the meridional winds is evident from 4°N on 27 January to 6°S on 29 January, which corresponds to the propagation of a signal of precipitation in Fig. C-7-3. The negative anomaly of meridional winds continues about one week at 6°S during and after the Jakarta Flood event. Another event of the propagation of negative meridional wind anomaly is seen from 4°N on 22 January to 14°S on 24 January with some correspondence to the enhancement of precipitation shown in Fig. C-7-3b.

A cold anomaly persists from 29 January to 4 February during and after the Jakarta Flood event around 6°S (Fig. C-7-4b). It is related to the cold anomaly propagation from the north associated with the propagation of negative meridional wind anomaly before the initial date as described above. The association of the cold anomaly with the northerly anomaly is indicative of a cold surge event. Continuation of the cold surge reaches 12°S on 29 January and the south end of the computational domain on 3 February. Note that there is no evidence of the cold anomaly around 22 January that corresponds to the strong negative meridional wind anomaly. This is a surge event but not a cold surge event. Larger variability of temperature anomaly exists to the south of Java Island for the two-month period, in which cold (warm) anomaly dominates during January (February).

Time-latitude variations of relative humidity (Fig. C-7-4c) shows similar pattern with those of the precipitation shown in Fig. C-7-3b. The period of late January to early February is also marked by a moist condition near the surface (at 850 hPa) with value of relative humidity exceeding 96% over the northern part of Java Island.

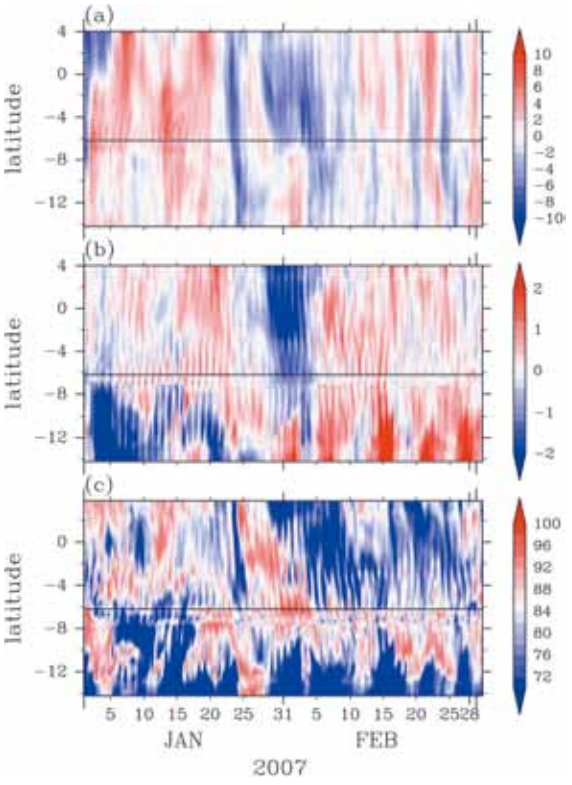

Fig. C-7-4. Same as Fig. C-7-3 except for the ensemble mean of the model simulated (a) meridional wind anomaly (m s^{-1}), (b) temperature anomaly (°C), and (c) relative humidity (%) at 850 hPa. Here, we define an anomaly as a deviation from the two-month average. 'After Trilaksono et al. (2011).'

Figure C-7-5 shows the horizontal distributions of the ensemble mean of the model simulated precipitation rate (shades) and horizontal winds at 850 hPa (arrows) averaged for each pentad. Here, we only show six pentads, pentad 3 - 8, including pentad 7 (31 January - 4 February) in which the heavy rainfall event occurred in Jakarta. In pentad 7, a zonally elongated rain band is formed around 106°E - 119°E, 5°S - 6°S. In that period, Jakarta is located at the western edge of the rain band. There is small amount of rainfall to the north and south of the rain band. The rain band in pentad 7 is consistent with the increase of convergence of horizontal winds at 850 hPa (not shown).

A cold surge is captured through pentad 5 - 7. In pentad 5, a typical Borneo vortex appears; the northeasterly winds over the South China Sea change their direction to southeastward over and around Sumatra Island, and the wind is roughly eastward over West Java. In pentad 6, eastern part of the vortex disappears, and further deformation of the vortex continues. In pentad 7, the winds over the South China Sea become almost northerly. The wind speed increases near West Java and the northerly component increases from pentad 6 to pentad 7. The northerly component of surface wind intensifies upward motion on the northern slope of the mountain range in West Java. The surge event terminates in pentad 8.

In association with the modulation of horizontal wind field, the horizontal distribution of heavy precipitation changes from pentad to pentad. In pentad 5, weak precipitation less than 1 mm hr^{-1} covers middle and northern parts of the computational domain with some intensification over the South China Sea. In pentad 6, heavy precipitation areas appear over the South China Sea and the Java Sea. In pentad 7, the former area disappears while the latter moves southward to form the zonally elongated rain band. The rain band disappears in pentad 8.

C-7-4. Discussion

The Borneo vortex is centered at (1°S, 111°E) in pentad 5, in which precipitation over West Java is relatively weak. Another Borneo vortex event is also captured by the model in pentad 3 (11 - 15 January, Fig. C-7-5a), when the heavy precipitation occurred in the southern tip of Malay Peninsula which faces the South China Sea, as reported by Tangang et al. (2008). Strong convergence associated with a northeasterly cold surge exists over a tip of Malay Peninsula during the event. Although Tangang et al. (2008) argued that this was not a vortex event, based on reanalysis data with the 2.5° × 2.5° resolution, our model output with the 20-km resolution shows the existence of the vortex.

In pentad 7, on the other hand, the vortex disappears, during which the heavy rainfall occurred at Jakarta. This is consistent with the fact that the regions to the south of the South China Sea (namely, the Java Sea) experience enhanced convection when the Borneo vortex is absent (Chang et al. 2005).

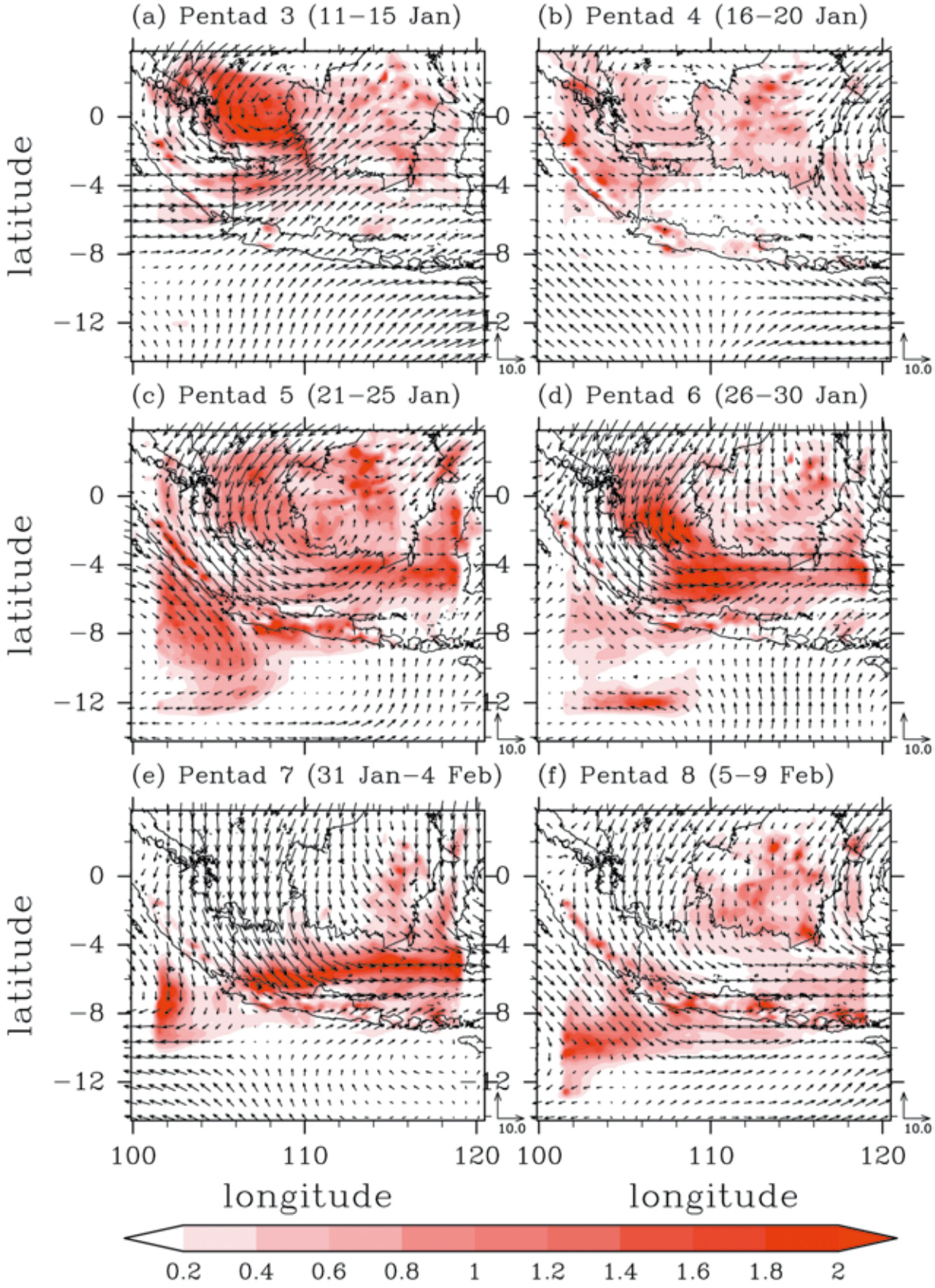

Fig. C-7-5. Horizontal distribution of the ensemble mean of the model simulated precipitation rate (mm hr^{-1}) and horizontal winds (m s^{-1}) at 850 hPa averaged for each pentad. Unit vectors are shown on the right bottom corner in each plot. 'After Trilaksono et al. (2011).'

C-7-5. Conclusions

A time-lagged ensemble forecast using a regional numerical model is employed to investigate the modulation of precipitation over West Java in the two-month period of January-February 2007. Comparison between the numerical results and the TRMM 3B42 data shows fundamental agreement on the temporal modulation of the spatial distributions of precipitation as shown in Figs. C-7-2 and C-7-3 including the enhancement of precipitation on the time scale of pentad during the period of heavy rainfall, from 31 January to 4 February, in the Jakarta Flood event.

In addition to the modulation of meridional winds reported by Wu et al. (2007), modulation of temperature and relative humidity is also shown in this study. During the two-month period, several monsoon surges are observed, among which only the surge event during the Jakarta Flood event is associated with the cold anomaly. The event is preceded by the Borneo vortex event shown in Fig. C-7-5c. We have shown pentad-to-pentad modulation of synoptic fields of precipitation and only pentad 7, which includes the Jakarta Flood event, has the banded structure of heavy precipitation to the north of Java Island (Fig. C-7-5e).

C-8. Simulation of low level cloud over the Western Ghats using a non hydrostatic model[1]

C-8-1. Introduction

The Western Ghats mountain range along the western coast of India, with an average elevation of about 1200 m, is important for providing sites for hydroelectric power generation. Western India has faced water shortages for many years from lack of rainfall. Artificial rainfall from cloud seeding is one possible solution. To explore this option to enhance rainfall over western India, a series of numerical experiments have been carried out using the high-resolution JMA nonhydrostatic model NHM (Saito et al., 2006). This study simulated the total cloud cover and cloud height at different times of day.

C-8-2. The model and simulation of cloud

NHM was installed on the C-MMACS multiscale forecasting platform. The model explicitly calculates the microphysical processes of hydrometeors such as cloud water, rain, and cloud ice. The typical high-resolution NHM configuration for cloud simulation includes a Lambert conformal mapping, time splitting gravity waves, and split-explicit sound waves. A bulk parameterization scheme that forecasts both the mixing ratio and number concentration is applied to the hydrometeors. The calculation domain of the 5 km NHM was 2500 × 2000 km covering India. The top height of the model domain was about 22 km and employed 40 variable vertical layers. The time integration for up to 48 h was conducted with a time step of 30 s. The NCEP-GFS forecast and analysis were used for initial and boundary conditions.

Figure C-8-1 represents the daily mean cloud coverage simulated 48 h in advance with a resolution of 20 km. The high-resolution (5 km) cloud coverage simulations over the Western Ghats are presented in Figure C-8-2. The three panels represent the simulations at 0500,1200, and 1700 IST on 14 July 2009.

[1] K.C. Gouda and P. Goswami (CSIR C-MMACS)

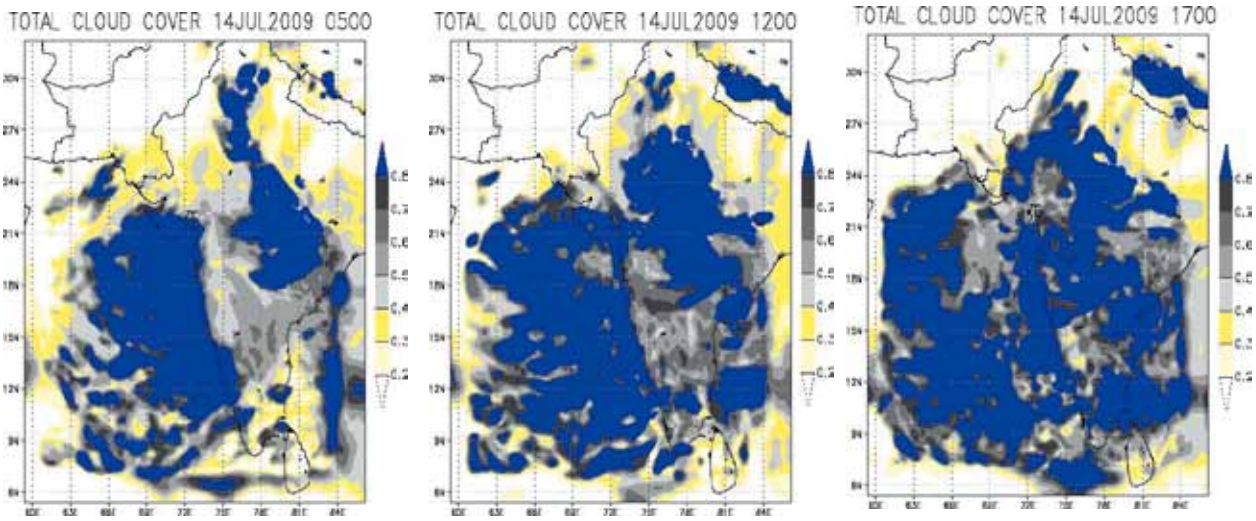

Fig. C-8-1. Cloud coverage simulated 48 h in advance at 0500, 1200, and 1700 IST on 14 July 2009 with a resolution of 20 km.

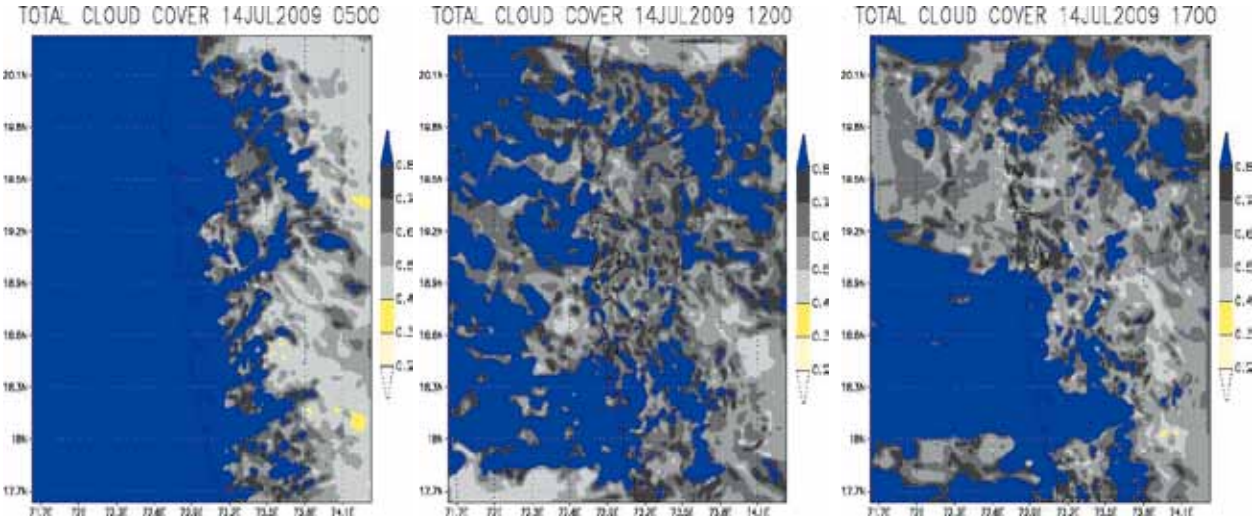

Fig. C-8-2. Cloud coverage simulated 48 h in advance at 0500, 1200, and 1700 IST on 14 July 2009 with a resolution of 5 km over the Western Ghats.

C-8-3. Validation of simulated cloud

A comparison of cloud cover over India from the NHM simulation and MODIS observations for three different days is presented in Figure C-8-3. The simulations are at 20 km resolution, while the observations are at 150 km resolution. The spatial structure of cloud coverage is well captured by the model over the Western Ghats.

The present study needs to be supplemented by extensive diagnostics to understand the effects of high resolution on the simulation of orographic clouds over the Western Ghats. The introduction of high resolution significantly changes model dynamics, and analysis of the circulation features is likely to yield significant insights. The significantly higher skill of the NHM configuration sets the stage for a more detailed diagnostics in terms of cloud coverage. An exciting possibility is to conduct more simulations with different temporal and spatial resolutions and for different seasons to test the robustness of the model in simulating cloud properties.

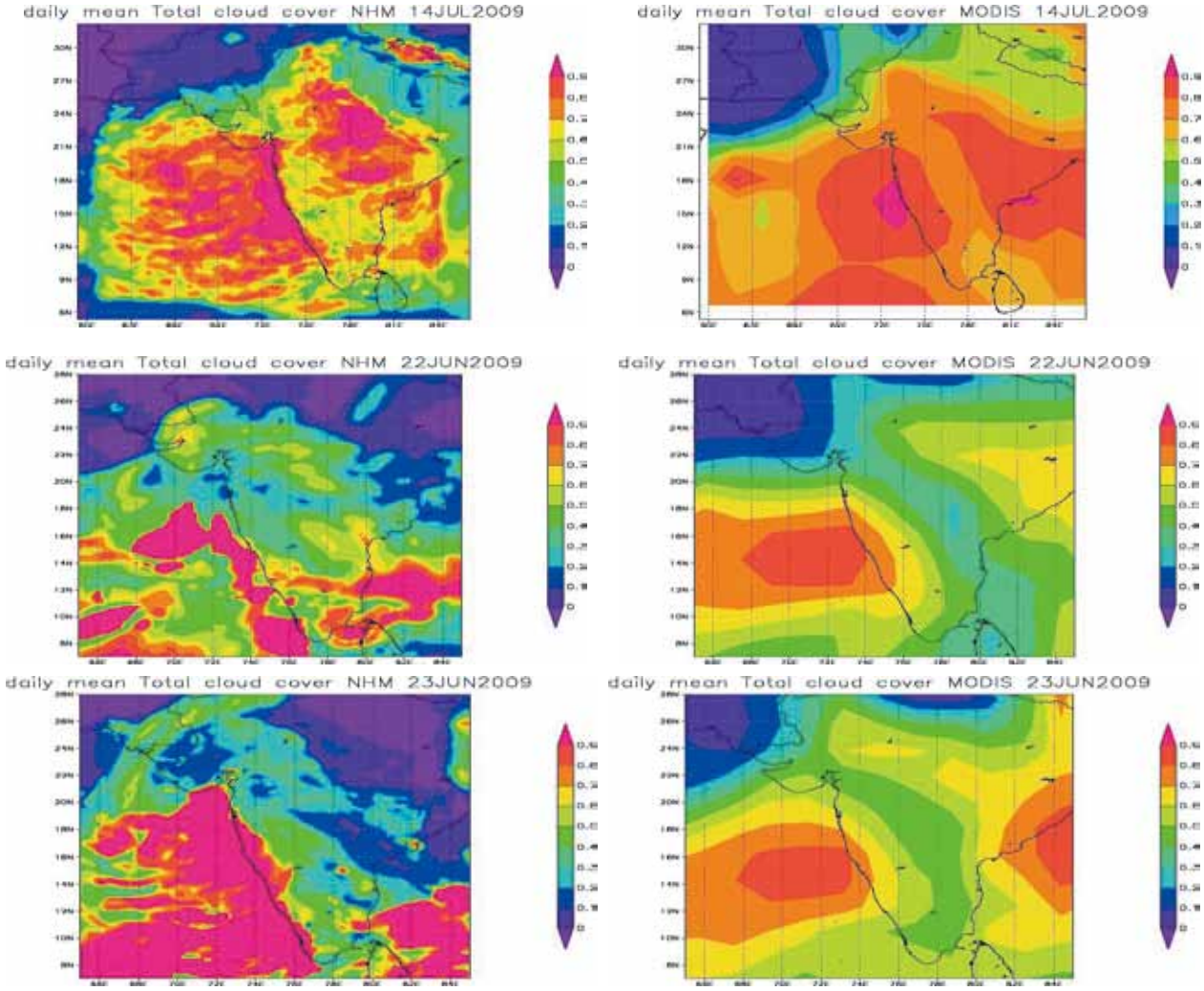

Fig. C-8-3. Comparison of simulated (left) and observed (right; MODIS) daily mean total cloud cover over India on selected days.

C-8-4. Conclusion

Success in cloud seeding critically depends on the ability to determine the window of opportunity as well as the right direction of seeding. It is also necessary to generate quantitative knowledge about the response of local cloud systems to different seeding conditions in a cost-effective manner. Simulation and forecasting thus may transform cloud seeding to a precision exercise from what would be otherwise simply blind shooting. With our emphasis on orographic clouds, we have first focused on simulating clouds over the Western Ghats. We found that the present configuration of NHM yields a good cloud simulation over the Western Ghats. Various sensitivity studies of the effect of cloud seeding experiments need to be conducted in NHM.

D. Numerical experiments for tropical cyclones

D-1. Forecast experiment with a nonhydrostatic model and simulation of storm surge on cyclone Nargis[1]

D-1-1. Introduction

Severe meteorological phenomena such as tropical cyclones (TCs) sometimes cause catastrophic damage to human society; therefore, their prediction is significantly important for preventing and mitigating meteorological disasters. In the areas around the Bay of Bengal, historically, there have been several cases in which storm surges induced by TCs gave rise to severe floods (Webster 2008). At the end of April 2008, cyclone Nargis was generated in the center of the bay and moved eastward in contrast with typical northward motion of cyclone of the bay such as the 1970 Bohla cyclone or the 1991 Bangladesh cyclone. Nargis reached its maximum intensity of category 4 around 06–12 UTC on 2 May, then it made landfall in southern Myanmar, and caused a destructive storm surge over the Irrawaddy Delta and other low-lying areas that claimed more than one hundred thousand lives. Figure D-1-1 shows the development of Nargis estimated by the Regional Specialized Meteorological Center (RSMC) New Delhi and the US Navy Joint Typhoon Warning Center (JTWC). The minimum center pressure by JTWC was 937 hPa, while the RSMC New Delhi estimated its intensity as 962 hPa. For disaster prediction and mitigation in these areas, forecasts of TCs and the associated storm surges based on numerical weather prediction (NWP) are particularly important. In this study, numerical simulations of the 2008 Myanmar cyclone Nargis and the associated storm surge were conducted using the Japan Meteorological Agency (JMA) Nonhydrostatic Model (NHM; Saito et al. 2001; Saito et al. 2006) and the Princeton Ocean Model (POM; Blumberg and Mellor 1987). The JMA operational global analysis (GA) and the global spectral model (GSM) forecast have been operated, but they underestimated Nargis' intensity probably due to its coarse horizontal resolution (T213) or inaccuracy of initial conditions. We show that downscale experiments by NHM using GA and GSM forecast data reproduced the development of Nargis more properly as bellow. This work also aims to demonstrate the applicability of downscale NWP in Southeast Asia and to propose a decision support for preventing and mitigating meteorological disasters, in view of the recent situation that the numerical simulation models and the data are available and accessible to registered users in Southeast Asia as shown in Section E-3.

D-1-2. Cyclone forecast experiments

NHM forecast experiments with a horizontal resolution of 10 km were conducted with using GA and GSM forecast data as the initial and the lateral boundary conditions, respectively. The model domain is a square of 3400 km size (1˚S-30˚N, 73˚E-107˚E) which covers the Bay of Bengal and the surrounding areas including Myanmar (Fig. D-1-2). We assumed a minimum lead time of two days before the landfall in order to effectively mitigate Nargis' storm surge damage and set the initial time of our simulation as 12 UTC on April 30 2008, when Nargis started its eastward movement and one

[1] T. Kuroda, K. Saito, M. Kuni and N. Kohno (JMA)

day before its rapid development. As a result, the minimum sea-level pressure of the experiment was 974 hPa while that of GSM was 993 hPa (Fig. D-1-3), which implied that NHM could predict Nargis' rapid development more accurately than GSM. The higher resolution of NHM contributed to the better representation of the cyclone center. Another possible cause is the difference in the physical processes, especially the convective parameterization schemes. The Kain–Fristch (K–F) scheme (Kain and Fritsch 1993) employed in NHM tends to heat the atmosphere at lower levels than does the Arakawa-Schubert (A-S) scheme in GSM (Shindo et al. 2008), which would enhance the intensification of Nargis. With respect to the cyclone center position at the landfall time, positional lag of NHM (124 km) was smaller than that in GSM (193 km), although the forecasted track of NHM deviated northwardly from the best track. The maximum surface wind speed predicted by GSM was less than 20 m/s, while that predicted by NHM was more than 30 m/s. Moreover, the NHM forecast well captured Nargis' characteristics of the compact central dense overcast (CDO) with spiral rainbands to the west and south observed by the Tropical Rainfall Measuring Mission's Microwave Imager (TRMM/TMI) (Fig. D-1-4).

Sensitivity experiments were conducted to investigate the effects of ice phase, sea surface temperature (SST), and horizontal resolutions to Nargis' rapid development. In a warm rain experiment, Nargis developed earlier and the eye radius became larger than the case with ice phase. As for the SST experiment, it was shown that a high SST anomaly preexistent in the Bay of Bengal led to the rapid intensification of the cyclone, and that SST at least warmer than 29 °C was necessary for the development seen in the experiment. In a simulation with a horizontal resolution of 5 km, the cyclone exhibited more distinct development and attained a center pressure of 968 hPa.

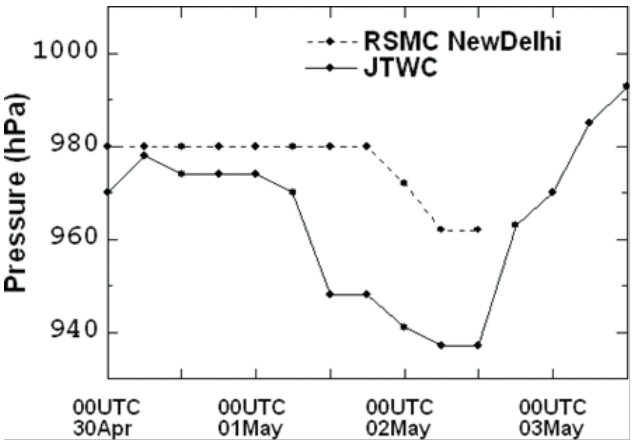

Fig. D-1-1. Time sequence of sea level center pressure estimated by the RSMC New Delhi and JTWC. After Kuroda et al. (2010).

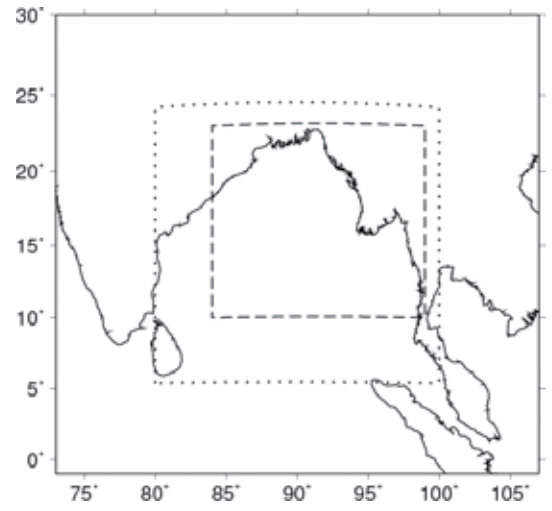

Fig. D-1-2. Domain used for NHM forecasts with the 10 km horizontal resolution. Dotted square is the domain of nested experiment with a horizontal resolution of 5 km, and broken rectangle indicates the domain of POM for storm surge simulations. After Kuroda et al. (2010).

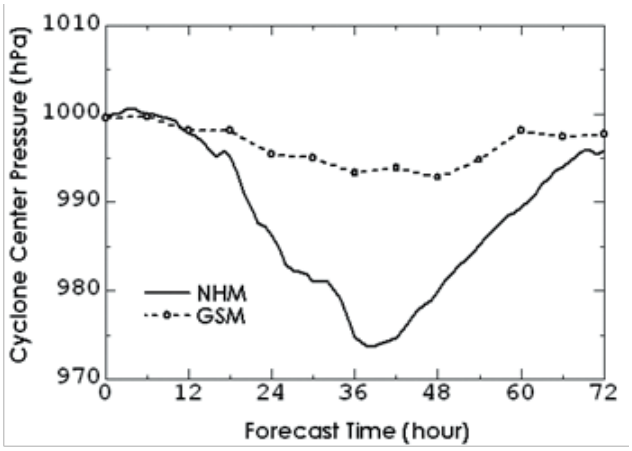

Fig. D-1-3. Time evolution of sea level center pressure of Nargis by NHM (GAGSM) and GSM forecasts. Initial time is 12 UTC 30 April 2008. After Kuroda et al. (2010).

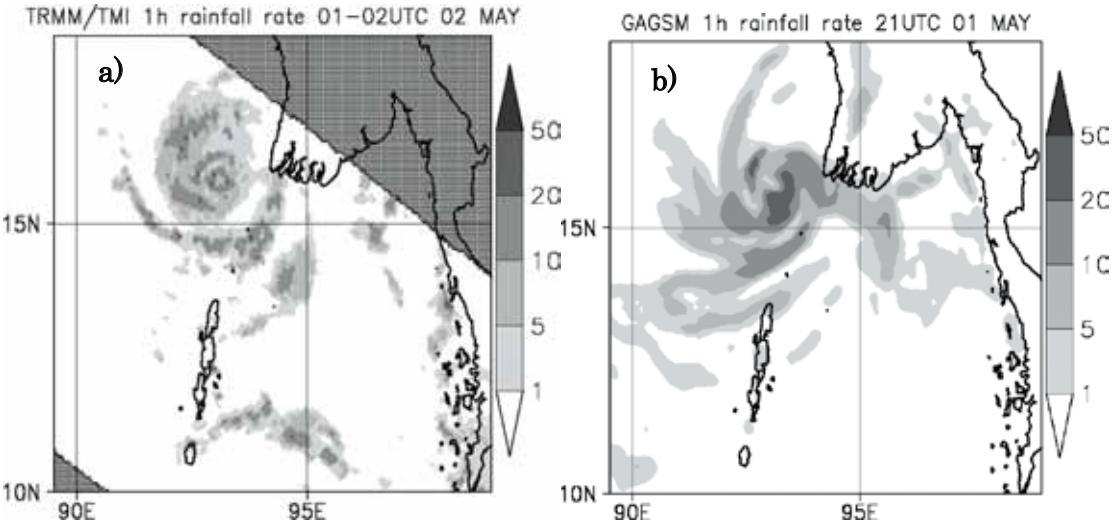

Fig. D-1-4. a) Rainfall rate (mm/hr) observed by TRMM/TMI at 0137 UTC 2 May 2008. After JAXA/EORC Tropical Cyclone Database (http://sharaku.eorc.jaxa.jp/TYP_DB/index_e.shtml). b) Rainfall rate (mm/hr) simulated by NHM at FT=33. After Kuroda et al. (2010).

D-1-3. Storm surge simulation

Numerical experiments on the storm surge were performed with POM with a horizontal resolution of 3.5 km. Oceanic currents and water levels were calculated with sigma (terrain-following) coordinates using the surface pressure and winds from NWP models. The open-sea boundary was assumed to follow a static balance with the atmospheric surface pressure, and deviations from the statically balanced level caused inflow or outflow current and gravitational waves. The astronomical tide was not taken into account, and thus, only the deviation of water level was computed with respect to the ocean's vertical motion. We conducted simulations by POM using surface pressure and wind fields from the GSM and the NHM forecasts. An experiment with POM using GSM forecast could not reproduce the storm surge (Fig. D-1-5c), while a simulation using NHM forecast predicted a realistic rise in the sea surface level by over 3 m (Fig. D-1-5f) at the Irrawaddy point (Fig. D-1-6). The rise was roughly of the same magnitude as the displacement due to the storm surge at the Yangon River reported by Shibayama et al. (2008), although a simulated maximum rise at the Yangon point (Fig. D-1-6) was 1.5m. In the simulation using NHM forecast, surface wind speeds reached 25 m s^{-1} (Fig. D-1-5d), and were much higher than those obtained in the GSM forecast which were less than 6 m s^{-1} (Fig. D-1-5a). Since the sea-level rise due to pressure depression (the inverse barometer effect) was less than 0.5 m, the major part of the storm surge was caused by the ocean current generated by strong wind in the simulation. A southerly sub-surface current driven by strong surface winds of the cyclone caused a storm surge in the river mouths in southern Myanmar facing the Andaman Sea as shown in Fig. D-1-6. We showed that the storm surge produced by Nargis was predictable two days before landfall by a downscale forecast with a mesoscale model using accessible operational NWP data and application of an ocean model.

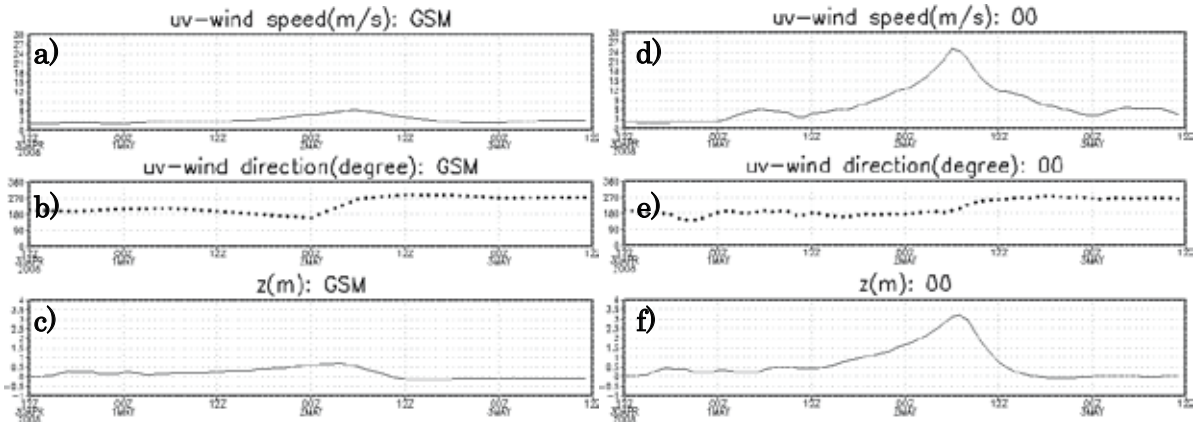

Fig. D-1-5. a) Time sequence of the surface wind speed by the GSM forecast at the Irrawaddy point (16.10˚N, 95.07˚E). b) Same as in a) but for wind directions. c) Same as in a) but water levels simulated by POM. d)-f) Same as in a)-c) but with the NHM forecast. After Kuroda et al. (2010).

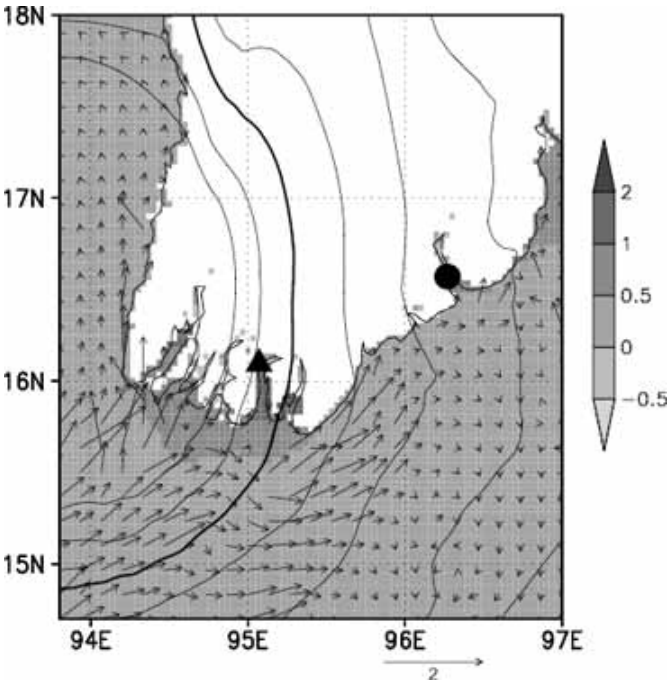

Fig. D-1-6. Enlarged view (FT=36) depicts the beginning of the sea level rise (gray scale) with showing the sea level pressure (thick contour indicates 1000 hPa and contour interval is 1 hPa) and vertically averaged current (arrows, m/s) which flows into the river mouths in southern Myanmar. Triangle and circle indicate the Irrawaddy and Yangon points, respectively. After Kuroda et al. (2010).

D-1-4. Concluding remarks

Although our results demonstrated the predictability of Nargis' storm surge given a lead time of two days, there were several quantitative discrepancies between the forecast and the real situations involving the cyclone intensity, track, and timing. For example, the storm surge at the Yangon River was about 4 m (Shibayama et al. 2008), while the maximum level at the Yangon point in our simulation was 1.5 m. These errors would be caused by inaccuracies in the initial and boundary conditions and SST, as well as insufficiencies of the model resolutions and physics. Thus, if the northward bias of the TC track predicted by NHM were reduced, a higher water level might have been simulated at the Yangon point. Risk management should be undertaken considering forecast errors and reliability.

D-2. Mesoscale LETKF Data Assimilation on Cyclone Nargis[1]

D-2-1. Introduction

Nargis was a severe tropical cyclone (TC) that formed on 27 April 2008 in the Bay of Bengal and made landfall on 2 May in southwestern Myanmar. Nargis caused a destructive storm surge over the Irrawaddy Delta, claiming more than 100,000 lives. If an appropriate warning had been issued by about 2 days before the landfall, the number of casualties might have been reduced.

JMA global analysis (horizontal resolution about 20 km) and GSM forecast data (horizontal resolution about 60 km and valid time every 6 h) expressed Nargis' track to some degree, but the expression on the storm's development was inadequate in both the early and mature stages. Thus, it was difficult to foresee a severe storm from these data. Recently, a downscale NWP using the JMA nonhydrostatic model (NHM) and JMA data was conducted as a forecast experiment of Nargis by Kuroda et al. (2010). They carried out the NHM forecast with a horizontal resolution of 10 km for a square region of 3400 km around the Bay of Bengal, using the JMA global analysis (GA) and the GSM global forecast as initial and boundary conditions, respectively (GAGSM). The initial time of the simulation was set to 12 UTC 30 April, 2008. At this time, GA expressed Nargis as a weak depression of 999 hPa although the intensity was less than 985 hPa in the best track. After 42 hours (06 UTC on 2 May), NHM intensified the depression to a cyclone of 974 hPa, and predicted its landfall in southern Myanmar although the point was northwardly deviated to the best track. The development of the cyclone predicted by NHM was considerably better than that by GSM (994 hPa; Fig.D-1-3), but the intensity was still weaker compared with the best track data (Fig. D-1-1). A reason for the inadequate depression in the NHM forecast may be a weak expression of the initial vortex in GA. Therefore, it is necessary to prepare more accurate initial fields using another data assimilation approaches in order to improve the cyclone forecast.

D-2-2. Data assimilation experiment

The local ensemble transform Kalman filter (LETKF) is an assimilation method based on the ensemble forecast. Miyoshi and Aranami (2006) applied this method to NHM (NHM-LETKF), and performed a data assimilation experiment. We applied NHM-LETKF to the Nargis' case with data assimilation cycles as depicted in Fig. D-2-1. To obtain the analysis at 12 UTC on 30 April, the first cycle began at 12 UTC on 28 April. The initial seed consisted of 20 (or 40) JMA global analyses before 12 UTC on 30 April. Then a 6-hourly ensemble forecast with a 40km resolution was conducted using the seed as the initial values. The observation data were assimilated with LETKF and the resultant analysis ensemble was used as the initial values for the next 6-hourly forecast. After iterating these steps, an analysis ensemble at 12 UTC on 30 April was obtained finally. Each member of the analysis ensemble was then used as the initial condition for the extended ensemble forecast with a 10 km resolution. The analysis ensemble mean was used for the control run of the extended forecast as well.

---

[1] T. Kuroda, K. Saito, M. Kunii and H. Seko

Selection of observation data is essential since it affects the accuracy of the analysis. Observation data used in the JMA analysis are stored in a dataset called CDA (Onogi 1998), and the each element has a quality control (QC) flag. Among the observed data, sea surface winds observed by QuikSCAT are the most important for the TC analysis over the sea because it captures surface circulation around the center of TC (Fig. D-2-2a). However, QuikSCAT data shown in Fig. D-2-2b were rejected in the QC process of the JMA global analysis in spite of their distribution around the cyclone center. These rejected data may affect the analysis around the TC center where the intensity was not well represented by both GA and GSM. In this study, in addition to the control experiment using the global analysis quality controlled CDA data (GAQC) we conducted an experiment using all QuikSCAT observations (ALLSCAT) in order to investigate the sensitivity of observations on analysis.

D-2-3. Results

The minimum center pressure of Nargis in the most deepening members reached 962 hPa and 960 hPa in the extended ensemble forecasts of GAQC and ALLSCAT, respectively (Fig. D-2-3). Although these members attained deeper center pressures than the GAGSM downscale experiment (974 hPa), the cyclone tracks were considerably deviated northwardly compared with the GAGSM case. On the other hand, the track of the extended forecast using the ALLSCAT analysis mean was encouraging, showing the favorably suppressed northward deviation of the cyclone track in comparison to the GAGSM downscale experiment (Fig. D-2-4). In order to justify the utilization of these QC-rejected data, new QC criteria are necessary. GAQC uses the GSM forecast as the first guess, but the NHM forecast should be used in the LETKF cycles. Also, GAQC automatically rejects all wind observation data exceeding 30 m/s, but such the wind speed may not be rejected around the cyclone center. Thus, criterion modification of QC is considerable. Besides, investigation of the influence of other analysis factors (e.g., localization and covariance inflation) is a significant future subject.

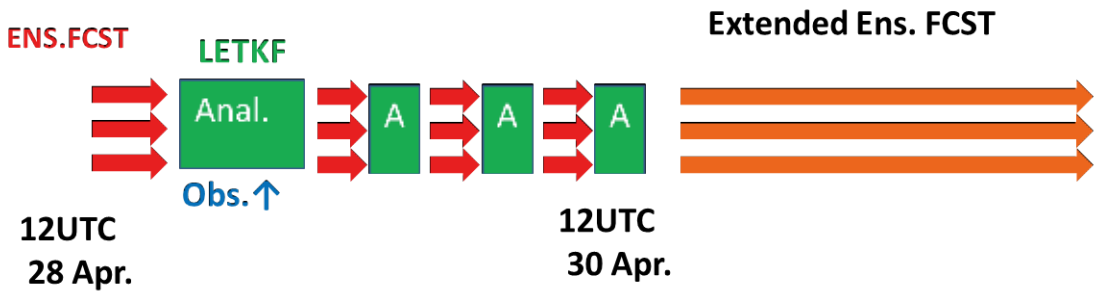

Fig. D-2-1. Data assimilation cycle and the extended ensemble forecast.

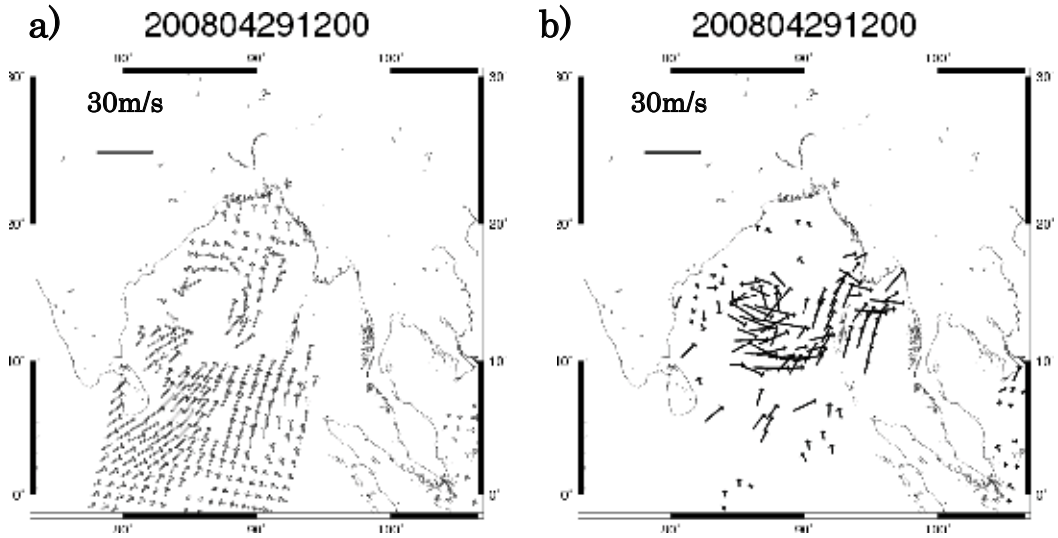

Fig. D-2-2. Surface wind distribution at 12 UTC on 29 April 2008 in the Bay of Bengal observed by QuikSCAT Seawinds. a)Winds used in the JMA global analysis. b) Winds rejected in QC.

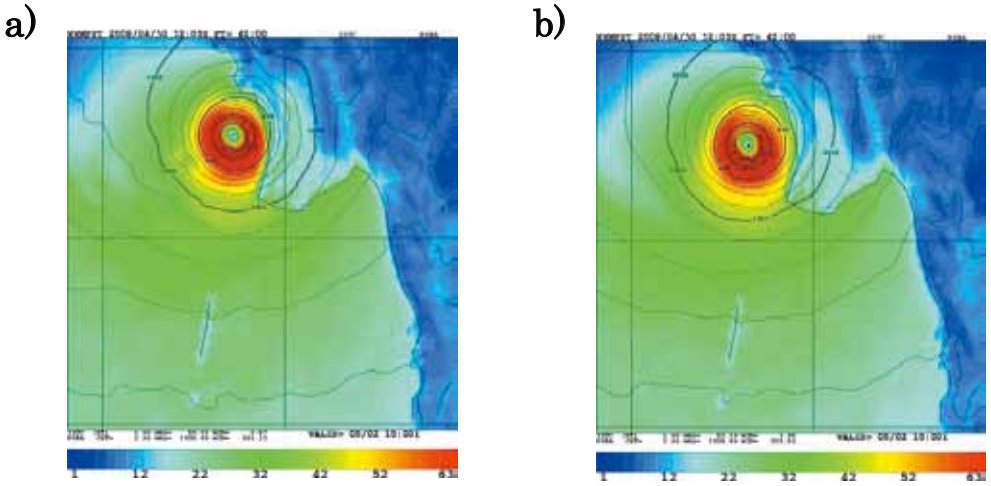

Fig. D-2-3. Wind speed field of most depressed member in the extended ensemble forecast at 06 UTC on 2 May. a) GAQC case. The center pressure is 962 hPa. b) ALLSCAT case. The center pressure is 960 hPa.

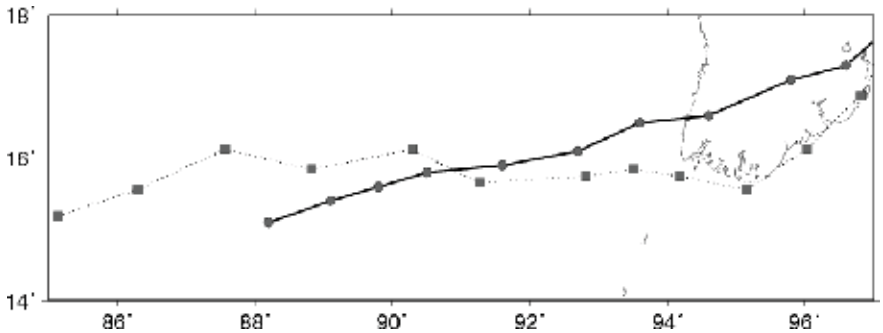

Fig. D-2-4. Forecasted cyclone tracks from 12 UTC 30 to 06 UTC 3 May. Thick solid line indicates the downscale experiment (GAGSM), and thin dotted line represents the extended forecast from the LETKF analysis (ALLSCAT) with the ensemble size of 20.

D-3. Ensemble prediction of cyclone Nargis and the associated storm surge[1]

D-3-1. Introduction

In Section D-1, numerical simulations of the Myanmar cyclone Nargis and the associated storm surge using the JMA nonhydrostatic model (NHM; Saito et al., 2006a; 2007) and the Princeton Ocean model (POM; Blumberg et al., 1987) were presented, based on Kuroda et al. (2010). A storm surge of about 3.2 m was simulated in southern Myanmar, but the cyclone center lagged about 120 km in position at the 48 h forecast and the predicted intensity of the cyclone was weaker than the analyses by the Regional Specialized Meteorological Center (RSMC) New Delhi and the Joint Typhoon Warning Center (JTWC).

It is well known that the magnitude of a storm surge highly depends on the track and intensity of tropical cyclone (TC) and NWP has unavoidable forecast errors due to uncertainties of initial and boundary conditions and the model's dynamics and physics. Therefore, probabilistic forecasts accounting for these uncertainties can contribute to the mitigation strategies for natural disasters. In this study, a mesoscale ensemble forecast of cyclone Nargis using the JMA nonhydrostatic mesoscale model with a horizontal resolution of 10 km and simulation of the associated storm surge were conducted by Saito et al. (2010a).

D-3-2. Mesoscale ensemble prediction using NHM

A mesoscale ensemble prediction system (EPS) was developed to consider errors in the forecast of cyclone Nargis. NHM which covers the Bay of Bengal and its surrounding areas (Fig. D-1-2) with a horizontal resolution of 10 km was employed as the forecast model. JMA's high-resolution global model plane analysis at 12 UTC 30 April 2008 is used as the initial condition and the 6 hourly GSM forecast GPV (0.5 x 0.5 degrees, 17 levels) supplied from the Japan Meteorological Business Support Center (JMBSC) is used as the boundary condition of the control run. The EPS runs up to 72 h with 21 ensemble members including the control forecast.

To provide the initial conditions of ensemble runs, perturbations from JMA's operational one-week EPS (WEP), which were obtained based on the global model singular vector method, are extracted by subtracting the control run forecast from the first 10 positive ensemble members in WEP. Since the highest level of the archived pressure plane forecast GPV of WEP is 100 hPa and is lower than the model top of the 40 level NHM (22.1 km ~ 40 hPa), forecast GPVs of WEP are first interpolated to the 32 level hybrid NHM model planes (model top is located at 13.8 km ~ 160 hPa), and perturbations are extracted by subtracting the interpolated field of the control run from perturbed runs. The perturbations are then normalized and added to the initial condition of the control run of the 40 level hybrid NHM. This procedure was originally developed for the WWRP Beijing Olympics 2008 Research and Development project (Saito et al. 2010b). For further details of normalization, see Saito et al. (2010a).

D-3-3. Ensemble prediction with initial perturbations

[1] K. Saito, T. Kuroda, M. Kunii and N. Kohno (JMA)

Figure D-3-1a plots tracks of Nargis until the valid time of 0600 UTC 2 May (FT=42) predicted by the 10 km NHM ensemble with initial perturbations. Most ensemble members predicted center positions of the cyclone east of the best track, and the landfall times are earlier than those observed. One of the reasons for this error is the positional lag of the cyclone center at the initial time (FT=0). Predicted positions of the cyclone center at FT=42 are distributed in an elliptical area elongated in the moving direction, and all ensemble members except one made landfall on the west coast of southern Myanmar. The average of relative displacements of the cyclone centers from the control in ensemble members is about 90 km.

Figure D-3-1b indicates the time evolution of center pressures. Despite the small initial perturbation in pressure, predicted cyclone center pressures range from 972 to 982 hPa at FT=42. One members intensified Nargis up to 966 hPa at FT=38 (0200 UTC 2 May). This intensity is weaker than the JTWC's best track data (941 hPa at 0000 UTC and 937 hPa at 0600 UTC 2 May), but comparable to the best track data of RSMC New Delhi (Fig. D-1-1; 972 hPa at 0000 UTC and 962 hPa at 0600 and 1200 UTC).

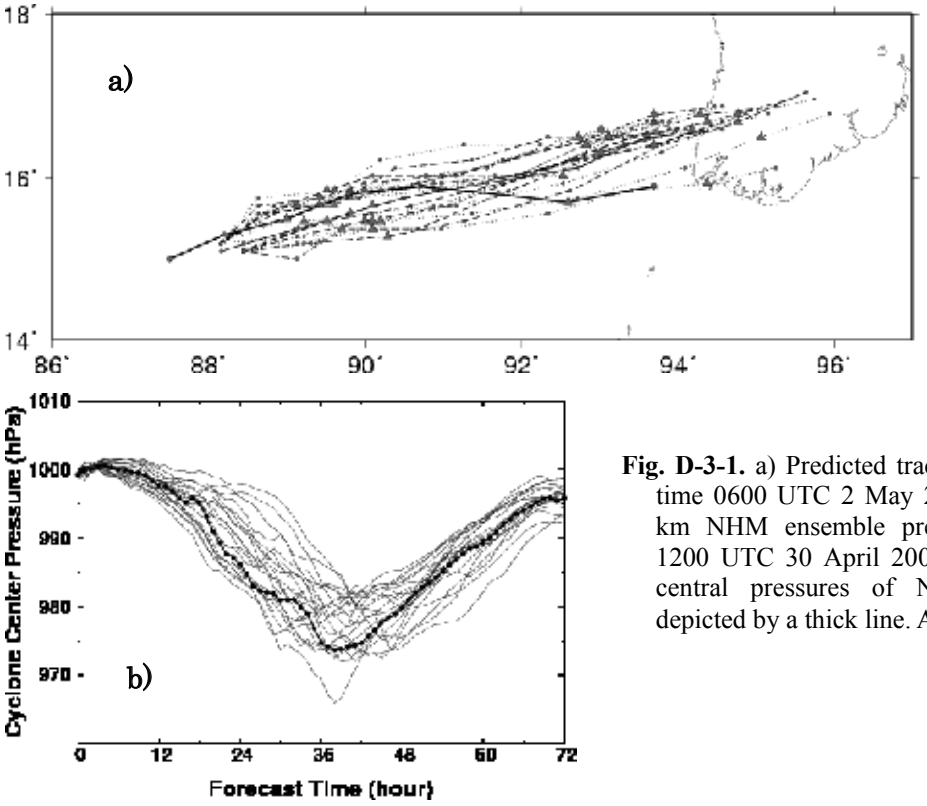

Fig. D-3-1. a) Predicted tracks of Nargis until valid time 0600 UTC 2 May 2008 (FT=42) by the 10 km NHM ensemble prediction. Initial time is 1200 UTC 30 April 2008. b) Time sequence of central pressures of Nargis. Control run is depicted by a thick line. After Saito et al. (2010a).

D-3-4. Ensemble prediction with initial and lateral perturbations

Figure D-3-2 illustrates tracks and evolution of center pressures of Nargis predicted by the NHM ensemble with both initial and lateral boundary perturbations. The center positions at FT=42 are distributed in an elliptical area with a major axis in the moving direction but are obviously dispersed over a wider area than those in the case without lateral boundary perturbations. Evolution of cyclone pressures (Fig. D-3-2b) also exhibits a larger spread, about 15 hPa in intensity, and timing of minimum pressures ranges from FT=36 to FT=60. Most cyclone tracks have northerly biases, but some members in Fig. D-3-2a have no northerly biases.

RMSEs of ensemble means are smaller than those of the control run and also smaller than those for the case without lateral boundary perturbations (see Fig.13 of Saito et al. (2010a)). Magnitudes of ensemble spreads are smaller than RMSE but reach about 70 % of RMSEs. These results suggest that the ensemble forecast is further improved by including lateral boundary perturbations.

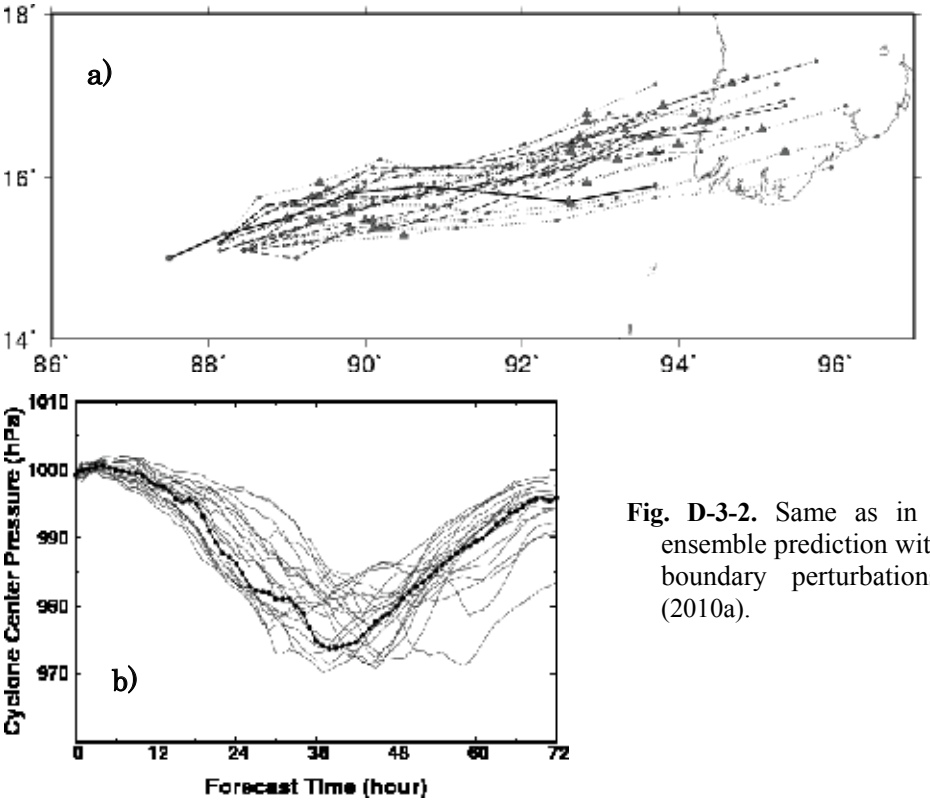

Fig. D-3-2. Same as in Fig. D-3-1 but NHM ensemble prediction with both initial and lateral boundary perturbations. After Saito et al. (2010a).

D-3-5. Storm surge simulation

Storm surge simulations were performed using surface winds and pressure from ensemble predictions. The Princeton Ocean Model with a horizontal resolution of 3.5 km was used as in section D-1. The initial time of this simulation was 1200 UTC 30 April 2008, and the ocean model was initiated from a static state. As the input data, 10 m horizontal winds and sea level pressures were given in every 10 minutes from WEP forecasts or NHM ensemble forecasts.

Figures D-3-3a-c plots the time sequence of wind speeds, wind directions and water levels predicted by WEP at the Irrawaddy point (16.10N, 95.07E). Maximum surface wind speed from the WEP control run at the Irrawaddy point is about 5 m/s at 1200 UTC 2 May (FT=48). Maximum wind speed in all ensemble members is about 7.5 m/s (Fig. D-3-3a). In Fig. D-3-3b, wind directions of most ensemble members became clockwise, but became counterclockwise in two members. A small storm surge was simulated by WEP winds. Consequently, the maximum water level is about as low as 0.3 m in the control run and 0.6 m in all ensemble members (Fig. D-3-3c).

Figures D-3-3d-f plots the time sequence of wind speeds, wind directions and water levels at Irrawady point by the NHM ensemble prediction. The maximum surface wind speed (25 m s^{-1}) was attained by the control run (Fig. D-3-3d). Several members predicted strong winds exceeding 20 m s^{-1}, but timings of the strongest wind are dispersed within 30 hours from 2000 UTC 1 May (FT=32) to

0200 UTC 3 May (FT=62). Wind directions (Fig. D-3-3e) in most members were southerly until 2000 UTC 1 May (FT=32) and changed to westerly after 1700 UTC 2 May (FT=53), suggesting that the simulated cyclone in each member passed north of the Irrawaddy point (except in two members). The water level at the Irrawaddy point reached 3.2 m at 0700 UTC (FT=43) in the control run. Two members predict high water levels near 4 m at FT=33 and FT= 37, while two other members simulated 3.1 m storm surges at FT=45 and FT=56.

From the time sequences plotted in Fig. D-3-3f, we can compute the maximum, minimum and center magnitudes of water levels. Assuming equal weight for all ensemble members, we can compute 25 % and 75 % probability values from the number of members that exceeds the corresponding thresholds (Fig. D-3-4). We can see that at the Irrawaddy point, a storm surge of about 1.8 m is expected with a probability exceeding 50 %, and 2.2 m with a probability of about 25 %. In the worst cases, water levels may reach about 4 m. We can notice that the possibility of the peak water level becomes maximum around FT=42, but the highest water level may occur earlier or later such as FT=33 or FT=60. This kind of figure is obtained only by the high resolution ensemble prediction, and gives important information on forecast errors and reliability for effective risk management.

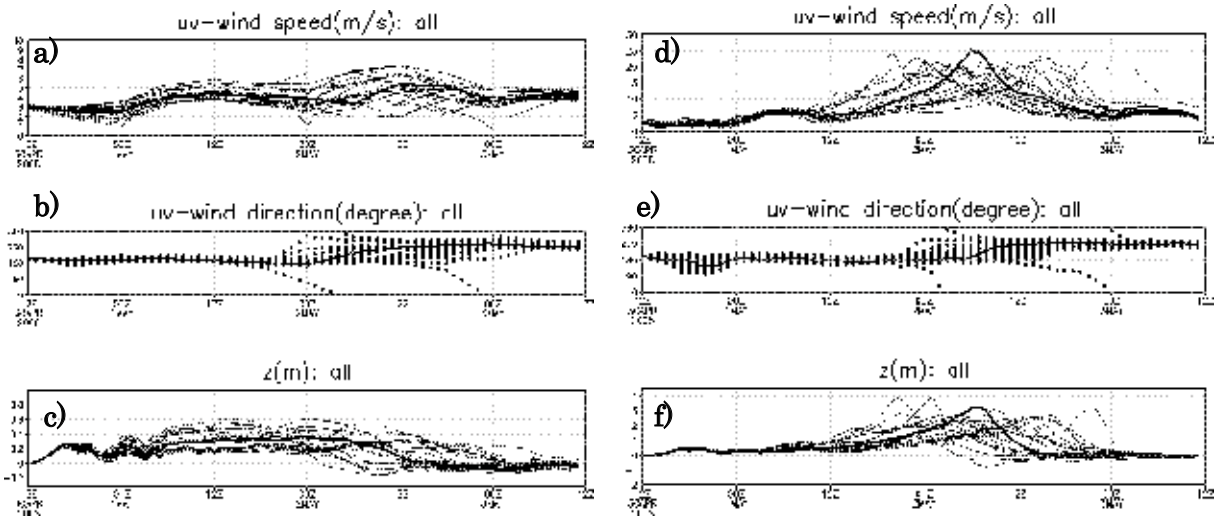

Fig. D-3-3. a) Time sequence of wind speeds by the WEP ensemble prediction at the Irrawaddy point. Control run is depicted by a thick line. b) Same as in a) but for wind directions. c) Same as in a) but water levels simulated by POM. d)-f) Same as in a)-c) but by the NHM ensemble prediction. After Saito et al. (2010a).

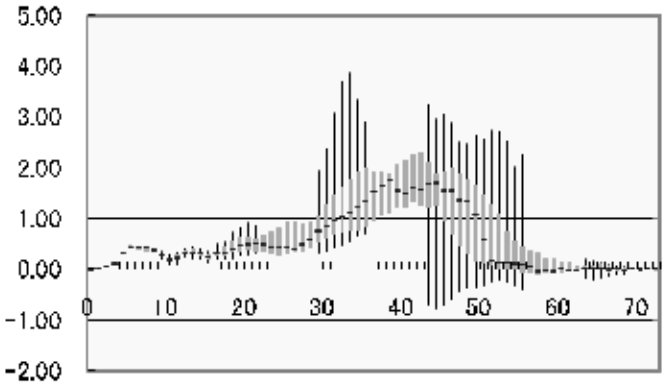

Fig. D-3-4. Time sequence of the maximum, minimum and center magnitudes of tide levels at the Irrawaddy point. Widths between 25 % and 75 % probability values are depicted with solid rectangles, whose upper and lower sides correspond to 25 % and 75 %, respectively. After Saito et al. (2010a).

D-4. Mesoscale data assimilation experiment of Myanmar cyclone Nargis[1]

It is important to prepare accurate initial fields for the forecast of tropical cyclones (TCs) with numerical models, and the resolution of the models is critical to predicted TC intensity. However we are usually forced to use the coarse-meshed initial fields produced by global model analysis in low latitudes, where tropical cyclones originate and develop. In this study, a mesoscale data assimilation (DA) system was developed for low latitudes, and DA experiments for tropical cyclone Nargis were conducted. A tropical cyclone bogus (TCB) procedure was also developed for the Bay of Bengal, and its impact was investigated.

D-4-1. Development of a data assimilation system in the low latitudes

To develop a low-latitude DA system, we modify the mesoscale 4 dimensional variational data assimilation system (Meso 4D-Var; Ishikawa and Koizumi 2002; Koizumi et al. 2005) of Japan Meteorological Agency (JMA) and apply it to the tropics. Meso 4D-Var was used as the operational mesoscale DA system at JMA from March 2002 to April 2009. The dynamical core of this system is based on JMA's hydrostatic spectral model (MSM). The system consists of a nonlinear forward model and a simplified adjoint model whose horizontal resolution is 20km. An incremental approach is employed where the analysis field is made by an outer model with a horizontal resolution of 10km.

In this study, we shift the domain of Meso 4D-Var to a low-latitude region that covers the Bay of Bengal (Fig. D-4-1). Map projection is also changed from the Lambert conformal projection to the Mercator projection for low latitudes. Topography, land-sea distribution, and climatological sea-surface temperature data were newly prepared according to change of the domain. Specifications of the new 4D-Var system in the tropics are listed in Table D-4-1.

In addition to above-mentioned some modifications, the regression coefficient for balanced wind was modified in order to appropriately perform Meso 4D-Var in low latitude. Meso 4D-Var control variables consist of virtual temperature (T_v), model surface pressure (P_s), specific humidity (q), and unbalanced wind (u_U, v_U). These variables are regarded as uncorrelated with each other. The relationship between unbalanced and balanced (geostrophic) wind is defined by

$$\begin{pmatrix}\Delta u_U\\ \Delta v_U\end{pmatrix}_k = \begin{pmatrix}\Delta u\\ \Delta v\end{pmatrix}_k - \mathbf{G}\nabla\left(\Delta\Phi + \frac{R_d\overline{T_v}}{\bar{p}}\right)_k, \tag{D-4-1}$$

where ϕ is the geopotential height, p is the atmospheric pressure, R_d is the gas constant for dry air, T_v is the virtual temperature in basic field, and k is the vertical level. Here, $\mathbf{G}$ is the regression coefficient matrix of wind expressed as

$$\mathbf{G} = \begin{pmatrix} r_{xx} & r_{xy}\\ r_{yx} & r_{yy}\end{pmatrix}. \tag{D-4-2}$$

The term in parentheses in the second term on the right-hand side of Eq. (D-4-1) is called the mass variable.

In the operational Meso 4D-Var, the unbalanced wind is calculated as

[1]M. Kunii, Y. Shoji, M. Ueno and K. Saito

$$\begin{pmatrix} u_U \\ v_U \end{pmatrix} = \begin{pmatrix} u \\ v \end{pmatrix} - \begin{pmatrix} r_{xx} & r_{xy} \\ r_{yx} & r_{yy} \end{pmatrix} \begin{pmatrix} u_g \\ v_g \end{pmatrix}, \quad \text{(D-4-3)}$$

where u_g and v_g are the geostrophic wind components, and r_{xx} is the regression coefficient for components between east-west and east-west, r_{yy} is that for components between north-south and north-south, r_{xy} is that for components between east-west and north-south, and r_{yx} is that for components between north-south and east-west.

In the operational Meso 4D-Var system, the coefficient matrix $\mathbf{G}$ was determined statistically in the original mid-latitude domain. Figure D-4-2a presents the regression coefficients in mid-latitude used in the operational Meso 4D-Var as a function of vertical level (Ishikawa and Koizumi 2002). The geostrophic balance argument has some validity at mid-levels, while it is decreased at low levels due to surface friction.

In this study, it is conceivable that the geostrophic balance argument is not necessarily valid in the new domain since the analysis domain is extended to low latitudes. To solve this problem, we reconstructed $\mathbf{G}$, which was applicable to the tropics. First we executed preliminary forecast experiments in the domain with low latitudes in order to investigate the degree of geostrophic balance statistically. We then divided the whole domain into some equal parts in the north-south direction, and calculated the regression coefficients for each of sub-domains. The result indicated that the geostrophic balance argument was valid in mid-latitude, but was not satisfied fully near the equator. We determined a new weighting coefficient as a function of latitude based on the amplitudes of coefficients in each partial domain (Fig.D-4-2b).

Since the statistical period above seems insufficient for constructing background error covariance matrix(**B**) itself, we merely utilize the weighting function from the statistical results in order to take into account the latitudinal dependency of the geostrophic balance. We used **B** designed for the operational model and multiplied the regression coefficients of mid-latitude by the new weighting coefficient.

D-4-2. Tropical Cyclone Bogus (TCB)

In low latitudes where cyclones are generated, the density of observations is generally sparse. Therefore, in cyclone predictions, especially in the operational NWP, it is common to use pseudo-data, called TCB, which expresses typical structures of TCs based on cyclone central pressure (P_C) and gale-force wind (exceeding 15 m/s) radius (R_{15}). The R_{15} and P_c of a typhoon in the western North Pacific are determined by JMA's forecasters every 3h. However, the JMA estimates of the TC parameters are not routinely available over the Bay of Bengal. To prepare TCB data for Nargis, we tested the following two TC parameter estimation methods and assessed the impact of resulting TCB data on the forecast.

(a) TCBa

With this method, Nargis' central pressure P_C (or gale-force wind radius R_{15}) was estimated by using a statistical regression formula between the 10-min maximum wind and central pressure (or

gale-force wind radius) obtained from the JMA best-track data from 2004 to 2007.

(b) TCBb

In the second method, we intended to use the data available for real-time prediction, specifically using the central pressure estimated by RSMC New Delhi's best-track data for P_C. Also, instead of resorting to a statistical approach as in the first method, R_{15} was estimated from satellite-based scatterometer (QuikSCAT) sea-wind data. Depending on the availability of QuikSCAT surface-wind observations, R_{15} was first obtained at 1500 UTC on 28 July, 1200 UTC on 29 July, and 0600 and 1200 UTC on 30 July for the analysis period. A linear interpolation of the values was then made between the corresponding times in order to determine R_{15} every 6 h over the entire period.

D-4-3. Numerical experiment for cyclone Nargis

We performed numerical experiments using the JMA NHM (Saito et al. 2006; 2007) with a horizontal resolution of 10km. We focused the initial time in our experiments on 1200 UTC 30 April 2008, two days before the landfall of Nargis. In order to assess the impact of DA, the following initial conditions were tested.

(1) GA

JMA's high-resolution global analysis (GANAL) at 1200 UTC 30 April.

(2) MA12

Initial field produced by a successive 12h DA using Meso 4D-Var from 0000 UTC to 1200 UTC 30 April, which included four 3-h assimilation windows.

(3) MA24

Same as MA12, except that the data assimilation period is 24h from 1200 UTC 29 to 1200 UTC 30 April.

(4) TCBa12

Same as the MA12 experiment, except that TCBa data were assimilated into the model.

(5) TCBa24

Same as the MA24 experiment, except that TCBa data were assimilated into the model.

(6) TCBb12

Same as the MA12 experiment, except that TCBb data were assimilated into the model.

(7) TCBb24

Same as the MA24 experiment, except that TCBb data were assimilated into the model.

Vertical profiles of relative humidity averaged over the whole domain at the initial time are presented in Fig. D-4-3. A glance at this figure reveals that the moisture field of GA is drier than those of MA12 and MA24, especially at the 850 to 300 hPa levels. This is probably a manifestation of the dry bias at middle and lower levels in JMA's global spectral model (GSM), which was pointed out by Miyamoto (2009). It seems that DA experiments conducted in this study more appropriately modified

the mean bias of moisture fields that appeared in the first guess. In this case, the assimilation of the PWV and 1 h accumulated precipitation data retrieved from the satellite-based microwave radiometer effectively ameliorated the analysis fields over the ocean, where observational data were scarce.

Surface-wind fields at the initial time also indicate certain differences between the GA and other experiments (MA12 and MA24). In GA, southwesterly flow dominates over a wide area southeast of the cyclone. In other experiments, southwesterly flows are limited south of the cyclone, and over the sea east of 90°E southerly winds prevail. These southwesterly and southerly flows converge in the area between the cyclone and the Andaman Islands. This convergence of surface flows in the humid environment mentioned above seems to cause the increase of PWV in the MA12 and MA24 experiments. For detail, see Kunii et al. (2010).

Figure D-4-4 presents time series of pressure (Figs. D-4-4a, D-4-4c, and D-4-4e) and track (Figs. D-4-4b, D-4-4d, and D-4-4f) of the cyclone center predicted by NHM using different initial conditions, along with the best track of RSMC New Delhi and the estimated sequence by the Indian National Centre for Ocean Information Services (INCOIS) (hereafter, collectively called “best tracks”).In the GA experiment, the center pressure became minimum (969hPa) at FT = 36 (0000 UTC 2 May). In best tracks, the center pressures reached minimum values at 0600 UTC 2 May. In this case, the simulated cyclone moved faster than best tracks and made landfall between 0000 and 0600 UTC 2 May at southern Myanmar. This earlier landfall could be the cause of the earlier occurrence of minimum pressure. In MA12, the cyclone central pressure at the initial time is almost the same as with the GA experiment. However, improvements in the prediction of cyclone intensity and speed are obtained. In this experiment, the timing of the minimum pressure is the same as in the INCOIS analysis, and the cyclone central pressure is consistently deeper than that in the GA experiment. Amelioration of dry bias at lower levels in analysis fields (Fig. D-4-3) may have helped the cyclone’s development.

Assimilation of TCB (TCBa12, TCBa24, TCBb12, and TCBb24) intensifies the cyclone. Cyclone central pressures at 1200 UTC 30 April (FT = 0) become deeper compared with experiments without TCB. Predicted cyclone center pressures at the mature stage in the TCBa experiments are between the RSMC New Delhi best track and the INCOIS estimation. The cyclones in the TCBb experiments tend to develop at a slower rate and to a lesser degree than in TCBa. A smaller gale-force wind radius in TCBb cyclones may have caused this difference. If we assume comparable reliabilities of the two cyclone intensity analyses, the center pressure predicted by TCBa24 seems best.

D-4-4. Summary

We developed a mesoscale data assimilation system in low latitudes and conducted forecast experiments for tropical cyclone Nargis. The JMA Meso 4D-Var system, which was designed for operational mesoscale data assimilation in the mid-latitudes, was modified for application to the tropics. In addition, a procedure for TCB calculation in the Bay of Bengal was developed based on the JMA’s operational scheme. At first, we statistically estimated the gale-force wind radius from the 10 min averaged maximum wind to make TCB profiles (TCBa) since no information about the gale-force

wind radius was available for Nargis.

The results show that the DA system developed in this study is useful for the real-time simulation for TCs in Bay of Bengal. It is expected that in the future such a DA system will contribute to mitigating meteorological disasters in the low-latitude region, including Southeast Asia.

Table D-4-1. Specifications of the original Meso 4D-Var and this study. After Kunii et al. (2010).

		Original	This Study
Method		Incremental method	
Forward model		A hydrostatic spectral model with a horizontal resolution of 10 km and 40 vertical levels up to 10 hPa. Three types of precipitation scheme; a large-scale condensation scheme, amoist convective adjustment scheme for mid-level convection and a prognostic Arakawa-Schbert scheme for deep cumulus convection.	
Adjoint model		Same dynamical process as the forward model but has only a few physical processes: simplified vertical diffusion, simplified long-wave radiation, grid-scale condensation and moist convection adjustment.	
Lateral boundary condition		Forecast of Global Spectral Model (GSM; TL959L60)	
		1 hourly original data (0.1875 degree gausian grid, 60 model planes)	6 hourly data distributed from Japan Meteorological Business Support Center (JMBSC) (0.5 degree, 17 pressure levels)
Assimilation window		6 hours	3 hours
Observational data *All observation data are treated as observed hourly. That is all data between -30 and +29 minutes to the clock time are regarded as observation s at the clock time.		Radio-sonde, synop (surface), ship, buoy, aircraft,wind and PWV fields retrieved from satellite-based microwave scatterometer/radiometer, tropical cyclone bogus. Wind-profiler, doppler-radar radial wind, Radar-AMeDAS analyzed rainfall.	Radio-sonde, synop (surface), ship, buoy, aircraft,wind and PWV fields retrieved from satellite-based microwave scatterometer/radiometer, tropical cyclone bogus (only TCB experiments).
Map projection		Lambert conformal projection	Mercator projection
Horizontal grid resolution (grid size)	Outer model	10 km (361 x 289)	10 km (401 x 301)
	Inner model	20 km (181 x 145)	20 km (201 x 151)

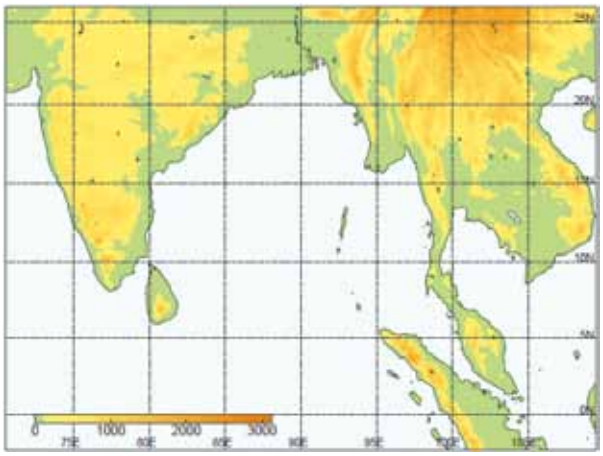

Fig. D-4-1. Domain of Meso 4D-Var in this study. After Kunii et al. (2010).

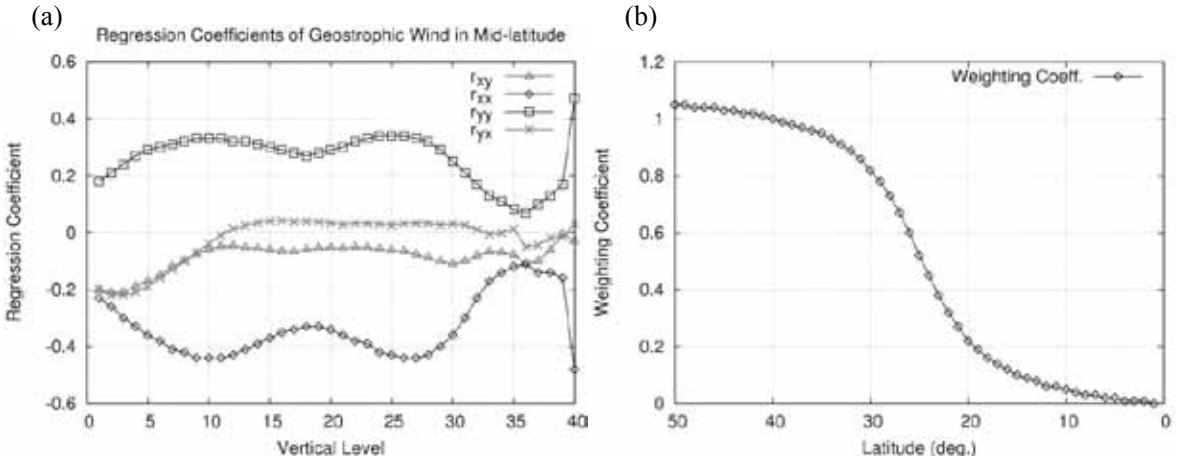

Fig. D-4-2. (a) Regression coefficients of geostrophic wind in mid-latitude. X- and Y-axis represent the model vertical level and the regression coefficient. Here, r_{xx} represents the regression coefficient for components between east-west and east-west, r_{yy} represents that for components between north-south and north-south, r_{xy} represents that for components between east-west and north-south, and r_{yx} represents that for components between north-south and east-west (Ishikawa and Koizumi 2002a). (b) Weighting coefficients for the regression coefficients of geostrophic wind in mid-latitude. After Kunii et al. (2010).

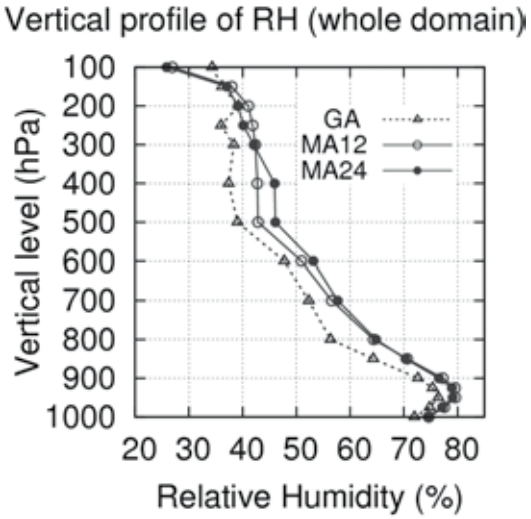

Fig. D-4-3. Vertical distributions of relative humidity averaged over the whole domain for the experiments of GA (dashed line with open triangle), MA12 (gray line with circle), and MA24 (black line with dot). After Kunii et al. (2010).

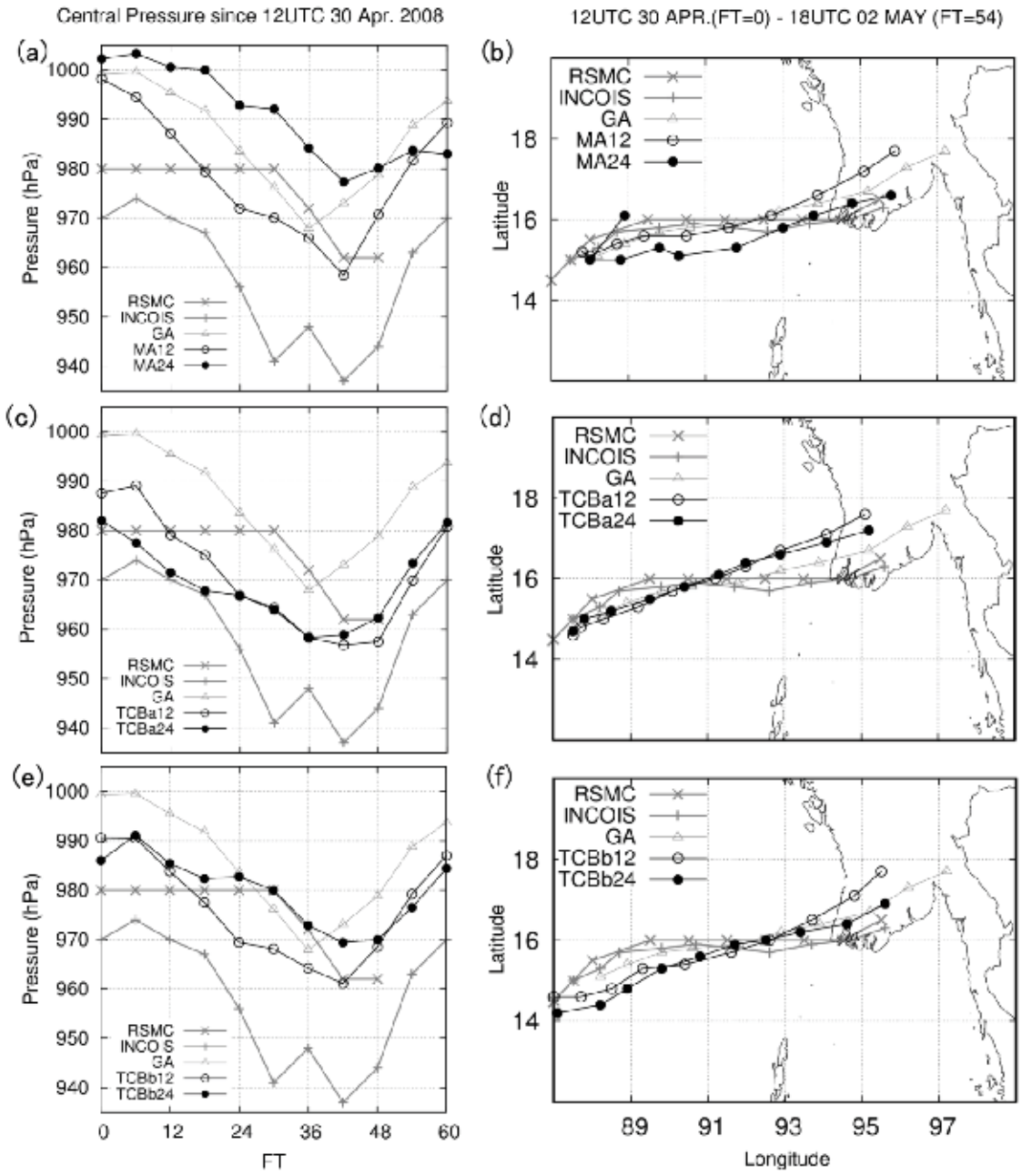

Fig. D-4-4. Time series of pressure (a, c, and e) and track (b, d and f) of the cyclone center predicted by NHM using different initial fields, along with RSMC New Delhi's best-track sequence (gray line with cross marks) and INCOIS's estimated sequence (gray line with plus marks). After Kunii et al. (2010).

D-5. Near realtime retrieval of GNSS precipitable water vapor in low latitudes and mesoscale data assimilation experiment of Myanmar cyclone Nargis[1]

D-5-1. Abstract

A trial of near realtime (NRT) analysis of precipitable water vapor (PWV) using global ground based GPS (Global Positioning System) network was performed. Preliminary evaluation of the NRT retrieved GPS PWV in Singapore showed comparable accuracy with those obtained by posterior analyses that use IGS (International Global navigation satellite system Service) precise ephemeris.

Four-dimensional variational (4D-Var) data assimilation (DA) experiments using the NRT derived GPS PWV were conducted for the tropical cyclone (TC) Nargis in 2008. In order to analyze the initial field at 1200 UTC 30 April 2008, 12, 24, 36, and 48 h sequential DA experiments with 3 h assimilation windows were performed. The initial fields made by these DA experiments were applied to subsequent forecast experiments using a nonhydrostatic model (NHM) with a horizontal resolution of 10 km.

NHM predictions using initial fields produced by DA experiments that used only ordinary observational data (without GPS PWV) exhibited a large variation of predicted maximum TC intensity (958 to 983 hPa) for each experiment. In these experiments, a longer assimilation period did not necessarily result in better prediction. The DA of GPS PWV yielded a smaller variation of predicted maximum TC intensity (964 to 974 hPa), and a longer assimilation period tended to bring deeper depression of TC central pressure. Overall, with GPS data assimilated, the predicted TC intensities became closer to the best track data produced by the Regional Specialized Meteorological Centre (RSMC) New Delhi.

D-5-2. NRT analysis of PWV with global IGS stations

Shoji (2009) introduced a procedure of NRT GPS analysis for the Japanese nationwide GPS network named GEONET (GPS Earth Observation Network). In this study, the procedure proposed by Shoji (2009) was enhanced in order to enable NRT analysis for GPS stations not only in Japan but also all around the world.

In order to serve an operational numerical weather prediction (NWP), NRT GPS analysis refers to the retrieval of the PWV within several tens of minutes after the observation. The procedure of this study is based on the Precise Point Positioning (PPP) method (Zumberge et al. 1997). The PPP method enables us to analyze each GPS station independently with relatively low computational load. Therefore the method befits the NRT analysis of large number of GPS stations. However, the PPP requires precise value for orbits (positions and clock) of GPS satellites because the method treats satellite orbits as known parameter. Satellite orbit accuracy is crucial for PWV retrieval in the PPP method.

---

[1] Y. Shoji, M. Kunii and K. Saito

Representative examples of GPS satellite orbits are provided by the IGS. Table D-5-1 summarizes the nominal accuracy of the IGS ephemerides. From the point of latency, IGU is only option for our NRT analysis. The nominal accuracy of an orbit in the IGU predicted part is about 5 cm. It is about twice as worse as those stored in IGF and IGR. On the other hand, the clock accuracy of the IGU predicted part is about 45 cm in length (about 70 mm in PWV). It is much worse than those stored in the IGF and the IGR. This suggests that correction to the clock offsets in the IGU predicted part is inevitable.

Table D-5-1. IGS Ephemerides as of January 2011.

Type		Abbreviation in this study	Nominal Accuracy	
			Orbits	Clocks
Ultra-Rapid	Predicted Half	IGU	~5cm	~1.5ns (~45cm)
	Analyzed Half		~3cm	~0.05ns (~1.5cm)
Rapid		IGR	~2.5cm	~0.025ns (~0.75cm)
Final		IGF	~2.5cm	~0.02ns (~0.6cm)

Shoji (2009) selected an IGS station USUD which has been equipped with hydrogen maser atomic clock, as a reference station to analyze the clock offsets of GPS satellites. This station was installed in July 1990, on the building roof of the Usuda Deep Space Center of the Japan Aerospace Exploration Agency (JAXA) in Saku city, Nagano Prefecture (red triangle in Fig. D-5-1 (a)). Firstly, the clock offset of USUD was analyzed by using the IGS rapid orbit (IGR), and then, the offset of USUD station clock was extrapolated for the next two days. Secondly, the offsets of GPS satellite clocks were analyzed while the extrapolated offsets of the USUD clock were kept fixed as a time reference. In this step, 23 GEONET stations (blue diamonds in Fig. D-5-1 (a)) were analyzed simultaneously while the satellites positions were kept fixed at orbits in IGU.

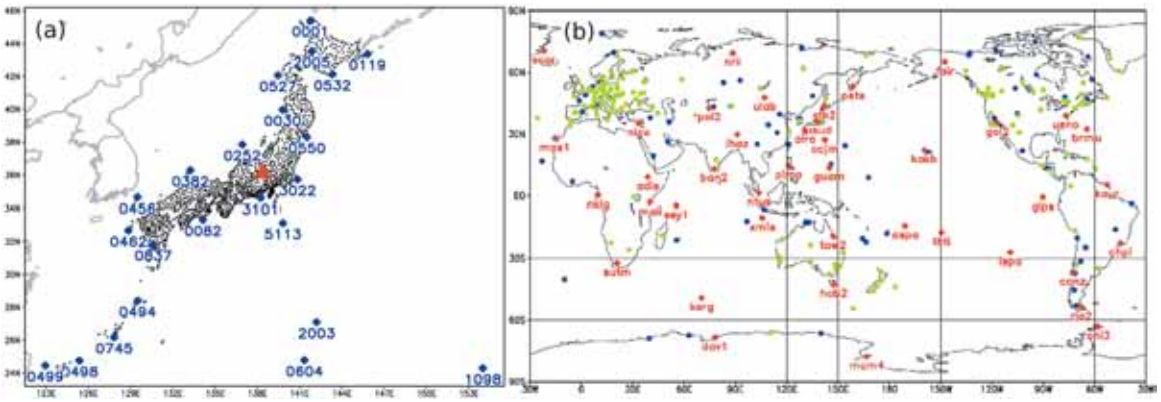

Fig. D-5-1. (a) Locations of GEONET GPS stations. Small dots: GEONET stations; large blue diamonds (◆): GEONET station used for the analysis of satellite clock offsets in Shoji (2009); filled red triangle (▲): USUD IGS station. (b) Locations of IGS stations. Red diamonds (◆): IGS station used for the analysis of satellite clock offset in this study; green dots (●): hourly sites; blue dots (●): non hourly sites.

The network which Shoji (2009) adopted for satellite clock correction (Fig. D-5-1 (a)) modifies satellite clock information around Japan. In order to correct crock information of all GPS satellites, IGS's global GPS network was used as shown in Fig. D-5-1 (b).

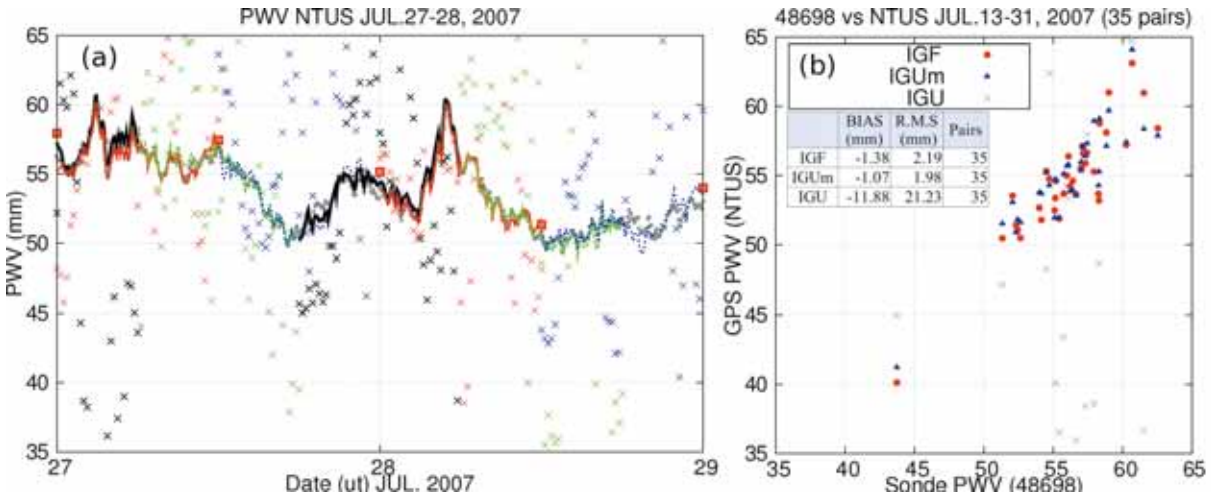

Fig. D-5-2. (a) Two days PWV sequence at IGS site "NTUS" in Singapore from 27 to 28 July 2007. Gray dots (●): GPS PWVs obtained by using IGF; x marks: those by using IGU; lines: those by using corrected IGU in this study; red squares (□) radio-sonde in Singapore (48698). (b) Scatter diagram of PWV comparison between radio-sonde and GPS for 19 days in July 2007. Red squares (■); GPS PWVs obtained by using IGF; blue triangles (▲): those obtained by using corrected IGU in this study; gray x marks (×): those obtained by using IGU.

Figure D-5-2 shows the comparison of the PWV retrieved by GPS and radio-sonde in Singapore. GPS PWVs obtained by using modified IGU (IGUm) in this study represent much the same performance with those obtained by using IGF. Those two agreed with radio-sonde observation with approximately 2 mm in root mean square (RMS) differences, whereas those obtained by using IGU resulted in large amount of errors (~21 mm in RMS).

D-5-3. Mesoscale data assimilation experiment of NRT GPS PWV for Myanmar cyclone Nargis

Kunii et al. (2010) modified the Meso 4D-Var in order to apply the system to low latitudes, and conducted DA experiments on Myanmar cyclone Nargis in 2008. Their results demonstrated the effectiveness of the DA system for the prediction of Nargis. They succeeded to reproduce the cyclone's minimum central pressure lower than 960 hPa. Also, they suggested the significance of observation enhancement around the Bay of Bengal.

In order to assess the impact of GPS PWV for TC prediction in low latitudes, we conducted DA experiment using DA system developed by Kunii et al. (2010). We targeted 1200 UTC 30 April 2008 as the initial time for the NHM forecast experiments. It is about two days before landfall of Nargis in the Irrawaddy river delta around 1200 UTC 2 May.

The following initial conditions were tested.

(a) GA:

JMA operational Global Analysis (GANAL) at 1200 UTC 30 April is used as the initial field.

(b) MA12, 24, 36, and 48:

Successive DA cycles with 3 h assimilation windows were performed. Assimilation periods of the DA experiments were 12, 24, 36, and 48 h. Radio-sonde, synop (surface), ship, buoy, aircraft, wind and PWV fields retrieved from satellite-based microwave scatterometer/radiometer were assimilated with hourly data slots. GANAL at 1200 UTC 28 April was used as the initial condition for the first DA window and produced the first-guess field by the hydrostatic mesoscale spectral model of JMA (MSM) prediction. Fields analyzed by previous DA windows were used as initial conditions of subsequent DA windows.

(c) GPS12, 24, 36, and 48:

These experiments are the same as the above MA experiments, except that GPS PWV is added to the assimilation data during the entire assimilation period. Figure D-5-3 shows the domain of our DA and NWP experiments together with locations of assimilated GPS sites.

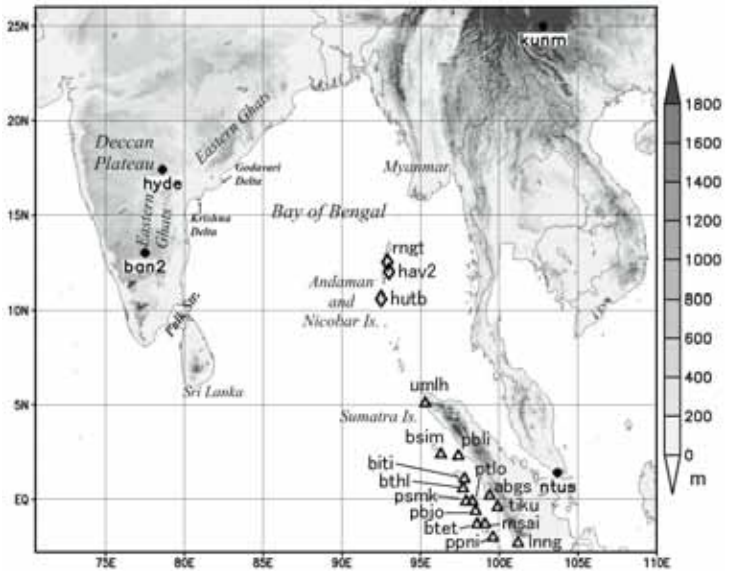

Fig. D-5-3. Locations of the 21 GPS stations used in this study. Black dots (•) denote IGS stations; open triangles (△) denote Sumatran GPS Array (SuGAr); open diamonds (◇) denote GPS stations in the Andaman Islands. Station IDs expressed in four characters are placed near each station's position. The ground surface altitude is expressed in shade. After Shoji et al. (2011).

Figure D-5-4 plots the time series of TC central pressures predicted by NHM, along with RSMC New Delhi's best track and estimated sequence by the Indian National Centre for Ocean Information Services (INCOIS) (hereafter, labeled "best tracks" for descriptive purposes).

When GANAL at 1200 UTC 30 April was used as the initial field (GA), NHM predicted a minimum TC central pressure of 969 hPa at FT = 36. The 12 h DA of ordinary observational data (MA12) resulted in a deeper depression of 958 hPa at FT = 42. However, NHM predictions using initial fields produced by ordinary observational data (MA12, 24, 36, and 48) indicated a large variation of the minimum TC central pressures (958 to 983 hPa). Among these four experiments, 12 h data assimilation (MA12) produced the deepest pressure dip. The 24 h and 36 h DA resulted in a decrease of pressure depression of more than 10 hPa from MA12. Furthermore, MA48 had the poorest performance.

By assimilating GPS PWV (GPS12, 24, 36, and 48), the variation of predicted TC central pressures became smaller (964 to 974 hPa). GPS12 resulted in 6 hPa larger minimum pressure than that of

MA12. However, other experiments (GPS24, 36, and 48) predicted significantly deeper minimum pressures than MA24, 36, and 48. Cyclone development was quite insufficiently predicted by MA48, whereas GPS48 successfully predicted the second deepest minimum central pressure among the four experiments that assimilated GPS PWV (GPS12, 24, 36, and 48). Overall, TC intensities predicted by DA experiments with GPS data (Fig. D-5-4b) were closer to the best track produced by RSMC New Delhi than the DA experiments without GPS data (Fig. D-5-4a). The cause of such a significant difference is discussed in Shoji et al. (2011).

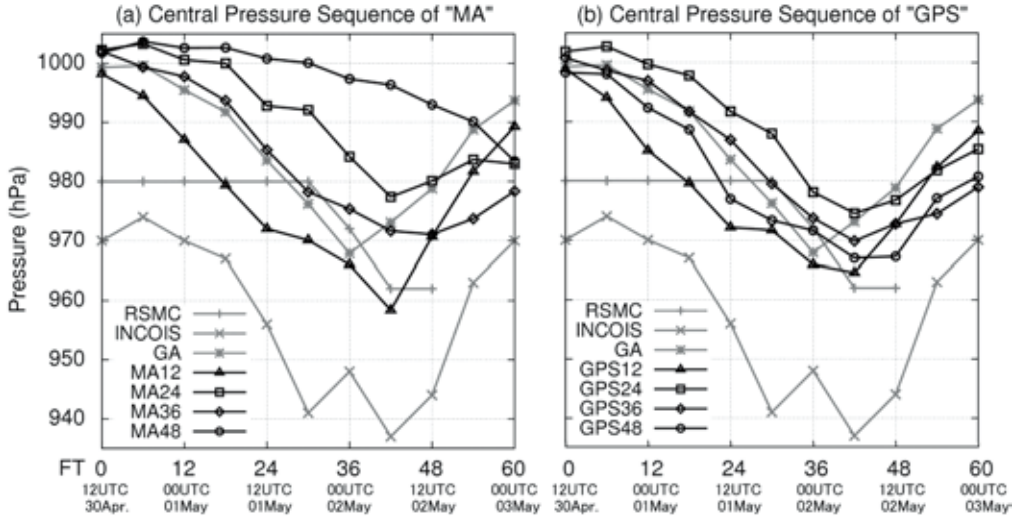

Fig. D-5-4. Time series of TC central pressure predicted by the NHM using different initial fields, along with best track sequence by RSMC New Delhi (gray line with "+" marks) and estimated sequence by INCOIS (gray line with "x" marks). After Shoji et al. (2011).

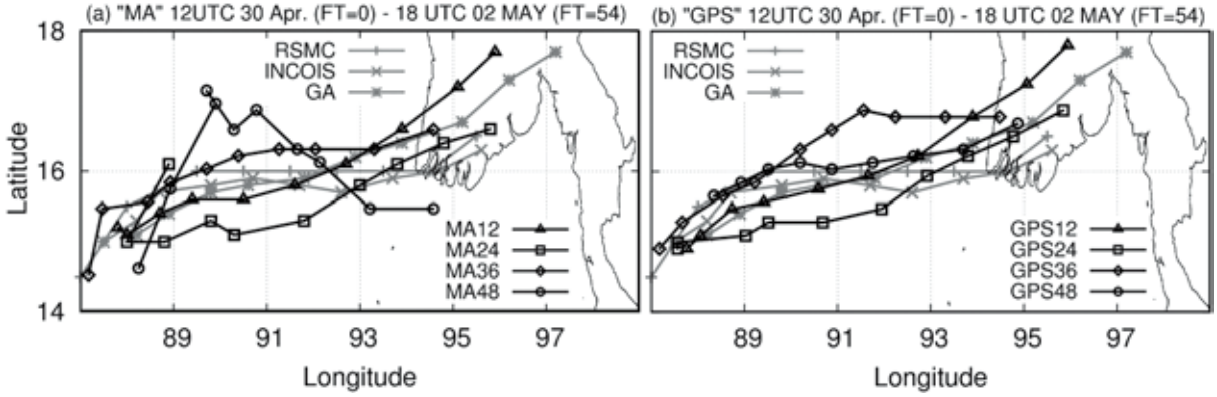

Fig. D-5-5. Time series of the Nargis track predicted by NHM using different initial fields, along with best track sequence produced by RSMC New Delhi (gray line with "+" marks) and estimated sequence analyzed by INCOIS (gray line with "x" marks). After Shoji et al. (2011).

Figure D-5-5 plots the predicted cyclone track, along with best tracks from 1200 UTC 30 April (FT = 00) to 1800 UTC 02 May (FT = 54). In the GA experiment, the simulated cyclone moved faster than best tracks and made landfall at 0200 UTC 2 May in southern Myanmar. This predicted landfall time is 10 h earlier than best tracks. The predicted TC pressure at FT = 42 in GA decayed, while INCOIS analyzed the deepest pressure at that time. This disagreement can be attributed to too early landfall in the GA prediction. In MA12, though a northward bias was observed in the latter half of the prediction,

moving speed and landfall time improved compared to GA. At FT = 42 in MA12, the predicted TC center was still located over the ocean, which might have led to further development of the TC at FT = 42.

MA24 exhibits a small southward bias in the first half of the prediction but decreases the bias in the latter half. As a result, the landfall location became closer to that of best tracks. Kunii et al. (2010) discussed the causes of these differences in the predicted TC track from the perspective of differences in steering flow.

No large differences in tracks between MA12 and GPS12, or between MA24 and GPS24, are apparent. GPS36 had a larger northward bias than MA36 from FT = 00 to FT = 36; after that, its moving direction changed to eastward. The predicted track of MA48 meandered largely north and south, even though the speed was slower than best tracks and landfall time was several hours delayed. GPS48 roughly followed the path of best tracks.

Overall, the large variation of predicted TC pressures and tracks represents the high sensitivity of TC prediction to the initial field and indicates the significance of precise analysis of the initial field. As pointed out by Kunii et al. (2010), poor observation density around the Bay of Bengal might cause the large variation in prediction results.

D-5-4. Summary

Our results suggest the importance of accurate analysis around the TC center in the early stage. Assimilation of GPS PWV improved prediction of intensity and track. However, the analyzed location of the TC center indicated a gap of several hundred kilometers from the best tracks. These facts indicate the necessity of further enhancing the observational network. Space-based Microwave radiometer and scatterometer data tend to be rejected around the TC center from DA in the quality check process. Novel approaches of quality control and/or direct assimilation of brightness temperatures may be needed in order to use more space-based remote sensing data. GPS observation is not affected by weather conditions; thus, it is always available as a continuous water vapor sensor. The results obtained in this study encourage the use of GPS, especially in data-sparse areas like the Bay of Bengal.

D-6. Asymmetric features of near-surface wind fields in typhoons revealed by the JMA mesoscale analysis data[1]

Recently the relationships between azimuthal wavenumber-one inner-core structures of tropical cyclones (TCs), and environmental vertical wind shear, have been increasingly investigated with numerical simulations at high resolution and theoretical considerations. However, due to the lack of detailed observations, which are usually obtained through a special field observational program, the results have not been endorsed by observational studies in a systematic manner. A viable alternative for detailed observations is analytical gridded data produced with a relatively high resolution by using a state-of-the-art data assimilation technique, such as the mesoscale analysis (hereafter referred to as "meso-analysis") data operationally produced at the Japan Meteorological Agency (JMA).

Over the years, researchers have developed parametric wind models to depict the surface winds within a TC. Parametric models have shown utility in creating wind fields as input to models such as the wave model, storm surge model, statistical-parametric model to predict TC wind radii, and pressure–wind model to relate the minimum central pressure to maximum surface winds in TCs. In most of such studies storm motion is assumed to be the only contributor to the near-surface wind asymmetry in TCs. Furthermore, most of previous theoretical studies on the wind distribution in the TC boundary layer have focused on the effect of TC translation on the wind distribution. Based on results from a real data simulation of Typhoon Chaba (2004), however, Ueno (2008) suggested that vertical wind shear could play a dominant role in determining the wind structure in the TC boundary layer insofar as the shear is significantly large. In the simulation low-level inflow tends to occur in the downshear-left quadrant, in accordance with the preferred location of rainfall maximum, and the strongest tangential wind is about 90° of azimuth downstream of the maximum inflow. A better knowledge of the role of vertical wind shear in determining the near-surface wind asymmetry would help to significantly improve parametric wind models.

The purpose of the present study is to document, in an extensive manner using the meso-analysis data, the influence of environmental vertical wind shear on the wavenumber-one asymmetries of near-surface wind components in the TC inner-core region. As a first step to quantify the shear contribution to the near-surface wind asymmetry in real TCs, we analyze the wind fields at about 20 m height (the lowest analysis level) obtained from the JMA operational meso-analysis, putting emphasis on the azimuthal location of wind maximum and its relevance to shear and storm motion. For the purpose a total of 190 cases from 35 typhoons observed during 2004–2007 seasons are examined. Figure D-6-1 shows the directional relationship between shear and tangential wind maximum. The azimuth of tangential wind maximum is found by performing the first-order Fourier decomposition of earth-relative wind field with respect to the surface center. In the figure both the shear direction and azimuth of tangential wind maximum are defined relative to the direction of storm

---

[1] M. Ueno and M. Kunii

motion. The storm motion vector is calculated from the JMA best-track position fixes. As expected, and in accordance with various earlier observational studies, the wind maxima are found predominantly to the right of TC motion. Interestingly, however, a small fraction (17 %) of the total cases exhibit a left-of-motion maximum and it occurs only in cases in which the shear direction is nearly equal to the storm heading. This result is in qualitative agreement with expectations from the simplified formulae derived in the study, which predict the tangential wind maximum in storm-relative coordinates to the left of TC center facing in the direction of enhanced eyewall convection (see Ueno and Kunii (2009) for more details).

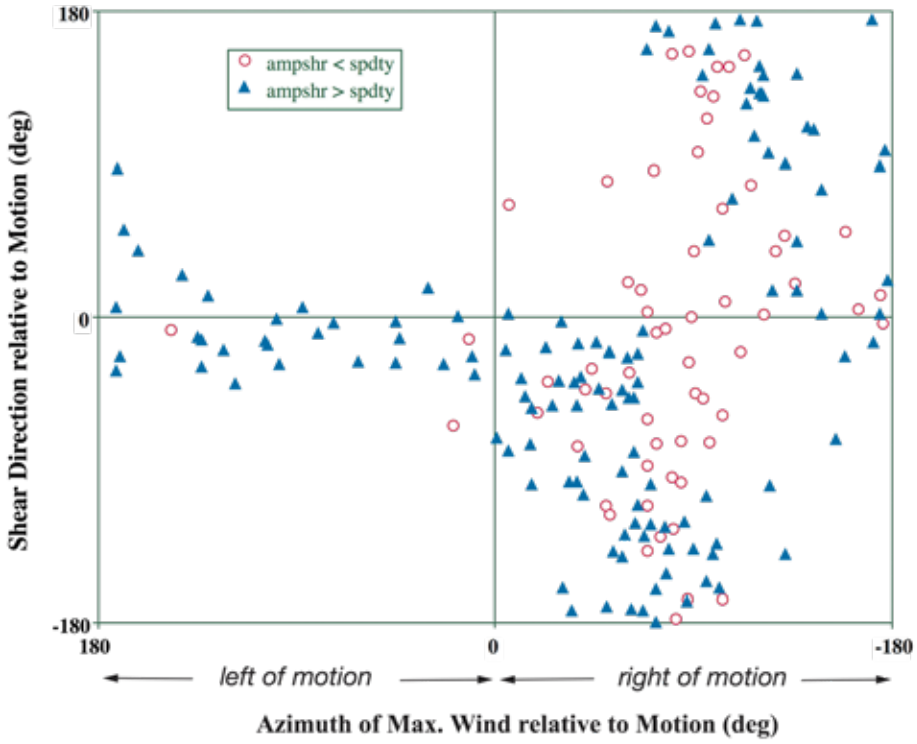

Fig. D-6-1. Directional relationship between vertical wind shear and tangential wind maximum. Vertical axis denotes the direction (in degree) of shear relative to that of storm motion vector with positive (negative) values for the shear to the left (right) of the motion, while horizontal one represents the azimuthal direction (in degree) of tangential wind maximum relative to storm heading. The sampled cases are stratified into two groups according to whether the shear magnitude is greater than storm translation speed (closed triangles) or not (open circles). After Ueno and Kunii (2009).

D-7. Preliminary validation of TC structure function used in the JMA typhoon bogussing procedure[1]

D-7-1. Introduction

Tropical cyclone (TC) vortex initialization is one of the most crucial aspects of mesoscale TC modeling (Chen 2008). The mesoscale models used for the prediction of TC intensity and/or wind and rainfall distributions associated with TCs are required to be initialized with a realistic inner-core structure. However the conventional observational network does not capture the detailed inner-core structure. As a result, the initial vortex obtained by assimilating observational data is mostly weaker than the observed one with a larger radius of maximum wind (RMW) (Ueno and Mashiko 2005; Braun et al. 2006). The lack of storm-scale details in the initial conditions likely prevents the model from producing an accurate forecast of TC intensity due mainly to a vortex spinup problem (Elsberry 2002). Indeed, a comparative numerical study conducted by Bender et al. (1993) has demonstrated that it is essential to start with TC vortex of realistic intensity for accurate TC intensity forecasts.

At present, from an operational point of view, a feasible option to prepare a realistic TC inner-core structure in the initial fields for high-resolution models such as JMA mesoscale model is to use the so-called "TC bogus observations". At JMA, a typhoon bogussing procedure has been applied to model initialization for TC forecasting. In the procedure, a climatological TC structure is constructed based on real-time TC analysis at the RSMC (Regional Specialized Meteorological Center) Tokyo, and a set of pseudo observations (or bogus observations) describing the TC structure are created around the TC center and assimilated into the initial fields for the mesoscale model.

A noteworthy aspect of the JMA typhoon bogussing method is that the symmetric portion of the three dimensional typhoon structures is totally determined by using an analytical TC structure function (Ueno 1989). The analytical function was originally developed to reproduce the climatological typhoon structure obtained by Frank (1977) in the initial fields for an early version of the JMA global model. Although the analytical function has been used since then to generate TC bogus observations, little attention has been paid to the validity of its use in the current modeling environments, especially in the high-resolution modeling ones. For example, detailed inner-core structures such as RMW are not always correctly specified by the method since the wind fields of bogus typhoon are basically determined from gale-force wind radius and central pressure through the analytical function. Furthermore, some key parameters to determine the thermal structure of bogus typhoon is best tuned to the models with a resolution of several tens of kilometers.

In the present study the possibility of improving the accuracy of structure function is explored using mesoscale analysis data (Ueno and Kunii 2009), JTWC (Joint Typhoon Warning Center) best-track data, and radiosonde observations for 2004–2007, as a first step toward appropriately applying the typhoon bogussing method to high-resolution modeling framework.

---

[1] M. Ueno

D-7-2. TC structure function

In the typhoon bogussing procedure, an empirical radius parameter (hereafter referred to as RTY), which demarcates a typhoon vortex from its environment, is determined at first from the gale-force wind radius and the latitude of the storm center. RTY is defined as the radius at which the rotation speed around the storm center of an air-ring initially located at the gale-force wind radius becomes zero as it expands outward conserving absolute angular momentum. In most cases the values of RTY are within the range of 300 to 1000 km. Once RTY is determined, then axisymmetric surface pressure profile is specified by using an empirical formula (Fujita 1952) from the JMA real-time warning track information regarding the central pressure and gale-force wind radius, and ambient surface pressure (Ueno 1989). To avoid possible aliasing or wrong projection of near-core small-scale features onto the large-scale ones, which could occur by imposing a tight eyewall on the model grid beyond its resolution, the surface pressure profile is modified (or smoothed) in a somewhat arbitrary manner so as to fit the model grid.

The D-value (deviation of axisymmetric geopotential height (Z) from ambient) at pressure P can be expressed as

$$\begin{aligned} D = Z(r) - Z_B &= -\frac{R}{g}\int_{P_s}^{P} T d\ln p + \frac{R}{g}\int_{P_B}^{P} T_B d\ln p \\ &= -\frac{R}{g}\int_{P_s}^{P} (T - T_B) d\ln p + \frac{R}{g}\int_{P_B}^{P_s} T_B d\ln p \end{aligned}, \qquad \text{(D-7-1)}$$

where the subscript B denotes an azimuthal average (reference-value) at the RTY of the relevant quantities. r is radial distance from the storm's center and R is the gas constant for dry air. P_s is surface pressure as a function of r and P_B is the value of P_s at the RTY. Remaining symbols are conventional. The right-most first term is a measure of vertically integrated temperature deviation. On the other hand, the second term indicates the D-value of P_B isobaric surface, which becomes increasingly negative value with decreasing P_s. Note here that the environmental fields, which need to calculate the reference-values such as T_B, are taken from the most recent forecast (i.e., first guess for the analysis). Then the problem is to determine the first term. To solve the problem it is assumed that the term can be expressed by the following analytical function,

$$\beta(\ln p - \ln P_s) \times \left\{(\ln p - \ln P_{Ta0})^2 + \varsigma\right\}^{-n} \times \exp\left\{\delta(\ln p - \ln P_{Tax})^2\right\} \equiv \Delta Z(r, p). \qquad \text{(D-7-2)}$$

The function includes some parameters that determine the warm core structure of the bogus typhoon. The left-hand first term in Eq. (D-7-2) increases with height (or decreasing p) with a negative constant β. The second term is symmetric in the vertical about $p = P_{Ta0}$ in terms of $\ln p$ and takes a maximum value there for a positive integer n. ΔZ decreases with increasing ς (>0). The third term is symmetric in the vertical about $p = P_{Tax}$ in terms of $\ln p$ and takes a maximum value there with the peakedness determined by the parameter δ (<0). By a combined effect of these three terms ΔZ takes

a maximum value at a pressure level between $p = P_{Tax}$ and $p = 0$. The exact pressure level where ΔZ is the largest depends on the relative contribution of the three subsidiary parameters, β, ς and δ.

The analytical function ΔZ was developed to reproduce the axisymmetric warm core structure of typhoons presented in the Frank's composite study. The vertical profile of temperature anomaly for the warm core is obtained by differentiating ΔZ with respect to $\ln p$. The key parameters included in the function are P_{Tax} and P_{Ta0}. P_{Tax} denotes the pressure level where the maximum temperature anomaly occurs. On the other hand, P_{Ta0} is considered to be the pressure level where the temperature anomaly vanishes above the P_{Tax}-level. Then the relationships between the key and subsidiary parameters are easily obtained and can be represented as

$$\delta = -\frac{1}{2\left(\ln P_s - \ln P_{Ta0}\right)\left(\ln P_{Tax} - \ln P_{Ta0}\right)}, \tag{D-7-3}$$

$$\begin{aligned}\varsigma &= n\left(\ln P_{Tax} - \ln P_{Ta0}\right) \\ &\times \frac{A + \sqrt{A^2 + \dfrac{4(n+1)}{n}\left(\ln P_s - \ln P_{Tax}\right)^2\left(\ln P_{Tax} - \ln P_{Ta0}\right)\left(\ln P_s - \ln P_{Ta0}\right)}}{\ln P_s - \ln P_{Tax}} \\ &- \left(\ln P_{Tax} - \ln P_{Ta0}\right)^2\end{aligned}, \tag{D-7-4}$$

where

$$A \equiv \left(\ln P_s - \ln P_{Ta0}\right)\left\{2\left(\ln P_{Tax} - \ln P_{Ta0}\right) - \left(\ln P_s - \ln P_{Tax}\right)\right\}. \tag{D-7-5}$$

Note here that both δ and ς could vary with radius because P_s is a function of radius. As for β, its calculation is done separately for the TC center and other places. If both P_{Tax} and P_{Ta0} are prescribed with $n = 1$, which is the current JMA operational setting, then β is the only parameter to be determined. The value of β at the TC center can be obtained from Eq. (D-7-2) by giving D-value at a certain pressure level. In the current operational setting, D-value at 700 hPa is used for this purpose since geopotential height at 700 hPa can be estimated from the central pressure with acceptable accuracy based on an empirical formula. If the resulting D-value at $p = P_{Tax}$ is found positive, then β is modified so as to make the D-value reduce to zero there. The value of β outside the center is obtained based on the assumption that the temperature anomaly at $p = P_{Ta0}$ decreases linearly with radius and becomes zero at the RTY. The assumption is reasonably consistent with Frank (1977) (see Figs. 3 and 4 therein) and necessary for a smooth transition in thermal structure from bogus typhoon to environment at the RTY.

The wind fields are derived from the geopotential height fields assuming the gradient wind balance between mass and wind fields. In the boundary layer the gradient winds are modified to include the surface friction. Asymmetric components of bogus typhoon are retrieved from the first guess fields and added to the symmetric ones before the bogus observations are utilized in the data assimilation system

(Ueno 1995). In the current JMA data assimilation system, only wind bogus observations are assimilated.

As mentioned above, the value of β at the TC center is derived from D-value at 700 hPa (algorithm I) or D-value ($=0$) at $p = P_{Tax}$ (algorithm II). Ueno (2000) revealed that in most cases β is determined through algorithm II, suggesting the importance of the specified value of P_{Tax} in determining the bogus TC structure. Nevertheless, P_{Tax} has long been used as a substitute for the pressure level (P_{Za0}) at which D-value becomes zero, without sufficient validation of the setting.

D-7-3. Validation of TC structure

The three-dimensional typhoon structure constructed using the TC structure function outlined in the foregoing section may strongly depend on the previously specified surface pressure profile. In the current bogussing procedure, the surface pressure profile is tailored to fit the model grid length to avoid a kind of aliasing error. This modification usually results in a weaker cyclone with a larger RMW. Figure D-7-1 compares the RMW of meso-analysis typhoon with that from the best-track data archived by JTWC. The JTWC values of RMW are mostly confined to less than 100 km, while the meso-analysis ones are distributed much more broadly extending up to 300 km. While this discrepancy might be mostly attributable to the insufficient horizontal resolution of the data assimilation system, there is a possibility that the use of Fujita's formula in the operational bogussing procedure, which determines the axisymmetric component of sea-level pressure, is also responsible for the large RMW bias. The RMW of bogus typhoon is basically determined through the formula from the following three parameters, central and ambient sea-level pressures, and gale-force wind radius. This means that even if reliable RMW value is available on a real-time basis, it cannot be directly used to modify the sea-level pressure profile due to the limited degrees of freedom of the formula. The use of other formula such as that proposed by Holland (2008) has the potential to overcome the disadvantage and generate improved sea-level pressure profile including RMW.

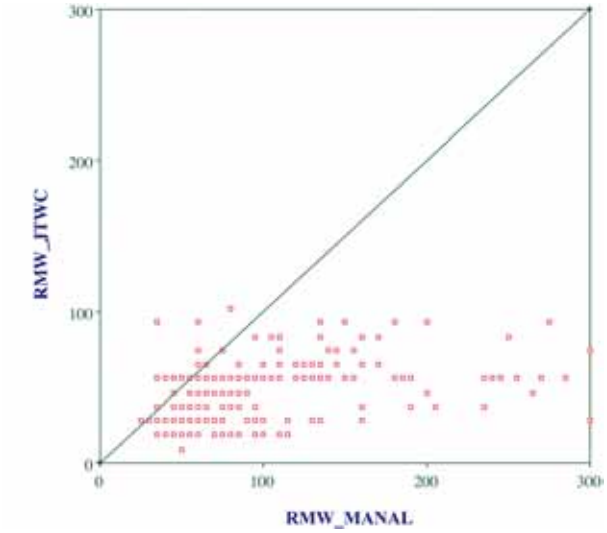

Fig. D-7-1. Scatter diagram of JTWC best track (ordinate) versus meso-analysis (abscissa) for RMW (km). The total number of cases evaluated is 240.

As described in the previous section, the thermal structure of bogus typhoon is primarily determined by the two key parameters characterizing the warm-core structure, P_{Tax} and P_{Ta0}. They respectively indicate the pressure level that gives maximum temperature anomaly at the storm center, and the pressure level where the temperature anomaly vanishes above the P_{Tax}-level. Since the resultant warm core structure of meso-analysis typhoons is built up from not only bogus observations, but also past and current observations through the influence of the assimilating model, there is no assurance that the parameters retrieved from meso-analysis typhoons coincide with those used in the bogussing procedure. Figure D-7-2 plots the retrieved pressure levels. The retrieved P_{Tax} tends to be significantly larger than the value specified in the bogussing procedure (i.e., 250 hPa), especially for the cases with strong environmental vertical wind shear. On the other hand, an overall shift to smaller values is found in the retrieved P_{Ta0}, as compared to the specified value (i.e., 100 hPa). Note that the retrieved values could change with the definition of environments (e.g., RTY).

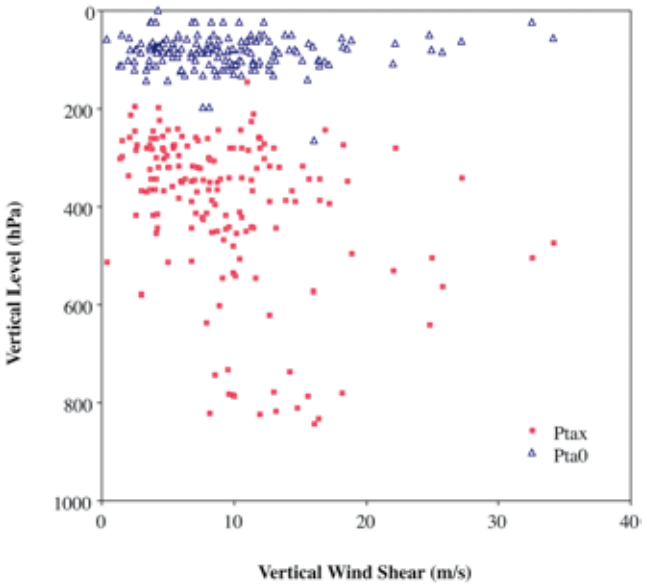

Fig. D-7-2. P_{Tax} (red square) and P_{Ta0} (blue triangle) retrieved from the meso-analysis typhoons. The vertical and horizontal axses indicate vertical level in pressure (hPa) and environmental vertical wind shear (m s^{-1}), respectively. The total number of cases evaluated is 166.

As mentioned in the foregoing section, the pressure level (P_{Za0}) where the D-value becomes zero has long been set to P_{Tax} in the operational bogussing procedure possibly as a result of some early empirical efforts to best tune the parameter to the numerical models of the time. Here in the present study the validity of the P_{Za0} setting is examined using the radiosonde and surface synoptic observations obtained in the near-core region of typhoons during the period 2004–2007. The validation study is done using the bogus observations that include asymmetric components extracted from the first guess fields. Table D-7-1 shows the errors of bogus observations produced with the operational setting, comparing with those with a trial parameter setting. The trial setting follows Ueno (2000) who found that the setting $P_{Za0} = P_{Ta0}$ leads to a smallest mean error irrespective of TC intensity when the fitting process to the model grid is not applied to the surface pressure profile. Note that the fitting process usually results in reducing the sharp pressure gradients near the center of an intense storm. So the parameters tuned with the process being skipped are considered more appropriate for very high-resolution models. As seen in

the table, the trial set of parameters yields smaller errors throughout the depth of troposphere, consistent with the verification results of Ueno (2000).

Table D-7-1. Root-mean-square (RMS) difference between bogus and radiosonde observations evaluated for geopotential height (left three columns) and wind (right ones) within the radius obtained by multiplying the typhoon radius by factor 0.3. OPE and TRI denote the RMS differences obtained with an operational and a trial setting of key parameters, respectively. The numbers of cases evaluated are around 2000 for the surface and around 200 for the rest.

GPH (m)			Wind (m/s)		
Level	OPE	TRI	Level	OPE	TRI
Surf.	38.90	38.90	Surf.	16.77	16.77
850	40.57	37.87	850	11.97	11.73
700	37.84	33.66	700	9.50	8.98
500	32.89	32.31	500	9.12	8.04
400	36.96	34.59	400	9.74	8.27
300	41.62	32.88	300	8.88	7.74
250	45.43	33.04	250	8.31	7.58
200	38.68	36.71	200	8.51	7.99

D-7-4. Summary

In the present study, initial data problems arising with high-resolution TC modeling are discussed, focusing on the validity of TC structure function used in the JMA bogussing procedure. It is found from the study that (i) the radius of maximum wind (RMW) of the meso-analysis typhoons tends to be significantly larger than that estimated by JTWC on the whole, (ii) the warm core structures of the meso-analysis typhoons are significantly different from those intended by bogus observations, and (iii) a modification of key parameters in the structure function could provide the inner-core TC structure more consistent with radiosonde observations. These results suggest that there is still plenty room for improvement in the current TC vortex initialization using the TC bogussing method, especially in the context of high-resolution modeling.

D-8. Re-Analysis and re-forecast of Typhoon Vera (1959)[1]

D-8-1. Introduction

Typhoon Vera attacked Japan around 18 JST (Japan Standard Time) on 26 September 1959. Vera caused the most tragic disasters after World War II, especially to the Ise Bay area located at middle part of the Japan Island, i.e. total amount of death toll was 5,098 and total number of total lost houses was 40,838. These were mainly induced by the storm surge, whose tide level at Nagoya port was 383 cm. The location of the Ise Bay and Nagoya To prevent such the tragic disaster, it is necessary that forecasts of its track and intensity are really precise.

Japan Meteorological Agency (JMA) has started the long-term global-reanalysis project from 1958 to 2012, called as the JRA-55 (Ebita et al. 2009), which is a successor for the JRA-25 (Onogi et al. 2007). The JRA-55 project provided us the pilot analysis and observational data associated with Vera. In addition, we found the flight level and drop sonde observations by the US air force in the report for Vera of JMA (JMA 1961), and decided to use these observations in our study. The purposes of this study are a) the confirmation that the JMA operational meso scale analysis and forecast system are useful for super typhoon Vera, b) the challenge to assimilate the typhoon center pressure observations by direct observations.

D-8-2. Typhoon Vera

Typhoon Vera was generated 200 km west of Eniwetok Atoll on 20 September 1959 as a tropical cyclone, developed to a typhoon at 15 JST on 23 September, and was recorded minimum pressure of 894 hPa (Fig. D-8-1, Fig. D-8-2). At the same time, the maximum wind speed of 70 m h^{-1} was estimated, and Vera became “super typhoon”. At 18 JST on 26 September, Vera made landfall on the Kii Peninsula and surface pressure of 929 hPa was recorded at the Shionomisaki observatory very near from the landfall point. This value is the second record as the surface pressure at landfall time in Japan. After the landfall, Vera passed the Japan Island within 6 h.

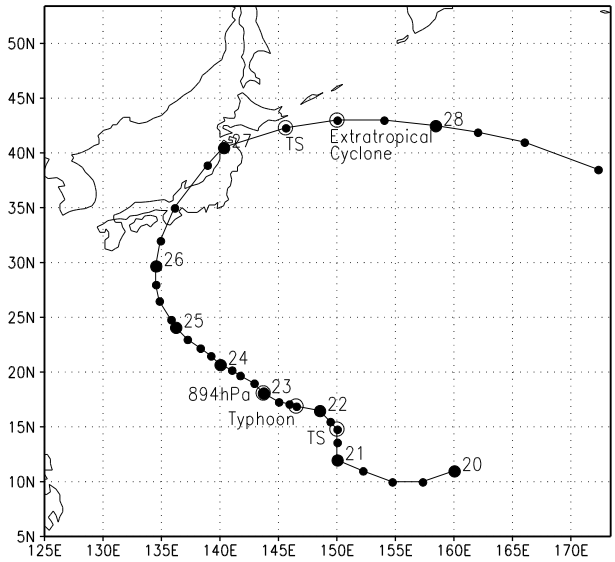

Fig. D-8-1. Best track of Typhoon Vera. Dates are indicated with UTC.

D-8-3. Methodology

D-8-3-1. Observations, assimilation and forecast systems

In this study, upper sounding, surface observation, ship, aircraft data were used (Fig. D-8-3). The aircraft observations are

[1] T. Kawabata, M. Kunii, N. Kohno (JMA), K. Bessho, T. Nakazawa, Y. Honda (JMA) and K.Sawada (JMA)

distributed in area of 20-30 N, 130-140 E. Aircraft data consists of flight level data by air-born sensor around 700 hPa height and drop sonde observations in the typhoon center and around the typhoon.

An assimilation system in this study is the JMA operational meso scale nonhydrostatic 4-dimensional variational assimilation system (JNoVA; Honda et al. 2005). Horizontal resolutions of inner and our loop of JNoVA are 15 and 5 km, respectively. In JNoVA, an adjoint scheme of large scale condensation as moisture process is implemented. A forecast system is the JMA operational meso scale nonhydrostatic model (JMANHM; Saito et al. 2006). Its horizontal resolution is 5 km. A bulk cloud microphysics and the KF parameterization (Kain and Fritsch 1993) schemes are implemented.

D-8-3-2. Experimental design

First, forecast using the JMA operational Global Spectrum Model (GSM) with 60 km grid spacing was conducted using JRA-55 analysis as initial conditions. Next, forecast using JMANHM with 20 km grid spacing was conducted, nested in the GSM result (hereafter NHM-20km) from 09 JST 25 September to 09 JST 26 Sep.. Finally, forecast using JMANHM with 5 km grid spacing was conducted, nested in NHM-20km from 03 JST 25 Sep. to 09 JST. This result was used as a first guess field.

Assimilations using JNoVA were conducted from 09 JST 25 Sep. to 09 JST 26 Sep. with 3-h assimilation window. After that, 36-h forecast by JMANHM with

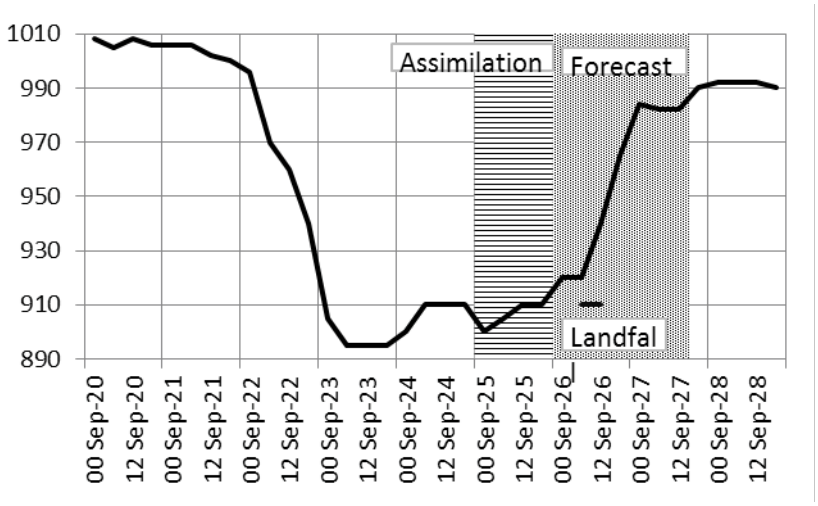

Fig. D-8-2. Time series of sea level pressure at the Typhoon Vera center. Assimilation term is shown in the horizontal line area and forecast term is shown in the shaded area.

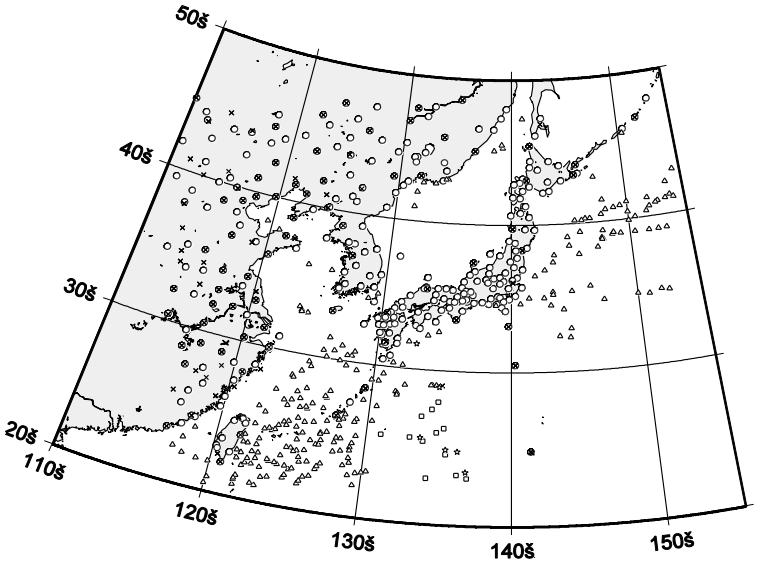

Fig. D-8-3. Distribution of observational data in the 24-h assimilation term.. Surface (circles), ship (triangles), upper soundings (crosses), aircraft data at flight levels (squares), and drop sonde (stars).

5 km grid spacing was conducted (NHM-5km) from 09 JST 26 Sep. to 21 JST 28 Sep.. Assimilation and forecast term associated with the Vera life time are indicated in Fig. D-8-2. Assimilation and forecast region is illustrated in Fig. D-8-4.

D-8-3-3. Assimilation method of drop sonde observations in the TC center

In general, numerical models can not represent strong tropical cyclone (TC) similar with actual one, because of its coarse resolution and simplified physical processes. It is reasonable to suppose that observations in the TC center have bias error which is introduced by the model representativeness.

In this study, since assimilation term was very short, the error was considered as random, that is, the error was treated as observational error, instead of bias. We gave the observational error using following method: When departure value (first guess – observation) is just 70 hPa, the value of observational error is set to 4.0 hPa which is five times of default value in JNoVA. When departure value is 10 hPa, the value is set to default value of 0.8 hPa (Eq. D-8-1). This specific value was determined under consideration of that a value of cost function when the observation in the TC center was assimilated became similar magnitude to that when not assimilated.

$$\mathrm{ERRobs} = 0.8\mathrm{hPa} * \left(\frac{\mathrm{departure}}{15} + \frac{1}{3}\right) \quad \text{if } (\mathrm{departure} > 10\mathrm{hPa}). \quad \text{(D-8-1)}$$

When the TC location in first guess field is far from the observational location, “twin cyclones” problem, which means that two cyclones, a bogus cyclone in the first guess field and an actual observed cyclone, exist in the analysis field may be induced. In our method, the problem hardly occurs, because the observational error becomes large under the situation, and the observation in the TC center is weekly assimilated. Our method could not correct the displacement error without other observations. Accordingly, our strategy is that typhoon is intensified by the assimilation of the TC center observation, and the displacement error is corrected by the other observations around the typhoon.

D-8-4. Results

D-8-4-1. Drop sonde assimilation in the TC center

In this section, effects of drop sonde assimilation in the TC center are discussed. Three observations were used in the assimilation term at 11 JST 25 Sep., 17 JST 25 Sep. 06 JST 26 Sep, respectively. Observations, analysis, first guess, and observational errors are illustrated in Fig. D-8-5. Since there are large departures (first guess – observation) in the first and second assimilation, observational errors are also set to large value. After several assimilations were conducted, departure became small at 06 JST 26 Sep.. Since observational error was set to small amount, the analysis of the center pressure and the location

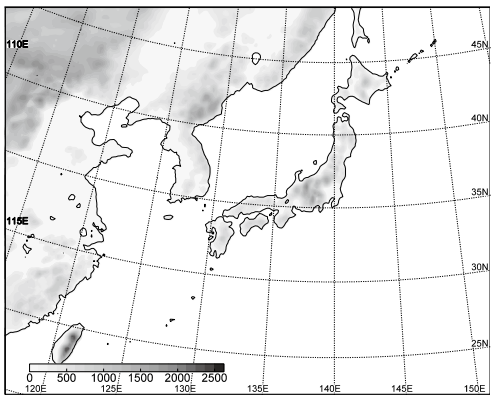

Fig. D-8-4. Model domain and orography of JNoVA and NHM-5km. After Kawabata et al. (2011).

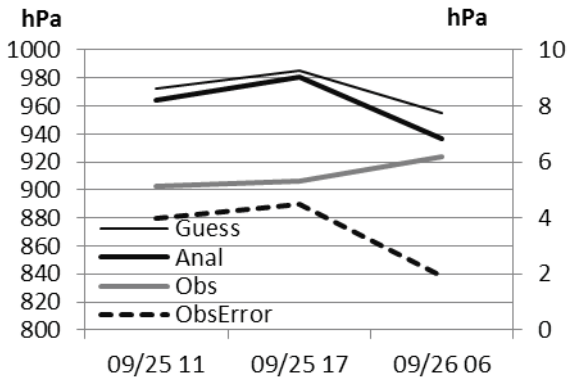

Fig. D-8-5. Surface pressure of first guess (thin black line), analysis results (thick black line) and observation (thick gray line). Observational errors (black dashed line) used in JNoVA are indicated with right axis. After Kawabata et al. (2011).

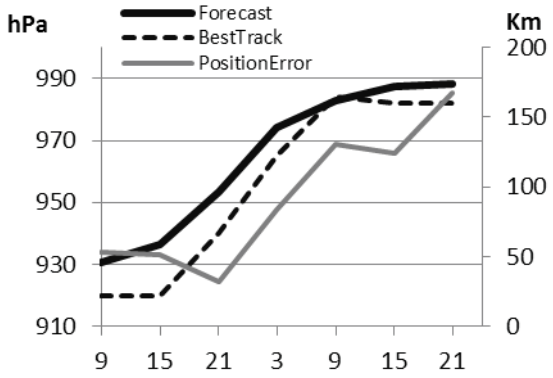

Fig. D-8-6. Forecast results of NHM-5km. Time sequence of center pressure of forecast result (thick line), best track (thin dashed line), and position error comparison with best track data (thin gray line) are indicated. Time sequence of position error uses right axis. After Kawabata et al. (2011).

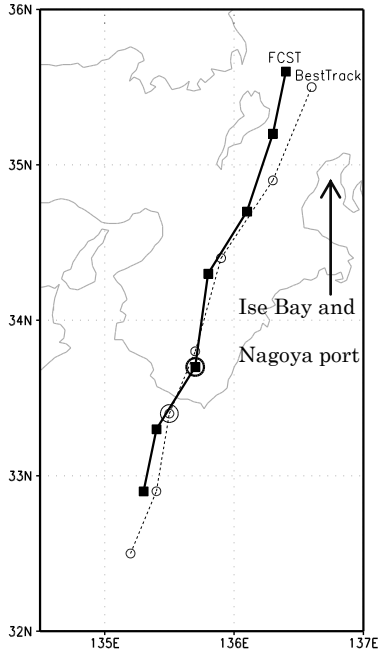

Fig. D-8-7. Typhoon tracks of forecast result (solid line) and best track (dashed line) around the landfall time. Large circles indicate the locations at 18 JST in each track. After Kawabata et al. (2011).

significantly closed to the observation.

D-8-4-2. Forecast results

The TC center pressure and the position error in forecast result are compared with best track data (Fig. D-8-6). The value of center pressure at the initial time is 930 hPa, and difference between the forecast and observation is a small value of 10 hPa. The center pressure becomes large similarly to the observations during forecast time. Position error is also small less than 60 km during 12-h forecast. Forecast tracks around landfall time (Fig. D-8-7) is almost same with best track. Moving speed of forecast is slightly faster than that of observation, but difference is smaller than 1 h.

Next, forecast results are compared with surface weather map. Surface pressure distribution in forecast results (middle panels in Fig. D-8-8) are very similar to the surface weather map (upper panels in Fig. D-8-8). The location and contour distribution of Vera, subtropical high pressure, cold and warm front are same. Especially, frontal rainfall distribution in the forecast result at 03 JST 27 Sep. are agreeing with frontal line

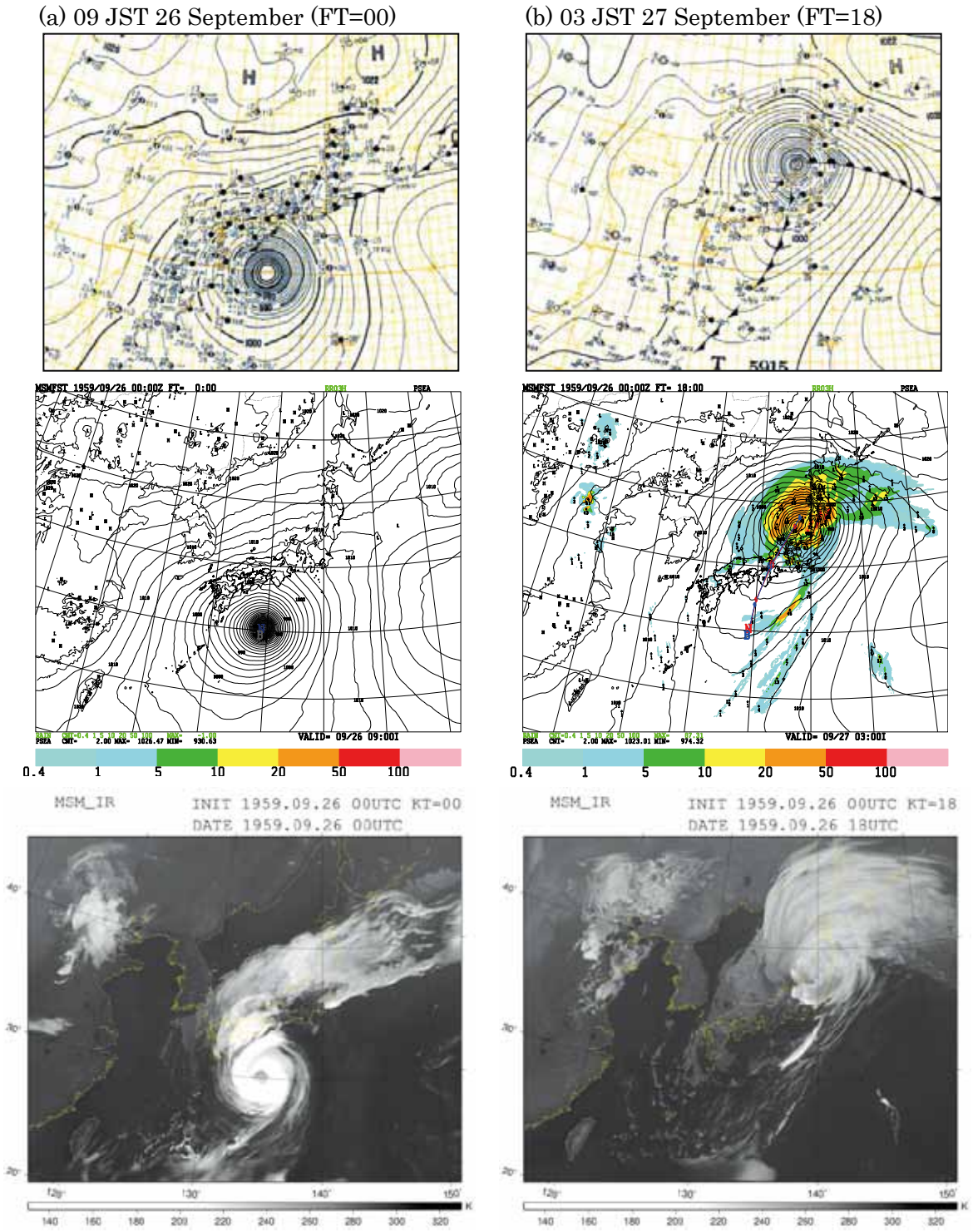

Fig. D-8-8. Upper panels are surface weather map, middle panels show surface pressure and 3-h accumulated rainfall amount, and bottoms are pseudo satellite images derived by forecast results. Blue lines in middle panels illustrate best tracks and reds illustrate forecast tracks.

in the weather map. Weather distribution is estimated by pseudo satellite image (bottoms in Fig. D-8-8). These images are calculated through radiative transfer equations using model forecast results. Rainy or cloudy weather distributions in weather map are match to the estimated weather in the forecast results.

Finally, time sequence of tide level in the forecast result is compared with the observation at Nagoya port in Fig. D-8-9. The tide level was calculated using Princeton Ocean Model (POM) with NHM-5km. The highest tide height of 389 cm in the observation is the maximum record in Japan. Correspondingly, forecast reproduced 352 cm height. Time sequence of forecast strongly resembles observation.

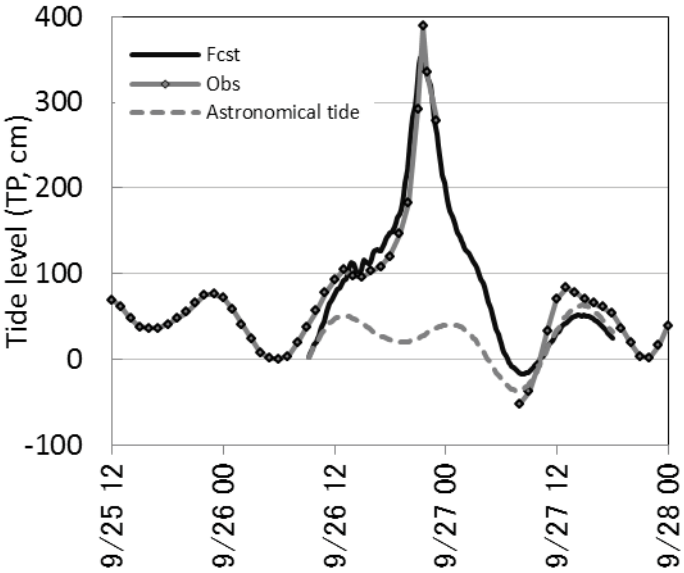

Fig. D-8-9. Time sequence of tide level of forecast (black line), observation (gray line with markers), and astronomical tide (gray dashed line).

D-8-5. Conclusion

Typhoon Vera made landfall Japan in 1959 and induced tragic disaster. Our motivations are confirmation of performance of JMA operational assimilation and forecast system for the typhoon, and challenge to assimilate directly the drop sonde observation in the TC center.

We introduced the observational-error adjustment method, which the value of error is adjusted according to the departure value. This method provided the successful analysis of Vera. In the third assimilation, the departure became small, the analysis of the center pressure and the location significantly closed to the observation.

In the forecast, time sequences of center pressure and location are very similar to best track data. Especially, track around landfall is almost same. Weather distribution in the forecast estimated by rainfall distribution and pseudo satellite image is comparable to the weather map. Finally, tide level calculated through POM is excellent compared with the observation.

Super typhoon Vera before 50 years was well reanalyzed and re-forecasted using JNoVA and JMANHM. Direct assimilation of the drop sonde observation in the TC center was contributed to this result. The basic framework for meteorological disaster prevention was established after Vera and has been still valid. Our result can provide a realistic numerical 4-dimensional data and be useful for the validation on the framework.

Acknowledgement

The authors are grateful to the U.S. army for their courageous observational work. The authors are thankful to the JRA-55 development team, the Climate Prediction Division of JMA, and the global

model team of the ReVera project, especially, Dr. H. Kamahori, Mr. A. Ebita and Mr. Y. Ohta, Mr. Shindo. They provided us pilot data, observation data, and the forecast result of GSM.

This study was partly supported by the Japanese Ministry of Education, Culture, Sports, Science and Technology (MEXT) through a Grant-in-Aid for Scientific Research (21244074) "Study of advanced data assimilation and cloud resolving ensemble technique for prediction of local heavy rainfall".

D-9. Development of Air-Sea Bulk Transfer Coefficients and Roughness Length in JMA Non-Hydrostatic Model[1]

D-9-1. Introduction

New formulation of air-sea bulk transfer coefficients and roughness lengths are introduced in JMA-NHM (Saito *et al.* 2006) to improve the representation of exchange of momentum, sensible and latent heat flux over the ocean surface applied to intense tropical cyclone (TC) (Wong *et al.* 2010). Prediction of TC movement using numerical weather prediction (NWP) model has improved in recent decades due to the advance made in model dynamics and physical processes, data assimilation methods and ensemble prediction system to facilitate the disaster preparedness and mitigation. In addition, TC intensity and wind distribution are inevitably important to assess the impact of high winds and vulnerable areas of wind destruction. More accurate prediction requires development of key physical processes, such as air-sea interaction, to simulate realistic structure and evolution of TC in NWP model. For instance in Powell *et al.* (2003) and Donelan *et al.* (2004), the drag coefficient of momentum or surface momentum flux are found to level off as wind speeds increase above hurricane force. Results from other field experiments (Belamari 2005) also suggest similar saturation properties of bulk coefficients in high wind regime. The existing drag coefficient formulation adopted in operational NWP models, for example in JMA-NHM, based on extrapolation of results from past field studies of surface momentum flux measurement under low and moderate wind speed situations, is therefore likely to be inadequate when applied to intense TC and extreme wind conditions. In the present work, the new bulk transfer coefficients and roughness lengths are implemented in NHM to study an intense TC affecting the South China Sea. Positive impacts are found on the forecasts of TC intensity, wind structure and precipitation pattern.

According to the bulk formulation of aerodynamics, the momentum flux, heat flux and moisture flux are expressed as follows,

$$-\overline{w'u'} = u_*^2 = C_m|U|^2$$
$$-\overline{w'\theta'} = u_*\theta_* = C_h|U|(\theta_s - \theta)$$
$$-\overline{w'q'} = u_*q_* = C_q|U|(q_s - q)$$

where C_m, C_h, C_q are respectively bulk transfer coefficients for momentum, heat and moisture, |U| the mean horizontal wind speed at 10 m above surface. In the original scheme of bulk transfer coefficients in JMA-NHM based on Kondo (1975) and Beljaars (1995), the coefficients vary linearly with the wind speed larger than moderate wind strength (~15 ms^{-1}). A saturation behaviour of C_m for wind speeds exceeding 30 ms^{-1} is introduced as a new formulation of surface momentum flux in NHM following Powell *et al.* (2003) and Donelan *et al.* (2004). Similar level-off in C_h and C_q (Lebeaupin et al. 2007) are implemented in the new scheme. Fig. D-9-1(a) shows the variation of the bulk transfer coefficients in the new scheme against wind speeds at 10 m under neutral condition. In order to consider effects of wave parameters like wave height and periods, modifications of roughness length according to Taylor and Yelland (2001) and Oost *et al.* (2002) are implemented in the roughness lengths of momentum

[1] W.K. Wong, S. Sumdin (TMD) and S.T. Lai (HKO)

(z_{om}). The roughness lengths for heat (z_{oh}) and moisture (z_{oq}) following Fairall *et al.* (2003) are also adopted in the new scheme. Fig. D-9-1(b) shows the variations of roughness lengths under different wind speed.

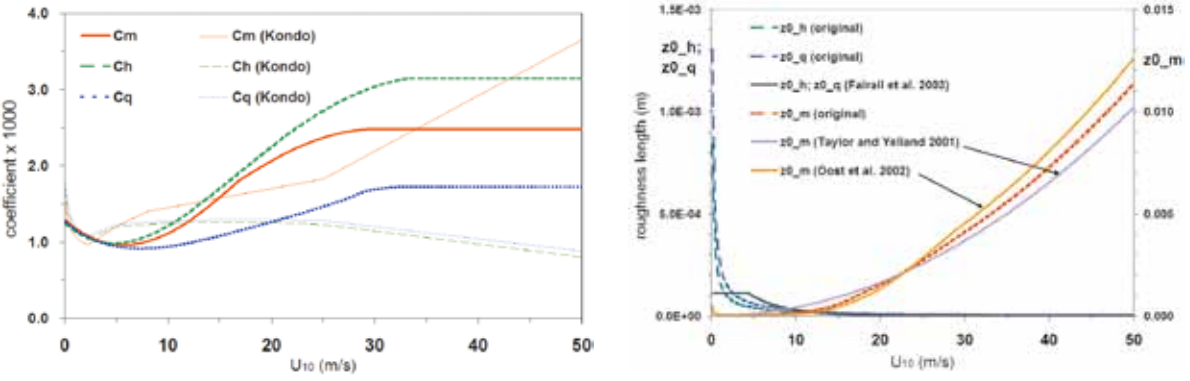

(a) (b)

Fig. D-9-1. (a) Variation of bulk transfer coefficients in the new scheme for momentum (C_m), heat (C_h), and moisture (C_q) against wind speed (ms^{-1}) at 10 m above the surface. Thin lines depicting bulk transfer coefficients in Kondo (1975) scheme. (b) Variation of roughness lengths for momentum (z_{0m}), heat (z_{0h}) and moisture (z_{0q}) against wind speeds at 10 m altitude (in ms^{-1}) under neutral condition. After Wong *et al.* (2010).

D-9-2. Model experiment using new surface scheme

Numerical simulation with NHM is configured in three domains with horizontal resolution at 20 km (RF20), 10 km (RF10) and 5 km (RF5) to perform numerical simulations of Typhoon Hagupit (0814) affecting the South China Sea in September 2008. Model setup can be referred to Wong *et al.* (2010).

a. Impact on intensity prediction and wind radii

Fig.D-9-2 shows the time series of forecast maximum wind near the centre of Hagupit from RF20, RF10 and RF5 experiments. In the new scheme, the reduction of drag coefficient over the high wind regime results in decrease of momentum flux near the centre of Hagupit, leading to increase in maximum wind speed and a larger hurricane wind area. In the outermost domain (RF20), the model cannot resolve the convection and storm structure due to coarse resolution, and the predicted maximum wind from both schemes are lower than the best track values by more than 10 ms^{-1}. In RF10 and RF5, however, the new scheme can give a higher wind speed in general, and similar wind speeds are obtained as compared with the best track data. Maximum wind in RF10 exceeding 40 ms^{-1} is forecast from 1500 UTC 22 September to 0000 UTC 24 September and the highest maximum wind speed and minimum central pressure forecasts are respectively 48 ms^{-1} and 946 hPa. It agrees better with the Hong Kong Observatory (HKO) best track data (49 ms^{-1} and 940 hPa) than using the original scheme (42 ms^{-1} and 952 hPa). Similarly in RF5 experiments, the new scheme gives an improved intensification trend and forecast the highest maximum wind at 53 ms^{-1} (minimum central pressure at 943 hPa), although the initial condition is obtained by downscaling the forecast of RF20 which has much weaker storm intensity than the best track data. RF5 forecast with the original scheme also produces the highest maximum wind at 50 ms^{-1} (minimum pressure at 949 hPa), but the intensification

trend is slower than that from the new scheme. Therefore, the improved forecasts of maximum wind speed and central pressure for Hagupit suggest that the new scheme works effectively to enhance the intensity of strong tropical cyclone in NHM with horizontal grid resolution of 10 km or above.

In wind distribution forecasts, both RF10 experiments using original and new schemes (Fig.D-9-4a and Fig.D-9-4b) can predict areas of hurricane force wind. Moreover, a comma shape annular pattern of distribution is reproduced using the new scheme. Hurricane wind radii are about one degree over the northwestern, northeastern and southeastern quadrants while a smaller radius is forecast to the southwest. This compares favourably with the wind distribution from the NOAA Multi-Platform Satellite Wind (MPSW) Analysis (Knaff and DeMaria, 2006) (Fig.D-9-3), with hurricane wind radii (red shade) ranged from 100 to 140 km over the four quadrants. Fig.D-9-4c and Fig.D-9-4d show the wind distribution forecasts from RF5 experiments. Annular region of hurricane wind area is also forecast by the original scheme, but the area over northwest quadrant is smaller than both the new scheme and the MPSW analysis.

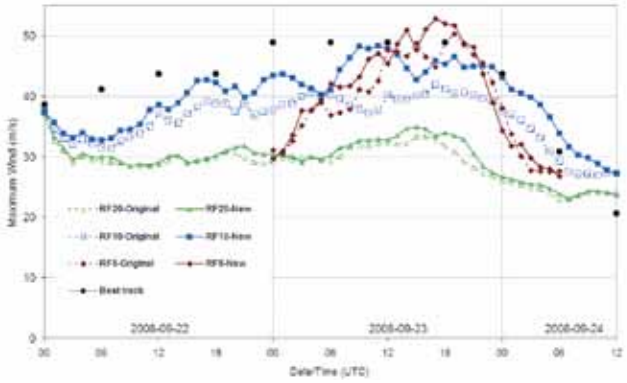

Fig. D-9-2. Time series of maximum wind near the centre of Hagupit from RF20, RF10 and RF5 using the original (dashed line) and new schemes (solid line). Maximum winds from HKO best track analysis are given in black dots. After Wong *et al.* (2010).

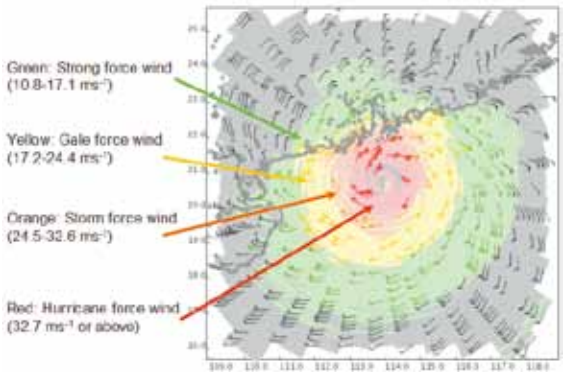

Fig. D-9-3. Surface wind distribution at 1200 UTC 23 September by NOAA Multi Platform Satellite Wind Analysis. After Wong *et al.* (2010).

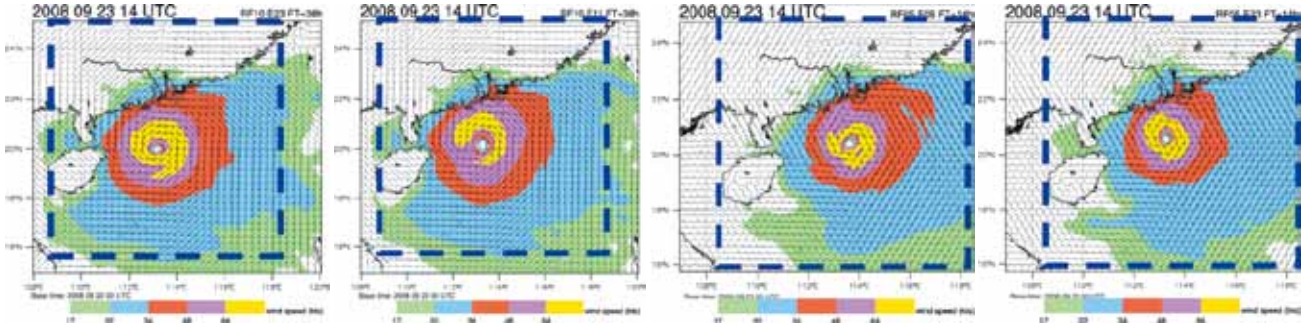

(a) RF10 (original scheme) (b) RF10 (new scheme) (c) RF5 (original scheme) (d) RF5 (new scheme)

Fig. D-9-4. Forecasts of surface wind barbs and isotach at 1400 UTC 23 September 2008 using the (a) original and (b) new schemes in RF10 experiments. The color shading of green / blue / red / violet / yellow represents areas of fresh (8.0-10.7 ms^{-1}) / strong / gale / storm / hurricane force winds respectively. (c)-(d) Similar forecasts from RF5 experiments. Area in Fig.D-9-4 is shown by dashed line boxes. After Wong *et al.* (2010).

b. Effects in precipitation forecast

Heat and moisture fluxes are enhanced due to larger heat and moisture bulk coefficients in the

new scheme, resulting in enhancement of vertical eddy transport of moisture and heat to sustain the development of Hagupit, as well as an increase of moisture in cloud and convective parameterization processes of NHM. Fig. D-9-5 (a)-(c) show the forecasts of sea level pressure and 1-hour accumulated rainfall at 1400 UTC 23 September 2008 from RF20, RF10 and RF5 using the original (top panel) and new scheme (bottom panel). Using the new scheme, spiral rainbands are better predicted when compared to radar reflectivity and TRMM rainfall rate. Improvements in the model forecast on the intensity and structure of rainbands are useful for nowcasting application and very-short-range forecast of the heavy precipitation due to passage of intense tropical cyclones (Lai and Wong 2006).

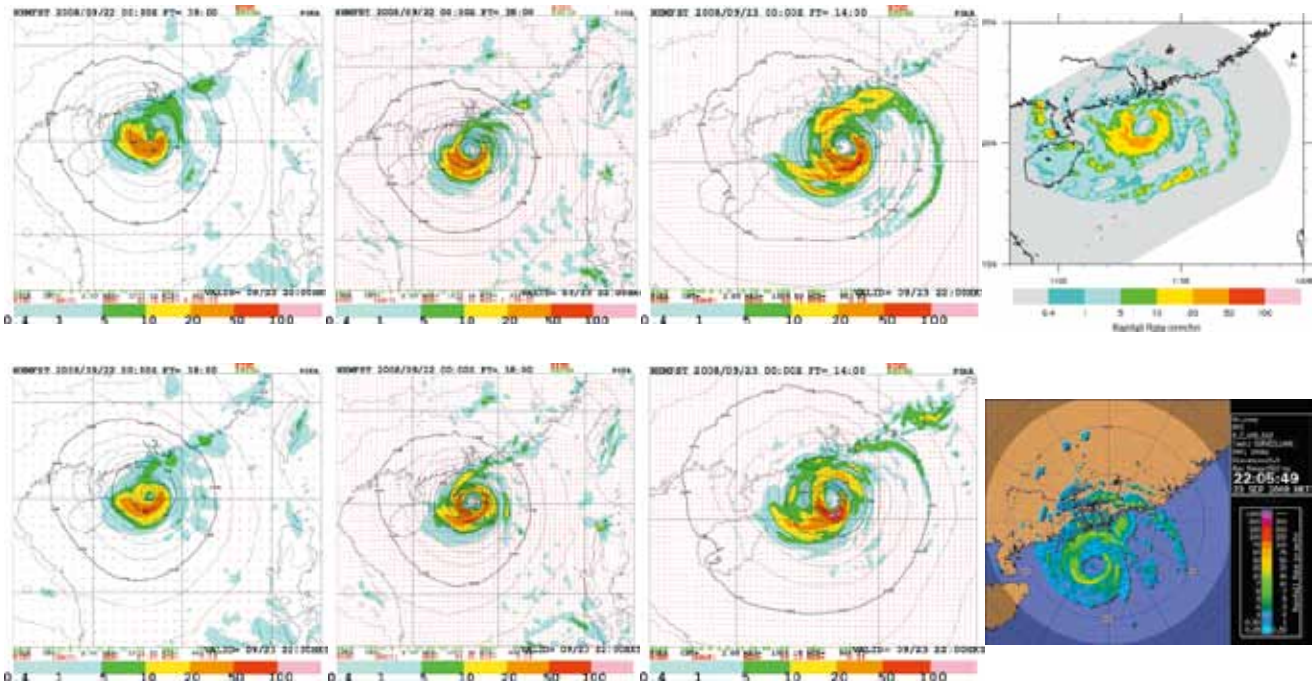

(a) RF20 (b) RF10 (c) RF5 (e)

Fig. D-9-5. Forecast mean-sea-level pressure (contour) and 1-hr accumulated rainfall (color shade) by (a) RF20, (b) RF10 and (c) RF5 at 14 UTC 23 September 2008 using the original scheme (top panel) and new scheme (bottom panel); (d) Rainfall rate estimate at 1425 UTC from TRMM (2A12 product from JAXA/EORC Tropical Cyclone Database); (e) Plan position indicator (PPI) display of radar reflectivity at 1405 UTC. After Wong *et al.* (2010).

D-9-3. Summary and Future Development

Using the new scheme of air-sea bulk transfer coefficients and roughness lengths in JMA-NHM, an increase in forecast maximum wind speed with a lower central pressure of Typhoon Hagupit are obtained, due to reduced drag coefficient and larger heat and moisture bulk coefficients in high wind regime. They contribute positively to the exchange of surface fluxes to sustain the development of Hagupit, distribution of high wind areas and rainbands near the centre of Hagupit. The new scheme thus provides potential benefits in using NHM to simulate other intense tropical cyclones and effects of bulk coefficients in high wind regime for weather forecasts and climate studies on wind-pressure relationship of intense tropical cyclones. The roughness lengths are modified and sea-wave effect is considered in the new scheme, though more accurate specification of wave parameter values requires future in-depth study using coupled atmosphere-wave model or field experiments.

E. Observation and NWP in Southeast Asia

E-1. Towards a mesoscale observation network for Southeast Asia[1]

Current conventional meteorological observations in Southeast Asia are clustered around the coastal regions due to the maritime nature and unique topography of the region. Coupled with the standard time interval of 6 to 12 hours between sampling, the region's conventional observation network lacks the spatial and temporal resolution to adequately capture the convective weather systems dominant in the region for weather forecasting and research.

The deployment of a transnational mesoscale testbed comprising ground-based remote and in situ sensors around the Straits of Malacca to investigate the Sumatra squalls could be a possible first step towards realizing a Southeast Asian mesoscale observation network. Improvement to the regional observational network could be achieved in parallel through integrating the existing weather radars operated by the various national weather agencies. Promoting the judicious use of weather satellite data in weather forecast and research should augment the lack of weather observations over the seas. These radar and satellite data if optimally assimilated, is expected to improve NWP forecast accuracies given the current dearth of conventional observations.

Although the sharing of radar data and the assimilation of more satellite data would be significant initial steps forward, more could be achieved through gradual, sustained and coordinated regional efforts in deploying in situ and remote-sensing instruments first in testbeds, but eventually as multi-sensor weather monitoring clusters. The mature mesoscale observation network is envisioned to comprise several coordinated radar, remote sensor subnets, in situ instruments, and satellite data receiving stations (Koh and Teo 2009). Due to the region's rich diversity, managing this mesoscale observation network could be through a confederation of the national or private stakeholders of this network (Fig. E-1-1). Apart from benefiting weather forecasts, the data collected by the network would act as a stimulus for much needed research into Southeast Asian weather systems.

Fig. E-1-1. Schematic diagram of the envisioned mesoscale observation network with its component subnets and various stakeholders. After Koh and Teo (2009).

[1] T.-Y. Koh and C.-K. Teo (NTU)

E-2. Development of Operational Rapid Update Non-hydrostatic NWP Model and Data Assimilation System in the Hong Kong Observatory[1]

E-2-1. Introduction of NWP System in HKO

A mesoscale NWP model system has been operated by the Hong Kong Observatory (HKO) using the Operational Regional Spectral Model (ORSM) since 1999. ORSM is formulated using the hydrostatic governing equations to provide numerical model guidance for short-term weather prediction up to 3 days ahead. The finest horizontal resolution is 20 km and the model run is updated every 3 hours. With the recent advances made in NWP modeling, HKO commenced the implementation and experimental trials of non-hydrostatic models a few years ago, with a view to enhance the capability of quantitative precipitation forecast (QPF) and prediction of severe weather phenomena and mesoscale convective systems. In April 2004, HKO started to operate the JMA Non-hydrostatic Model (NHM) (Saito *et al.* 2006) in trial basis to provide very-short-range (1-12 hours) forecasts which are rapidly updated at every hour with a high resolution (grid spacing at 5 km) covering an area of about 600 km x 600 km centred over Hong Kong. The initial and boundary conditions are obtained from the ORSM. In order to reduce the spin-up time of the model and improve the model QPF, the specific humidity fields of the cloud hydrometeors in NHM are initialized by the 3-dimensional cloud analysis output from the Local Analysis and Prediction System (LAPS) (Albers *et al.* 1996). Radar reflectivity, Doppler radial wind and geostationary satellite cloud data (visible albedo and infrared brightness temperature) are ingested into LAPS to generate the humidity fields of hydrometeors. Improvements in model QPF are obtained that facilitate the development of blending technique with nowcast QPF (Wong and Lai 2006). At the same time, forecasts from NHM are used to provide background data to LAPS for mesoscale real-time analysis with horizontal resolutions from few kilometres to few hundreds metres.

With experience gained on using JMA-NHM over the last few years, HKO has developed a new NWP system based on NHM, also called the Atmospheric Integrated Rapid cycle (AIR) forecast model system, and has been put into operation since June 2010. AIR forecast model system has two forecast domains with horizontal resolutions at 10 km and 2 km. With substantial increase in the horizontal resolution, use of non-hydrostatic governing equations and more advance model physics, the new system enhances the capability to resolve mesoscale and local-scale weather phenomena, and their evolution from very-short-range to 3 days ahead.

In this paper, the design and experimental results of the AIR forecast model system are described. In the next two sections, specifications of NHM and its data assimilation system will be presented. Performance of NHM in a couple of case studies on QPF, tropical cyclone movement and intensity, as well as the model verification on upper-level wind forecasts against aircraft data will be illustrated in E-2-4. A short summary including aspects of future research and development of AIR system will be given in section E-2-5.

[1] W.K. Wong

E-2-2. Description of NHM in AIR Forecast Model System

Figure E-2-1 shows the coverage of the two NHM domains in AIR forecast model system. The outer domain, denoted by Meso-NHM, has the horizontal resolution of 10 km with 50 terrain-following vertical levels. Meso-NHM has an analysis-forecast cycle of 3 hours to provide the forecast up to 72 hours ahead. It is targeted to simulate rainstorm, tropical cyclone track and intensity, and other mesoscale weather systems. The boundary condition of Meso-NHM is obtained from the forecasts of JMA Global Spectral Model (GSM;JMA 2007) that are updated every 6 hours (initial times at 00, 06, 12 and 18 UTC) with a horizontal resolution of forecast data at 0.5 degree in latitude and longitude. The sea-surface temperature (SST) is specified by the NCEP high resolution real-time daily SST analysis at 0.083 degree. The inner domain, called the RAPIDS-NHM, has a horizontal resolution of 2 km with 60 vertical levels. Its boundary condition is based on the forecasts from Meso-NHM. RAPIDS-NHM provides forecasts up to 15 hours ahead and the model forecast is rapidly updated at every hour with a view to enhance the analysis and prediction of mesoscale and convective weather phenomena as well as to provide an improved model QPF to blend with the radar-based precipitation nowcast. More details on the specification of Meso-NHM and RAPIDS-NHM are given in Table E-2-1.

E-2-3. Data Assimilation System of AIR/NHM

The data assimilation of NHM in AIR forecast model system is developed on the basis of JNoVA-3DVAR (**J**MA **No**n-hydrostatic model based **V**ariational data **A**ssimilation system). It is implemented as the hourly analysis system in JMA and the design is originated from the JNoVA-4DVAR (Honda *et al.* 2005) which is the operational data assimilation system for JMA Mesoscale Model (MSM) using NHM with a horizontal resolution of 5 km (JMA 2007). Like the other variational data assimilation system, JNoVA-3DVAR computes the best linear unbiased estimate of the control variables representing the model states that minimize the following cost function:

$$J(\mathbf{x}) = \frac{1}{2}(\mathbf{x}-\mathbf{x_B})\mathbf{B}(\mathbf{x}-\mathbf{x_B})^T + \frac{1}{2}(\mathbf{y}-\mathbf{Hx})\mathbf{R}(\mathbf{y}-\mathbf{Hx})^T ,$$

where $\mathbf{x}$, $\mathbf{x_B}$ are respectively control variable vector and model background field. They include horizontal wind components (u,v), surface pressure (p_s), potential temperature (θ) and pseudo relative humidity representing the ratio of specific humidity of water vapour to its saturation value. $\mathbf{y}$ represents a state vector containing observation data and $\mathbf{H}$ is the observation operator. $\mathbf{B}$ and $\mathbf{R}$ are respectively observation and background error covariance matrices where $\mathbf{B}$ matrix is estimated based on the NMC method (Parrish and Derber 1992).

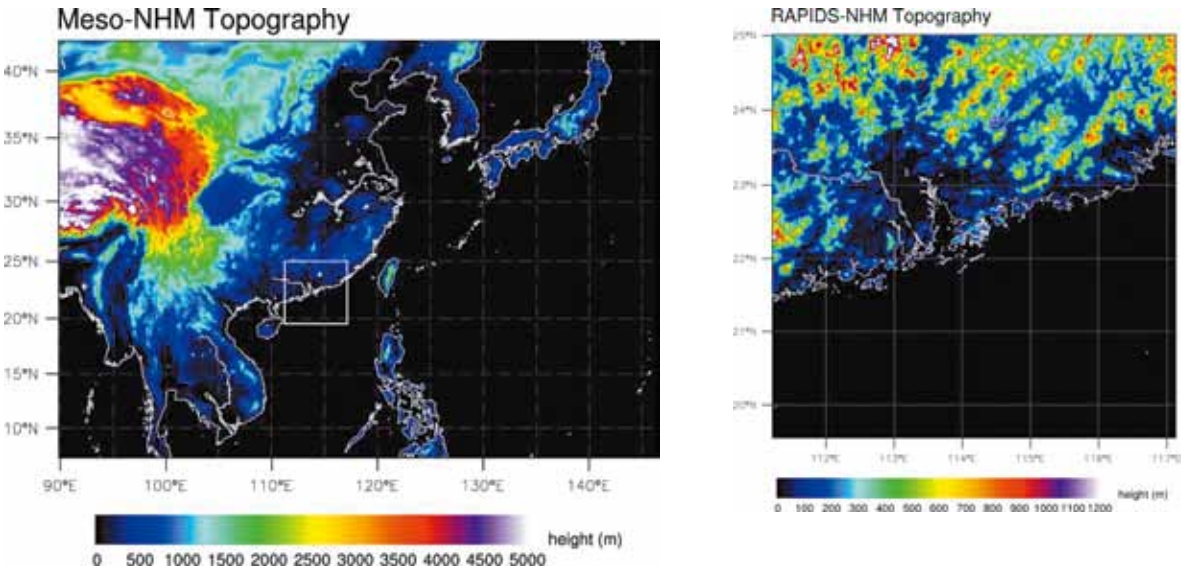

Fig. E-2-1. Spatial coverage of Meso-NHM and RAPIDS-NHM. Altitude of model topography (in metre) is given in color shading.

Table. E-2-1. Specification of Meso-NHM and RAPIDS-NHM in AIR Forecast Model System.

	Meso-NHM	**RAPIDS-NHM**
Horizontal resolution	10 km	2 km
Horizontal grid	Arakawa-C	
Map projection	Mercator	
No. of grid points	585x405	305x305
Vertical coordinates	Terrain following height coordinates using Lorenz grid	
No. of vertical levels	50	60
Time step	30 s	8 s
Initial time	00, 03, 06,…, 21 UTC	Every hour
Forecast range	72 hours	15 hours
Initial condition	JNoVA-3DVAR with background from JMA GSM forecast	JNoVA-3DVAR with background from Meso-NHM
Boundary condition	JMA GSM forecast data at 0.5 degree resolution in lat/lon	Meso-NHM forecasts
Nesting configuration	One-way nesting	
Topography	USGS GTOPO30 (30 second data smoothed to 1.5 times horizontal resolution) with modifications over HK areas based on USGS-SRTM (Shuttle Radar Topography Mission)	
Land-use characteristics	USGS Global Land Cover Characterization (GLCC) 30 second data and 24 land-use types with modification over HK areas	
Dynamics	Fully compressible non-hydrostatic governing equations solved by time-splitting horizontal-explicit-vertical-implicit (HEVI) scheme using 4-order centred finite differencing in flux form	
Cloud microphysics	3-ice bulk microphysics scheme	
Convective parameterization	Kain-Fritsch scheme (JMA version)	-
Surface process	Flux and bulk coefficients: Beljaars and Holtslag (1991), Donelan et al. (2004), Belamari (2005); Roughness length: Beljaars (1995) and Fairall et al. (2003); Stomatal resistance and temporal change of wetness included; 4-layer soil model to predict ground temperature and surface heat flux.	
Turbulence closure model and planetary boundary layer process	Mellor-Yamada-Nakanishi-Niino Level 3 (MYNN-3) (Nakanishi and Niino, 2004) with partial condensation scheme (PCS) and implicit vertical turbulent solver. Height of PBL calculated from virtual potential temperature profile.	
Atmospheric radiation	Long wave radiation process follows Kitagawa (2000) Short wave radiation process using Yabu and Kitagawa (2005) Prognostic surface temperature included; Cloud fraction determined from PCS.	

The observation data that can be assimilated in JNoVA-3DVAR include conventional observations from synoptic weather stations, radiosonde, buoy and ship reports, as well as data from automatic weather stations in Hong Kong and the Guangdong province, wind profilers, aircraft (AMDAR reports), atmospheric motion vector (AMV) from MTSAT-1R/MTSAT-2 geostationary satellite and retrieved ATOVS (Advanced TIROS Operational Vertical Sounder) temperature profile from NOAA polar-orbiting satellites. Total precipitable water vapour (TPWV) retrieved from microwave sounders (SSM/I and AMSR-E) is ingested in the Meso-NHM analysis, while TPWV from the local Global Positioning System (GPS) network signals are assimilated in RAPIDS-NHM to analyse the humidity contents. For the initialization of tropical cyclone, JNoVA-3DVAR includes a bogus scheme that is based on the forecaster's analysis on central pressure, maximum wind and radius of strong wind to construct vertical profiles of horizontal wind components around the tropical cyclones, with asymmetric effects of storm structure taken into account. The wind profiles are then assimilated into JNoVA-3DVAR in a similar way as the other upper-air wind data but using different error characteristics. Furthermore, Doppler radial velocity data from the two weather radars in Hong Kong are also assimilated in RAPIDS-NHM analysis.

E-2-4. Case Studies

In this section, discussions will be given to illustrate the performance of NHM in a couple of cases on significant convection and tropical cyclone forecasts. Verification on the analysis and forecast performance of NHM on weather elements and a comparison with ORSM will also be discussed.

a. Rainstorm on 24 May 2009

On 24 May 2009, a broad area of low pressure affected the northern part of the South China Sea. Meanwhile, a ridge of high pressure was established over southeastern part of China that resulted in convergence of easterly and southerly airstreams and successive development of rainbands over the coastal areas (Fig. E-2-2a - c). Figure E-2-3a depicts the forecasts of sea-level pressure and hourly accumulated rainfall at 0400 UTC on 24 May 2009 from Meso-NHM initialized at 1800 UTC on 23 May. Meso-NHM can successfully simulate the rainbands over the coastal water. It can be revealed from the forecasts of winds and relative humidity on 850 hPa and 700 hPa levels (Figs. E-2-3b and E-2-3c) that the development of the rainbands was associated with the low-level jet of moist southeasterly winds (areas enclosed by the red isotach representing 20 knots and above). As the convection predicted by Meso-NHM is quite shallow, the precipitation forecast by the model is less than the actual rainfall from radar estimate. Figure E-2-3d shows the forecast at the same time by RAPIDS-NHM which is initialized by the 3-hour forecast from Meso-NHM including the mixing ratio of the cloud hydrometeors. In general, the forecasted rainbands from RAPIDS-NHM have more detailed structures due to increased horizontal resolution, which are more consistent with the rainbands shown on the radar imagery in terms of their size and orientation in northwest-southeast direction.

(a)

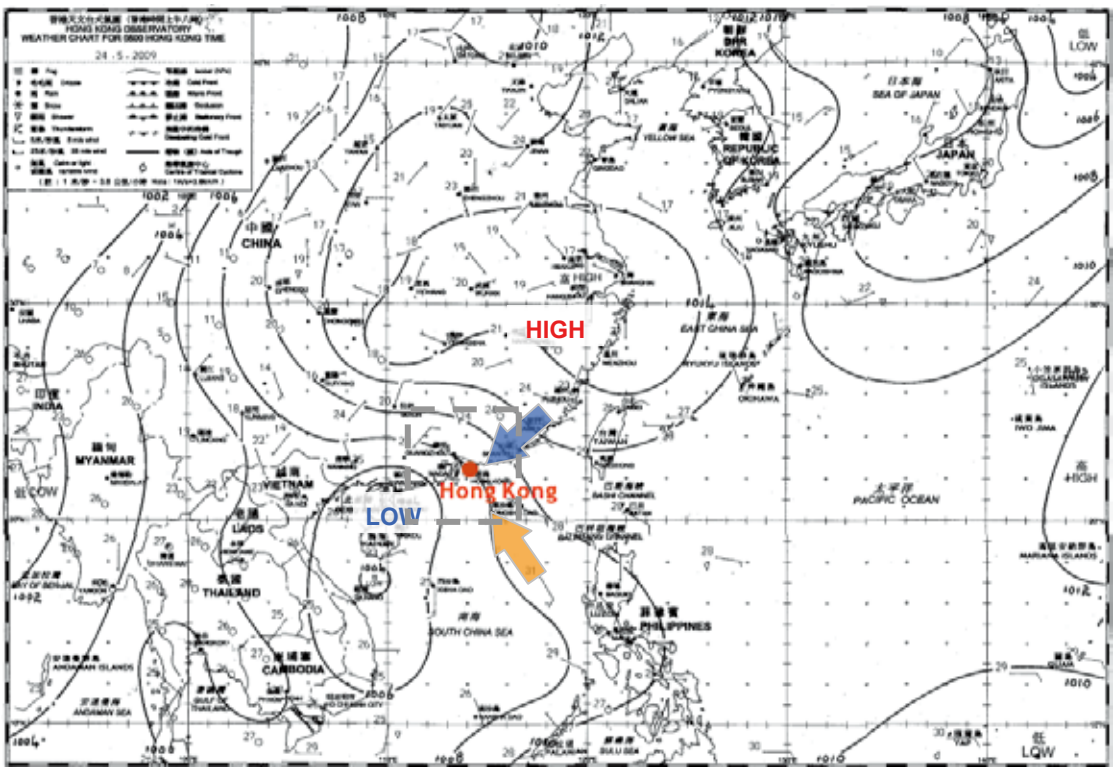

(b)

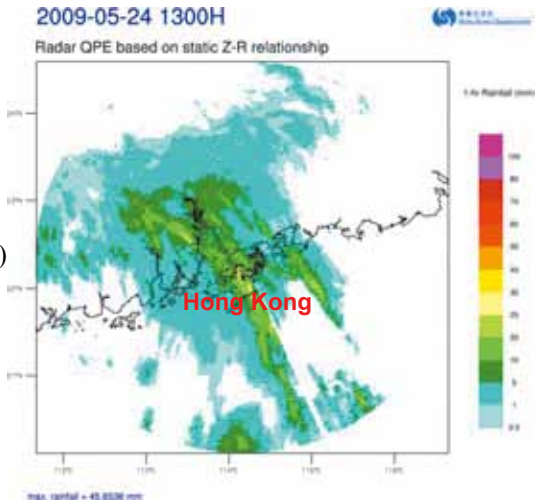

(c)

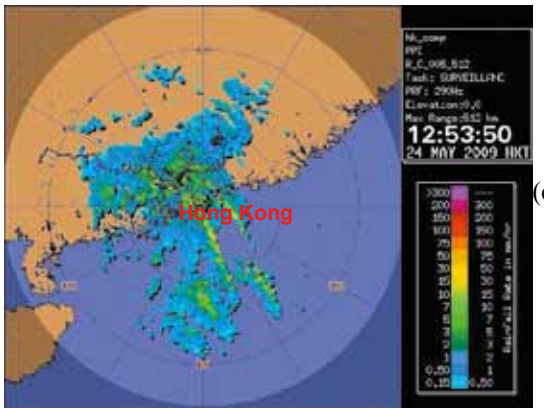

Fig. E-2-2. (a) Synoptic analysis at 0000 UTC (0800 HKT) 24 May 2009 (0800 HKT); (b) Radar rainfall analysis of 1-hr accumulated rainfall (in mm) at 1300 HKT and its spatial coverage is shown by grey dash line in (a); (c) radar reflectivity imagery at 1253 HKT.

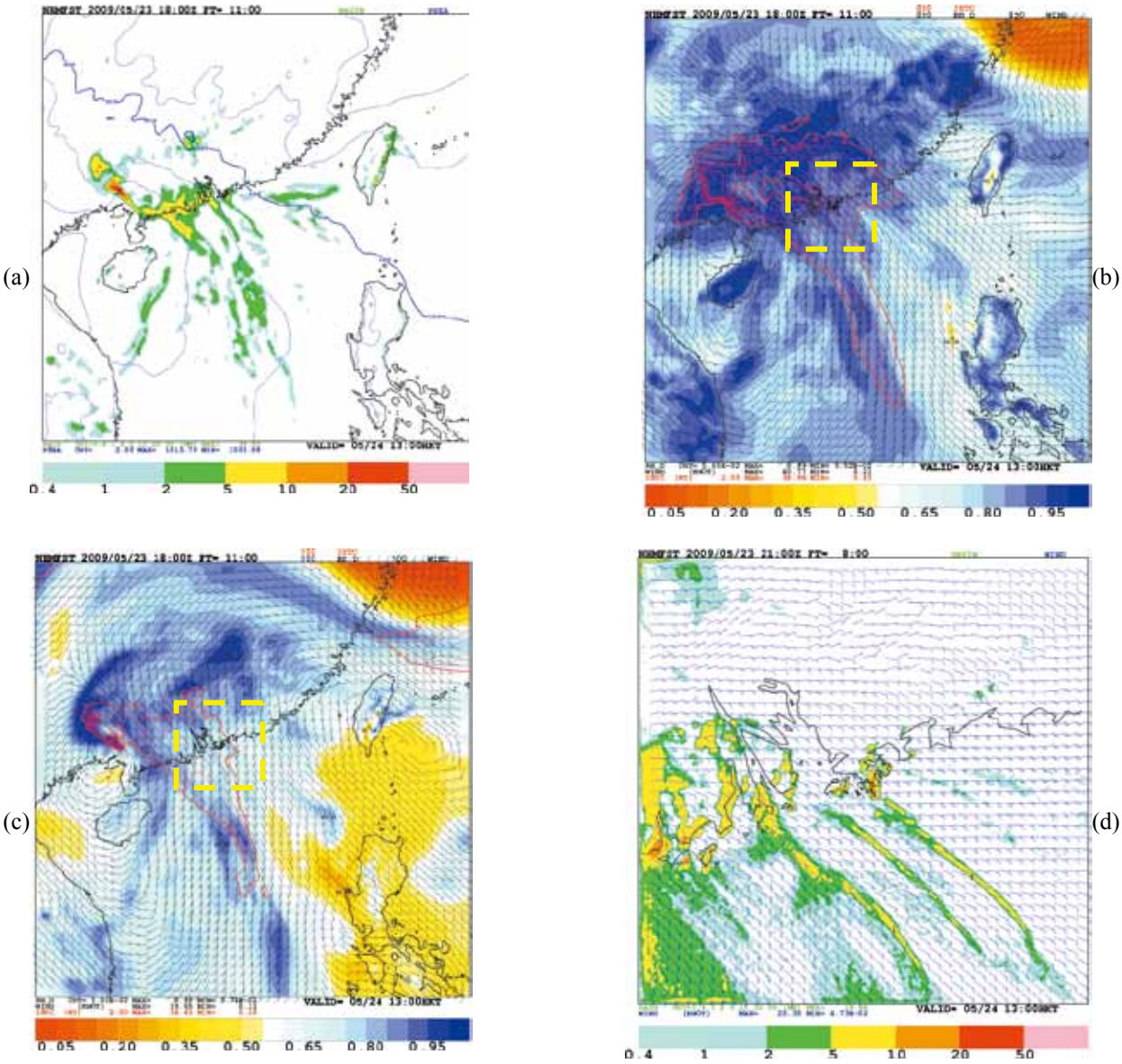

Fig. E-2-3. (a) Forecast of sea-level pressure and 1-hour accumulated rainfall (in mm) at 1200 HKT 24 May 2009 by Meso-NHM; Forecast of relative humidity (color in percentage) and winds on (b) 850 hPa and (c)700 hPa levels, areas enclosed by red contour representing wind speed exceeding 20 knots; (d) Forecast of 1-hour accumulated rainfall and surface wind at 1200 HKT by RAPIDS-NHM. Coverage of RAPIDS-NHM is shown in yellow dash line in (b) and (c).

b. Typhoon Koppu (0915) – Effects of bogus in TC intensity analysis and forecast

Figure E-2-4a shows the 3DVAR analysis of Meso-NHM on the surface wind and sea-level pressure of tropical cyclone Koppu (0915) at 1200 UTC 13 September 2009. Bogus wind profiles are assimilated in the analysis. At that time, Koppu had just intensified into a tropical storm with maximum wind at about 35 knots. The analysed central pressure is 991 hPa that agrees with the forecaster's real-time analysis. Compared to the background field (Fig. E-2-4d) as interpolated by the GSM forecasts, the intensity of Koppu is improved through the bogus data assimilation as the central pressure is deepened by about 10 hPa. The 24 hour and 48 hour of forecasts using the above 3DVAR analysis (first guess from GSM) as initial conditions are given in Figs. E-2-4b and c (E-2-4e and f),

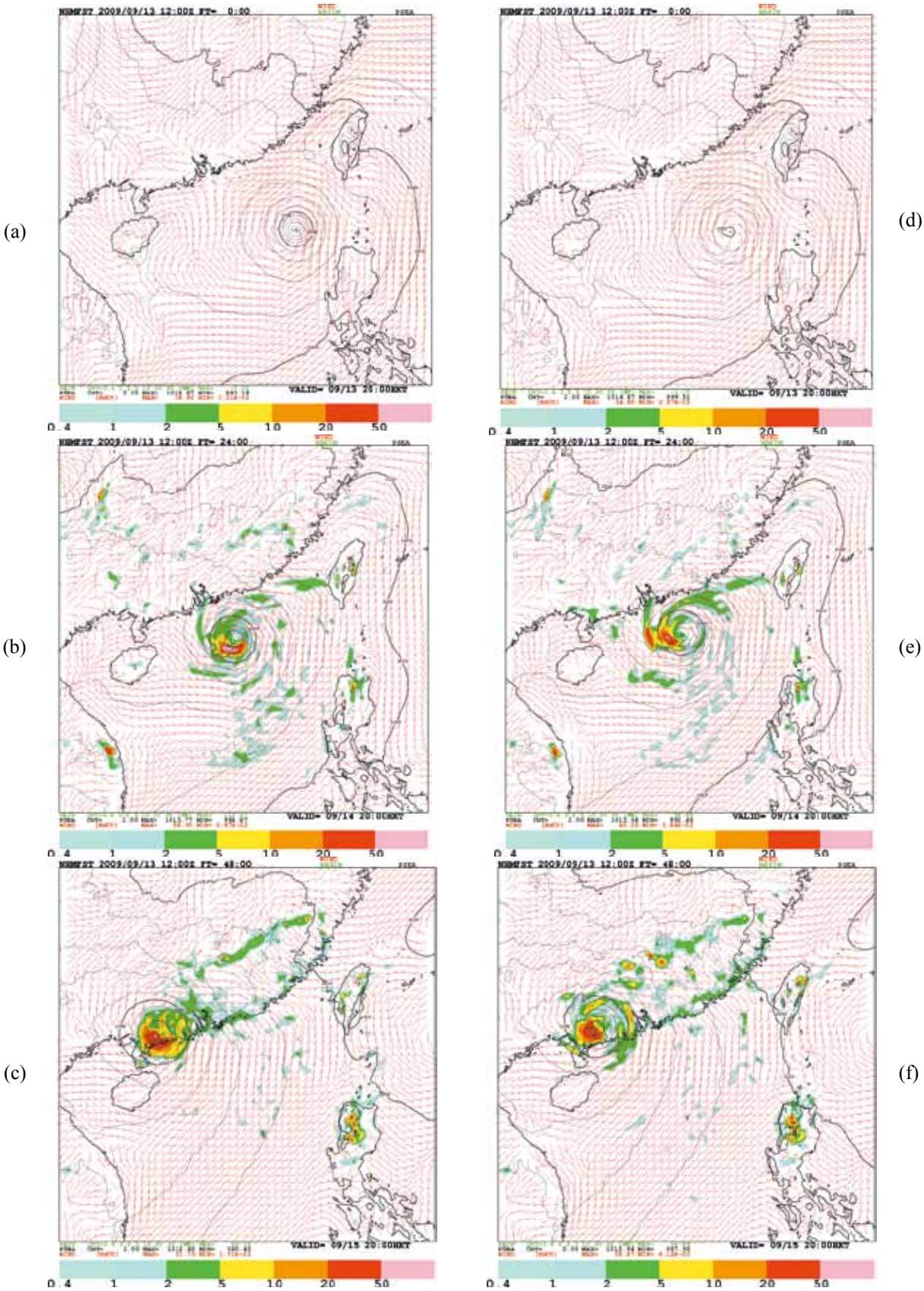

Fig. E-2-4. (a) JNoVA-3DVAR analysis of surface wind, sea-level pressure at 12 UTC 13 September 2009 by Meso-NHM; (b)-(c) 24 hour and 48 hours forecast overlaid with 1-hour accumulated rainfall (color in mm). Corresponding initial field and forecasts without 3DVAR analysis are shown in (d)-(f).

respectively. The forecast tracks are shown in Fig. E-2-5a, indicating that tracks from the two experiments are quite similar, although the time of landfall from the two experiments both lag behind the actual track by about 12 hours. Nevertheless, the bogus data assimilation results in a better intensification trend of Koppu (Fig. E-2-5b) as the winds on upper levels within the bogus region are strengthened. The maximum wind speed (MWS) near surface is increased by 22 knots in the 24 hour forecasts with bogus data assimilation while MWS is increased by only 5 knots in the other case.

(a)

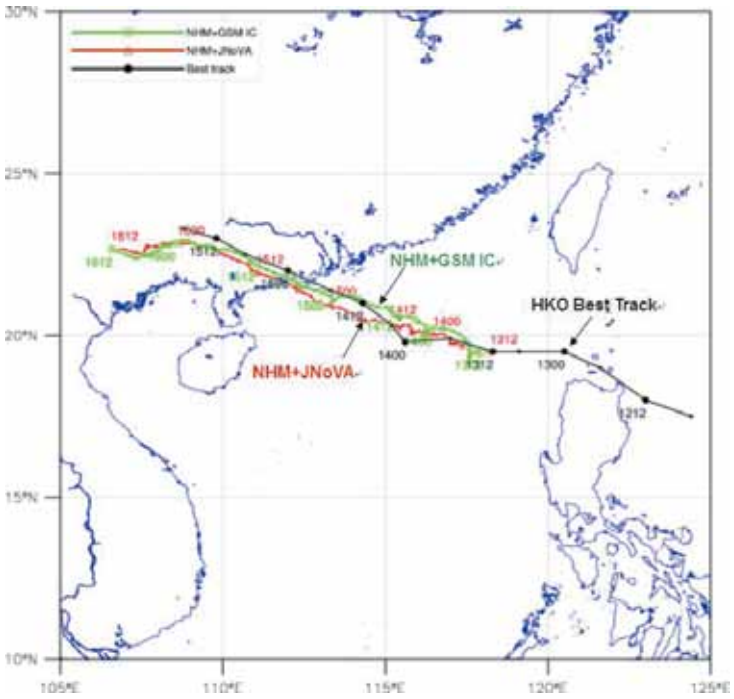

(b)

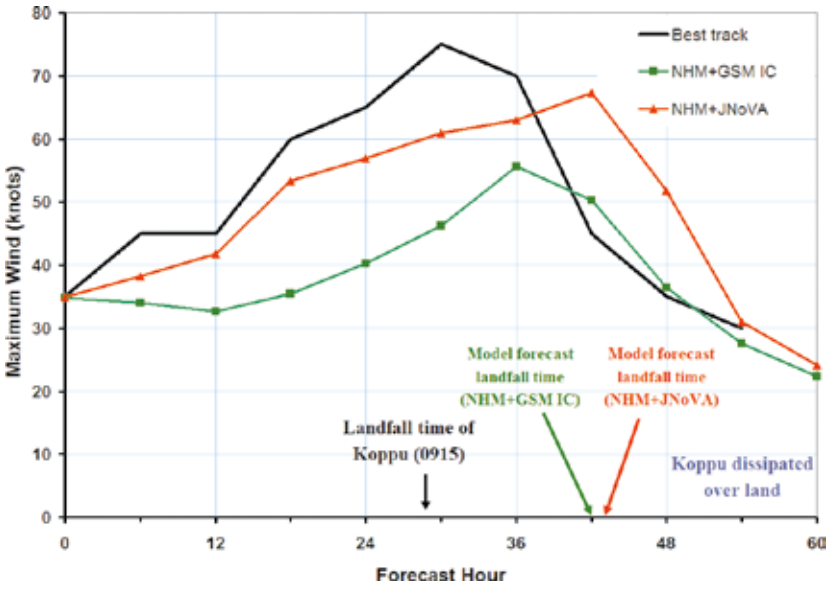

Fig. E-2-5. (a) Forecast tracks of Koppu (0915) by Meso-NHM using JNoVA-3DVAR analysis (red line with triangle marks) and initial condition interopolated from GSM forecast (green line with square marks). HKO best track is shown in black line with dots indicating the 6-hourly positions; (b) Maximum wind near centre of Koppu by the two experiments. HKO best track data is shown in black line.

c. Severe thunderstorm on 8 September 2010

In late evening on 8 September 2010 to the following early morning, widespread thunderstorms and significant convection affected the coastal regions of Guangdong and Hong Kong. During the day on 8 September, under the influence of the subsistence effect associated with the outer circulation of tropical cyclone Meranti (1010) near Taiwan, the weather was very hot over southeastern China that favoured a widespread development of convective cells under this strong thermal forcing. From successive RAPIDS-NHM runs initialized in the afternoon (Fig. E-2-6a-c), intense precipitation is forecasted to develop over Guangdong coastal area and later affects Hong Kong and Pearl River Delta region. The indication on the convective development during the overnight period is consistent based on forecasts from successive model runs, though the timing on the passage of severe thunderstorm is lagged behind the actual by about 2 hours. RAPIDS-NHM also suggests the severe convective system will bring high wind gusts upon its passage. Figure E-2-7a shows the forecasted surface wind vector (white arrow) and the total wind gust (summation of forecast surface wind at 10 m level and the wind gust component depicted in color shading) at 0200 HKT 9 September, indicating that wind gusts exceeding 30 knots affect western part of the territory including the Hong Kong International Airport (HKIA). At 975 hPa, the gale force wind is forecasted near HKIA (region X; Fig. E-2-7b). From the cross section along line AB (Fig. E-2-7c), the wind speed exceeds 37 knots at 900-950 hPa levels which agrees well with an aircraft observation taken upon descend of flight towards HKIA. RAPIDS-NHM successfully forecasts the whole structure of thunderstorm and associated gust front system. Figure E-2-7c depicts the vertical cross section equivalent potential temperature (EPT in color shade) along the line AB where large EPT gradient can be seen near the gust front region (near the middle of XB). Warm moist air mass to the southwest is lifted up by the gust front while significant downdraft (Fig. E-2-7d) is found along XA that the cooler air mass is brought from about 3-4 km in altitude to near surface and spread out laterally.

With further development in data assimilation and the forecast model, the spatial-temporal error of model quantitative precipitation forecast (QPF) associated with severe convective systems could be further reduced. Moreover, through the use of an optimal phase correction technique, the model QPF can provide useful guidance on the development of significant precipitation through the blending with nowcast QPF based on extrapolation technique of radar imagery (Wong *et al.* 2009). Figures E-2-8a and b show the T+5 hour radar nowcast QPF and blending QPF at 01HKT on 9 September. It is clearly seen that RAPIDS-NHM provides signs of significant rainfall over HK during 00-01 HKT. The phase correction is applied to relocate the model QPF pattern when radar imagery is made available every 6 minutes. In this case, the blending output is also found to give a consistent scenario on the significant precipitation over Hong Kong during the overnight period. Further development will be conducted to study the techniques to improve both model forecasts and blending algorithms, in order to enhance the capability in forecasting significant convection to support both aviation and public weather services.

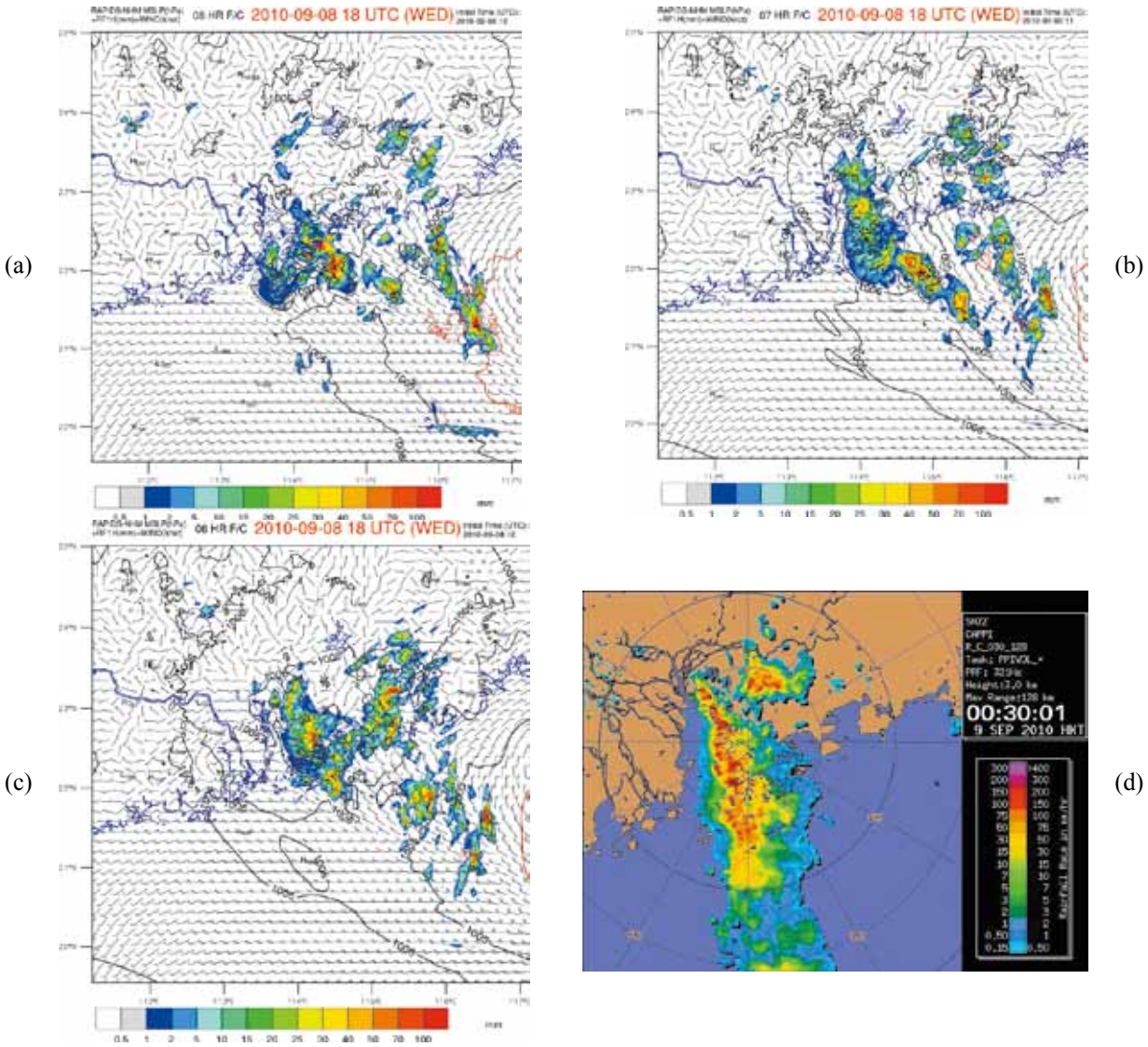

Fig. E-2-6. RAPIDS-NHM forecasts of hourly accumulated rainfall (color in mm) and mean-sea-level pressure at 02:00 HKT 9 September 2010, with model runs initialized from 10 to 12 UTC 8 September shown in (a)-(c) respectively; radar reflectivity image at 00:30 HKT 9 September 2010 shown in (d).

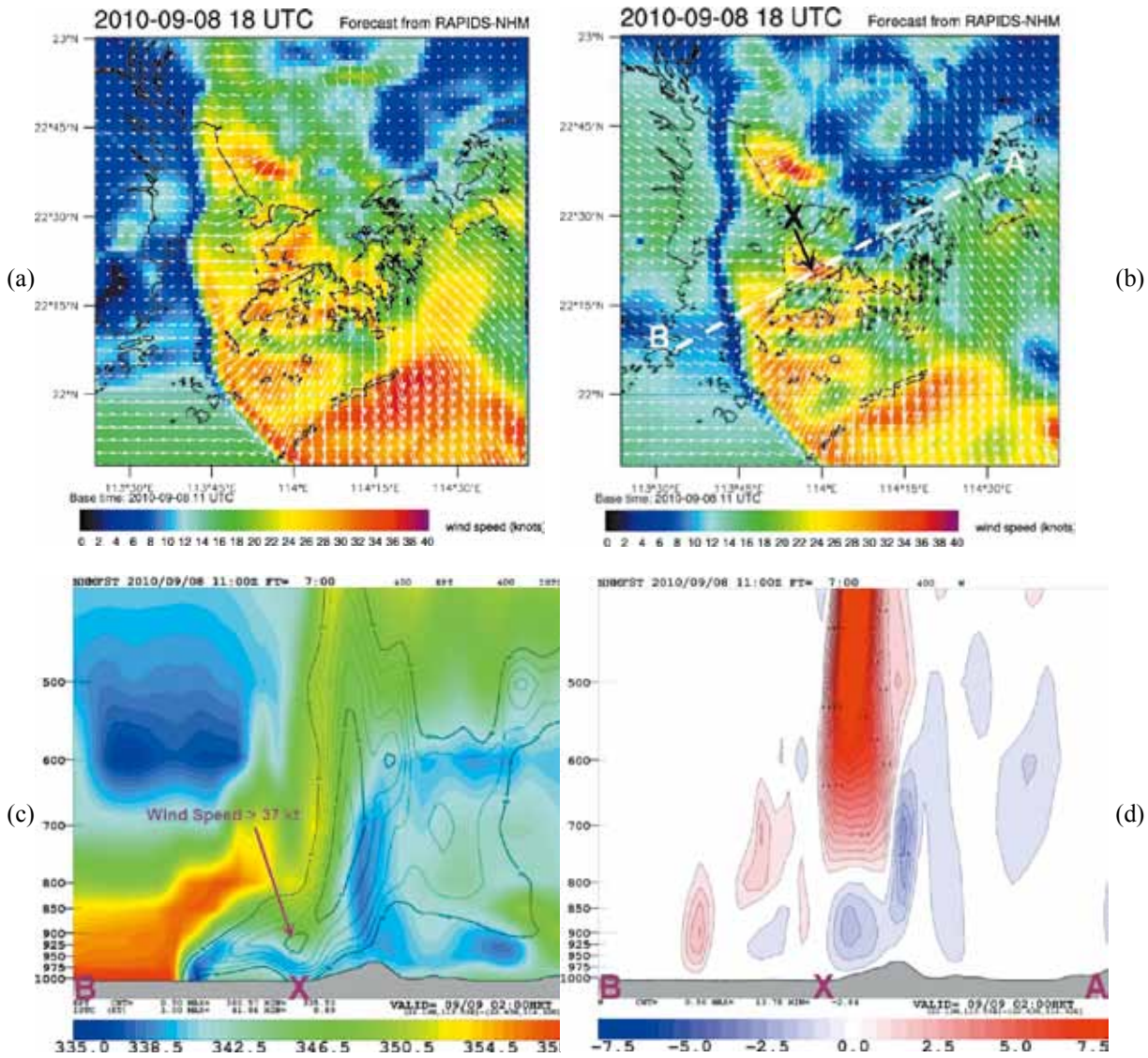

Fig. E-2-7. RAPIDS-NHM T+7h forecasts at 02 HKT 9 September 2010 on: (a) surface wind direction (white arrows) and magnitude of wind gust (color shade in knots); (b) wind speed (color in knots) and wind direction on 975 hPa 975; (c) vertical cross section along AB on wind speed (black contours covering areas exceeding 22 knots with an interval of 3 knots); and (d) vertical wind speed with positive value in red (in m/s) and negative in blue shading.

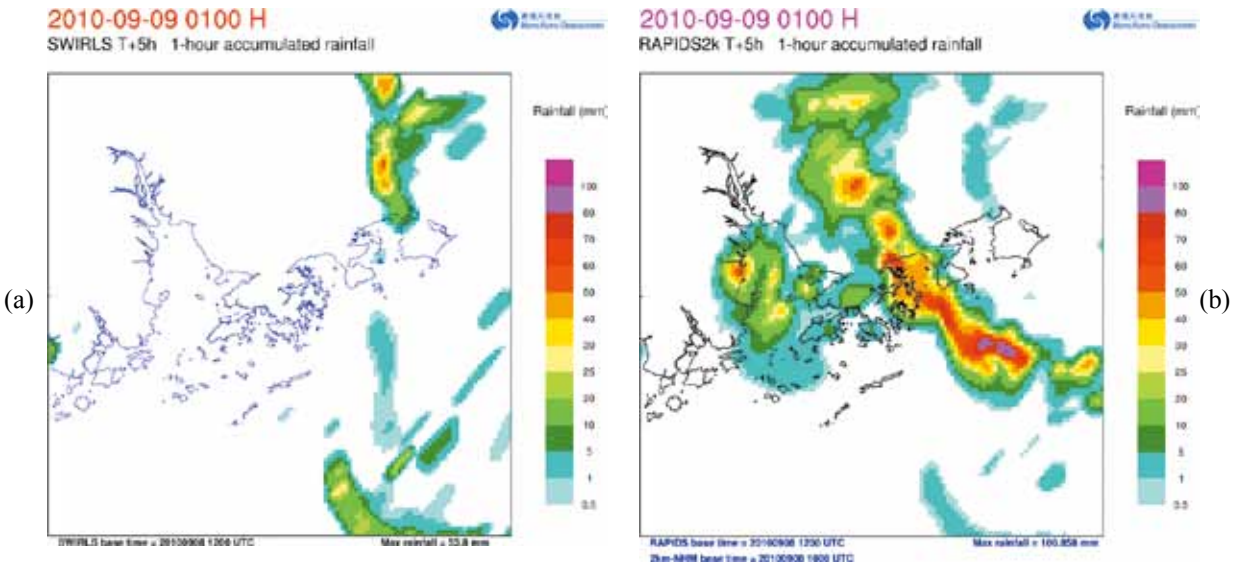

Fig. E-2-8. (a) QPF on 1-hour accumulated rainfall (color in mm) ending at 0100 HKT 9 September 2010 using radar extrapolation techniques; (b) Blending QPF by combining radar nowcast and phase corrected RAPIDS-NHM forecast.

d. Verification of NHM Analysis and Forecast

To monitor the performance of the model analysis and forecast, monthly verification is conducted for various weather elements like wind, temperature and humidity against meteorological station data. In case for Meso-NHM, 50 selected stations over the model domain are used to verify the model performance. Figures E-2-9a-d show the root-mean-square errors of Meso-NHM analysis and forecast (solid lines) for mean-sea-level pressure (MSLP), temperature, surface wind vector magnitude and relative humidity from March to December 2010. Comparing to the results from ORSM (dotted lines), the new NWP system show clear improvements owing to the use of more advanced data assimilation technique and forecast model. For instance, the RMSE of 72 hour forecast of MSLP for Meso-NHM is around 2 hPa that is smaller than that of ORSM by about 1 hPa. Improvements are clearly seen in the forecasts of surface wind and temperature that their RMSEs are generally reduced by 20-30%. Improvement in humidity forecast is also found in Meso-NHM though the gain is smaller than other weather elements. From the verification of upper level wind, Meso-NHM also shows improvements over ORSM throughout the analysis and 3-day forecast period (Fig. E2-10a-d). Using the aircraft wind data, it is also found that the performance of Meso-NHM is similar to global NWP model output that we can further enhance the development of forecast guidance and products related to upper air wind condition (e.g. en-route turbulence intensity) based on Meso-NHM output (Wong *et al.* 2011).

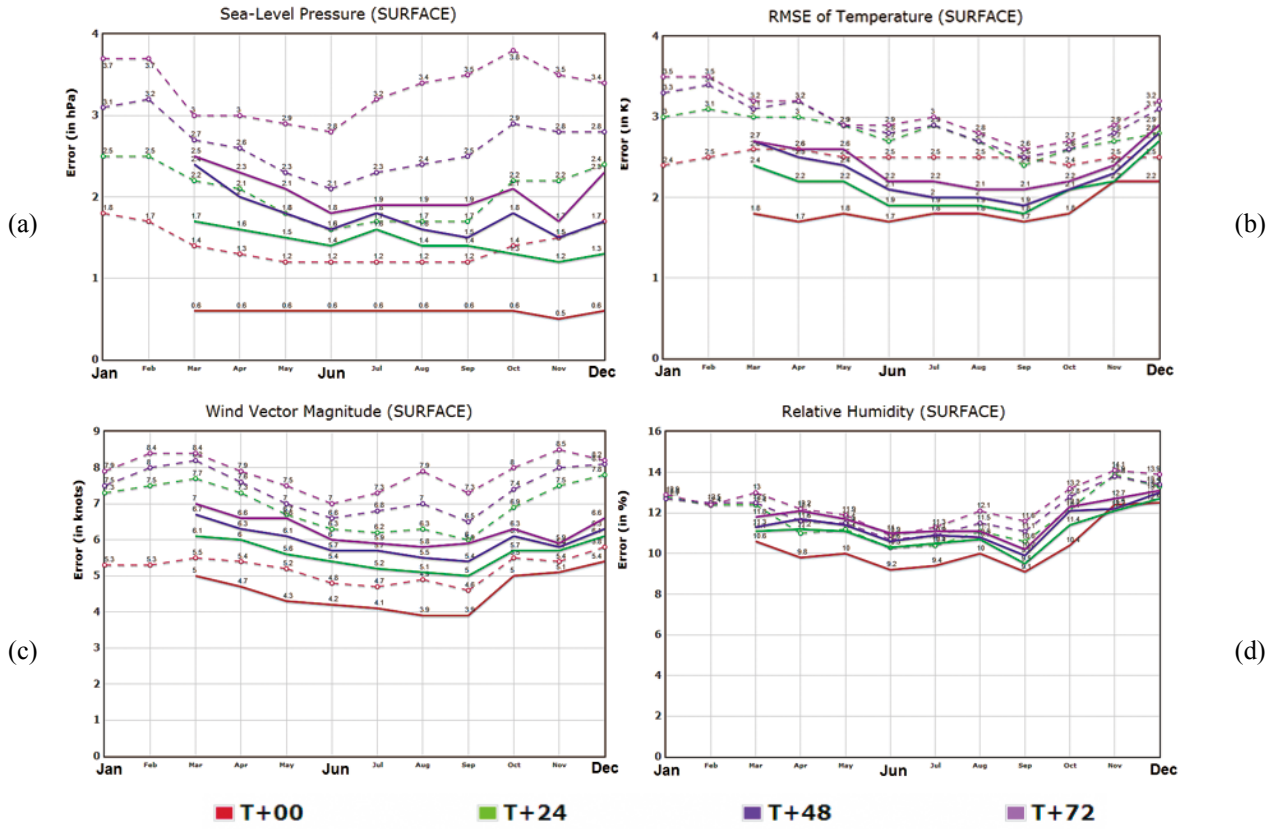

Fig. E-2-9. RMSE of analysis and forecast of surface elements from Meso-NHM (solid lines) and ORSM (dotted lines) during Mar-Dec 2010 on (a) mean-sea-level pressure, (b) temperature, (c) wind vector and (d) relative humidity.

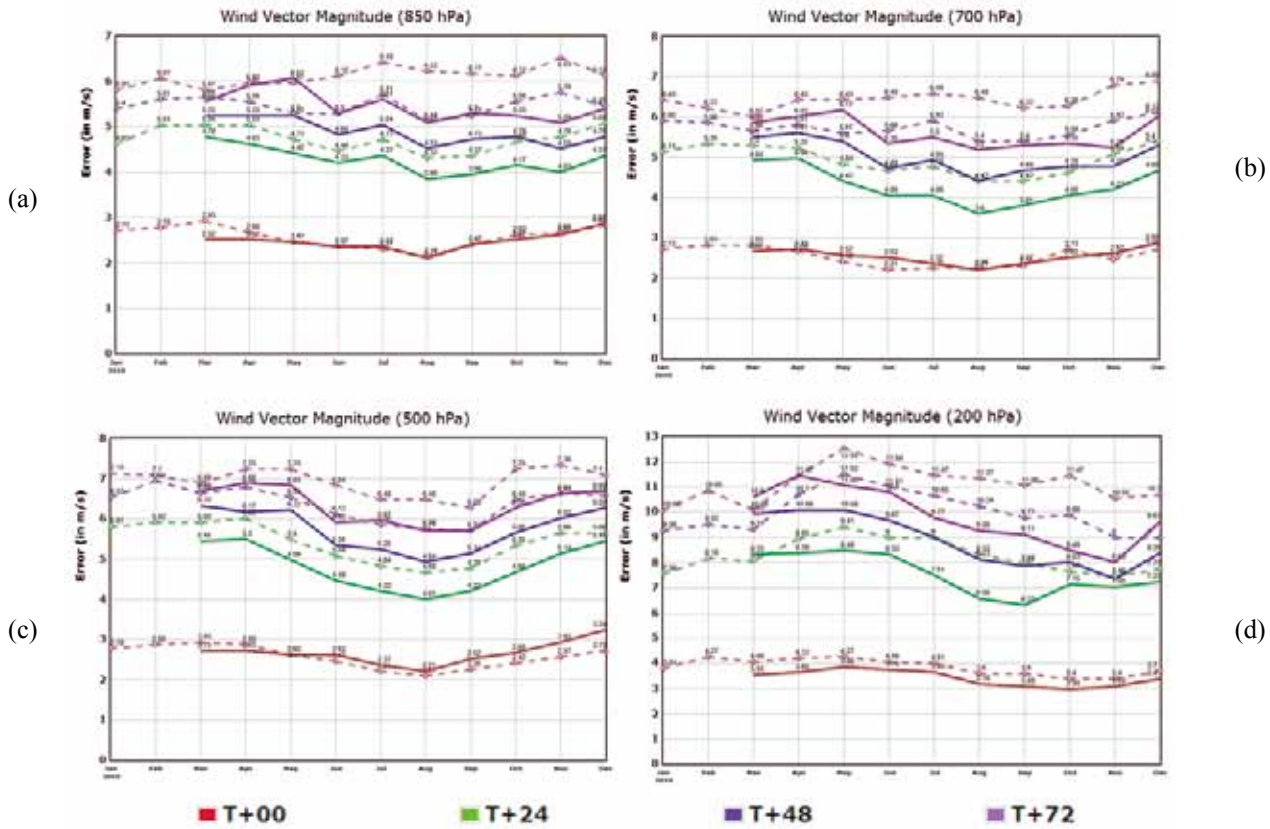

Fig. E-2-10. RMSE of analysis and forecast of wind vectors from Meso-NHM (solid lines) and ORSM (dotted lines) during Mar-Dec 2010 on (a) 850 hPa, (b) 700 hPa, (c) 500 hPa and (d) 200 hPa.

E-2-5. Summary and Future Development

The design and implementation of the AIR forecast model system - the new operational NWP model and data assimilation systems in HKO, are presented in this paper. With the increase in the model resolution, use of non-hydrostatic governing equations and more advanced model physics, the AIR forecast model system shows promising results to enhance the forecast capability of mesoscale and convective weather systems.

To further enhance the AIR forecast model system over the next few years, research and development will be made on aspects like (a) the studies of optimal parameters in physical parameterization processes, (b) development of direct assimilation of satellite microwave radiance data, (c) ingestion of radar reflectivity in JNoVA-3DVAR or retrieved moisture profiles from a separate cloud or moisture analysis algorithm (e.g., LAPS), (d) ingestion of new types of remote sensing observation (e.g., moisture and temperature retrievals from ground-based radiometer) and (e) development NHM with sub-kilometre resolution to forecast local-scale or terrain-induced severe weather phenomena in Hong Kong. Applications of NHM for aviation forecast guidance and supporting collaborative research activities on NWP will also be explored.

E-3. Available input data for NHM real-data simulation[1]

E-3-1. Introduction

Until recently, NHM was able to use only JMA's original formatted data only (e.g., NuSDaS) and the available input data formats were restricted. Through the "International Research for Prevention and Mitigation of Meteorological Disasters in Southeast Asia," more datasets became available as input data for NHM and other research activities improved the usability of NHM. Previous sections of this report show some of the recent research that has been conducted using these newly available datasets.

This section briefly introduces the kinds of datasets available for NHM input and their specifications. It also lists the sections of this report where the datasets are used.

E-3-2. Available input dataset for NHM

Available input datasets for NHM are listed in Table E-3-1 with their horizontal resolutions, vertical layers, time intervals, and file formats. The data suppliers are as follows.

JRA-25 and JCDAS data are available on the JMA website (http://jra.kishou.go.jp/). Registration is needed to access the data for research purposes, and the data are not available for commercial purposes. In addition, JRA-55, a 55-year reanalysis dataset with a 60-km horizontal resolution and 60 vertical layers starting in 1958, is underway in JMA and will soon become available for NHM.

Global Analysis data, Meso Analysis data and two sets of ensemble forecast data (1-Week Ensemble for RSMC Tokyo region and 1-Week Ensemble forecast for Global Troposphere) are released to users outside JMA on the Meteorological Research Consortium website (http://www.mri-jma.go.jp/Project/cons/index.html) as part of a joint research activity between JMA and the Meteorological Society of Japan (MSJ). Foreign researchers who collaborate with a member of MSJ are eligible to access these datasets.

Forecast data by GSM and MSM of JMA are released by the Japan Meteorological Business Support Center (http://www.jmbsc.or.jp/). These datasets are also archived by the Research Institute for Sustainable Humanosphere at Kyoto University (http://database.rish.kyoto-u.ac.jp/arch/glob-atmos/) for research purposes.

Another set of high-resolution GSM forecast data for WMO Region II countries has been released by JMA and distributed to WMO affiliation member countries in region II for operational or research purposes.

NCEP-GFS forecast and analysis (including final-analysis) datasets are released by the National Climate Data Center (http://nomads.ncdc.noaa.gov/) with full and open access.

NHM outputs are also available for one-way self-nesting applications of NHM

[1] S. Hayashi, T. Kuroda and K. Saito

Table E-3-1. Available input datasets for NHM.

Data	Horizontal Resolution	Vertical Levels & Coordinate	Time Interval	File Format	Ensemble Members	Sections
JRA25 & JCDAS (JMA)	1.25 x 1.25 deg.	24 p-levels	Every 6 hour	GRIB1	---	C-4, C-5 D-8 (JRA55)
Global Analysis (JMA)	0.1875 deg. ~ 20km	60 η-levels	Every 6 hour	NuSDaS	---	C-3, D-1, D-2, D-3, D-4, D-5
Meso Analysis (JMA)	5km Lambert map (Japan region only)	50 z* hybrid-levels	Every 3 hour	NuSDaS	---	
GSM 1-Week EPS RSMC Tokyo region (JMA)	1.25 x 1.25 deg.	12 p-levels	Initial: 12UTC valid: every 6hour	NuSDaS	51	
GSM 1-Week EPS Global Troposphere (JMA)	1.25 x 1.25 deg.	11 p-levels	Initial: 12UTC valid: every 12hour	NuSDaS	51	D-4
GSM Forecast (JMA)	0.5 x 0.5 deg. (1.25 x 1.25 deg. before 2007-11-21)	18 p-levels	Initial: every 6 hour valid: every 6 hour	GRIB2 (GRIB1 for 1.25deg.)	---	D-1, D-2, D-3, D-4
MSM Forecast (JMA)	0.1 x 0.125 deg. (Japan region only)	17 p-levels	Initial: every 3 hour valid: every 3hour	GRIB2	---	
GSM forecast (JMA) (only for WMO Region II)	0.5 x 0.5 deg.	22 p-levels	Initial: every 6 hour valid: every 3hour	GRIB2	---	
GFS Forecast (NCEP)	1.0 x 1.0 deg. 0.5 x 0.5 deg.	27 p-levels	Initial: every 6 hour valid: every 3 hour	GRIB1 GRIB2 for 0.5 deg.	---	C-1, C-2 C-8
GFS (Final) Analysis (NCEP)	1.0 x 1.0 deg. 0.5 x 0.5 deg.	27 p-levels	Every 6 hours	GRIB1 GRIB2 for 0.5 deg.	---	C-7
NHM outputs (JMA)	any	any	any	NuSDaS	---	

F. Decision support system

F-1. Experimental development of a decision support system for prevention and mitigation of meteorological disasters based on ensemble NWP Data[1]

F-1-1. Introduction

Ensemble NWP (Numerical Weather Prediction) is a technique that utilizes multiple runs with slightly perturbed initial conditions and/or different parameterization of models to evaluate uncertainty introduced by chaos on initial conditions, uncertainty in imperfection of numerical models, and chaotic behavior of the atmosphere (e.g., Kalnay 2003). Nowadays, most of the operational forecast centers adopt the ensemble NWP technique to quantify the uncertainty of numerical predictions.

Exponential growth of computer power allows us to perform high resolution forecasts and increase the number of ensemble members (Yoden et al. 2008). Southeast Asia region is threatened by meteorological disasters such as flood, strong wind, storm surge, and torrential rain caused by tropical cyclones and other tropical disturbances. Accurate prediction in weather would help risk management. Ensemble forecasting helps to generate a representative sample of the possible future status.

Raw output of ensemble NWPs is not suitable for dissemination to public because the size of information is much larger than that of deterministic NWPs. This requires data conversion to the user-friendly form before dissemination. The actual form depends on each user of the information. Decision support system is a system that conveys information from the NWP sector to decision makers in social, political, and economical sectors in an appropriate way. Especially, commercial decisions are often made, not on the basis of events which are likely to occur, but on the basis of events which are unlikely to occur, but which, if they did occur, would involve serious financial loss (Palmar 2002). This fact requires us to provide reliable probabilistic forecasts. We have to consider not only the development of ensemble prediction systems, but also the development of decision support systems to utilize the output from ensemble NWPs.

For this purpose, we started to develop an experimental decision support system. We have developed tools to store ensemble NWP data on a database and handle probabilistic information obtained from ensemble NWP data, depending on purposes. This report briefly introduces the system, based on Otsuka and Yoden (2010).

Fig. F-1-1. Data finder on Gfdnavi. Left panel shows data tree. Right panel shows items in the selected folder. After Otsuka and Yoden (2010).

[1] S. Otsuka and S. Yoden

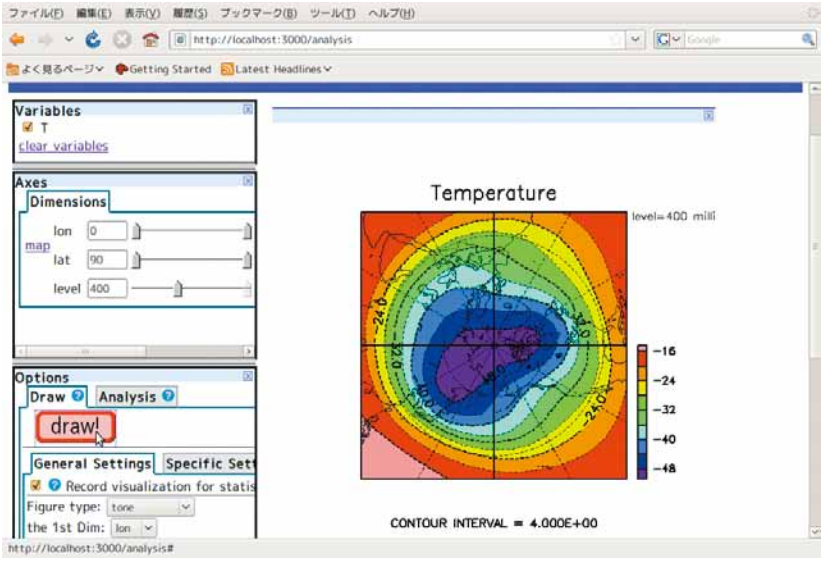

Fig. F-1-2. Visualization window on Gfdnavi. Control panels are located in the left column. Right panel shows the results. After Otsuka and Yoden (2010).

F-1-2. Test data

Cyclone Nargis attacked Myanmar in May 2008. More than 13,800 people were killed and economical loss was reported more than 10 billion dollars. This is the worst natural disaster in Myanmar's recorded history (Webster 2008; Fritz et al. 2009). This meteorological disaster is used as an example of analyses to make a tutorial document, in which analyses of ensemble NWP data are demonstrated to obtain information which is useful for prevention and mitigation of meteorological disasters when disasters are likely to occur.

Output from the experimental ensemble NWP on cyclone Nargis is used as the test data of the decision support system. The atmospheric model is Japan Meteorological Agency Non-Hydrostatic Model (JMA-NHM, Saito et al. 2007). The period of the experiment is from 30 April 2008 12 UTC to 3 May 12 UTC. The horizontal resolution is 10 km. The initial and boundary conditions for the control run of NHM are taken from JMA's high resolution global analysis and forecast, and the initial and boundary perturbations are produced from JMA's one-week global ensemble prediction system. The Princeton Ocean Model (POM, Blumberg and Mellor 1987) is used for the simulation of the storm surge. The input to POM is the output from NHM (wind at 10 m and sea level pressure). The horizontal resolution in POM is 3.5 km. See details in sections D-1 and D-3.

F-1-3. Experimental development of decision support system

a. Unified database and visualization server

We use Gfdnavi (Horinouchi et al. 2010; Nishizawa et al. 2010) for the experimental development of a decision support system. Gfdnavi works as a database server and enables us to distribute and share geophysical fluid data on a computer network. It is also useful for personal use because it has analysis tools and visualization tools which work on web browsers. Gfdnavi is distributed at http://www.gfd-dennou.org/arch/davis/gfdnavi/index.en.htm. Gfdnavi has basic analysis functions such as mean and standard deviation and visualization tools such as contour plot and line plot so that we can analyze NWP data.

Data for analyses is selected via the tree view as shown in Fig. F-1-1. If a dataset is selected in the left panel, available variables are shown in the right panel. When variables are selected, the analysis/visualization window will appear.

A graphical user interface is used to visualize datasets as shown in Fig. F-1-2. In the left panel, there are options for visualization. First, the plot type is selected from the menu in the bottom-left panel. After selecting abscissa and ordinate, ranges for them can be specified by the sliders in the middle-left panel. Then, one can execute visualization and obtain the results. Detailed parameters can be specified in the "specific settings" panel. The diagram will appear in the right-hand side.

b. Visualization of ensemble NWP data

In addition to the intrinsic functions of Gfdnavi, we implement visualization functions which are specific to ensemble NWP data. These functions enable us to utilize probabilistic information of ensemble NWP data. The following sections show the details.

(1) 1D-diagrams of ensemble data

A plume diagram consists of superimposed 1D line plots. Typically, time series of a quantity is superimposed for all the ensemble members. At the initial time, the differences among the ensemble members are small. As time evolves, the difference becomes large (the reliability of the forecast becomes low), which makes the superimposed line plots spread away with each other. This looks like a plume rising from a chimney. The plume diagram is often used to display 1D time series of ensemble NWP data.

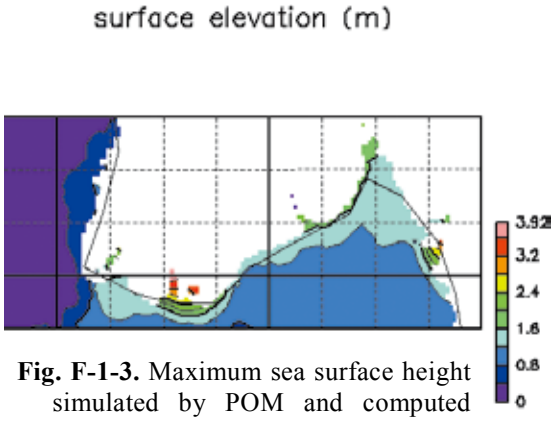

Fig. F-1-3. Maximum sea surface height simulated by POM and computed using all the ensemble members and all the time steps. After Otsuka and Yoden (2010).

Box plot or box-and-whisker plot is introduced by Tukey (1977). This plot shows five quantities: the minimum, the lower quartile, the median, the upper quartile, and the maximum. There are many variations.

In this section, analyses with the decision support system are demonstrated using sea surface height simulated by POM. Figure F-1-3 shows the horizontal distribution of the maximum sea surface height for all the time steps and all the ensemble members. The largest sea surface height is obtained at the mouth of the Irrawaddy River (Ayeyarwady River). Next, the time evolution of sea surface height at the mouth of the Irrawaddy River (95.07E, 16.1N), where the maximum sea surface height is obtained, will be shown.

The top-left panel of Fig. F-1-4 is the plume diagram of the sea surface height at the mouth of the Irrawaddy River. The ensemble member that shows the largest sea surface height is highlighted with the red color. The value and timing of the maximum sea surface height vary much from member to member. The top-right panel of Fig. F-1-4 shows the ensemble mean and spread (standard deviation) of the same data. The spread becomes larger when the sea surface height becomes higher. The bottom-left panel of Fig. F-1-4 shows a box plot for the same data, in which the maximum, the minimum, and the standard deviation are shown. With this plot, it is possible to see the distribution of extreme values (outliers), which are not shown in the spread. The bottom-right panel of Fig. F-1-4 shows the percentiles of the distribution of the same data. For example, most of the members show the sea surface height of about 1 m at around 2 May 00UTC, whereas some members show the sea surface height of nearly 4 m. After 2 May 00UTC, on the other hand, ensemble members show a variety of sea surface heights. As seen above, we can extract many kinds of information from 1D diagrams of the same ensemble NWP data by using different plotting methods.

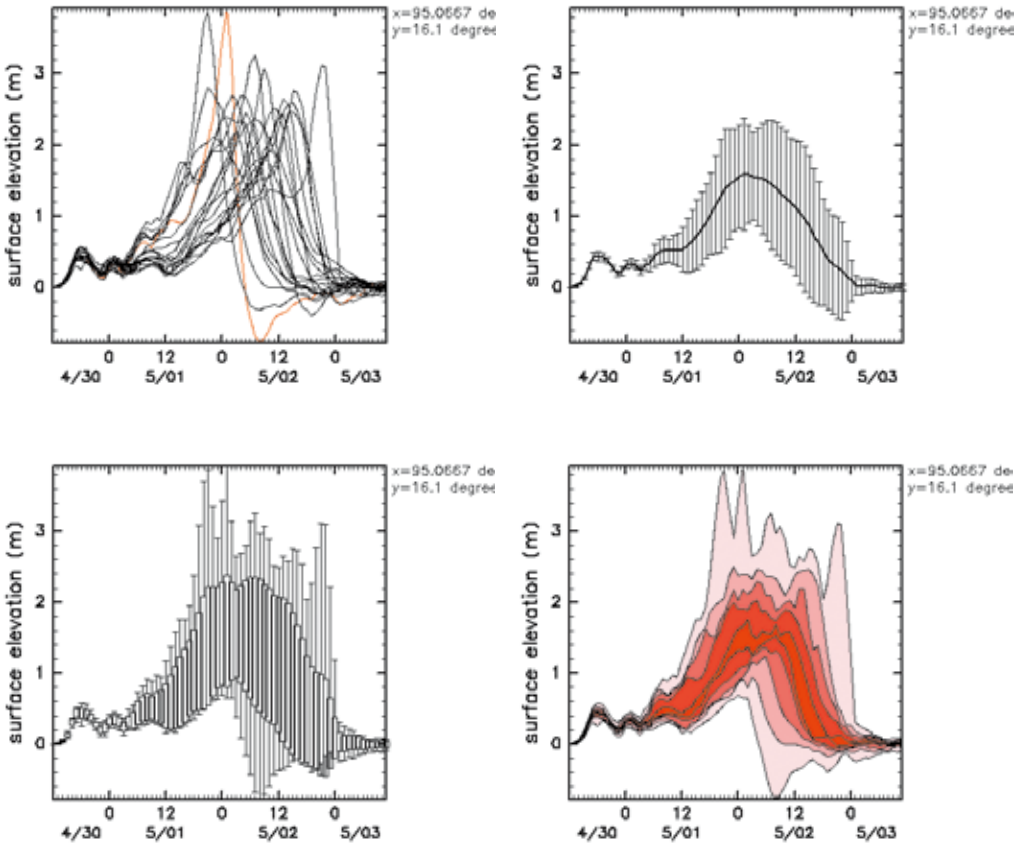

Fig. F-1-4. Sea surface height at the mouth of the Irrawaddy River (95.07E, 16.1N). Top left: plume diagram. Top right: mean and spread. Bottom left: box plot. Bottom right: percentile. After Otsuka and Yoden (2010).

(2) 2D-diagrams of ensemble data

Three kinds of 2D plots for ensemble NWP data are implemented: ensemble mean and spread, so-called spaghetti plot, and distributions of probability exceeding a threshold value. The spaghetti plot shows the same isopleth lines for all the ensemble members in a single plot. Higher density of the contour lines means higher reliability of the forecast, and the lower density of the lines, which look like spaghetti on a plate, means lower reliability. For example, a spaghetti plot of the geopotential height at 500 hPa with isopleth lines of 5,640 m is shown as the cover illustration of Kalnay (2003).

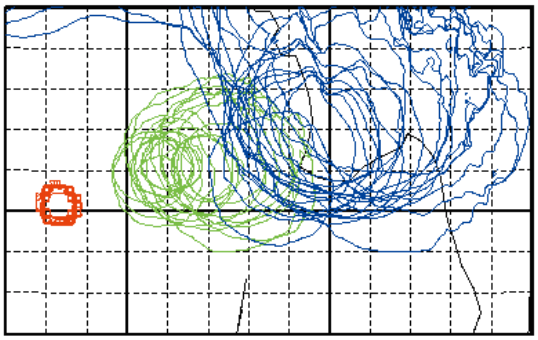

Fig. F-1-5. Spaghetti diagram of sea level pressure of NHM. Each contour shows 1000 hPa in each ensemble member. Red: initial time. Green: t=24 h. Blue: t=48 h. After Otsuka and Yoden (2010).

In this section, analyses with the system are demonstrated using the sea level pressure simulated by NHM. Figure F-1-5 shows a spaghetti plot of the sea level pressure with the contour lines of 1000 hPa at the initial time, 24 hours, and 48 hours. As time evolves, the low pressure region, which corresponds to cyclone Nargis,

becomes larger and the difference between different members becomes larger. Especially, the speed of eastward movement of the cyclone differs from member to member, which makes the differences of the value and the timing of the maximum sea surface height shown in Fig. F-1-4.

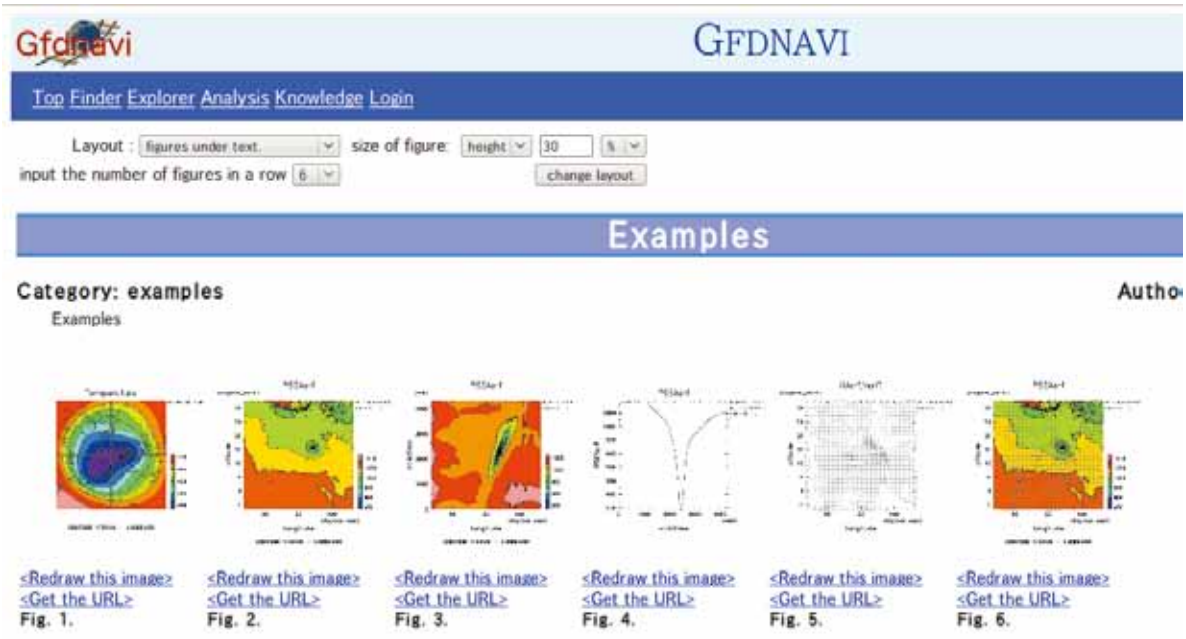

Fig. F-1-6. Examples of the diagrams in the interactive document on the decision support system. After Otsuka and Yoden (2010).

F-1-3-3. User's guide of the decision support system

We created an interactive tutorial document on how to analyze ensemble NWP data by using the experimental version of the decision support system to obtain information which is necessary for prevention and mitigation of meteorological disasters (see I-2).

The user's guide consists of systematic explanations of drawing methods on the system. As generic draw methods, there are explanations for 1D plots (line, marker, and bar), 2D plots (contour, tone, and vector arrow), and statistical plots (scatter and histogram). Especially, how to extract information by slicing data along each axis is demonstrated for five-dimensional ensemble NWP data as a function of latitude, longitude, height, time, and ensemble member.

As draw methods which are specific to ensemble NWP data, 1D diagrams such as plume diagram and 2D diagrams such as the spaghetti plot are described. As analyses with simple mathematical operations, how to compute the ensemble mean and spread is explained.

These sample diagrams shown in the tutorial document are also provided in an interactive document on the decision support system, using the knowledge documenting system of Gfdnavi (Fig. F-1-6). This enables us to modify parameters of the diagrams and redraw them. This also enables us to save the diagrams on the database and write documents on the diagrams. By using this tool, it is possible to archive and share knowledge which are needed to analyze and interpret NWP data. By archiving many case studies, the system will provide useful information and tools for specialists of ensemble NWP data, and the system will also serve as a tool for education.

F-1-4. Summary

We have developed an experimental decision support system for prevention and mitigation of meteorological disasters, using a unified database and visualization tool Gfdnavi. The system

enables us to analyze and visualize ensemble NWP data easily. The system is demonstrated using the data of the experimental ensemble NWP on cyclone Nargis. The tutorial document on the system is produced, including the interactive document of sample diagrams. Further efforts are needed to enrich the contents to provide useful information for those who make decisions for mitigation of meteorological disasters in various sectors.

G. International partnership

G-1. Workshops and meetings[1]

G-1-1. The First International Workshop

The First International Workshop on "Prevention and Mitigation of Meteorological Disasters in Southeast Asia" was held on March 3-5, 2008, at the Palace Side Hotel in Kyoto, Japan. In total, 58 researchers participated from 12 countries and regions in East Asia, Southeast Asia and South Asia. A brief report of the meeting including a group photo is seen in the Newsletter No. 2 (see I-1).

= Program =

March 3 (Mon)

9:00 Opening
9:10 Shigeo YODEN (Department of Geophysics (DG)/ Kyoto University, JAPAN)
International research for prevention and mitigation of meteorological disasters in Southeast Asia

Session I: High-resolution numerical weather predictions (chair: S. Yoden)

9:30 Emmy SUPARKA (Institut Teknologi Bandung(ITB), INDONESIA)
Reduction of geohazard risks for sustainable development in Indonesia
9:50 Tri Wahyu HADI (ITB, INDONESIA)
Mesoscale NWP model intercomparisons for the maritime continent: preliminary results and future plan
10:30 (*coffee break*)
11:00 Kazuo SAITO (Meteorological Research Institute (MRI)/JMA, JAPAN)
Contribution of MRI to the international research for prevention and mitigation of meteorological disasters in Southeast Asia
11:20 Tabito HARA (Japan Meteorological Agency (JMA), JAPAN)
Operational mesoscale NWP at the Japan Meteorological Agency
11:40 Md. Nazrul ISLAM (SAARC Meteorological Research Centre, BANGLADESH)
Use of regional climate model to study extreme weather events in and around Bangladesh
12:20 (*lunch break*)
13:30 KIEU Thi Xin (Vietnam National University of Hanoi, VIETNAM)
Numerical weather prediction with high resolution regional model-HRM in Vietnam.
Impact of convection parameterization on heavy rainfall forecast of HRM, verification and problems for very low latitudes
13:50 Mezak Arnold RATAG (Indonesia National Meteorology and Geophysical Agency (BMG), INDONESIA)
Development of high resolution models and its applications for weather and climate risk reduction in Indonesia
14:30 Palikone THALONGSENGCHANH (DG/Kyoto University, JAPAN/LAO, PDR)
A down-scale experiment on numerical weather prediction in Indochina region (Lao PDR)
14:50 Krushna Chandra GOUDA (CSIR/Centre for Mathematical Modelling and Computer Simulation, INDIA)
Comparison of two strategies for simulation of extreme rainfall events
15:30 (*coffee break*)

Session II: Tutorials and demonstrations (chair: S. Yoden)

16:00 Shugo HAYASHI (MRI/JMA, JAPAN)
Basic usage of the NHM for numerical weather experiments
16:40 Seiya NISHIZAWA (DG/Kyoto University, JAPAN)

[1] S. Yoden and F. Furutani (Kyoto University)

Experimental development of a unified data base and decision support system for prevention and mitigation of meteorological disasters

March 4 (Tue)

Session III: High-impact weather and its simulation/prediction (chair: K. Saito)

9:00 Vinliam BOUNLOM (Hydrological Division, Department of Meteorology and Hydrology, LAO, PDR)
Country report on hydro-meteorological disasters in Lao PDR for the year 2006

9:20 Long SARAVUTH (Ministry of Water Resources and Meteorology, CAMBODIA)
Flash flood in Preas Vihear Province

9:40 Fredolin TANGANG (National University of Malaysia, MALAYSIA)
On the roles of the northeast cold surge, the Borneo Vortex, the MJO and the IOD during the worst 2006/2007 flood in Southern Peninsular Malaysia

10:20 Taiichi HAYASHI (DPRI/Kyoto University, JAPAN)
Disaster by the severe cyclone "Sidr" in the coastal region of Bangladesh in November, 2007

10:40 (*coffee break*)

11:10 Hiromu SEKO (MRI/JMA, JAPAN)
Numerical simulation of heavy rainfall events in South/Southeast Asia using NHM

11:30 Rosbintarti Kartika LESTARI (NTU, SIMGAPORE)
Preliminary study on the precipitation of maritime Southeast Asia

11:50 Kazuhisa TSUBOKI (Nagoya University, JAPAN)
Simulation experiments of typhoons and tornadoes using the cloud resolving model

12:10 Toshiki IWASAKI (Tohoku University, JAPAN)
Influences of cloud microphysical processes on structure and development of tropical cyclone

12:30 Mitsuru UENO (MRI/JMA, JAPAN)
Recent advancements in the understanding of typhoon inner-core structures and its implication for typhoon vortex initialization

12:50 (*lunch break*)

Session IV: Satellite observations, their applications and data assimilation (chair: T.-Y. Koh)

14:00 Toshitaka TSUDA (RISH/Kyoto University, JAPAN)
Utilization of GPS radio occultation data for the studies of atmosphere dynamics

14:40 Yoshinori SHOJI (MRI/JMA, JAPAN)
An experiment of near real-time precipitable water vapor retrieval using ground-based GPS stations in South East Asia

15:00 Perapol BEGKHUNTOD (RFMMC, Mekong River Commission, CAMBODIA)
Satellite-based rainfall estimation and hydro-meteorological networks for flood forecasting in the Mekong River Basin

15:40 (*coffee break*)

16:10 Hirohiko ISHIKAWA (DPRI/ Kyoto University, JAPAN)
Satellite monitoring of hazardous weather in Asia

16:30 Masaru KUNII (MRI/JMA, JAPAN)
Meso-scale data assimilation experiment in low latitudes

16:50 Le DUC (Vietnam National University of Hanoi, VIETNAM)
Development of a data assimilation system with HRM model and 3DVAR technique

17:10 Takeshi ENOMOTO (Japan Agency for Marine-Earth Science and Technology (JAMSTEC), JAPAN)
ALERA:AFES-LETKF experimental ensemble reanalysis

17:30 Vijapuapu S. PRASAD (National Center for Medium Range Weather Forecasting, INDIA)
Assimilation of direct satellite radiance data at NCMRWF

18:30 (*banquet*)

March 5 (Wed)

Session V: Model output statistics, predictability, and decision supports (chair: T. Satomura)

9:00 Tieh Yong KOH (NTU, SIMGAPORE)
Statistical verification of COAMPS model over SCSMEX period
9:20 Hongwen KANG (APEC Climate Center, KOREA)
Multi-model output statistical downscaling prediction of precipitation in the Philippines and Thailand
9:40 Edwin S. T. LAI (Hong Kong Observatory, P. R. CHINA)
Use of NWP and EPS products in support of location-specific forecasts
10:00 Hitoshi MUKOUGAWA (DPRI/Kyoto University, JAPAN)
Predictability of tropical circulation examined by breeding of growing mode(BGM) method for JMA ensemble prediction system
10:20 (*coffee break*)
10:50 Syozo YAMANE (Chiba Institute of Science, JAPAN)
Properties of ensemble perturbations evolving in an atmospheric general circulation model
11:10 Prawit JAMPANYA (Thai Meteorological Department (TMD), THAILAND)
The meteorological natural disasters warning system of Thailand
11:30 SANGA-NGOIE Kazadi (Ritsumeikan Asia Pacific University, JAPAN)
Our endangered costal ecosystems - an eco-climatic and risk analysis using GIS and remote sensing -
11:50 Kamol PROMASAKHA NA SAKOLNAKHON (TMD, THAILAND)
Integration NWP data and applied geographic information system(GIS) management for landslide at Amphure Pai, Mae Hong Son
12:10 Takeshi HORINOUCHI (RISH/Kyoto University, JAPAN)
Database and data-analysis infrastructure for atmospheric studies
12:30 (*lunch break*)

Session VI: High-resolution model as a fundamental research tool (chair: T.W. Hadi)
14:00 Takehiko SATOMURA (DG/Kyoto University, JAPAN)
Development of ultra-high resolution numerical model
14:20 Nurjanna Joko TRILAKSONO (ITB, INDONESIA)
Study of diurnal patterns of convection in Sumatra Island using weather research and forecasting-advanced research WRF (WRF-ARW) model
14:40 Shigenori OTSUKA (DG/Kyoto University, JAPAN)
Numerical experiments on vertically fine structures of water vapor in the Tropics
15:00 Yoichi ISHIKAWA (DG/Kyoto University, JAPAN)
Dependency of the tropical convective clouds on the sea surface temperature simulated by a high-resolution coupled model
15:20 Tetsuya TAKEMI (DPRI/Kyoto University, JAPAN)
Environmental stability control of the precipitation structure and intensity within mesoscale convective systems
15:40 (*coffee break*)

Session VII: Future research and collaborations
16:10 all participants
Open discussions
16:50 Closing

G-1-2. The Second International Workshop

The Second International Workshop on "Prevention and Mitigation of Meteorological Disasters in Southeast Asia" was held on March 2-5, 2009, at Jayakarta Hotel in Bandung, Indonesia. In total, 47 researchers participated from 12 countries and regions in East Asia, Southeast Asia and South Asia. A brief report of the meeting including a group photo is seen in the Newsletter No. 4 (see I-1).

= Program =

March 2 (Mon)

Opening session (Chair: Tri Wahyu HADI)

13:30 Tri Wahyu HADI (ITB, Indonesia)
Welcome, opening remarks, and logistics

13:40 Emmy SUPARKA (ITB, Indonesia)
Welcome address

14:00 Takashi NISHIGAKI (JST, Japan)
Welcome address

14:20 Shigeo YODEN (DG/Kyoto University, Japan)
International collaborations on prevention and mitigation of meteorological disasters in Southeast Asia

14:50 Mu MU (IAP/CAS, China)
Approaches to adaptive observation for improving high impact weather prediction: CNOP and SV

15:30 (*Coffee break*)

Session I: Downscale NWPs (Chair: KIEU Thi Xin)

16:00 Tri Wahyu HADI (ITB, Indonesia)
Prediction of diurnal variation over Java Island: A four-model intercomparison

16:30 Shugo HAYASHI (MRI/JMA, Japan)
Statistical verifications of short term NWP by NHM and WRF-ARW around Japan and Southeast Asia

17:00 Introduction of posters
Two minutes talk without ppt slides

17:30 (End of the first day sessions)

19:00 <<< Joint banquet with JSPS-AASP at the Jayakarta Hotel >>>

March 3 (Tue)

Session I: - continued (Chair: Toshiki IWASAKI)

08:30 Md. Nazrul ISLAM (SAARC/MRC, Bangladesh)
Regional climate model in prevention of meteorological disaster in SAARC region

09:00 KIEU Thi Xin (University of Hanoi, Vietnam)
Implementing regional hydrostatical models & NHM of MRI for the historical heavy rain case caused flooding in Hanoi in November 2008. Comparision
Development of a short-range ensemble prediction system at NCHMF: Preliminary results (Le DUC, NCHMF, Vietnam)

09:30 Wai-kin WONG (Hong Kong Observatory, Hong Kong)
Development and applications of JMA-NHM in support of severe weather forecasting in Hong Kong

10:00 (*Coffee break*)

Session II: Tropical disturbances and precipitation process (Chair: Chun-Chieh WU)

10:30 Hiromu SEKO (MRI/JMA, Japan)
Structure of the regional heavy rainfall system that occurred in Mumbai, India, on 26 July 2005

11:00 Tetsuya TAKEMI (DPRI/Kyoto University, Japan)
High-resolution modeling study of an extreme rainfall event in a complex terrain under the influence of typhoon Fung-Wong (2008)
11:30 (*Lunch*)

Session II: - continued (Chair: Tieh Yong KOH)
13:30 Toshiki IWASAKI (Tohoku University, Japan)
Influences of cloud microphysical processes on structure and development of tropical cyclone Part II: Effects of evaporation from rain
14:00 Yoichi ISHIKAWA (DG/Kyoto University, Japan)
Interaction between tropical convective clouds and ocean mixed layer simulated by a high-resolution coupled model
14:20 Madhavan N. RAJEEVAN (NARL, India)
Sensitivity of different microphysics parameterization schemes to the simulation of mesoscale convective systems observed over Gadanki, India
14:40 Tohru KURODA (MRI/JMA, Japan)
NHM utilities for SE Asian NWP and numerical experiments of myanmar cyclone Nargis
15:00 (*Coffee break*)

Session III: Observation network (joint with JSPS-AASP) (Chair: Toshitaka TSUDA)
15:30 Manabu D. YAMANAKA (JAMSTEC, Japan)
Overview and scientific background of JEPP-HARIMAU project: Long coastlines of maritime continent governing global climate
16:00 Masato SHIOTANI (RISH/Kyoto University, Japan)
Ozone and water vapor 0bservations in the equatorial Pacific
16:30 Tieh Yong KOH (Nanyang Technological University, Singapore)
Towards a mesoscale observation network in Southeast Asia
17:00 Basuki SUHARDIMAN (ITB, Indonesia)
Trans European information network 3 (TEIN3) and its potential use for the weather and climate research in Southeast Asia
17:20 (End of the second day sessions)

March 4 (Wed)
Session IV: New methods in observation, data assimilation, and NWPs (joint with JSPS-AASP) (Chair: Masato SHIOTANI)
08:30 Toshitaka TSUDA (RISH/Kyoto University, Japan)
Application of GPS radio occultation (RO) data for the studies of atmospheric dynamics and data assimilation into numerical weather prediction model
09:00 Seon Ki PARK (Ewha Womans University, Korea)
Data assimilation and parameter estimation to improve forecast accuracy of disastrous weather systems
09:30 Kevin CHEUNG (Macquarie University, Australia)
A statistical tropical cyclone rainfall model for the Taiwan area
10:00 (*Coffee break*)

Session IV: - continued (Chair: Mezak A. RATAG)
10:30 Chun-Chieh WU (National Taiwan University, Taiwan)
Targeted observation for improving tropical cyclone predictability – DOTSTAR and T-PARC
11:00 DODLA V. Bhaskar Rao (Andhra University, India)
Ensemble prediction of “SIDR” cyclone over Bay of Bengal using a high resolution mesoscale model
11:30 Kazuo SAITO (MRI/JMA, Japan)
Ensemble forecast experiment of cyclone Nargis
12:00 (*Lunch*)
Session V: Risk assessment and community preparedness (Chair: Kazuo SAITO)

13:30 Hirohiko ISHIKAWA (DPRI/Kyoto University, Japan)
Estimation of meteorological hazards using output from numerical weather prediction model
14:00 Kamol PROMASAKHA NA SAKOLNAKHON (TMD, Thailand)
Case Study: The atmospheric stability indices and applied GIS risk assessment severe thunderstorms in the northeastern of Thailand
14:30 Mezak A. RATAG (BMG, Indonesia)
Roles of high resolution weather and climate models in disaster risk management at district level
15:00 (*Coffee break*)

Tutorials
15:30 Kazuo SAITO, Shugo HAYASHI, and Tohru KURODA (MRI/JMA, Japan)
Introduction to non-hydrostatic model of MRI/JMA
17:00 *(End of the third day sessions*)

March 5 (Thu)
Session VI: Extended range NWPs (Chair: Mu MU)
08:30 Hitoshi MUKOUGAWA (DPRI/Kyoto University, Japan)
On the influence of the tropical intraseasonal oscillation to the predictability of the Pacific/North American pattern
09:00 Krushna C. GOUDA (CSIR/CMMCS, India)
Advance prediction of date of onset of monsoon: dynamical basis and skill evaluation
09:30 Donaldi Sukma PERMANA (BMG, Indonesia)
Comparisons between conformal cubic atmospheric model (CCAM) and global forecasting system (GFS): global model output over Indonesia in September – October – November (SON) 2008
10:00 (*Coffee break*)

Session VII: Data assimilation (Chair: Seon Ki PARK)
10:30 Yoshinori SHOJI (MRI/JMA, Japan)
Data assimilation of precipitable water vapor derived from GPS network in South East Asia
11:00 I Dewa Gede A. JUNNAEDHI (ITB, Indonesia)
Impact of local data assimilation on short range weather prediction in Indonesia : A preliminary result
11:30 (*Lunch*)

Poster session
13:00 Kosuke ITO (DG/Kyoto University, Japan)
Improved estimates of air-sea fluxes in a tropical cyclone using an adjoint method
Takuya KAWABATA (MRI/JMA, Japan)
Development and results of a cloud-resolving nonhydrostatic 4DVAR assimilation system
Hyun Hee KIM (Ewha Womans University, Korea)
Identification of adaptive observation area in typhoon Megi (2002) using an ensemble data assimilation method
Masaru KUNII (MRI/JMA, Japan)
Sensitivity analysis using the mesoscale singular vectors
Jalu Tejo NUGROHO (LAPAN, Indonesia)
Solar cycle prediction using periodicity analysis of weighted wavelet Z-transform
Shigenori OTSUKA (DG/Kyoto University, Japan)
Numerical experiments on formation processes of thin moist layers in the mid-troposphere over a tropical ocean
Kazuo SAITO (MRI/JMA, Japan)
Achievements and experiences of MRI/JMA at the WWRP Beijing Olympic research and development project
Hiromu SEKO (MRI/JMA, Japan)

Mesoscale ensemble experiments on potential parameters for tornado formation
Hiromu SEKO (MRI/JMA, Japan)
Mesoscale ensemble experiments on heavy rainfalls in Japan area using LETKF
Tri Handoko SETO (BPPT, Indonesia)
Weather modification technology for flood prevention in Indonesia
Ibnu SOFIAN (BAKOSURTANAL, Indonesia)
Simulation of wind-setup wave in the Indonesian Seas using the nesting wavewatch III
Elza SURMAINI (Dept. of Agriculture, Indonesia)
Validation of ECMWF seasonal forecast output in Indonesia

Closing session (Chair: Shigeo YODEN)

14:30 All Participants
Discussion for Future Activities
15:00 (*Adjourn*)

G-1-3. The Third International Workshop

The third international workshop on "Prevention and Mitigation of Meteorological Disasters in Southeast Asia" was held on March 1-3, 2010, and the open symposium on "Meteorological Disasters and Adaptable Society in the Asia-Pacific Region" was held on March 4, 2010, at Ritsumeikan Asia Pacific University (APU) in Beppu, Japan. 61 researchers and graduate students from 13 countries participated in the workshop, and 63 people including citizens of Beppu attended the open symposium. A brief report of the meeting including a group photo is seen in the Newsletter No. 6 (see I-1).

= Program =

March 1 (Mon)

Opening session (Chair: Sanga-N. KAZADI)

09:15 Sanga-N. KAZADI (APU, Japan)
Welcome, opening remarks, and logistics
09:20 Malcolm J. M. COOPER (APU, Japan)
Welcome address
09:30 Shigeo YODEN (DG/Kyoto U., Principal Investigator, Japan)
International collaborations on prevention and mitigation of meteorological disasters in Southeast Asia
10:00 Indratmo SOEKARNO (ITB, Vice President, Indonesia)
Flood protection in Bandung - West Java due to Citarum River
10:30 (*Coffee break*)

Opening session – continued (Chair: Kazuo SAITO)

11:00 Naoyuki HASEGAWA (Head of Office Int. Affairs/JMA, Japan)
Regional cooperation in meteorological services in Asia and the Pacific
11:30 Mu MU (IAP/CAS, China)
A comparison study on adaptive observation approaches: Singular vector, conditional nonlinear optimal perturbation and ensemble transform Kalman filter
12:00 Kaoru TAKARA (DPRI/Kyoto U., Leader of GCOE-ARS, Japan)
Sustainability science for a resilient society adaptable to extreme weather conditions
12:30 (*Group photo*)
12:40 (*Lunch*)

Session I: High-impact weather - prediction and analysis (Chair: Tieh Yong KOH)

14:00 Tetsuo NAKAZAWA (MRI/JMA, Japan)
Can the global ensemble forecast data detect high-impact weather events?
14:30 Venkata Bhaskar Rao DODLA (Jackson State University, US)
A new strategy for improvement in the prediction of tropical cyclone intensity and movement using FDDA and vortex initialization
15:00 Introduction of posters
15:30 (*Coffee break*)

Session I: - continued (Chair: Tri Wahyu HADI)

16:00 Fredolin TANGANG (National University of Malaysia, Malaysia)
Impact of the Madden-Julian Oscillation (MJO) on the maritime continent's rainfall
16:30 Samsul BAHRI (Weather Modification Unit/BPPT, Indonesia)
The use of radar for weather modification in order to mitigate weather and climate disaster in Indonesia
17:00 (End of the first day sessions)
18:00 (*Banquet*)

March 2 (Tue)

Session II: Tropical disturbances (Chair: Takehiko SATOMURA)

09:00 Chun-Chieh WU (National Taiwan University, Taiwan)
Targeted observation, data Assimilation, and tropical cyclone dynamics and predictability

09:30 Yoshinori SHOJI (MRI/JMA, Japan)
Data assimilation of GPS PWV for Myanmar cyclone NARGIS

09:50 Krushna Chandra GOUDA (CSIR/CMMCS, India)
Prediction of tropical cyclone over Bay of Bengal using NHM high resolution model

10:10 Hari Prasad DASARI (University of Evora, Portugal)
Numerical prediction and dynamical analysis of a super cyclonic system over north Indian Ocean

10:30 (*Coffee break*)

Session II: - continued (Chair: Chun-Chieh WU)

11:00 Takeshi ENOMOTO (JAMSTEC, Japan)
Precursory signals of typhoon genesis in analysis ensemble spread

11:30 Palikone THALONGSENGCHANH (LMNRRI/PMO, Lao PDR)
Flood event on meteorological disaster "TC Ketsana's Case FY 2009" in Lao PDR

11:50 Thanh NGO-DUC (AMO/NHMS, Vietnam)
Extreme climate events in Vietnam - tropical cyclones and heavy rainfall phenomena observed in the past

12:10 Shigenori OTSUKA (DG/Kyoto University, Japan)
Decision support system for prevention and mitigation of meteorological disasters based on ensemble NWP data: an experimental use for the forecasts of Nargis

12:30 (Lunch)

Session III: Heavy precipitation and microphysics (Chair: Thi Xin KIEU)

13:30 Takehiko SATOMURA(DG/Kyoto University, Japan)
Toward the mitigation of water disaster in countries in the Indochina Peninsula

14:00 Juneng LIEW (National University of Malaysia, Malaysia)
Numerical investigation of a severe afternoon thunderstorm over west coast of Peninsular Malaysia

14:20 Tetsuya TAKEMI (DPRI/Kyoto University, Japan)
Representation of extreme weather events in convection-resolving simulations at 100-m resolution

14:40 Siriluk CHUMCHEAN (Mahanakorn University of Technology, Thailand)
Bangkok rainfall forecasting system: An operational radar and RTC application

15:00 (*Coffee break*)

Session III: - continued (Chair: Hirohiko ISHIKAWA)

15:30 Seon Ki PARK (Ewha Womans University, Korea)
Characteristics of fog occurrence over the Korean Peninsula

16:00 Ryoji NAGASAWA (NPD/JMA, Japan)
Problem of cloud overlap in the radiation calculation in the JMA Nonhydrostatic Model

16:20 Chee-Kiat TEO (NTU, Singapore)
Nadir correction to AIRS radiances

16:40 Hiromu SEKO (MRI/JMA, Japan)
Data assimilation of side-looking radio occultation by observing system simulation experiment

17:00 (*End of the second day sessions*)

March 3 (Wed)

Session IV: Mesoscale NWP (Chair: Seon Ki PARK)

09:00 Kazuo SAITO (MRI/JMA, Japan)

Achievement of MRI for the International Research for Prevention and Mitigation of Meteorological Disasters in Southeast Asia

09:30 Takuya KAWABATA (MRI/JMA, Japan)
Cloud-resolving 4D-Var with Radar and GPS data

09:50 Masaomi NAKAMURA (MRI/JMA, Japan)
Projection of the change in future extremes around Japan using a nonhydrostatic regional model

10:10 Santi SUMDIN (TMD, Thailand)
The conversion operational Unified Model output to GrADS and GIS data for weather forecasting activities in Thai Meteorological Department

10:30 (*Coffee break*)

Session IV: - continued (Chair: Tetsuya TAKEMI)

11:00 Tri Wahyu HADI (ITB, Indonesia)
Multiscale precursors of extreme weather and climatic events in Indonesia: Process study and experimental predictions

11:30 Wai-kin WONG (Hong Kong Observatory, Hong Kong)
Development of operational rapid update non-hydrostatic NWP and data assimilation systems in the Hong Kong Observatory

11:50 Shugo HAYASHI (MRI/JMA, Japan)
Statistical verification of short range forecasts by NHM and WRF-ARW over Southeast Asia and Japan areas

12:10 Tieh Yong KOH (NTU, Singapore)
Improved diagnostics for NWP verification

12:30 (*Lunch*)

Session V: Global to regional scales and applications (Chair: Hiromu SEKO)

13:30 Hirohiko ISHIKAWA (DPRI/Kyoto University, Japan)
Reproduction of hazardous weather in Asia in 2009 using dynamic downscaling from global analysis

14:00 Kumarenthiran SUBRAMANIAM (MMD, Malaysia)
Performance of ensemble prediction for numerical weather prediction (NWP) models during the northeast monsoon over Peninsular Malaysia

14:20 Shozo YAMANE (Doshisha University, Japan)
Properties of ensemble perturbations evolving in an atmospheric general circulation model

14:40 Zhina JIANG (LaSW/CAMS, China)
A New Approach to the Generation of Initial Perturbations for Ensemble Prediction: Conditional nonlinear optimal perturbations

15:00 (*Coffee break*)

Session V: - continued (Chair: Shigeo YODEN)

15:30 Ivonne Milichristi RADJAWANE (ITB, Indonesia)
Sea level rise assessment in the northern part of Java coastal area

16:00 Yoichi ISHIKAWA (DG/Kyoto University, Japan)
Formation of ocean surface barrier layer simulated by high-resolution atmosphere-ocean coupled model

16:20 Rita Tisiana Dwi KUSWARDANI (Ocean University of China, China)
The effects of surface waves on the upper ocean and climate system and its application to the development of an ocean forecast system in Indonesian Seas

Closing

16:40 Yoshinori SHOJI (MRI/JMA, Japan)
Report on the 16th Session of the Asia-Pacific Regional Space Agency Forum and the first Asia Oceania Region Workshop on GNSS

16:50 Takashi NISHIGAKI (JST, Japan)

Concluding remarks
17:00 Shigeo YODEN (DG/Kyoto U., Japan)
Summary
17:10 (*End of the workshop*)

Poster presentations

P-1 Taiichi HAYASHI (DPRI/Kyoto U., Japan)
Recent research trend of heavy rainfall and severe local storm in the northeastern Indian subcontinent

P-2* Hitoshi HIROSE (DG/Kyoto University, Japan)
Comparison between cloud cover variations from satellite observations and those from surface observations

P-3* Kosuke ITO (DG/Kyoto University, Japan)
Estimation of air-sea fluxes in a tropical cyclone by using variational method with an intermediate atmosphere-ocean coupled mode

P-4 Thi Xin KIEU (Vietnam National University at Hanoi, Vietnam)
On some tests of rainfall forecast using NHM in Vietnam

P-5* Yoshiaki MIYAMOTO (DPRI/Kyoto University, Japan)
Axisymmetric and asymmetric processes of tropical-cyclone vortex during the rapid intensification phase

P-6 Findy RENGGONO (Weather Modification Unit/BPPT, Indonesia)
Precipitating cloud observed by C-band radar at Sorowako, Indonesia

P-7* Naoaki SAITO (DG/Kyoto University, Japan)
Interaction between thermal convection and mean flow in a rotating system

P-8 Tri Handoko SETO (Weather Modification Unit/BPPT, Indonesia)
Weather modification technology for flood prevention in Indonesia

P-9 Widada SULISTYA (Centre for Public Meteorology/BMKG, Indonesia)
Indonesian extreme weather

P-10 Fredolin TANGANG (National University of Malaysia, Malaysia)
Simulation of heavy precipitation episode over eastern Peninsular Malaysia using MM5: Sensitivity to cumulus parameterization schemes

P-11 Palikone THALONGSENGCHANH (LMNRRI/PMO, Lao PDR)
TC Ketsana's effect in Lao (FY2009)

P-12* Nurjanna Joko TRILAKSONO (DG/Kyoto University, Japan)
Study of heavy rainfall during Jakarta flood event January-February 2007

P-13* Hiroki YAMAMOTO (DG/Kyoto University, Japan)
Laboratory experiments on two coalescing axisymmetric turbulent plumes in a rotating fluid

P-14* Ryuji YOSHIDA (DPRI/Kyoto University Japan)
A Numerical simulation of tropical cyclogenesis with MCS merger

March 4 (Thu)
"Open Symposium on Meteorological Disasters and Adaptable Society in the Asia-Pacific Region

Open Symposium (Chair: Sanga-N. KAZADI)

10:00 Sanga-N. KAZADI (APU, Japan)
Opening remarks

10:10 Shigeo YODEN (DG/Kyoto University, Japan)
International collaborations on prevention and mitigation of meteorological disasters in Southeast Asia

10:30 Shunso TSUKADA (APU, Japan)
Socio-economic implications of meteorological disasters and possible measures to mitigate their impacts

10:50 Tieh Yong KOH (NTU, Singapore)
Towards a mesoscale observation network in Southeast Asia

11:10 Toshitaka TSUDA (RISH/Kyoto University, Research Leader of GCOE-ARS, Japan)
Fusion of science and engineering for extreme weathers and global warming

11:30 Takashi NISHIGAKI (JST, Japan)
Comments

11:40 Masahiro KOBAYASHI (JICA Kyushu, Japan)
Comments

11:50 Sanga-N. KAZADI (APU, Japan)
Closing remarks

12:00 (*end of the Symposium*)

12:15 – 13:15 ***Lunch buffet*** at the APU cafeteria
all participants are invited to have further discussions/conversations

13:30 – 18:00
Field observations at some key spots related to Geohazards in and around Beppu

G-1-4. The First Local Meeting

The first local meeting on "Prevention and Mitigation of Meteorological Disasters in Southeast Asia" was held on August 17-18, 2007, at Kyoto University in Kyoto, Japan. 24 Japanese researchers and 2 officers from JST participated in this meeting and discussed research plan and schedule of this program.

G-1-5. The Second Local Meeting

The second local meeting on "Prevention and Mitigation of Meteorological Disasters in Southeast Asia" was held on September 9-10, 2008, at MRI in Tsukuba, Japan and 28 Japanese researchers participated in this meeting.

= Program =

13:10-13:30 Opening

13:30-16:20 **Session I: Observation and Data**

Taiichi HAYASHI (DPRI/Kyoto University)
Recent research trend of mesoscale phenomena in South Asia

Takehiko SATOMURA (DG/Kyoto University)
Precipitation characteristics in northern Indochina

Noriyuki NISHI (DG/Kyoto University)
Detection of precipitation using split-window measurements by geostaionary satellite

Hirohiko ISHIKAWA (DPRI/Kyoto University)
Myanmar Cyclone Nargis: Satellite images and numerical experiments by WRF

Masato Shiotani (RISH/Kyoto University)
Stationary circulation observed in the upper troposphere over the western Indian Ocean

Yoshinori SHOJI (MRI/JMA)
Global realtime analysis of GPS data and plan of assimilation experiments

15:30-15:40 (*Coffee break*)

15:40-16:20 **Session 1 (continued)**

Takeshi HORINOUCHI (RISH/Kyoto University)
Gfdnavi: present and future prospects

Seiya NISHIZAWA (DG/Kyoto University)
Experimental development of a decision support system for prevention and mitigation of meteorological disasters with Gfdnavi

16:20-17:00 **Invited talks**

Shuichi MORI（JAMSTEC）
Present status of JEPP/HARIMAU radar-profiler network observations in Indonesia

Manabu YAMANAKA（JAMSTEC）
Coastline length governing equatorial rainfall amount

17:00-17:30 **Discussion on data archive and cooperation**

September 10 (Wed)

09:10-10:50 **Session 2: Numerical weather prediction**

Shigeo YODEN (DG/Kyoto University)
Ensemble forecasts with regional models

Kohei ARANAMI (JMA)
Improvements of utility tools to carry out NHM and introduction of DVD-NHM

Syugo HAYASHI (MRI/JMA)
Intercomparisons of NHM and WRF forecasts over topical and Japan areas
Tohru KURODA (MRI/JMA)
Development of utility tools for NHM execution in tropics and reproduce/forecast experiments of Nargis
Kazuo Saito（MRI/JMA）
Tidal wave simulation on ensemble forecast of Nargis
10:50-11:00 (*Coffee break*)

11:00-12:00 **Session 2（continued）**
Mitsuru UENO (MRI/JMA）
Some aspects of typhoon structure represented in the JMA meso-analyses and synthetic data
Masaru KUNII (MRI/JMA)
Regional data assimilation experiment in southeast Asia
Hiromu SEKO(MRI/JMA)
Structure of the regional heavy rainfall occurred at Santacruz, India on 26 July 2005

12:00-12:30 **Discussion on Bandung WS**

G-1-6. The Third Local Meeting

The third local meeting on "Prevention and Mitigation of Meteorological Disasters in Southeast Asia" was held on July 13-14, 2009, at Kyoto University in Kyoto, Japan. 13 Japanese researchers, one Indonesian researcher and two officers from JST participated in this meeting.

= Program =

July 13 (Mon)
09:30-12:00 **Session 1**
Shigeo YODEN (DG/Kyoto University)
Past, present and future of this JST project
Hirohiko ISHIKAWA (DPRI/Kyoto University)
The relationship between the development of Typhoon and the Ocean Heat Content
Tetsuya TAKEMI (DPRI/Kyoto University)
Representation and localization of severe local rainstorms and related disasters with high-resolution regional simulations
Tri Wahyu Hadi (ITB)
Improved NWP systems for hydrometeorological disaster risk reduction in Southeast Asia: economic imperatives and scientific challenges
Nurjanna Joko Trilaksono (DG/Kyoto University, ITB)
Study of heavy rainfall during Jakarta flood event January-February 2007
Shigenori OHTSUKA (DG/Kyoto University)
Experimental development of a decision support system for prevention and mitigation of meteorological disasters with Gfdnavi
12:00-13:30 (*Lunch break*)

13:30-16:00 **Session 2**
Masami Narita (JMA)
Development of a convection scheme for the JMA nonhydrostatic model
Masami Narita (JMA)
Using JMA models by the NWP research and development platform
Syugo HAYASHI (MRI/JMA)

Statistical verification of short range forecasts by NHM and WRF-ARW over Southeast Asia and Japan areas

Tohru KURODA(MRI/JMA)

Recent results and future plan of forecast experiments on Cyclone Nargis

Kazuo SAITO (MRI/JMA)

Ensemble prediction of Myanmar Cyclone Nargis and the associated storm surge

Masaru KUNII (MRI/JMA)

Mesoscale data assimilation of Myanmar Cyclone Nargis

Yoshinori SHOJI (MRI/JMA)

GPS data assimilation of Myanmar Cyclone Nargis

16:00-17:00 **Discussion on the project**
18:00- (*Banquet*)

July 14 (Tue)
09:30-14:30 **Individual discussions**

G-2. Newsletters[1]

Newsletters on "International Research for Prevention and Mitigation of Meteorological Disasters in Southeast Asia" were published six times for three years (see Appendix I-1).

・Newsletter No. 1 (Published on December 26, 2007)
Contents: 1. Outline
2. Major Research Subjects
3. Topics (The 1st International Workshop, JSPS-LIPI Workshop, The 5th AOGS Annual Meeting)

・Newsletter No. 2 (Published on March 10, 2008)
Contents: 1. MRI Scientists visit NTU and ITB
2. Report on the 1st International Workshop
3. Topics (Internet satellite "Kizuna" (WINDS))

・Newsletter No. 3 (Published on October 31, 2008)
Contents: 1. Report on the AOGS 2008 Session AS06
2. Topics (The WWRP Beijing Olympics 2008, Forecast Demonstration/Research and Development Project, The Second Domestic Workshop)

・Newsletter No. 4 (Published on March 23, 2009)
Contents: 1. Report on the 2nd International Workshop
2. Joint Sessions and Activities in Institut Teknologi Bandung
3. Topics (A workshop on "Ground based atmospheric observation network in equatorial Asia")

・Newsletter No. 5 (Published on October 30, 2009)
Contents: 1. MRI Scientist visited CMMCS in India
2. Visit to three institutions in Jakarta, Indonesia, for further international research collaborations
3. Lectures in KAGI21 International Summer School 2009

・Newsletter No. 6 (Published on March 29, 2010)
Contents: 1. Summary of the activities for three years
2. Topics (Report on the 3rd International Workshop)

[1] S. Yoden and F. Furutani (Kyoto University)

G-3. Mutual visits[1]

In addition to the international workshops, MRI scientists visited partner institutions in Southeast Asia and exchanged the scientific information during the project period (Table G-3-1).

Table G-3-1. List of visits of MRI scientists to partner institutions

Partner institutions	Country/ Region	Visitors	Period	Report in Newsletter (I-1)
ITB	Indonesia	Saito and Hayashi	2008.2.11-12	No. 2
NTU	Singapore	Saito and Hayashi	2008.2.14-15	No.2
CSIR C-MMACS	India	Hayashi	2009.3.23-25	No.5
VNU	Vietnam	Saito and Kuroda	2009.10.6-9	No.6
HKO	Hong Kong	Saito and Honda**	2009.2.9-13*	

*Invitation by Hong Kong Observatory

**Yuki Honda (Numerical Prediction Division/JMA)

Prior to the project T. Hadi of ITB and T. Koh of NTU visited MRI on 19 March 2007 with Prof. Yoden of Kyoto Univ. and made presentations (Fig. G-3-1).

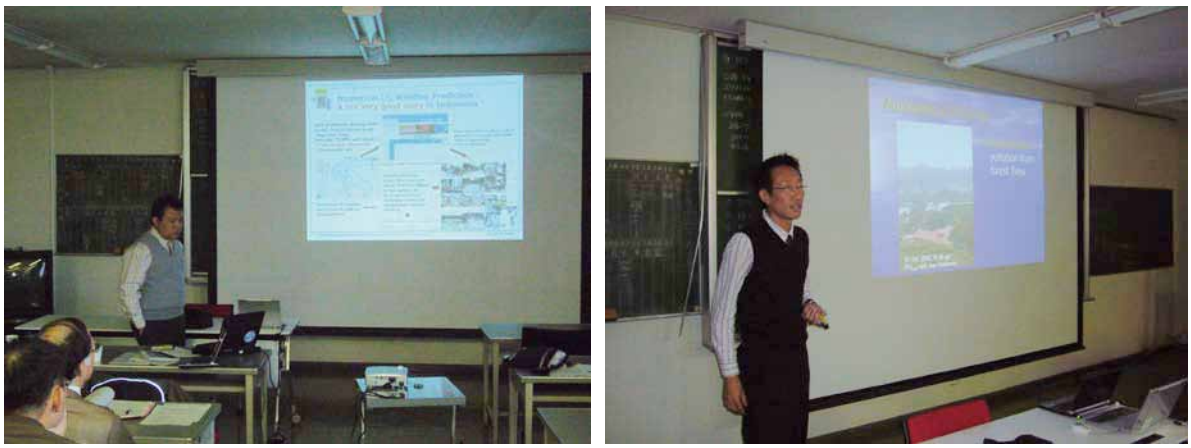

Fig. G-3-1. (Left) T. Hadi of ITB presents 'Numerical Weather Prediction in Indonesia: Demands, Prospects, and Challenges' at MRI. (Right) T.-Y. Koh of NTU presents 'Tropical Weather Research in Singapore'.

[1] K. Saito

G-4. Project web site at Kyoto University[1]

The web site of the project in English is provided by Kyoto University to serve researchers in Southeast Asia (http://www-mete.kugi.kyoto-u.ac.jp/project/MEXT/). The web site provides the following contents: the motivations of the project, the summary of the major research subjects (downscale NWPs, new data, and decision support system), topics, meetings, newsletters, the list of publications and presentations, reports of the project, and links to the related web sites. The top page (Fig. G-4-1) provides the general introduction of the project and the recent topics. The motivation of the project is written in the next page.

Fig. G-4-1. Top page of the web site of the project at Kyoto University.

On the pages of major research subjects, brief summaries are presented with schematic diagrams of (a) experimental downscale NWPs in the tropics with regional meso-scale models, (b) assessments of the impact of new observational data on NWPs with advanced data assimilation schemes, and (c) development of a unified data base and decision support system for prevention and mitigation of meteorological disasters. On the page of the topics, several reports on various topics are provided. The titles of the documents are shown below.

1. A session "Numerical Weather Prediction and Data Assimilation in Southeast Asia" (AS06) convened at the 5th Annual Meeting of Asia Oceania Geosciences Society (AOGS).
2. The International Symposium for Applications of "Kizuna" of Wideband InterNetworking engineering test and Demonstration Satellite (WINDS).
3. JSPS-LIPI workshop "Japan Indonesia Research Collaboration on Natural Disasters".

[1] S. Otsuka

4. A session "Applied Mesoscale Numerical Weather Prediction in Southeast Asia" (AS04) convened at the 3rd Annual Meeting of AOGS.
5. KAGI21 International Workshop "Regional Models for the Prediction of Tropical Weather and Climate"

On the page of the meetings, the programs of all the international and domestic workshops held by the project are provided. On the page of the newsletters, all the newsletters published by the project (volume 1-6) are distributed in the PDF format (Fig. G-4-2). The annual reports that are submitted to Japan Science and Technology Agency are also downloadable from the web site.

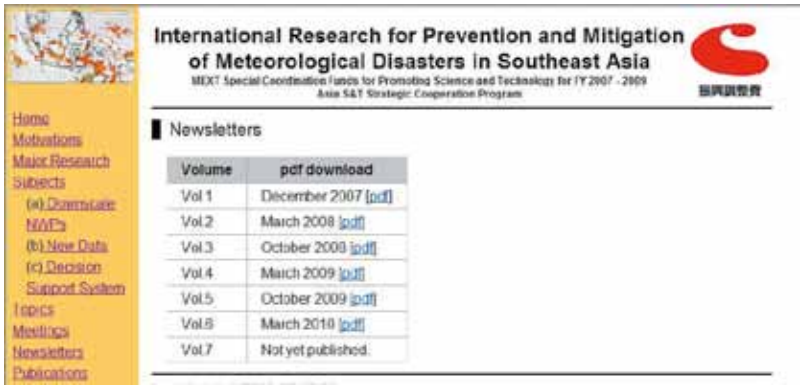

Fig. G-4-2. Download page of the newsletters.

G-5. Project web site at MRI[1]

The project web site on MRI's contribution was prepared as a part of the MRI's web page. The web site provided the following contents: News (topics), development of NWP models and application, meetings, information on NHM for the users outside JMA and links to the related web sites. The top page (Fig. G-5-1) provides the outline of the research and recent topics.

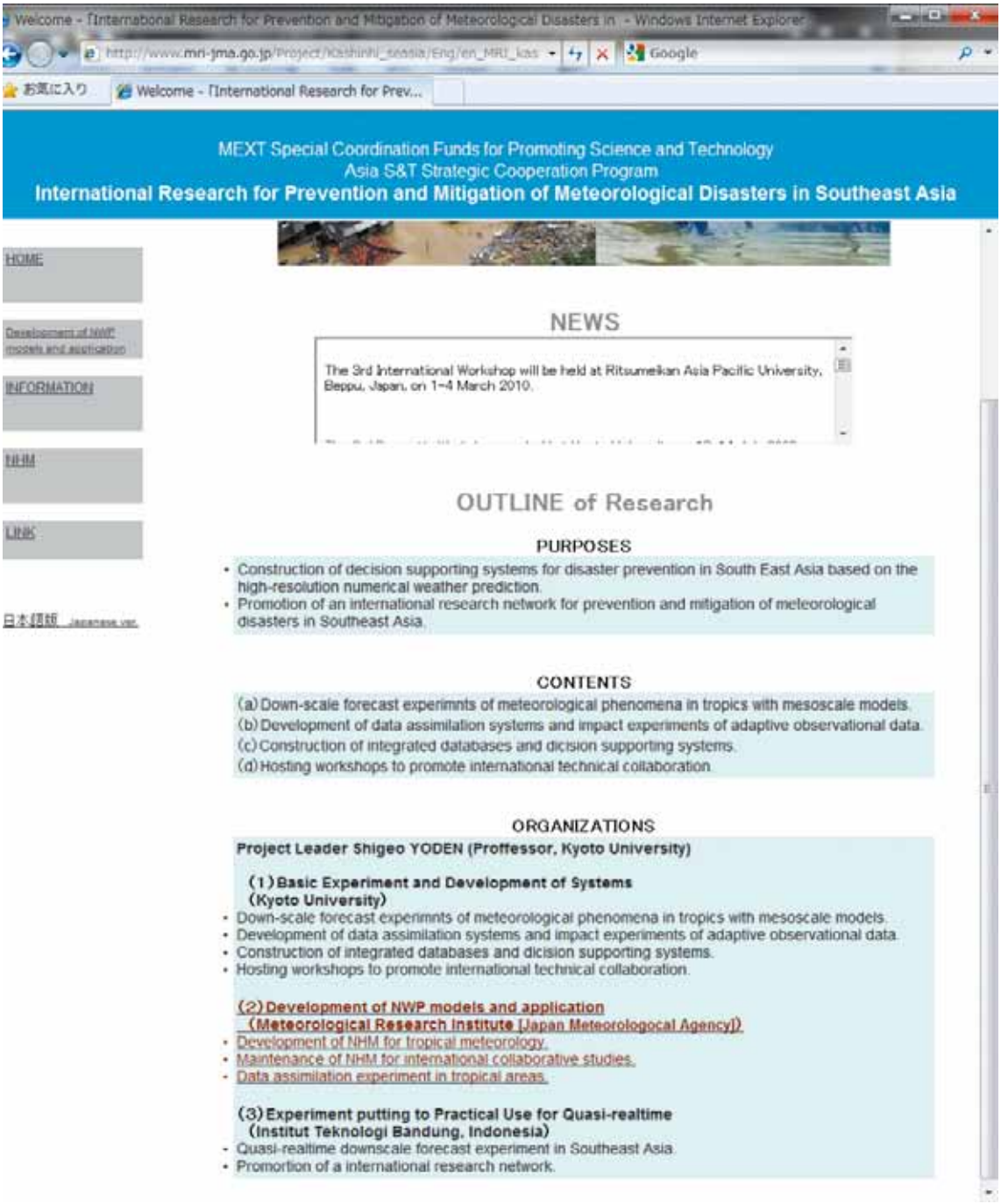

Fig. G-5-1. Top page of the web site of the project at MRI.
(http://www.mri-jma.go.jp/Project/Kashinhi_seasia/Eng/en_MRI_kashinhi.htm)

[1] K. Saito and T. Kuroda

On the pages of information, meeting programs, JMANHM information, and links are provided (Fig. G-5-2). The contents of JMANHM information include NHM user's guide (tutorials on NHM), a sample letter to ask for the permission to use NHM, publications and links to JRA25 and to Ruby-NusDaS(Fig. G-3-2).

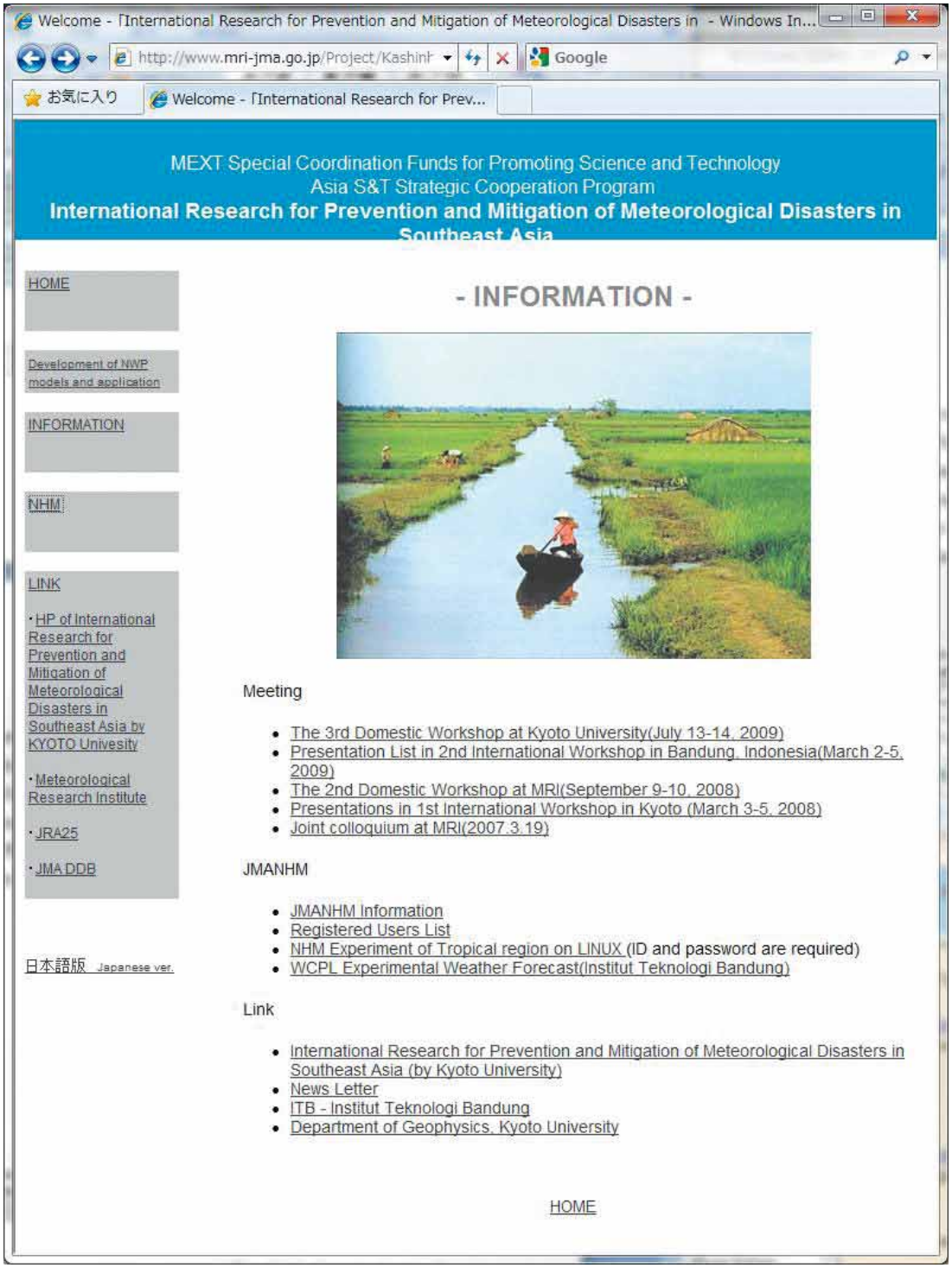

Fig. G-5-2. Information page.
(http://www.mri-jma.go.jp/Project/Kashinhi_seasia/Eng/en_MRI_kashinhi.htm)

H. References

Achtemeier, G. L., 1989: Modification of a successive corrections objective analysis for improved derivative calculations. *Mon. Wea. Rev.*, **117**, 78-86.

Albers S., J. McGinley, D. Birkenheuer, and J. Smart 1996: The Local Analysis and Prediction System (LAPS): Analysis of clouds, precipitation, and temperature. *Weather and Forecasting*, **11**, 273-287.

Asian Disaster Reduction Center, 2007: Natural Disasters Data Book 2006, (online), available from (http://www.adrc.or.jp /publications/databook/DB2006_e.html), (accessed 2008-9-29).

Belamari, S., 2005: Report on uncertainty estimates of an optimal bulk formulation for surface turbulent fluxes. *MERSEA IP Deliverable*, D.4.1.2.

Beljaars, A., 1995: The parametrization of surface fluxes in large-scale models under free convection. *Quart. J. Roy. Meteor. Soc.,* **121**, 255-270.

Bender, M. A., R. J. Ross, R. E. Tuleya, and Y. Kurihara, 1993: Improvements in tropical cyclone track and intensity forecasts using the GFDL initialization system. *Mon. Wea. Rev.*, **121**, 2046–2061.

Blumberg, A. F., and Mellor, G. L. 1987: A description of a three-dimensional coastal ocean circulation model. *Three-Dimensional Coastal Ocean Models, edited by N. Heaps, American Geophysical Union,* 208pp.

Bohra, A. K., S. Basu, E. N. Rajagopal, G. R. Iyengar, M. D. Gupta, R. Ashrit, and B. Athiyaman, 2005: Heavy rainfall episode over Mumbai on 26th July 2005: Assessment of NWP Guidance, *Report of NCMRWF*, 25 pp.

Branković, Č., T. N. Palmer, F. Molteni, S. Tibaldi, and U. Cubasch, 1990: Extended-range predictions with ECMWF models: Time-lagged ensemble forecasting. *Quart. J. Roy. Meteor. Soc.*, **116**, 867–912.

Braun, S. A., M. T. Montgomery, and Z. Pu, 2006: High-resolution simulation of Hurricane Bonnie (1998). Part I: The organization of eyewall vertical motion. *J. Atmos. Sci.*, **63**, 19–42.

Chan, S. T., T. F. Chan, and W. K. Wong, 2010: An Intercomparison of WRF-ARW and JMA-NHM Performance in Prediction of Tropical Cyclones over the South China Sea in 2008. *The 29th Conference on Hurricanes and Tropical Meteorology, American Meteorological Society, Tucson, Arizona, USA.*

Chang, C.-P., P. A. Harr, and H.-J. Chen, 2005: Synoptic disturbances over the equatorial South China Sea and western Maritime Continent during boreal winter. *Mon. Wea. Rev.*, **133**, 489–503.

Chen, S. S., 2008: Improving hurricane prediction through advanced data assimilation, modeling and observations. *AGU Fall Meeting, San Francisco, 15–19 December 2008.*

Cherubini, T., A. Ghelli, and F. Lalaurette, 2002: Verification of precipitation forecasts over the Alpine region using a high density observing network. *Wea. Forecasting*, **17**, 238-249.

Donelan, M. A., B. K. Haus, N. Reul, W. J. Plant, M. Stiassnie, H. C. Graber, O. B. Brown, and E. S.

Saltzman, 2004: On the limiting aerodynamic roughness of the ocean in very strong winds. *Geophys. Res. Let.,* **31**, L18306.

Ebita., A., K. Kobayashi, Y. Ota, M. Moriya, R. Kumabe, and K. Takahashi, 2009: JRA-55: Japanese 55-year reanalysis project status and plan, *Short abstracts of Fifth WMO Symposium on the Assimilation of Observations for Meteorology, Oceanography and Hydrology*, 46.

Elsberry, R. L., 2002: Numerical modeling for tropical cyclone intensity and precipitation. *USWRP Workshop on Numerical Modeling for Tropical Cyclone Intensity and Precipitation Prediction, San Diego, CA, 3–4 May 2002*.

Fairall, C. W., E. F. Bradley, J. E. Hare, A. A. Grachev, and J. B. Edson, 2003: Bulk parameterization of air-sea fluxes: Updates and verification for the COARE algorithm. *J. Climate,* **16**, 571-591.

Frank, W. M., 1977: The Structure and Energetics of the Tropical Cyclone I. Storm Structure, *Mon. Wea. Rev.*, **105**, 1119–1135.

Fritz, H. M., C. D. Blount, S. Thwin, M. K. Thu, and N. Chan, 2009: Cyclone Nargis storm surge in Myanmar, *Nature Geoscience*, **2**, 448-449.

Fujita, T., 1952: Pressure distribution within typhoon. *Geophys. Mag.*, **23**, 437–451.

Hayashi S., K. Aranami, and K. Saito, 2008:Statistical Verification of Short Term NWP by NHM and WRF-ARW with 20 km Horizontal Resolution around Japan and Southeast Asia., *SOLA*, **4**, 133-136.

Holland, G., 2008: A revised hurricane pressure−wind model. *Mon. Wea. Rev.*, **136**, 3432−3445.

Honda, Y., M. Nishijima, K. Koizumi, Y. Ohta, K. Tamiya, and T. Kawabata, 2005: A pre-operational variational data assimilation system for a non-hydrostatic model at the Japan Meteorological Agency: Formulation and preliminary results, *Quart. J. Roy. Meteor. Soc.*, **131**, 3465-3475.

Honda, Y., and K. Sawada, 2008: A New 4D-Var for Mesoscale Analysis at the Japan Meteorological Agency. *CAS/JSC WGNE Res. Act. Atmos. Ocea. Modell.*, **38**, 01.7-01.8.

Honda, Y., and K. Sawada, 2009: Upgrade of the Operational Mesoscale 4D-Var at the Japan Meteorological Agency. *CAS/JSC WGNE Res. Act. Atmos. Ocea. Modell*., **39**, 01.11-01.12.

Horinouchi, T., S. Nishizawa, C. Watanabe, A. Tomobayashi, S. Otsuka, T. Koshiro, and GFD Dennou Club, 2010: Gfdnavi, web-based data and knowledge server software for geophysical fluid sciences, part I: web application, *Lecture Notes in Computer Science*, **6913**, 93-104.

Huffman, G. J., R. F. Adler, D. T. Bolvin, G. Gu, E. J. Nelkin, K. P. Bowman, E. F. Stocker, and D. B. Wolff, 2007: The TRMM multisatellite precipitation analysis (TMPA): Quasi-global, multiyear, combined-sensor precipitation estimates at fine scales. *J. Hydrometeor.*, **8**, 38–55.

Ishikawa, Y., and K. Koizumi, 2002: Mesoscale 4-dimensional variational data assimilation. *Annual report of Numerical Prediction Division*, **48**, 37-59. (in Japanese)

Janjic, Z., R. Gall, and M. E. Pyle, 2010: Scientific Documentation for the NMM Solver. *NCAR Technical Note , NCAR/TN-477+STR*, 54pp

Japan Meteorological Agency, 1961: Official Report of Typhoon Vera, Japan Meteorological Agency.

Joseph, B., B. C. Bhatt, T. Y. Koh, and S. Chen, 2008: Sea breeze simulation over Malay Peninsula

over an intermonsoon period, *J. Geophys, Res*., **113**, p.D20122, doi:10.1029/2008JD010319.

Kain, J., and J. Fritsch, 1993: Convective parameterization for mesoscale models: The Kain-Fritsch scheme, The Representation of Cumulus Convection in Numerical Models, *Meteor. Monogr.*, **24**, 165-170.

Kalnay, E., 2003: Atmospheric Modeling, Data Assimilation, and Predictability, *Cambridge University Press*, 341 pp.

Kato T., and K. Aranami, 2005: Formation factors of 2004 Niigata-Fukushima and Fukui heavy rainfall and problems in the precipitations using a Cloud-resolving model, *SOLA*, **1**, 1-4.

Kawabata, T. H. Seko, K. Saito, T. Kuroda, K. Tamiya, T. Tsuyuki, Y. Honda, and Y. Wakazuki, An assimilation and forecasting experiment of the Nerima heavy rainfa11 with a cloud-resolving nonhydrostatic 4-dimensional variational data assimilation system, 2007, *J. Meteor. Soc. Japan*, **85**, 255-276.

Kawabata, T., M. Kunii, K. Bessho, T. Nakazawa, N. Kohno, Y. Honda, and K. Sawada, 2011: Reanalysis and Forecast of Typhoon Vera (1959) using a Mesoscale Four-Dimensional Variational Assimilation System. Part I: Impacts of Direct Observations and Bogus Data around the Eye of Typhoon. *J. Meteor. Soc. Japan* (submitted).

Kida, H., T. Koide, H. Sasaki, and M. Chiba, 1991: A New Approach for Coupling a Limited Area Model to GCM for Regional Climate Simulations. *J. Meteor. Soc. Japan*, **69**, 723-728.

Kitagawa, H., 2000: Radiation process. NPD Report No. 46, Numerical Prediction Division, JMA, 16-31. (in Japanese)

Knaff, J. A., and M. DeMaria, 2006: A multi-platform satellite tropical cyclone wind analysis system. *14th Conference on Satellite Meteorology and Oceanography*, *Atlanta, GA, U.S.A., 30 Jan. – 2 Feb. 2006.*

Koh, T. Y., and J. S. Ng, 2009: Improved diagnostics for NWP verification in the tropics. *J. Geophys. Res*., **114**, p.D12102, doi:10.1029/2008JD011179.

Koh, T. Y., and C. K. Teo (2009), "Towards a mesoscale observation network in Southeast Asia", *Bulletin of American Meteorological Society*, **90(4)**, 481-488, doi: 10.1175/2008BAMS2561.1.

Koizumi, K., Y. Ishikawa, and T. Tsuyuki, 2005: Assimilation of Precipitation Data to the JMA Mesoscale Model with a Four-dimensional Variational Method and its Impact on Precipitation Forecasts. *SOLA*, **1**, 45–48.

Kondo, J., 1975: Air-sea bulk transfer coefficients in diabatic conditions. *Bound.-Layer Meteor.,* **9**, 91-112.

Kunii, M., Y. Shoji, M. Ueno and K. Saito, 2010: Mesoscale data assimilation of Myanmar cyclone Nargis. *J. Meteor. Soc. Japan*, **88**, 455-474.

Kuroda, T., K. Saito, M. Kunii, and N. Kohno, 2010: Numerical simulations of Myanmar cyclone Nargis and the associated storm surge Part I: Forecast experiment with a nonhydrostatic model and simulation of storm surge. *J. Meteor. Soc. Japan*, **88**, 521–545.

Kuroda, T., K. Saito, M. Kunii, and H. Seko, 2010; Mesoscale LETKF Data Assimilation on cyclone Nargis. *CAS/JSC WGNE Res. Act. Atmos. Ocea. Modell.*, **40***,* 1.23-1.24.

Lai, S. T., and W. K. Wong, 2006: Quantitative precipitation nowcast of tropical cyclone rainbands – case evaluation in 2006. *39th Session of ESCAP/WMO Typhoon Committee, Manila, Philippines, 8 Dec. 2006.*

Lebeaupin, B.C., V. Ducrocq, and H. Giordani, 2007: Ocean-atmosphere interactions and coupling associated with torrential rainfall events. *International Conference on Alpine Meteorology*, *Chambéry, France, 4-8 June 2007.*

Majewski, D., 2009: HRM - User's guide. Deutscher Wetterdienst, Offenbach am Main, 120 pp.

Mittermaier, M. P., 2007: Improving short-range high-resolution model precipitation forecast skill using time-lagged ensembles. *Quart. J. Roy. Meteor. Soc.*, **133**, 1487–1500.

Miyamoto, K.,2009: Dry bias in the middle troposphere of the GSM. *Annual report of Numerical Prediction Division,* **55**, 68-70. (in Japanese)

Miyoshi, T., and K. Aranami, 2006: Applying a Four-dimensional Local Ensemble Transform Kalman Filter (4D-LETKF) to the JMA Nonhydrostatic Model (NHM), *SOLA*, **2**, 128-131 .

Nakanishi, M., and H. Niino, 2004: An improved Mellor-Yamada level 3 model with condensation physics: Its design and verification. *Bound.-Layer Meteor.*, **112**, 1–31.

Nakanishi, M., and H. Niino, 2006: An improved Mellor-Yamada level-3 model: Its numerical stability and application to a regional prediction of advection fog. *Bound.-Layer Meteor.*, **119**, 397–407.

Nishizawa, S., T. Horinouchi, C. Watanabe, Y. Isamoto, A. Tomobayashi, S. Otsuka, and GFD Dennou Club, 2010: Gfdnavi, web-based data and knowledge server software for geophysical fluid sciences, part II: RESTful web services and object-oriented programming interface, *Lecture Notes in Computer Science*, **6193**, 105-116.

Onogi, K. 1998: A Data Quality Control Method Using Forecasted Horizontal Gradient and Tendency in a NWP System: Dynamic QC. *J. Meteor. Soc. Japan.*, **76**, 497−516.

Onogi, K., J. Tsutsui, H. Koide, M. Sakamoto, S. Kobayashi, H. Hatsushika,T. Matsumoto, N. Yamazaki, H. Kamanori, K. Takahashi, S. Kadokura, K. Wada, K. Kato, R. Oyama, T. Ose, N. Mannoji, and R. Taira, 2007: The JRA-25 Reanalysis. *J. Meteor. Soc. Japan*, **85**, 369-432.

Oost, W.A., G.J. Komen, C.M.J. Jacobs, and C. van Oort, 2002: New evidence for a relation between wind stress and wave age from measurements during ASGAMAGE. *Bound.-Layer Meteor.,* **103**, 409-438.

Otsuka, S., and S. Yoden, 2010: Experimental Development of Decision Support System for Prevention and Mitigation of Meteorological Disasters Based on Ensemble NWP Data. *Annuals of Dias. Prev. Res. Inst., Kyoto Univ.,* **53B**, 377-382. (in Japanese with English abstract and figure captions)

Palmer, T. N, 2002: The economic value of ensemble forecasts as a tool for risk assessment: From days to decades, *Q. J. Roy. Meteor. Soc.*, **128**, 747-774.

Parrish, D., and J.C Derber, 1992: The National Meteorological Center's spectral statistical interpolation analysis system. *Mon. Wea. Rev.*, **120**, 1747-1763.

Powell, M. D., P. J. Vickery, and T.A. Reinhold, 2003: Reduced drag coefficient for high wind speeds in tropical cyclones. *Nature,* **422**, 279-283.

Saito, K., T. Kato, H. Eito, and C. Muroi, 2001: Documentation of the Meteorological Research Institute/Numerical Prediction Division unified nonhydrostatic model. *Tech. Rep. MRI*, **42**, 133pp.

Saito, K., T. Fujita, Y. Yamada, J. Ishida, Y. Kumagai, K. Aranami, S. Ohmori, R. Nagasawa, S. Kumagai, C. Muroi, T. Kato, H. Eito, and Y. Yamazaki, 2006: The operational JMA Nonhydrostatic Mesoscale Model. *Mon. Wea. Rev.*,**134**, 1266–1298.

Saito K., J. Ishida, K Aranami, T. Hara, T. Segawa, M. Narita, and Y. Honda, 2007: Nonhydrostatic Atmospheric Models and Operational Development at JMA. *J. Meteor. Soc. Japan*, **85B**, 271-304.

Saito, K., T. Kuroda, M. Kunii, and N. Kohno, 2010a: Numerical Simulations of Myanmar Cyclone Nargis and the Associated Storm Surge Part 2: Ensemble prediction. *J. Meteor. Soc. Japan*. **88**, 547-570.

Saito, K., M. Kunii, M. Hara, H. Seko, T. Hara, M. Yamaguchi, T. Miyoshi, and W. Wong, 2010b: WWRP Beijing 2008 Olympics Forecast Demonstration / Research and Development Project (B08FDP/RDP). *Tech. Rep. MRI*, **62**, 210pp.

Seko, H., and H. Nakamura, Analytical and Numerical Studies on Meso-β scale Precipitation Bands Observed over Southern Kyushu on 7 July 1996, 2005, *Papers in Meteorology and Geophysics*, **55**, 55-74.

Seko, H., S. Hayashi, M. Kunii and K. Saito, Structure of the Regional Heavy Rainfall System that Occurred in Mumbai, India, on 26 July 2005, 2008, *SOLA*, **4**, 129-132.

Shibayama, T., and Investigation Team of Japan Society of Civil Engineering, 2008: Prompt report on the storm surge disaster by the Myanmar Cyclone. *JSCE Magazine*, **93**, No.7, 41-43 (in Japanese).

Shindo, E., K. Saito, and M. Sugi, 2008: Typhoon formation and development experiment with a high resolution global model and a regional nonhydrostatic model. *Proceedings, 2008 Autumn Conference of the Meteorological Society of Japan,* **P109**. *(in Japanese)*

Shoji, Y., 2009; A study of Near Real-time Water Vapor Analysis using a nationwide Dense GPS Network of Japan, *J. Met. Soc. Japan*, **87**, 1-18.

Shoji. Y., M. Kunii, and K. Saito, 2011; Mesoscale Data Assimilation of Myanmar Cyclone Nargis Part II: Assimilation of GPS-Derived Precipitable Water Vapor, *J. Met. Soc. Japan*, **89**, 67-88.

Skamarock, W. C., J. B. Klemp, J. Dudhia, D. O. Gill, D. M. Barker, W. Wang, and J. G. Powers, 2005: A Description of the Advanced Research WRF Version 2. *NCAR Tech. Note*, **468**, 88p.

Skamarock, W. C., J. B. Klemp, J. Dudhia, D. O. Gill, D. M. Barker, M. G. Duda, X. Y. Huang, W. Wang, and J. G. Powers, 2008: A Description of the Advanced Research WRF Version 3. *NCAR Technical Note*, NCAR/TN-475+STR, 125 pp.

Tangang, F. T., L. Juneng, E. Salimun, P. N. Vinayachandran, Y. K. Seng, C. J. C. Reason, S. K.

Behera, and T. Yasunari, 2008: On the roles of the northeast cold surge, the Borneo vortex, the Madden-Julian Oscillation, and the Indian Ocean Dipole during the extreme 2006/2007 flood in southern Peninsular Malaysia. *Geophys. Res. Lett.*, **35**, L14S07, doi: 10.1029/2008GL033429.

Taylor, P. K., and M. A. Yelland, 2001: The dependence of sea surface roughness on the height and steepness of the waves. *J. Phys. Oceanogr.,* **31**, 572-590.

Teo, C. K., T. Y. Koh, C. F. Lo, and B. C. Bhatt, 2011: Principal Component Analysis of observed and modeled diurnal rainfall in the Maritime Continent. *J. Climate*, **24**, 4662-4675.

Trilaksono, N. J., S. Otsuka, and S. Yoden, 2011: A time-lagged ensemble forecast experiment on the modulation of precipitation over West Java in January-February 2007. *Mon. Wea. Rev.* doi:10.1175/MWR-D-11-00094.1.

Tukey, J. W., 1977: Exploratory Data Analysis, *Reading, Mass: Addison-Wesley Publishing Co.*, 688 pp.

Ueno, M., 1989: Operational bogussing and numerical prediction of typhoon in JMA. *JMA/NPD Tech. Rep.*, No. **28**, 48pp.

Ueno, M., 1995: A study on the impact of asymmetric components around tropical cyclone center on the accuracy of bogus data and the track forecast. *Meteorol. Atmos. Phys.*, **56**, 125–134.

Ueno, M., 2000: Typhoon forecast by numerical models. *Meteor. Res. Notes*, **197**, 131–286 (in Japanese).

Ueno, M., 2008: Effects of ambient vertical wind shear on the inner-core asymmetries and vertical tilt of a simulated tropical cyclone. *J. Meteor. Soc. Japan*. **86**, 531-555.

Ueno, M., and W. Mashiko, 2005: Current status and challenges of forecasting typhoon with high-resolution models. *Working Papers of CREST 2005*, 61–65 (in Japanese).

Ueno, M., and M. Kunii, 2009: Some aspects of azimuthal wavenumber-one structure of typhoons represented in the JMA operational mesoscale analyses. *J. Meteor. Soc. Japan*, **87**, 615–633.

Webster, P. J., 2008: Myanmar's deadly daffodil. *Nature Geoscience*, **1**, 488 – 490.

Wong, W.K. and E.S.T. Lai, 2006: RAPIDS – Operational Blending of Nowcast and NWP QPF. *2nd International Symposium on Quantitative Precipitation Forecasting and Hydrology, Boulder, USA, 4-8 June 2006.*

Wong, W. K., L. H. Y. Yeung, Y. C. Wang, and M. Chen, 2009 : Towards the Blending of NWP with Nowcast — Operation Experience in B08FDP, *WMO Symposium on Nowcasting, 30 Aug-4 Sep 2009, Whistler, B.C., Canada.*

Wong, W. K., P. W. Chan, and C. K. Ng, 2011: Aviation Applications of a New Generation of Mesoscale Numerical Weather Prediction System of the Hong Kong Observatory. *24th Conference on Weather and Forecasting/20th Conference on Numerical Weather Prediction, American Meteorological Society, 24-27 Jan 2011, Seattle, USA.*

Wong, W. K., S. Sumdin, and S.T. Lai, 2010: Development of Air-Sea Bulk Transfer Coefficients and Roughness Lengths in JMA Non-hydrostatic Model and Application in Prediction of an Intense Tropical Cyclone. *SOLA*, **6**, 65-68.

Wu, P., M. Hara, H. Fudeyasu, M. D. Yamanaka, J. Matsumoto, F. Syamsudin, R. Sulistyowati, and Y.

S. Djajadihardja, 2007: The impact of trans-equatorial monsoon flow on the formation of repeated torrential rains over Java Island. *SOLA*, **3**, 93–96.

Yabu, S., S. Murai, and H. Kitagawa, 2005: Clear-sky radiation scheme. *NPD Report, Numerical Prediction Division, JMA,* **51**, 53-64. (in Japanese)

Yamasaki, M., 1983: A further study of the tropical cyclone without parameterizing the effect of cumulus convection, 1983, *Papers in Meteorology and Geophysics*, **34**, 221-260.

Yamasaki, M., 1984: Dynamics of convective clouds and 'CISK' in vertical shear flow-with its application to easterly waves and squall-line systems, 1984, *J. Meteor. Soc. Japan*, **62**, 833-863.

Yamasaki, M., and H. Seko, Effect of the gravity wave on the convection cells, 1992, *Proceedings of Spring meeting of Meteorological Society of Japan*, A108 (in Japanese).

Yoden, S., K. Saito, T. Takemi, and S. Nishizawa, 2008: New stages of international collaborations which serves for mitigation of meteorological disasters in Southeast Asia, *Tenki*, **55**, 705-708. (in Japanese)

Zumberge, J. F., M. B. Heflin, D. C. Jefferson, and M. M. Watkins, 1997: Precise point positioning for the efficient and robust analysis of GPS data from large networks, *J. Geophys. Res.*, **102(B3)**, 5005–5017.

I. Appendix

I-1. Newsletters

I-2. Introduction to a web-based decision support tool for ensemble numerical weather prediction with Gfdnavi

International Research for Prevention and Mitigation of Meteorological Disasters in Southeast Asia

MEXT Special Coordination Funds for Promoting Science and Technology for FY 2007 - 2009
in Asia S&T Strategic Cooperation Program

Newsletter

No. 1 (Dec. 2007)

Contents

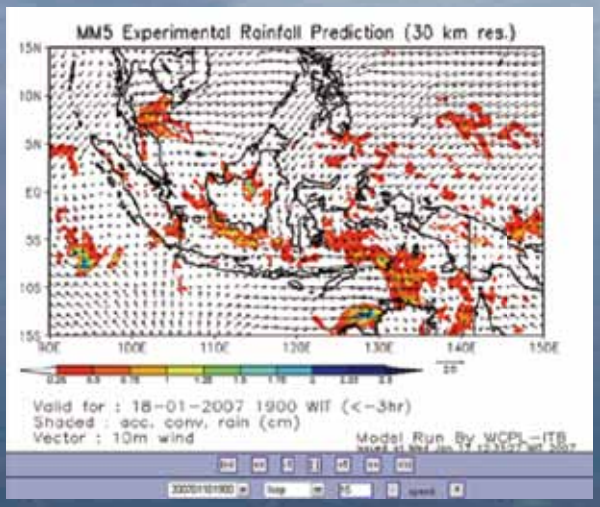

Outline

Motivations

Risk of high-impact weather in Southeast Asia is potentially increasing because of the economical development and urbanization. Global warming and climate change might become another factor for the increase of the risk. It would be a good timing for us to start an international research project for prevention and mitigation of meteorological disasters in Southeast Asia, because the research environment is rapidly changing by the growth of computer powers and the improvement of internet infrastructures. Regional meso-scale models can be run with personal computers for downscale numerical weather predictions (NWPs). Data transfer via internet is getting fast enough to perform near-real time NWPs. Utilization of probability information obtained by ensemble NWPs is a challenge for the development of decision support tools. Assessments of the impact of new observational data on the improvement of NWPs with advanced data assimilation schemes are also important subject in these days.

Thus, we have just started "International Research for Prevention and Mitigation of Meteorological Disasters in Southeast Asia" under the Ministry of Education, Culture, Sports, Science and Technology (MEXT) Special Coordination Funds for Promoting Science and Technology, supported for FY 2007-2009 under Asia S & T Strategic Cooperation Program.

Research Groups

Three main affiliations of this international research project are Kyoto University, Meteorological Research Institute (MRI) of Japan Meteorological Agency (JMA), and Institut Technologi Bandung (ITB) in Indonesia. Shigeo Yoden, Professor of Meteorology in Kyoto University, is the leader of this project, and Kazuo Saito, Head of the 2nd Research Laboratory, Forecast Research Department of MRI, and Emmy Suparka, Professor and Vice President of ITB are group leaders in these two institutes. As shown in Fig. 1, fundamental research and system development will be done at Kyoto University, while operational model development will be done at MRI/JMA. Real-time experiment will be done at ITB and other institutes outside Japan.

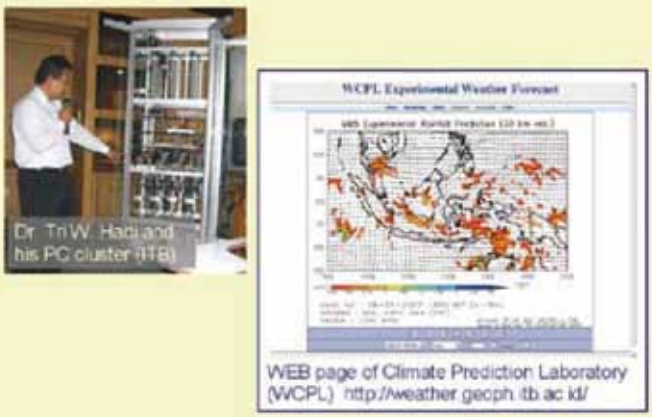

Figure 2. Recent attempt by Dr. Tri W. Hadi

Figure 2 shows an example of our recent preliminary attempts. Tri W. Hadi, Lecturer of ITB, constructed his own PC cluster by himself to perform downscale NWPs. Experimental weather forecast is on the web page of Weather and Climate Prediction Laboratory (WCPL) at http://weather.geoph.itb.ac.id/

Our purpose is to establish "International Scientist-Network for Prevention and Mitigation of Meteorological Disasters in Southeast Asia" through research and development of downscaling NWP systems.

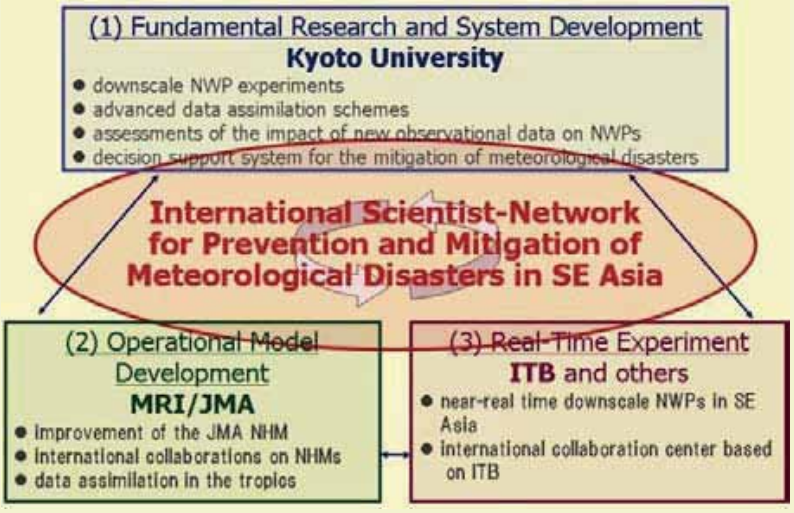

Figure 1. Research Groups

Major Research Subjects

(a) Experimental downscale numerical weather predictions (NWPs) in the tropics with regional meso-scale models

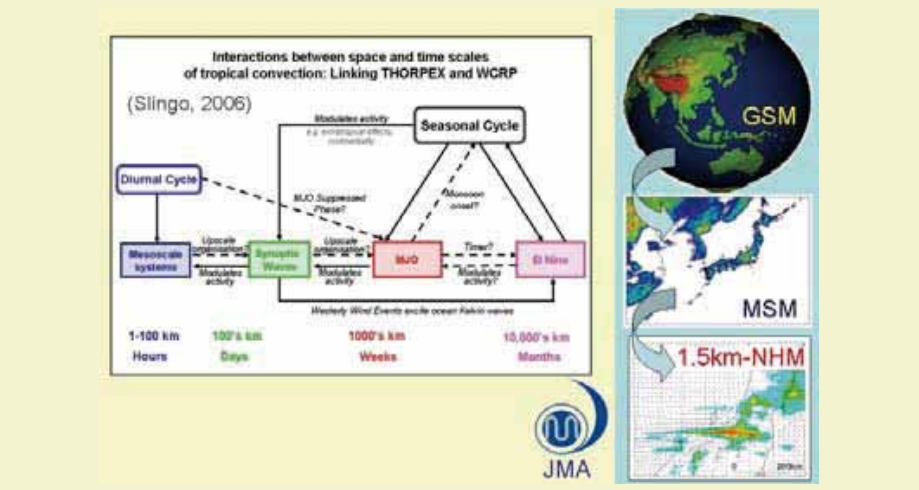

(b) Assessments of the impact of new observational data on the improvement of NWPs with advanced data assimilation schemes

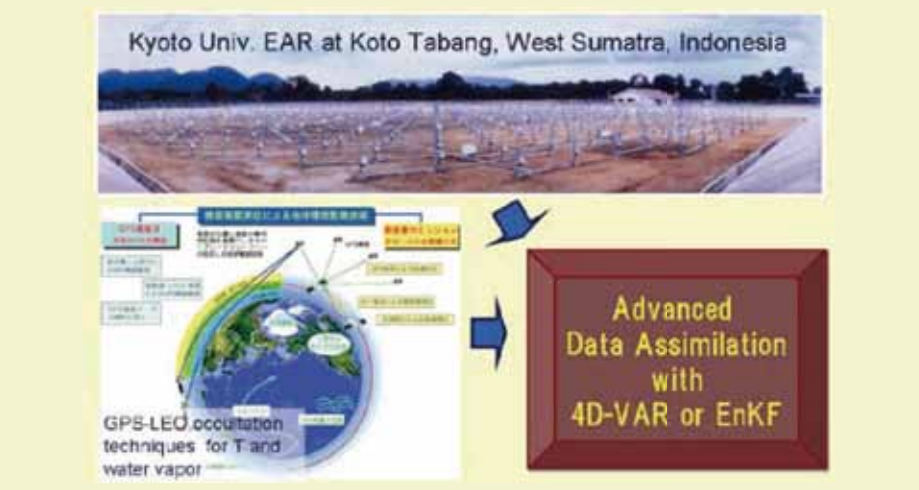

(c) Development of a unified data base and decision support system for prevention and mitigation of meteorological disasters

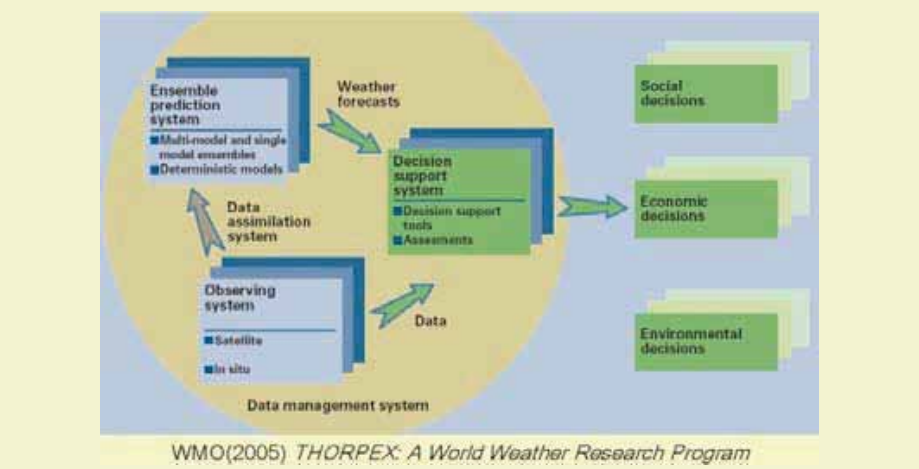

WMO(2005) *THORPEX: A World Weather Research Program*

Topics

The First International Workshop on Prevention and Mitigation of Meteorological Disasters in Southeast Asia

The first international workshop of this research project will be convened by Shigeo Yoden (Kyoto University) and Kazuo Saito (Meteorological Research Institute, Japan Meteorological Agency) in March 3-5, 2008, at the Palace Side Hotel in Kyoto, Japan. Details on this workshop will be announced in the following web page: http://www-mete.kugi.kyoto-u.ac.jp/project/MEXT/

JSPS-LIPI workshop "Japan Indonesia Reserch Collaboration on Natural Disasters"

This workshop was held on June 20, 2007 in Jakarta, Indonesia, under the auspices of JSPS (Japan Society for the Promotion of Science) and LIPI (Indonesian Institute of Sciences) to build strong networks of international cooperation to prevent natural disasters between Japan and Indonesia. Shigeo Yoden (Kyoto University) presented an overview paper on this new project.

The final report of the workshop can be found at the following web page: http://www.jsps.go.jp/english/e-astrategy/02_report070620.html

A session "Numerical Weather Prediction and Data Assimilation in Southeast Asia" (AS06) convened at the 5th Annual Meeting of Asia Oceania Geosciences Society

This session is convened by Tieh-Yong Koh (Nanyang Technological University), Shigeo Yoden (Kyoto University), and Tri Wahyu Hadi (Institut Teknologi Bandung) in the 5th AOGS Annual Meeting held in Busan, Korea, 16-20 June, 2008. Details can be seen in the following web page: http://www.asiaoceania.org/aogs2008/mars/pubSessionView.asp?sID=51

Session Description: Despite advances in numerical weather prediction (NWP) and data assimilation techniques for the recent decades, little discussion (and perhaps progress) has been made on these fronts in Southeast Asia. In this session, we want to share our experiences in actually trying to simulate realistically the region's synoptic and mesoscale weather over 1-2 day time scale. Downscaling of weather information in longer time scales in combination with global long-range forecasts is also an important subject of this session. Through the discussions we want to initiate a platform for scientists interested in mesoscale NWP and data assimilation in Southeast Asia to interact. We also welcome more theoretical work like data assimilation techniques for using data from advanced observational platforms like satellite and radar.

Abstract Submission Deadline: 24 January, 2008.

International Research for Prevention and Mitigation of Meteorological Disasters in Southeast Asia
Newsletter No.1 December 26, 2007

MEXT Special Coordination Funds for Promoting Science and Technology for FY 2007 - 2009
in Asia S&T Strategic Cooperation Program

Shigeo Yoden
Department of Geophysics, Kyoto University, Kyoto 606-8502, Japan
Tel: +81-75-753-3932
Fax: +81-75-753-3715
E-mail: yoden@kugi.kyoto-u.ac.jp
Web: http://www-mete.kugi.kyoto-u.ac.jp/project/MEXT/

International Research for Prevention and Mitigation of Meteorological Disasters in Southeast Asia

MEXT Special Coordination Funds for Promoting Science and Technology for FY 2007 - 2009
in Asia S&T Strategic Cooperation Program

Newsletter

No. 2 (Mar. 2008)

Contents

MRI Scientists visit NTU and ITB

Two scientists, Kazuo Saito and Syugo Hayashi of the Meteorological Research Institute (MRI), visited the Nanyang Technological University (NTU) of Singapore and the Institut of Teknologi Bandung (ITB) of Indonesia in February 2008. Their visit was done to discuss the collaboration on the International Research for Prevention and Mitigation of Meteorological Disasters in Southeast Asia and to confirm the portability of the JMA nonhydrostatic model (NHM) on computers at oversea research institutes.

On Monday 11 and Tuesday 12, Saito and Hayashi visited the Division of Applied Physics at the School of Physical and Mathematical Sciences of NTU, and met Assistant Professor Tieh-Yong Koh and Dr. Rosbintarti Kartika Lestari, who has been studying the regional atmospheric modeling under the guidance of Prof. Koh. At NTU, a cluster machine consists of IBM e-servers with AMD Opteron252 2.6GHz 16CPU and AMD Opteron Dual Core 275 2.2GHz 48CPU has been used for numerical weather prediction experiments with the COAMPS model. A test of NHM using JRA25 reanalysis data of JMA and visualization by 'Webpandah' (a visualization tool for NHM data developed at JMA) were conducted. Figure 1 shows the example of a simulation by NHM with a horizontal resolution of 30 km where JRA25 data at 00 UTC 7 January 1982 is used for the initial condition.

The duo also visited the satellite office of KAGI21 (Kyoto University Active Geosphere investigations for the 21st century COE Program) and the Faculty of Earth Sciences of ITB on Thursday 14 and Friday 15 February to meet Assistant Professor Tri Wahyu Hadi and his students, I Dewa Gede Junnaedhi and Nurjanna Joko Trilaksono (Fig. 2). At ITB, a cluster machine consists of 8 nodes 4 CPU Intel Quad-Core 660 2.4 GHz has been employed for near real time NWP experiments with MM5 and WRF models. A test of NHM using JMA' s high resolution GSM data distribute from the Japan Meteorological Business Support Center (JMBSC) was successively performed. Figure 3 shows the example of a simulation by NHM where high resolution GSM data at 00 UTC 14 February 2008 is used for the initial condition.

(Kazuo Saito, MRI/JMA)

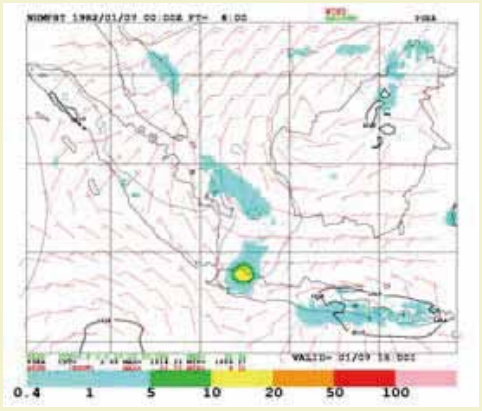

Figure 1. Surface wind and 6 hour accumulated precipitation by NHM with a horizontal resolution of 30 km. JRA25 data at 00UTC 7 January 1982 was used as the initial condition. 5 CPU of the NTU' s cluster machine was employed.

Figure 2. Photograph taken at the satellite office of KAGI21 of ITB. From left to right, Nurjanna Joko Trilaksono, Syugo Hayasi, Tri Wahyu Hadi, Kazuo Saito, I Dewa Gede Junnaedhi, and Ida Yayuk Purnamasari (Sectretary of the KAGI21 satellite office).

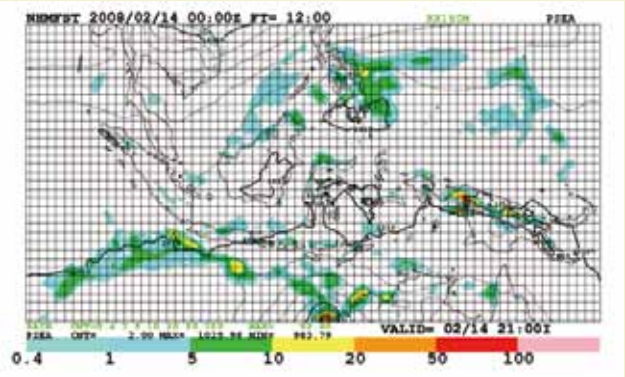

Figure 3. Surface pressure and 3 hour accumulated precipitation at 12 UTC 14 February 2008 by NHM with a horizontal resolution of 30 km. High resolution GSM data at 00UTC 14 February 2008 is used as the initial condition.

Report on the 1st International Workshop

The first international workshop of this research project on "Prevention and Mitigation of Meteorological Disasters in Southeast Asia" was held on March 3-5, 2008, at the Palace Side Hotel in Kyoto, Japan. In total fifty eight researchers participated from twelve countries and regions in East Asia, Southeast Asia and South Asia.

The workshop was opened by the address and introduction about the MEXT program by Dr. Hirokazu Kobayashi, Program Officer of JST (Japan Science and Technology Agency). After the keynote address about this project by the project leader, Shigeo Yoden (Kyoto University), there were seven sessions with a total of forty two invited talks: Suparka, Hadi, Saito, Hara, Islam, Xin, Ratag, Thalongsengchanh, and Gouda had presentations in the Session I "High-resolution numerical weather predictions"; S.Hayashi and Nishizawa in the Session II "Tutorials and demonstrations"; Bounlom, Saravuth, Tangang, T. Hayashi, Seko, Lestari, Tsuboki, Iwasaki and Ueno in the Session III "High-impact weather and its simulation/prediction"; Tsuda, Shoji, Begkhuntod, H. Ishikawa, Kunii, Duc, Enomoto, and Prasad in the Session IV "Satellite observations, their applications and data assimilation"; Koh, Kang, Lai, Mukougawa, Jampanya, Sanga, Promasakha and Horinouchi in the Session V "Model output statistics, predictability, and decision supports"; Satomura, Trilaksono, Otsuka, Y. Ishikawa and Takemi in the Session VI "High-resolution model as a fundamental research tool"; and all participants had open discussions in the Session VII "Future research and collaborations". Further details can be found in our Web page, http://www-mete.kugi.kyoto-u.ac.jp/project/MEXT/

There were presentations about new research results on numerical weather predictions, new observational data, and decision support tools/systems, and we also had enthusiastic discussions. We do hope this workshop will help us for making future international research collaborations among Asian scientists. We are going to have the second international workshop at ITB in Bandung, Indonesia in March 2009, and the third one at Ritsumeikan Asia Pacific University in Beppu, Japan in March 2010.

(Seiya Nishizawa, Kyoto Univ.)

Topics

The International Symposium for Applications of "Kizuna" of Wideband InterNetworking engineering test and Demonstration Satellite (WINDS) and successful launch of "Kizuna" on February 23, 2008

The International Symposium for Applications of "Kizuna" of Wideband InterNetworking engineering test and Demonstration Satellite (WINDS) was held on December 4 (Tuesday), 2007 at Meiji Kinenkan in Tokyo. There were 6 Addresses, including "ICT based e-health and disaster mitigation management system" by Professor Utoro Sastrokusumo (School of Electrical Engineering and Informatics, Institut Technologi Banding (ITB), Indonesia), and 5 Speeches. Shigeo Yoden (Kyoto University) participated in the Panel discussion "WINDS Application Experiments Now Needed in the Asia Pacific Region" as one of 6 panelists, and presented our international research activity, "An experimental down-scale numerical weather predictions in Southeast Asia with the aid of WINDS".

The "Kizuna" is a communications satellite that enables super high-speed data communications of up to 1.2 Gbps to develop a society without any information availability disparity, in which everybody can equally enjoy high-speed communications wherever they live (http://www.jaxa.jp/countdown/f14/index_e.html). The "Kizuna" was launched at 5:55 p.m. on February 23, 2008 (JST) successfully with H-IIA F14 from the Tanegashima Space Center. The multi-beam antennas had been successfully deployed at 8:35 p.m. on March 1 (JST) and the critical operation phase was completed. The "Kizuna" will further drift into the geostationary orbit at about 143 degrees east longitude in March. The initial functional verification of the onboard equipment will be done for about four months.

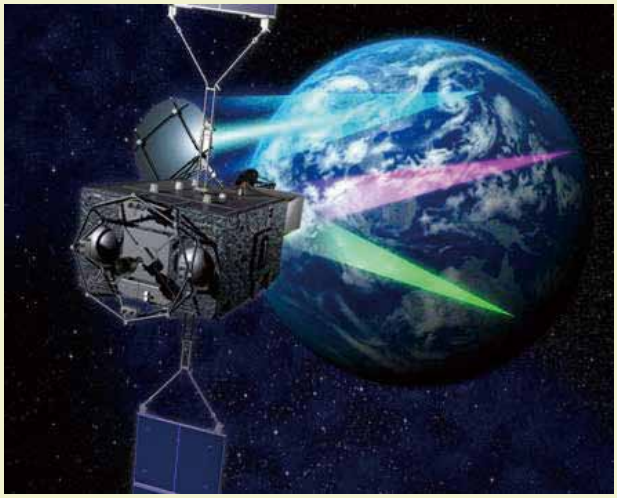

Photo No. : P-017-06848 in the KIZUNA Photo Gallery at the JAXA Web page, http://www.jaxa.jp/index_e.html

Our proposal for test use of the "Kizuna" has been accepted to transfer ensemble forecast data and adaptive observation data for downscale numerical weather predictions. We hope we can also use the "Kizuna" for teleconference between Kyoto University and ITB in the second International Workshop on Prevention and Mitigation of Meteorological Disasters in Southeast Asia, which will be held in March, 2009 in Bandung, Indonesia.

International Research for Prevention and Mitigation of Meteorological Disasters in Southeast Asia
Newsletter No.2; March 10, 2008

MEXT Special Coordination Funds for Promoting Science and Technology for FY 2007 - 2009 in Asia S&T Strategic Cooperation Program

Shigeo Yoden
Department of Geophysics, Kyoto University, Kyoto 606-8502, Japan
Tel: +81-75-753-3932
Fax: +81-75-753-3715
E-mail: yoden@kugi.kyoto-u.ac.jp
Web: http://www-mete.kugi.kyoto-u.ac.jp/project/MEXT/

International Research for Prevention and Mitigation of Meteorological Disasters in Southeast Asia

MEXT Special Coordination Funds for Promoting Science and Technology for FY 2007 - 2009
in Asia S&T Strategic Cooperation Program

振興調整費

Newsletter

No. 3 (Oct. 2008)

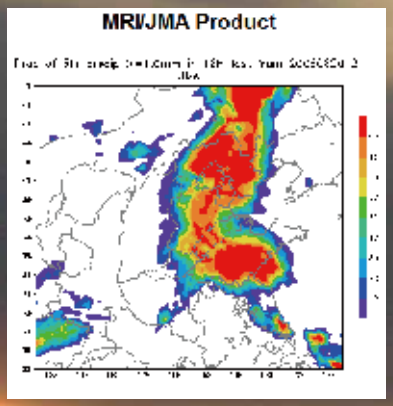

Contents

Report on the AOGS 2008 Session AS06

"Numerical Weather Prediction and Data Assimilation in Southeast Asia" on June 16, 2008

In conjunction with the program of International Research for Prevention and Mitigation of Meteorological Disasters in Southeast Asia (see Newsletter No. 1, Dec. 2007), Shigeo Yoden (Kyoto University), Tieh Yong Koh (Nanyang Technological University), and Tri Wahyu Hadi (Institut Teknologi Bandung) has successfully convened a session (AS06) entitled Numerical Weather Prediction and Data Assimilation in Southeast Asia at the 5th Annual Meeting of Asia-Oceania Geoscience Society (AOGS) that was held in Busan, Korea during 16-20 June 2008 (Photo 1). This session was aimed at setrengthening and widening the network of researchers interested in weather and climate prediction in Southeast Asia.

As many as 13 presentations were registered to the A06 session of the AOGS 2008 and only one was cancelled. The core members of the International Research for Prevention and Mitigation of Meteorological Disasters in Southeast Asia research team who attended this session are : Shigeo Yoden and Shigenori Otsuka (Kyoto University), Kazuo Saito and Shugo Hayashi (MRI), Tieh Yong Koh (NTU), and Tri Wahyu Hadi (ITB). An invited talk by Hongwen Kang of APEC Climate Center (APCC) highlighted some new results in multi-model outputs statistical downscaling prediction. In addition, there are contributed talks by Fredolin Tangang (National University of Malaysia), Der Song Chen (Central Weather Bureau of Taiwan), Kevin Kei Wai Cheung (Macquarie University, Australia), Che-Kiat Teo (NTU), Bhuwan Chandra Bhatt (NTU), and Ok-Yeong Kim (Pukyong National University, South Korea).

Photo 1. Opening talk by Dr. Tieh Yong Koh.

The A06 session of the AOGS 2008 has highlighted one fundamental problem in lieu of advanced NWP modeling i.e. the predictability of weather system in the Southeast Asian region. This confirms that the complexity of weather systems in Southeast Asia, that comprises the Maritime Continent, is one of the most challenging problem in atmospheric predictability due to dominant role of the mesoscale convective system. The very same problem that is also actually addressed by Professor Taroh Matsuno in his Axford Lecture of AOGS 2008 "Modeling of Tropical Convection by Use of an Ultra-High Resolution (3.5-7 km) Global Atmosphere Model – New Age of Tropical Meteorology". In such a situation, the "International Research for Prevention and Mitigation of Meteorological Disasters in Southeast Asia" is an excellent program to provide a knowledge hub for young scientists in Southeast Asian countries to access latest information on the ever developing science and technologies of weather and climate prediction.

As a side activity, the core members of the International Research for Prevention and Mitigation of Meteorological Disasters in Southeast Asia research team also visited the APEC Climate Center (APCC) in Busan on 16 June 2008. We would like to thank Dr. Hongwen Kang and Dr. Karumuri Ashok for their kind arrangement of the visit. Beside us, it turned out that many other scientists attending the 5th AOGS Annual Meeting were also interested in the program, so that in total there were more than 20 participants visiting APCC in the afternoon of 16 June 2008. Inline with the goals of our collaborative international research program, APCC has an excellent ensemble climate forecast data center that could help scientists in the APEC region (including those in Southeast Asia) to conduct research in the application of climate prediction. APCC has also been developing data management and data processing tools to make climate prediction more amenable for developing Asia-Pacific countries. Undoubtedly, closer collaboration with APCC in the future is necessary for the success of our program.

(Tri Wahyu Hadi, ITB)

Topics

The WWRP Beijing Olympics 2008 Forecast Demonstration / Research and Development Project

The WWRP Beijing Olympics 2008 Forecast Demonstration / Research and Development Project (B08FDP/RDP) is an international research project for a short range weather forecast of the WMO World Weather Research Programme (WWRP), which succeeded the Sydney 2000FDP. The B08FDP/RDP is divided into two components; the FDP component for a short range forecast up to 6 hours based on the nowcasting (http://www.b08fdp.org), and the RDP component for a short range forecast up to 36 hours based on the mesoscale ensemble prediction (MEP) system (http://www.b08rdp.org). Aims of the RDP project are to improve understanding of the high-resolution probabilistic prediction processes through numerical experimentation and to share experiences in the development of the real-time MEP system. In the 2008 experiment, six participating systems from Austria and France (ZAMG and Météo-France), Canada (MSC), China (NMC and CAMS), Japan (MRI/JMA) and United States (NCEP) joined B08RDP, and intercomparisons of MEP systems were conducted for one month from 24 July to 24 August, including the period of the Olympic games. Every participants ran their MEP forecasts in real-time and sent the 36 forecasts to the CMA's ftp server. The products were displayed every day on the B08RDP's website (Fig. 1) for reference of Beijing Meteorological Bureau's forecasters.

Collaborating with the Numerical Prediction Division of JMA, MRI developed its MEP system with a horizontal resolution of 15 km. It consists of 11 members: one control run and ten perturbed members. Initial conditions of the control run were given by the meso 4DVAR analysis which assimilated precipitation data over China, while initial perturbations were computed by the global targeted singular vector method. Lateral boundary perturbation method was newly implemented, and the latest version of NHM was employed as the forecast model. MRI also supported the Hong Kong Observatory (HKO) team by providing boundary conditions to NHM used in the HKO's B08FDP short range forecasting system SWIRLS. Results and outcome of the intercomprisons will be discussed at the 4th international B08FDP/RDP workshop held in 2009 at Beijing.

(Kazuo Saito, MRI)

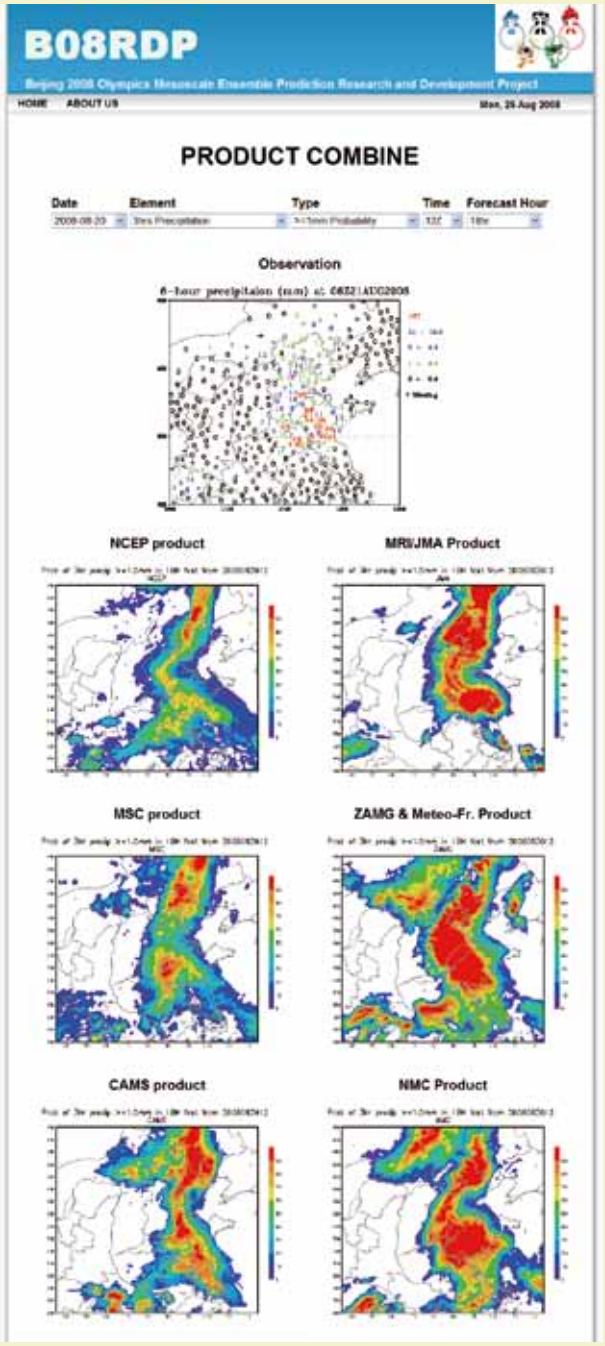

Figure 1. Example of the B08RDP product. Probability of precipitation greater than 1 mm in 3 hours from 03 UTC to 06 UTC 21 August 2008 predicted by MEP systems of 6 participants. Initial time is 12 UTC 20 August (FT=18). Observation shows accumulated 6 hour precipitation from 00 UTC to 06 UTC. After CMA's B08RDP website (http://www.b08rdp.org).

Topics

The Second Domestic Workshop

The second domestic workshop on the International Research for Prevention and Mitigation of Meteorological Disasters in Southeast Asia was held in September 9-10, 2008, at the Meteorological Research Institute in Tsukuba, Japan. There were 28 participants and we had active discussions. The program was as follows:

September 9 (Tue)
1310-1330 Opening
1330-1620 Session 1: Observation and Data
Taiichi HAYASHI (DPRI, Kyoto University)
Recent research trend of mesoscale phenomena in South Asia.
Takehiko SATOMURA (DG, Kyoto University)
Precipitation characteristics in northern Indochina.
Noriyuki NISHI (DG, Kyoto University)
Detection of precipitation using split-window measurements by geostaionary satellite.
Hirohiko ISHIKAWA (DPRI, Kyoto University)
Myanmar Cyclone Nargis: Satellite images and numerical experiments by WRF.
Masato SHIOTANI (RISH, Kyoto University)
Stationary circulation observed in the upper troposphere over the western Indian Ocean.
Yoshinori SHOJI (MRI, JMA)
Global realtime analysis of GPS data and plan of assimilation experiments.
Takeshi HORINOUCHI (RISH, Kyoto University)
Gfdnavi: present and future prospects.
Seiya NISHIZAWA (DG, Kyoto University)
Experimental development of a decision support system for prevention and mitigation of meteorological disasters with Gfdnavi.
1620-1700 Invited talks
Shuichi MORI (JAMSTEC/IORGC)
Present status of JEPP/HARIMAU radar-profiler network observations in Indonesia.
Manabu YAMANAKA (JAMSTEC/IORGC)
Coastline length governing equatorial rainfall amount.
1700-1730 Discussions on data archive and cooperation

September 10 (Wed)
0910-1200 Session 2: Numerical weather prediction
Shigeo YODEN (DG, Kyoto University)
Ensemble forecasts with regional models.
Kohei ARANAMI (NPD, JMA)
Improvements of utility tools to carry out NHM and introduction of DVD-NHM.
Syugo HAYASHI (MRI, JMA)
Intercomparisons of NHM and WRF forecasts over topical and Japan areas.
Tohru KURODA (MRI, JMA)
Development of utility tools for NHM execution in tropics and reproduce/forecast experiments of Nargis.
Kazuo SAITO (MRI, JMA)
Tidal wave simulation on ensemble forecast of Nargis.
Mitsuru UENO (MRI, JMA)
Some aspects of typhoon structure represented in the JMA meso-analyses and synthetic data.
Masaru KUNII (MRI, JMA)
Regional data assimilation experiment in southeast Asia.
Hiromu SEKO (MRI, JMA)
Structure of the regional heavy rainfall occurred at Santacruz, India on 26 July 2005.
1200-1230 Discussion on Bandung WS

International Research for Prevention and Mitigation of Meteorological Disasters in Southeast Asia
Newsletter No.3; October 31, 2008

MEXT Special Coordination Funds for Promoting Science and Technology for FY 2007 - 2009 in Asia S&T Strategic Cooperation Program

Shigeo Yoden
Department of Geophysics, Kyoto University, Kyoto 606-8502, Japan
Tel: +81-75-753-3932
Fax: +81-75-753-3715
E-mail: yoden@kugi.kyoto-u.ac.jp
Web: http://www-mete.kugi.kyoto-u.ac.jp/project/MEXT/

International Research for Prevention and Mitigation of Meteorological Disasters in Southeast Asia

MEXT Special Coordination Funds for Promoting Science and Technology for FY 2007 - 2009
in Asia S&T Strategic Cooperation Program

振興調整費

Newsletter

No. 4 (Mar. 2009)

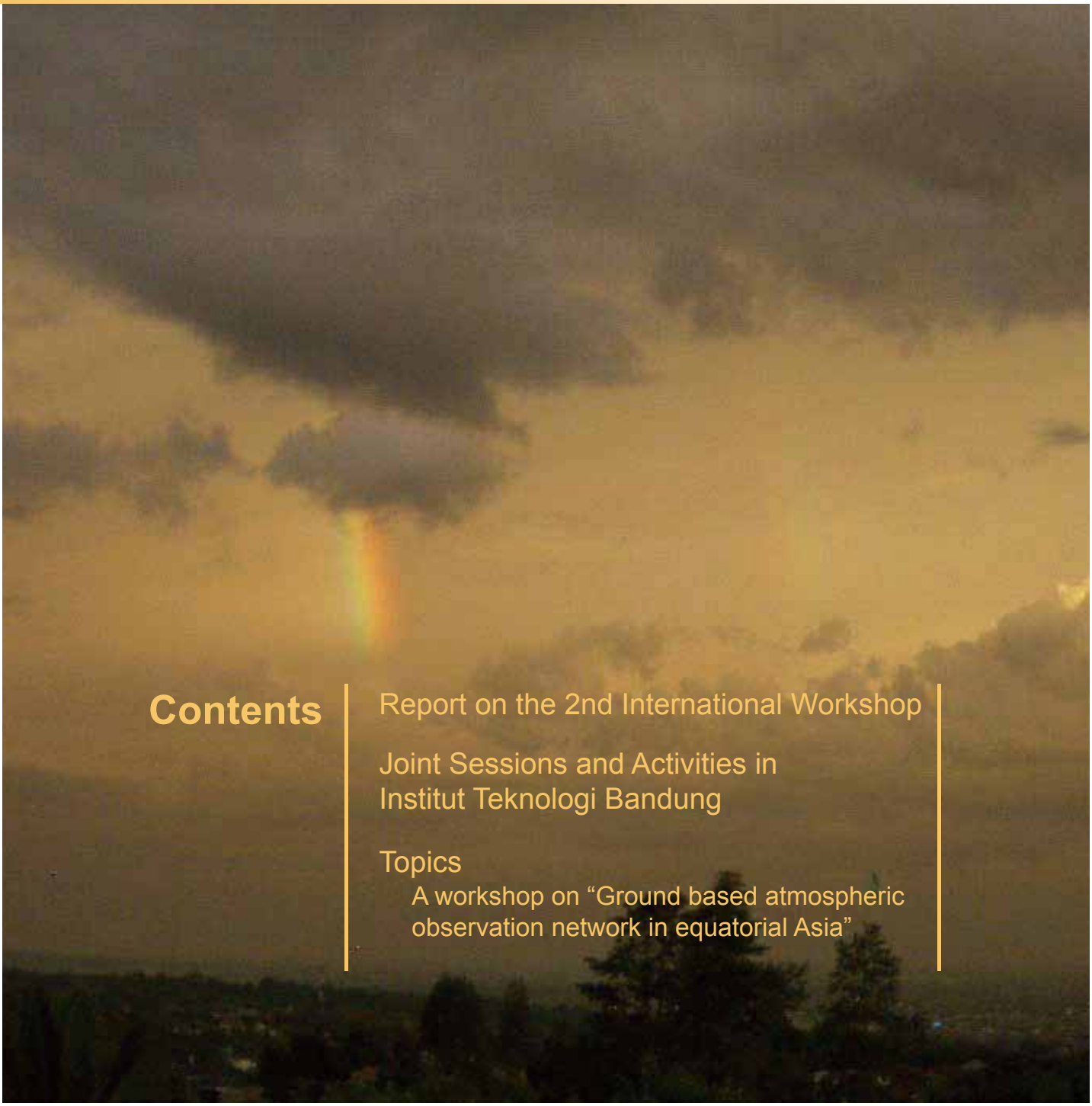

Contents

Report on the 2nd International Workshop

The second international workshop of this research project on "Prevention and Mitigation of Meteorological Disasters in Southeast Asia" was held on 2-5 March, 2009, at Jayakarta Hotel in Bandung, Indonesia. In total 47 researchers participated from 12 countries and regions in East Asia, Southeast Asia, and South Asia. This workshop was also partially suported by the Organization for the Promotion of International Relations of Kyoto University.

The workshop was opened by the welcome address by Dr. Emmy Suparka (Bandung Institute of Technology), followed by the welcome address by Dr. Takashi Nishigaki, Program Officer of JST (Japan Science and Technology Agency). After the keynote speech by the program leader Dr. Shigeo Yoden (Kyoto University) and the presentation by Dr. Mu Mu (Chinese Academy of Sciences), seven sessions were held. In session I, Hadi, Hayashi, Islam, Xin, and Wong gave talks on "Downscale Numerical Weather Predictions (NWPs)". In section II, Seko, Takemi, Iwasaki, Y. Ishikawa, Rajeevan, and Kuroda gave talks on "Tropical disturbances and precipitation process". Session III and IV were the joint sessions (see the next page). In session V, H. Ishikawa, Promasakha, and Ratag gave talks on "Risk management and community preparedness". After session V, Saito, Hayashi, and Kuroda from MRI (Meteorological Research Institute) demonstrated JMA (Japan Meteorological Agency)-MRI NHM (Non-Hydrostatic Model) as a tutorial seminar. In session VI, Mukougawa, Gouda, and Permana gave talks on "Extended range NWPs". In session VII, Shoji and Junnaedhi gave talks on "Data assimilation". During the workshop, 14 posters were presented by Ito, Kawabata, Kim, Kunii, Nugroho, Otsuka, Saito, Seko, Seto, Sofian, Surmaini, Putra, Listiaji, and Fithra.

In this workshop, various new results since the first international workshop in 2008 were presented. We will have the third international workshop at Ritsumeikan Asia Pacific University, Beppu, Japan in March 2010.

(Shigenori Otsuka, Kyoto Univ.)

Joint Sessions and Activities in Institut Teknologi Bandung

A joint banquet with the "Workshop on Ground-based Atmosphere Observation Network in Equatorial Asia" was held on March 2 at Jayakarta hotel, Bandung. Following a speech of welcome by Dr. Lambok Marinangan Hutasoit, the dean of the Faculty of Earth Sciences and Technology (ITB) at the beginning of the banquet, Dr. Toshitaka Tsuda (Kyoto University) addressed the importance of the collaborative relationship to prevent and mitigate meteorological disasters in South Asia. All the participants for both workshops enjoyed a delicious food and conversation.

The joint session "Observational network" and "New methods in observation, data assimilation, and NWPs" were held in March 3-4. As many as 10 speakers had impressive presentations on the observational network in South East Asia and the most recent research progresses in observation, data assimilation, and NWPs. Dr. Manabu D. Yamanaka (JAMSTEC) highlighted HARIMAU project, which is a high-resolution observational network with the meteorological radars and wind profilers for monitoring convective activities. Dr. Tieh Yong Koh (Nanyang Technological University) address a closer regional coordination in plans for developing infrastructure in the light of new observational networks and sophisticated numerical models. Dr. Toshitaka Tsuda (Kyoto Univ.) introduced an application of GPS radio occultation data to the temperature and humidity, and Dr. Seon Ki Park (Ewha Woman Univ.) addressed data assimilation and parameter estimation to improve forecast accuracy of disastrous weather system. Dr. Chun-Chieh Wu (National Taiwan Univ.) introduced a targeted observation for improving tropical cyclone predictability, DOTSTAR and T-PARK. The participants made an active discussion concerning the presentations across the research areas.

On May 5, many participants visited the Faculty of Earth Sciences and Technology of ITB. The dean illustrated the basic outlines of the faculty with a number of durians for hospitable reception. The participants asked the questions such as foreign exchange program and teaching system, and envisioned a future of the university.

(Kosuke Ito, Kyoto Univ.)

Topics

A workshop on "Ground-based atmospheric observation network in equatorial Asia"

For three years in FY2008-2010 we promote an international collaboration on “Elucidation of ground-based atmosphere observation network in equatorial Asia”, which has been selected as one of the projects of the Asia Africa Science Platform (AA-SP) program of JSPS.

Our project aims at establishing a concrete collaborative consortium among the Asian countries on atmosphere observations. In particular, LAPAN (National Institute of Aeronautics and Space) and NARL (National Atmosphere Research Laboratory) are the main counterpart which serve as the coordinating organization in Indonesia and India, respectively (http://www.rish.kyoto-u.ac.jp /radar-group/aaplat/index.htm). Within this program, we carry out four types of collaborative research and capacity building programs; (1) lecture courses, (2) on-job training, (3) exchange of scientists, and (4) workshop. We organized two series of intensive lectures in August and November 2008 at LAPAN, and the on-job training at EAR in October 2008. We also invited a few scientists from India and Indonesia to Japan for a collaborative research.

On 2-4 March 2009 we organized a workshop dedicated to ground-based and satellite observations of the equatorial atmosphere and ionosphere in Bandung. The meeting was jointly coordinated with the second workshop on “Prevention and Mitigation of Meteorological Disasters in Southeast Asia” of JST lead by Prof. Shigeo Yoden.

We first held a separate meeting at LAPAN for 1.5 days on 2-3 March, which was opened by a welcome address by Dr. Bambang Teja, the deputy chairman of LAPAN, followed by three overview talks by representatives of RISH, LAPAN and NARL. The oral sessions consist of nine invited papers and four contributed talks. In addition, 47 poster papers were presented, where most of them were associated with active discussions. A total of more than 80 participants attended the workshop, including eight from Japan, two from India and one from Vietnam.

From the afternoon of 3 March, we joined the 2nd JST workshop at Jayakarta hotel, which we found very useful in stimulating interactions between observations and numerical modeling of the equatorial atmosphere. We hope our collaborative activities will be more enhanced in the coming years.

(Toshitaka Tsuda, Kyoto Univ./RISH)

International Research for Prevention and Mitigation of Meteorological Disasters in Southeast Asia
Newsletter No.4; March 23, 2009

MEXT Special Coordination Funds for Promoting Science and Technology for FY 2007 - 2009 in Asia S&T Strategic Cooperation Program

Shigeo Yoden

Department of Geophysics, Kyoto University, Kyoto 606-8502, Japan
Tel: +81-75-753-3932
Fax: +81-75-753-3715
E-mail: yoden@kugi.kyoto-u.ac.jp
Web: http://www-mete.kugi.kyoto-u.ac.jp/project/MEXT/

International Research for Prevention and Mitigation of Meteorological Disasters in Southeast Asia

MEXT Special Coordination Funds for Promoting Science and Technology for FY 2007 - 2009
in Asia S&T Strategic Cooperation Program

振興調整費

Newsletter

No. 5 (Oct. 2009)

Contents

Topics

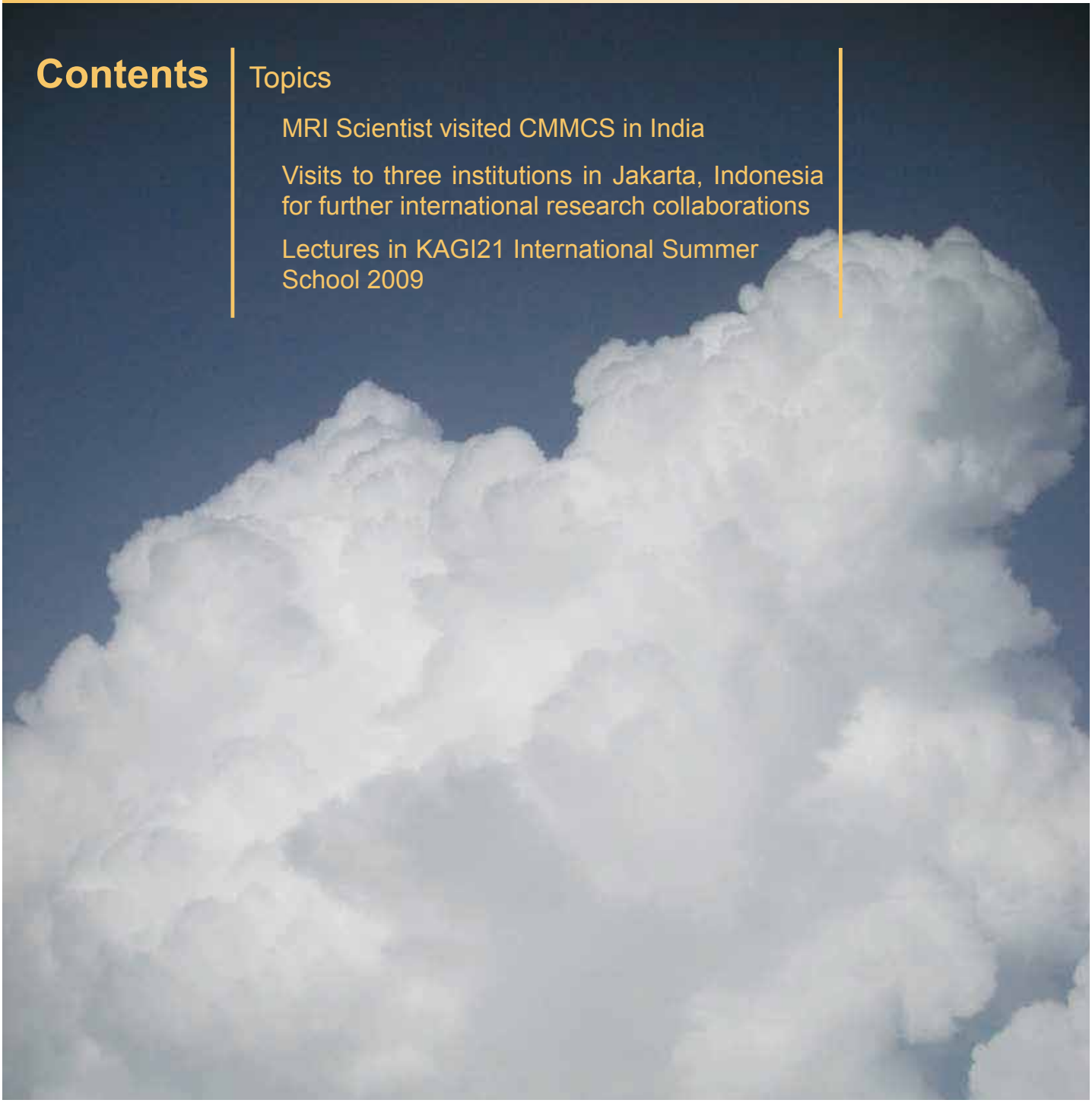

MRI Scientist visited CMMCS in India

Syugo Hayashi of the Meteorological Research Institute visited CSIR / CMMCS (Council of Scientific and Industrial Research / Centre for Mathematical Modeling and Computer Simulation) of India in March 2009. His visit was done to help the installation of the JMA nonhydrostatic model (NHM) to the CMMCS's computer system and to promote the mutual collaboration between MRI and CMMCS.

From 23rd to 25th March, Hayashi visited CMMCS and met Krushna Chandra Gouda, a research scientist of CMMCS (Photo. 1). NHM was installed in the CMMCS's super computer SGI ALTIX 3700 BX2, which has 24 CPUs of Itanium2 processor at 1.6GHz clock speed, 96GB physical memory. Intel Fortran and C compilers and MPI libraries are available for parallel computing. To see NHM's output with the NuSDaS format (JMA original data format), a visualization software package 'WEBPANDAH' was installed in the web-server SGI ORIGIN. As the disk storages of both machines are shared, access from ORIGIN to the result of NHM by ALTIX is easy.

For a test, a heavy rain case in south India on 22nd March 2008 was selected. The 24 hour simulation was conducted with the 20 km horizontal resolution. The NCEP final analysis with 1 degree is used for initial and boundary conditions. Figure 1 shows the 24 hour accumulated precipitation, sea level pressure and surface wind at 00 UTC 22 March 2008 predicted by NHM. The observed intense rain was well simulated, but some positional errors remained.

Photo 1. Photograph taken at the hotel Basil Ikon (Bangalore, India). Krushna Chandra Gouda (left) and Syugo Hayashi (right).

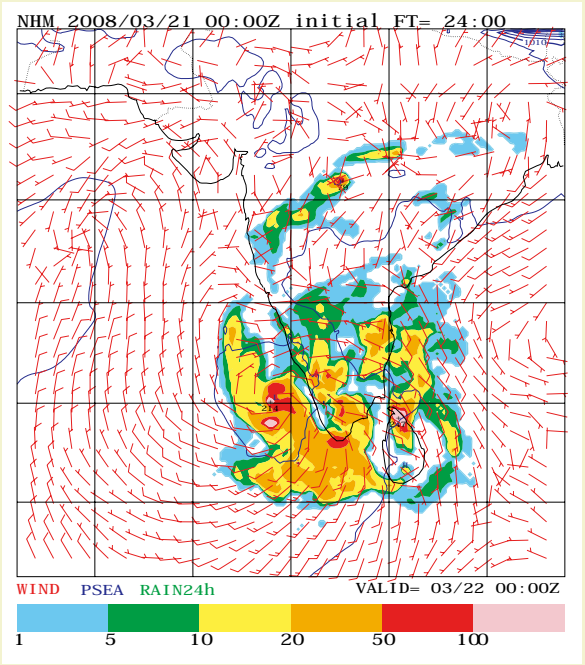

Figure 1. Predicted 24 hour accumulated precipitation, sea level pressure and surface wind at 24-hour forecast by NHM with a horizontal resolution of 20 km. NCEP final analysis at 00 UTC 21 March 2008 was used as the initial condition.

In the afternoon of 25th March, Hayashi made a presentation at the CMMCS seminar. The introduction of NHM and the performance of NHM in mid- and low- latitudes were shown. At low latitudes, NHM performance is insufficient compared with mid-latitudes. Therefore, tuning of the model for low-latitudes is needed to improve the forecast accuracy. In addition, it has to be confirmed that the model performance improves with finer horizontal resolutions (e.g., 5 km). Cooperation of researchers in various countries/regions is needed for further model's improvements.

(Syugo Hayashi, MRI / JMA)

Visits to three institutions in Jakarta, Indonesia for further international research collaborations

On August 14, 2009, Prof. Shigeo Yoden took an early flight from Singapore and arrived around 08:30 local time at the Sukarno-Hatta International Airport, Jakarta. I picked him with a chartered car and we started a "one day tour" to three institutions in Jakarta, Indonesia : (1) Japan International Cooperation Agency (JICA) – Indonesia Office, (2) Southeast Asian Ministers of Education Organization, Regional Open Learning Center (SEAMOLEC), and (3) Meteorological, Climatological, and Geophysical Agency (BMKG) Head Quarter. The main purpose of our visit was to explore new possibilities to promote collaboration between Kyoto University, Bandung Institute of Technology (ITB), and other institutions in Indonesia on the development of weather prediction technology for mitigating hydrometeorological disasters in Indonesia and other tropical Asian Countries through a JST-JICA program, Science and Technology Research Partnership for Sustainable Development (SATREPS).

The most important institution that we visited this time was the JICA Indonesia Office, which is located at Jl. Sudirman in Central Jakarta. Our purpose for visiting JICA was to obtain detailed information on the implementation of SATREPS in Indonesia. Mr. Kiichi Tomiya, a senior representative of JICA, kindly accepted our visit from 11:30 until 12:00 local time (Photo 1). From this visit, we learned the possibility for Kyoto University and ITB to submit a proposal to SATREPS.

The second institution we visited was SEAMOLEC, which is located in Ciputat area, South Jakarta. It was unfortunate that we could not see the Director, Dr. Gatot Haripriyanto because of his health problem. Mr. Ith Vuthy (Deputy Director of Program) and Ms. Dina Mustafa (Research and Development Manager) cordially met us and gave comprehensive explanations about the center's activities (Photo 2). We found out that, with wide access to educational resources in Southeast Asian countries, SEAMOLEC is one of potential counterpart to enhance "weather and climate literacy" in the region.

The visit to BMKG office was planned just a few days before Prof. Yoden's arrival in Jakarta. In spite of very limited time, we decided to visit BMKG because our partnership with the national weather service will be crucial for the envisioned proposal to SATREPS. Due to the timing, it was difficult to see higher authorities at BMKG but we met Dr. Dodo Gunawan (staff of Research and Development Center) and Mr. Sasmito (operational staff) (Photo 3). We found that they, who represent the work force of the institution, were very supportive to our ideas on the new collaboration between Kyoto University, ITB, and BMKG.

Photo 1.

Photo 2.

Photo 3.

Our tour of the day was completed but we had to catch up with Prof. Yoden's flight through a terrible traffic jam. I was relieved when I saw Prof. Yoden finally came out of the check in counter several minutes before it was closed, but I kept thinking about the big work on the preparation of our new proposal during my trip back to Bandung.

(Tri Wahyu HADI , Bandung Institute of Technology)

Lectures in KAGI21 International Summer School

Two lectures on “Decision support system for prevention and mitigation of meteorological disasters” and “DVD-NHM” were given during the 5th KAGI21 International Summer School in Ohmi-Maiko, Siga on 26-27 September 2009. There were 14 participants (7 from Asian countries and 7 from Japan).

Shigenori Otsuka was the lecturer of the former. In the lecture, the participants learned how to utilize ensemble numerical weather forecasting data for disaster prevention and mitigation, in which a decision support system built on a web-based visualization tool and database server "Gfdnavi" was used. The data for the exercise was an output of an experimental ensemble numerical weather forecasts on cyclone Nargis, which attacked Myanmar in May 2008. The data was provided by Dr. Kuroda (MRI / JMA) and his colleagues. The participants used laptop PCs to run the decision support system and tried several visualization methods to extract information from ensemble numerical weather predictions.

Syugo Hayashi (MRI/JMA) was the lecturer of the latter. In his lecture, the participants learned how to perform numerical simulations using a nonhydrostatic regional weather forecasting model JMA-NHM installed on a bootable DVD-ROM (DVD-NHM). Using DVD-NHM on the laptop PCs, the participants performed numerical experiments on a low-pressure system over Japan on 23rd April 2008, following instructions shown on a web-browser. The horizontal resolutions were 20 km and 5 km with one-way nesting. The participants learned how to analyze the result with a web-based visualization tool "web-pandah".

(Shigenori Otsuka, Kyoto University)

Photo 1.

Photo 2.

International Research for Prevention and Mitigation of Meteorological Disasters in Southeast Asia
Newsletter No.5; October 31, 2009

MEXT Special Coordination Funds for Promoting Science and Technology for FY 2007 - 2009 in Asia S&T Strategic Cooperation Program

Shigeo Yoden
Department of Geophysics, Kyoto University, Kyoto 606-8502, Japan
Tel: +81-75-753-3932
Fax: +81-75-753-3715
E-mail: yoden@kugi.kyoto-u.ac.jp
Web: http://www-mete.kugi.kyoto-u.ac.jp/project/MEXT/

International Research for Prevention and Mitigation of Meteorological Disasters in Southeast Asia

MEXT Special Coordination Funds for Promoting Science and Technology for FY 2007 - 2009
in Asia S&T Strategic Cooperation Program

振興調整費

Newsletter

No. 6 (Mar. 2010)

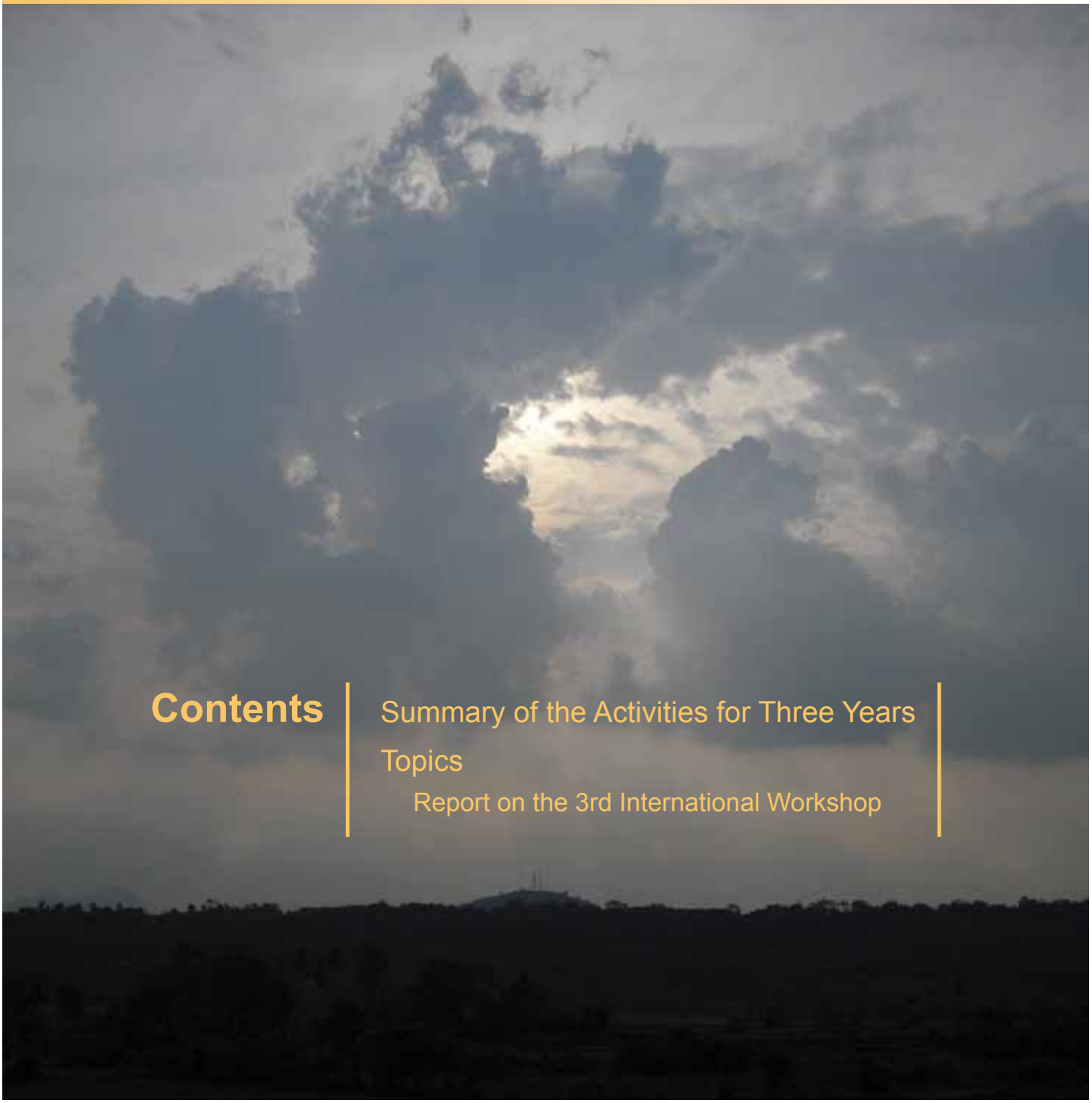

Contents

Summary of the Activities for Three Years

(1) Fundamental Research and System Development (Kyoto University)

In Kyoto University, a number of experimental downscaling Numerical Weather Predictions (NWPs) were performed to investigate meteorological disasters in Southeast Asia (a flood event in Jakarta in February 2007, Myanmar cyclone Nargis, etc). In those experiments, several regional atmospheric models including JMA-NHM were used. New observational data were utilized in those research activities for model validation. For example, performance of downscaling NWPs over Indochina region was investigated using surface station data in Laos for validation. Numerical experiments with very high resolution (~ 100 m in horizontal) were also performed to investigate highly isolated heavy rainfall events such as a flash flood event in Kobe city.

A prototype of a decision support system for prevention and mitigation of meteorological disasters is developed, by which ensemble NWP data can be analyzed and displayed. The system was developed based on Gfdnavi, a web-based database server and analysis tool. Using the output of an experimental ensemble NWP on Myanmar cyclone Nargis which was provided by MRI as a test dataset, how to analyze and display ensemble NWPs on tropical cyclones is documented with an interactive documentation system.

(Shigenori Otsuka, Kyoto Univ.)

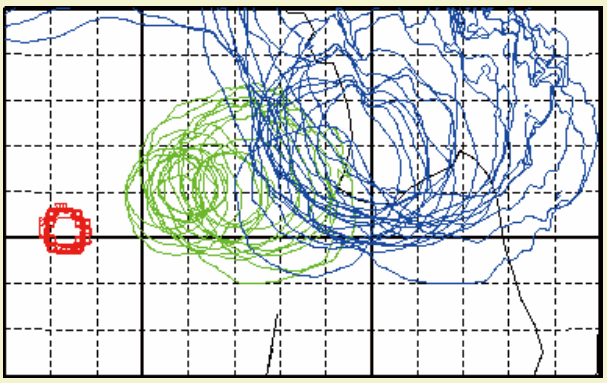

Figure 1. Spaghetti diagram of surface pressure for the experimental ensemble NWP on cyclone Nargis. The figure was produced by the prototype of a decision support system.

(2) Operational Model Development (Meteorological Research Institute / Japan Meteorological Agency)

Among the research groups of the International Research for Prevention and Mitigation of Meteorological Disasters in Southeast Asia, the Meteorological Research Institute of the Japan Meteorological Agency (MRI/JMA) was in charge of the part of 'Operational model development'. This part was divided into the following three subjects:

-- Development of NHM and verification of its performance in the tropics.
-- Preparation of experimental tools and collaborations for tropical NWP.
-- Data assimilation experiment in the tropics.

As for the first subject, Seko et al. (2008) conducted a numerical simulation of the Mumbai heavy rainfall which occurred in July 2005 in India. Using the global analysis data of JMA for initial and lateral boundary conditions, the intense rainfall system was successfully reproduced. Hayashi et al. (2008) conducted statistical verification of short term NWP over Southeast Asia and compared two mesoscale models (NHM and WRF) using the same conditions. Threat scores for precipitation from the two models were comparable, while WRF tended to predict more rains than NHM.

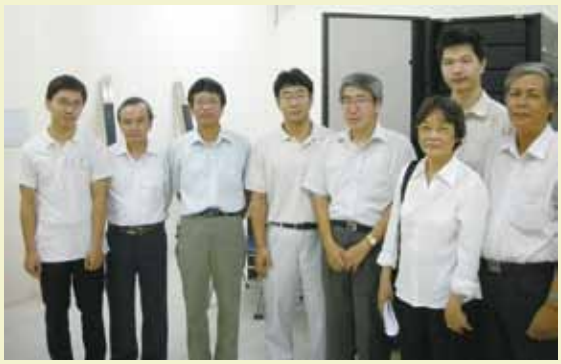

Figure 2. Group photo taken at the High Performance Computing Center of VNU on 6 October 2009. From left, Dr. L. Duc of NHMS, Prof. D. Uu and Prof. P. Anh of VNU, Dr. Kuroda and Dr. Saito of MRI, Prof. K. Xin of VNU and Dr. Son and Dr. N.H. Dien of HPCC.

As for the second subject, experimental tools using the JMA's NWP data were prepared for oversea collaborators. Information on tropical NWP is on the project website of MRI. (http://www.mri-jma.go.jp/Project/Kashinhi_seasia/Eng/ en_MRI_kashinhi.htm). As the link of the international partnership, MRI scientists visited partner institutes and discussed collaborations (Table 1). The latest visit was on 6-9 October for Vietnam [Vietnam National University (VNU; Figure 2), National Hydro-Meteorological Service of Vietnam (NHMS), and Department of Meteorology, Hydrology and Climate Change of the Ministry of Natural Resources and Environment].

On 2 May 2008, a cyclone 'Nargis' made landfall in Myanmar and caused the worst natural disaster in the country. Numerical simulations and mesoscale ensemble prediction (MEP) of Nargis and the associated storm surge (Kuroda et al., 2010; Saito et al. 2010) and data assimilation experiments (Kunii et al. 2010; Shoji et al. 2010) were conducted. A prototype of the decision support system was developed using the MEP result as the input data.

Table 1. Visits of MRI scientists to partner institutes.
(*Visit to HKO was supported by HKO.)

Partner Institute	Country/ Region	Period	Report in Newsletter
ITB	Indonesia	2008.2.11-12	
NTU	Singapore	2008.2.14-15	No.2
CSIR	India	2009.3.23-25	No.5
VNU	Vietnam	2009.10.6-9	No.6
HKO	Hong Kong	2009.2.9-13*	

(Kazuo Saito, MRI)

(3) Real-Time Experiment (Institute Teknologi Bandung in Indonesia and partners in the other countries)

The "International Research on Prevention and Mitigation of Meteorological Disaster in Southeast Asia (IRPMMDSEA)", in a sense, is some sort of a survey on implementation of high resolution Numerical Weather Prediction (NWP) and its potential to mitigate the meteorological disasters in Southeast Asia through a series of workshops in Indonesia and Japan. At least, the need to increase the accuracy of weather and climate prediction through enhanced utilization of NWP in Southeast Asian countries has been successfully raised as one consensus in these workshops. I observed that more indigenous efforts to develop better NWP systems in each of the countries have also been demonstrated in the last workshop in Beppu, Japan.

During the 3-year implementation of IRPMMDSEA, we are trying to focus on developing "NWP literacy" among key meteorological communities in Indonesia. Academically, introductory courses on NWP have been included in the new curriculum (2008) of undergraduate program of meteorology at ITB. NWP is also being socialized on the official web site of ITB (http://www.itb.ac.id/). It has also been reported that NWP experiments are now being set up and carried out at several research and operational institutions in Indonesia.

IRPMMDSEA is approaching its end in March 2010 but efforts to develop "NWP literacy" in Indonesia must not stop. Rather, it requires more concrete and sustainable programs. Our new initiatives include submission of a new proposal that aims mainly for a real implementation of operational NWP and establishment of a local forum on NWP development in Indonesia. I hope the snow ball of NWP in Southeast Asia will keep rolling and growing for the advances of tropical meteorology and the betterment of mankind in the region where meteorological disasters are a common problem.

Figure 3. A screen shot of ITB web site. Red circle indicate the link to our experimental NWP results.

(Tri Wahyu Hadi, ITB)

Topics

Report on the 3rd International Workshop

The third international workshop on "Prevention and Mitigation of Meteorological Disasters in Southeast Asia" was held on March 1-3, 2010, and the open symposium on "Meteorological Disasters and Adaptable Society in the Asia-Pacific Region" was held on March 4, 2010, at Ritsumeikan Asia Pacific University (APU) in Beppu, Japan. 61 researchers and graduate students from 13 countries participated in the workshop, and 63 people including the citizens of Beppu participated in the open symposium.

At the workshop, 41 researchers made oral presentations and 15 researchers and graduate students presented their posters.

At the open symposium, Dr. Sanga-N. Kazadi (APU) took the chair and gave opening and closing remarks. And Dr. Shigeo Yoden (Kyoto University), Dr. Shunso Tsukada (APU), Dr. Tieh Yong Koh (Nanyang Technological University) and Dr. Toshitaka Tsuda (Kyoto University) gave talks related to meteorological disasters and adaptable society. We also had valuable comments from Dr. Takashi Nishigaki (Japan Science and Technology Agency) and Mr. Masahiro Kobayashi (Kyushu International Center, Japan International Cooperation Agency).

After the open symposium, the lunch buffet party was held at Pacific Café, APU, and the participants had further discussion on the theme of the symposium.

International Research for Prevention and Mitigation of Meteorological Disasters in Southeast Asia
Newsletter No.6; March 29, 2010

MEXT Special Coordination Funds for Promoting Science and Technology for FY 2007 - 2009 in Asia S&T Strategic Cooperation Program

Shigeo Yoden
Department of Geophysics, Kyoto University, Kyoto 606-8502, Japan
Tel: +81-75-753-3932
Fax: +81-75-753-3715
E-mail: yoden@kugi.kyoto-u.ac.jp
Web: http://www-mete.kugi.kyoto-u.ac.jp/project/MEXT/

Introduction to a web-based decision support tool for ensemble numerical weather prediction with Gfdnavi

Shigenori Otsuka
Department of Geophysics, Kyoto University

Ver. 0.1

Contents

1 Introduction

- For mitigation of meteorological disasters, probabilistic information derived from ensemble forecasts are valuable.
- Quick-look of output data from ensemble forecasts is needed to build a decision support system.

- We developed a prototype of a decision support system based on Gfdnavi, which is a database server with an interactive data visualizer on web browser.

- In this tutorial seminar, we demonstrate this prototype decision support system using output of an ensemble experiment on cyclone Nargis.

2 How to use Gfdnavi

Gfdnavi is distributed in the following page:

`http://www.gfd-dennou.org/arch/davis/gfdnavi/index.en.htm`

Basic flow of analysis

1. Open a terminal emulator (Application → Accessory → Terminal, or a shortcut icon on your desktop)
2. type "cd gfdnavi-kashinhi" and enter key

   ```
   $ cd gfdnavi-kashinhi
   ```

3. Boot a Gfdnavi server by typing "ruby script/server" and enter key

   ```
   $ ruby script/server
   ```

4. Open a web browser
5. Open the top page by typing "http://localhost:3000" in the address bar
6. Click "Start from here"

7. Data tree

8. Click folder icons (or plus marks) to open folders

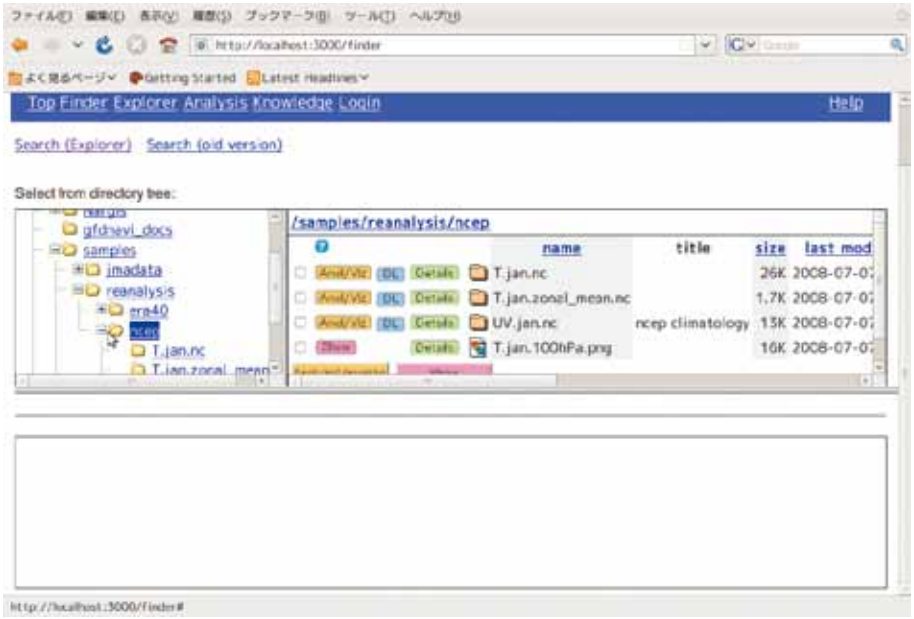

9. Click file names to show details

10. Click check-box if there is “Anal/Viz”

or you can directly move to the analysis page by clicking “Anal/Viz”

11. Click “Analyze/Visualize checked items” to move to the analysis page

12. When a variable (i.e., "T") is selected in the upper left panel, "Axes" window and "Options" window are updated.

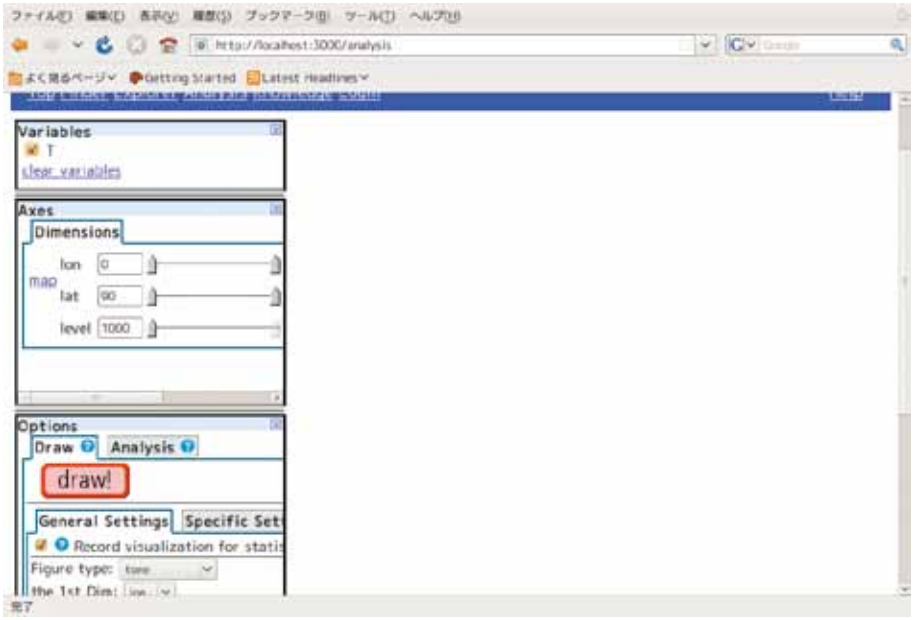

13. Select dimensions, draw settings, etc

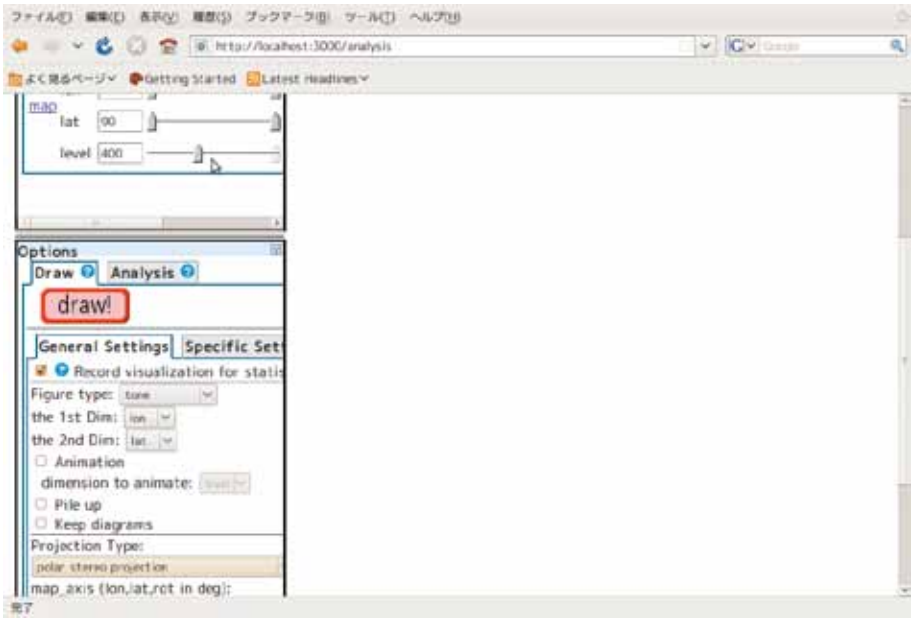

14. Click “draw!” button to execute visualization methods

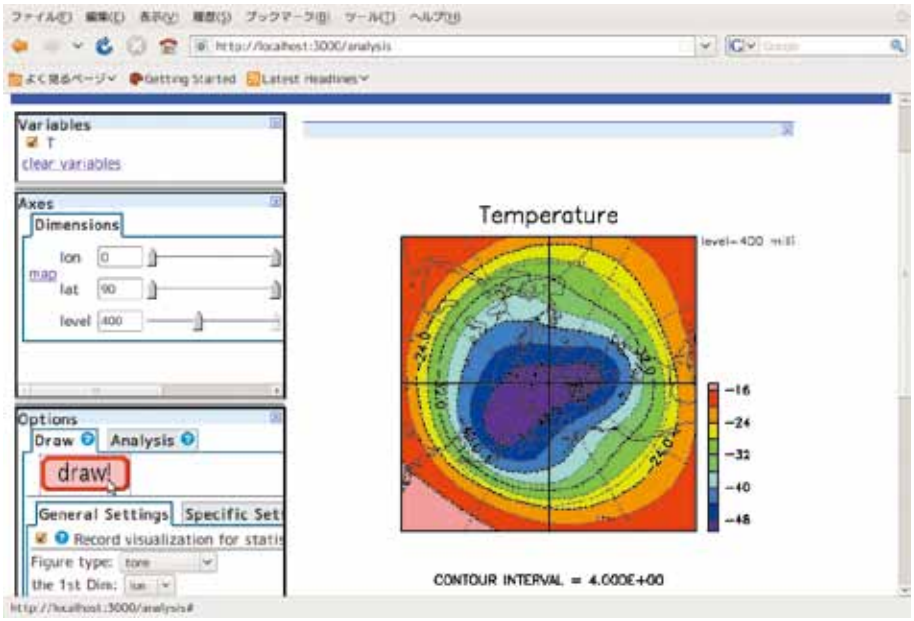

15. Many types of figures are available (line plot, vector plot, overlay of multiple figures, etc)

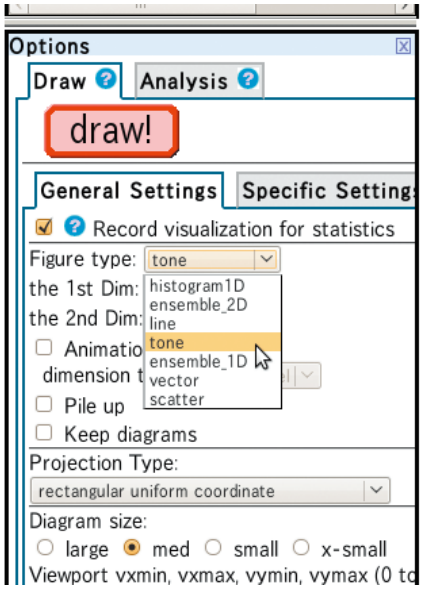

16. Click figures to open drop-down menu

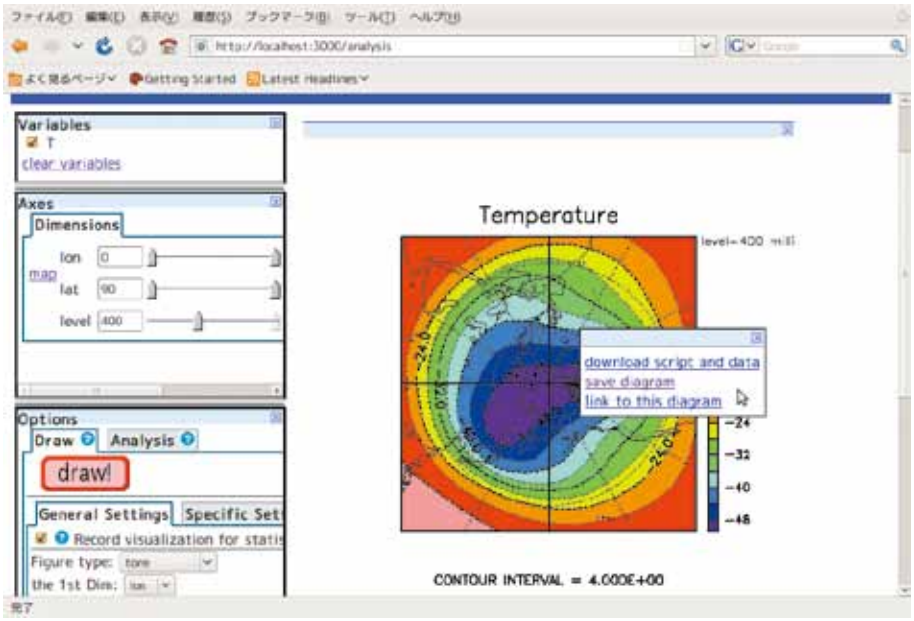

17. When Analysis is selected in the lower left panel, mathematical operation can be executed

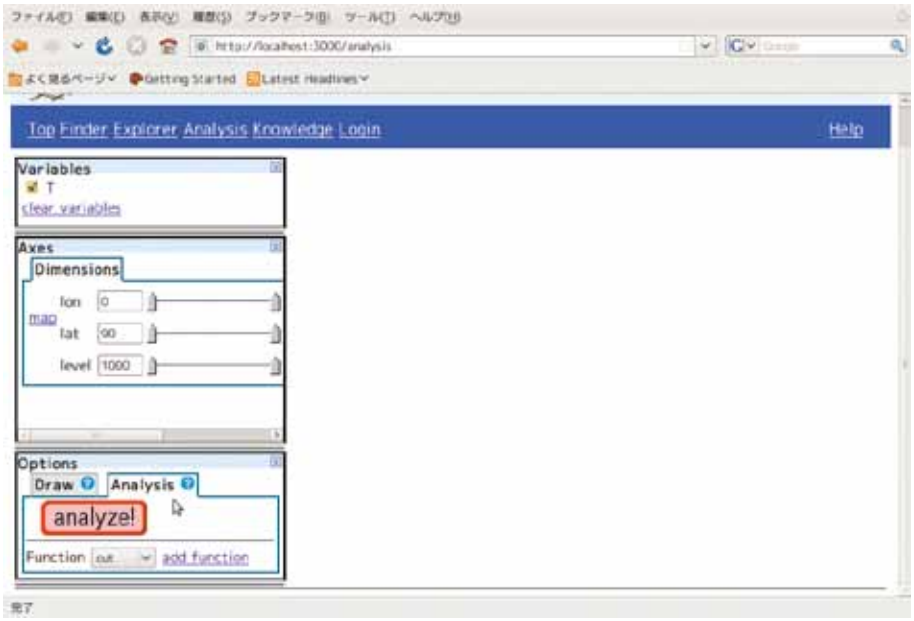

3 Test data: Cyclone Nargis (2008)

Sattelite image of Nargis FY2 image

`http://ssrs.dpri.kyoto-u.ac.jp/~okusan/nargis/indexj.htm`

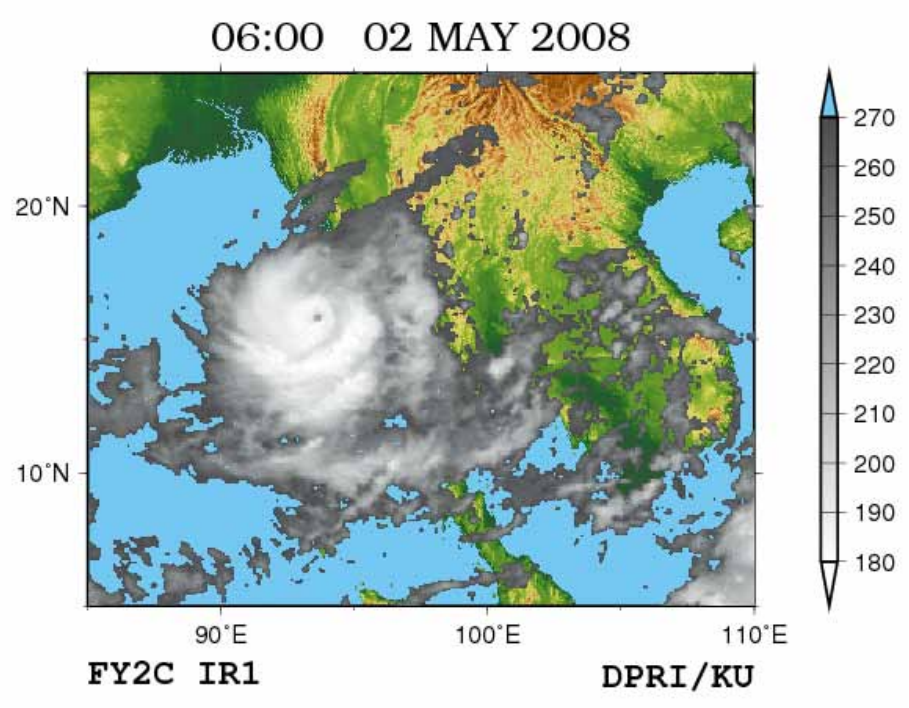

Best track of Nargis (from Joint Typhoon Warning Center)

`http://metocph.nmci.navy.mil/jtwc/atcr/2008atcr/2008atcr.pdf`
`http://metocph.nmci.navy.mil/jtwc/best_tracks/2008/2008s-bio/bio012008.txt`

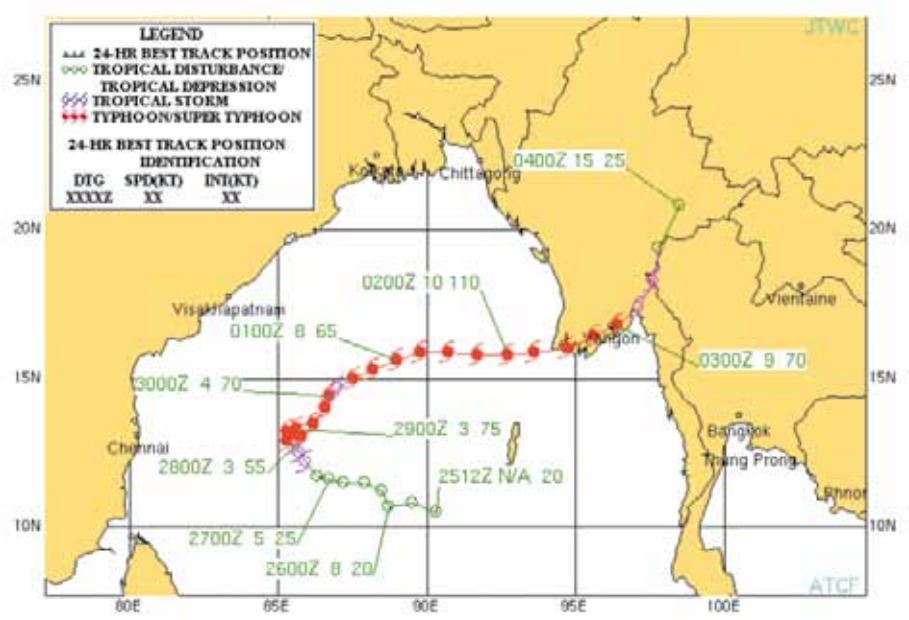

Available data Ensemble numerical weather forecasting experiments of cyclone Nargis (Kuroda et al., 2009; Saito et al., 2009)

1. Simulation of cyclone Nargis with Japan Meteorological Agency (JMA) nonhydrostatic model (NHM)

   - Period: 1200 UTC 30 Apr 2008 – 1200 UTC 03 May 2008 (3 days)
   - location in the data tree of Gfdnavi: /Nargis/NHM/
   - variables:

     PSEAsrf.nc sea level pressure
     Tsrf.nc surface temperature
     Usrf.nc surface wind (U)
     Vsrf.nc surface wind (V)
     uv_abs.nc surface wind speed ($\sqrt{U^2 + V^2}$)
     precip_hr.nc hourly precipitation
     precipitation.nc accumulated precipitation

2. Simulation of storm surge with Princeton Ocean Model (POM) driven by the output of the atmospheric model described above

   - location in the data tree of Gfdnavi: /Nargis/POM/
   - variables:

     h.nc surface elevation
     ps.nc surface pressure
     u.nc surface wind (U)
     v.nc surface wind (V)
     uc.nc surface current (U)
     vc.nc surface current (V)

4 Basic visualization on Gfdnavi

Notation

- A(lon, lat, $time$, $member$)
  A physical quantity "A" which is a function of lon, lat, $time$, and $member$.
- A_{member}(lon, lat, $time$)
  A physical quantity "A" which is a function of lon, lat, $time$ for each $member$.
- lon = 10°E
  Fix lon.
- lon = [10, ..., 20]
  Specify the range of lon for visualization.
- (X) lon = [10, ..., 20]
  Use lon as the x axis and specify the range for visualization.
- (Y) lon = [10, ..., 20]
  Use lon as the y axis and specify the range for visualization.
- (Ens) lon = 10, ..., 20
  Use lon for parameter sweep (especially ensemble members) and specify the range for visualization.
- (Anim) lon = [10, ..., 20]
  Use lon for animation and specify the range for visualization.
- lon = <10, ..., 20>
  Specify the range of lon for mathematical operations.

4.1 2D tone and contour plot for a scalar field

Data /Nargis/NHM/PSEAsrf.nc (lon, lat, $validtime$, $member$)

- PSEAsrf(lon, lat)
  - (X) lon = [73.45°E, ..., 106.54°E]
  - (Y) lat = [1.37°S, ..., 30.22°N]
  - $validtime$ = 2400 min (forecast time since 1200 UTC 30 Apr 2008)
  - $member$ = 0 (control run)

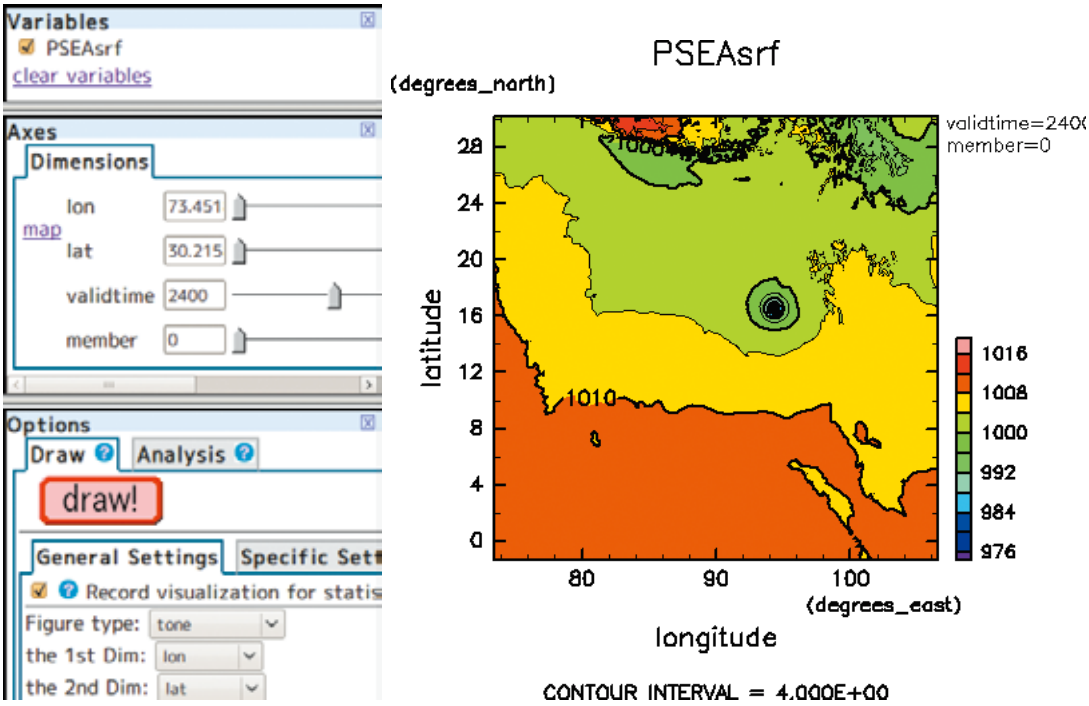

Cyclone Nargis is located at (94.5°E, 16.5°N).

- PSEAsrf(lon, t)
  - (X) lon = [73.45°E, ..., 106.54°E]
  - lat = 16.49°N
  - (Y) $validtime$ = [0 min, ..., 4320 min]
  - $member$ = 0

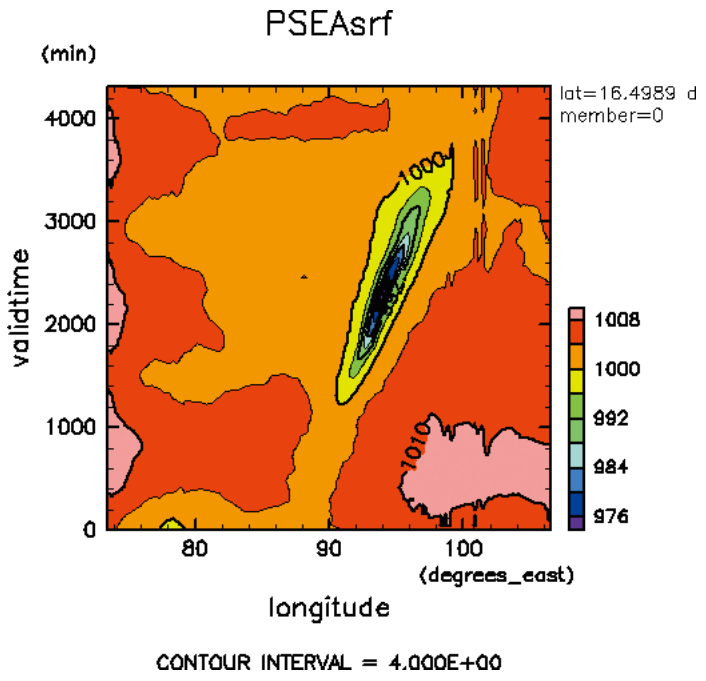

Here, eastward movement of the low pressure system (Nargis) is clear.

Excercise

- Try other quantities.

4.2 1D line plot for a scalar field

- PSEAsrf(*validtime*)
  - *lon* = 94.5°E
  - *lat* = 16.5°N
  - (X) *validtime* = [0 min, ..., 4320 min]
  - *member* = 0 (control run)

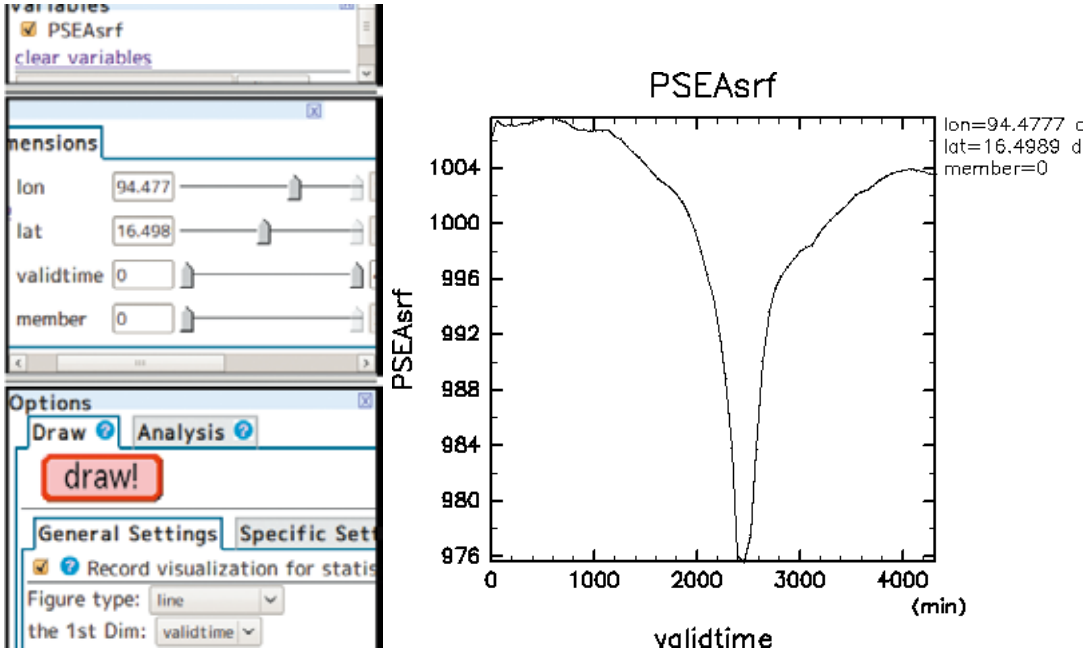

Excercise

- Take *lon* or *lat* as the x axis (= the 1st Dim).
  - PSEAsrf(*lon*)
  - PSEAsrf(*lat*)
- Try other quantities.

4.3 2D arrows for a vector field

Data /Nargis/NHM/Usrf.nc (*lon*, *lat*, *validtime*, *member*)
/Nargis/NHM/Vsrf.nc (*lon*, *lat*, *validtime*, *member*)

- (Usrf(*lon*, *lat*), Vsrf(*lon*, *lat*))
  - (X) *lon* = [73.45°E, ..., 106.54°E]
  - (Y) *lat* = [1.37°S, ..., 30.22°N]
  - *validtime* = 2400 min
  - *member* = 0

  Parameters for visualization:
  - interval of grids in x = 10
  - interval of grids in y = 10

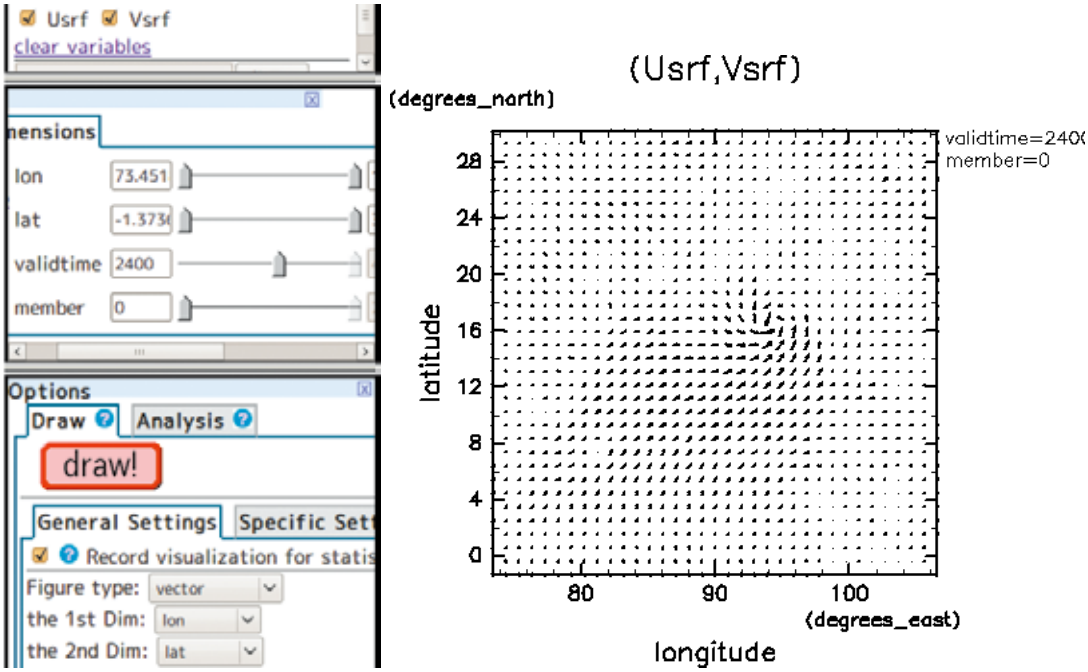

Pile up If you check "keep diagrams", old diagrams will stay in the window.

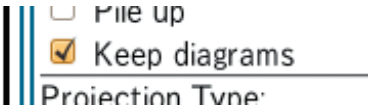

If you drag and drop a diagram onto another diagram, the former will be superimposed on the latter.

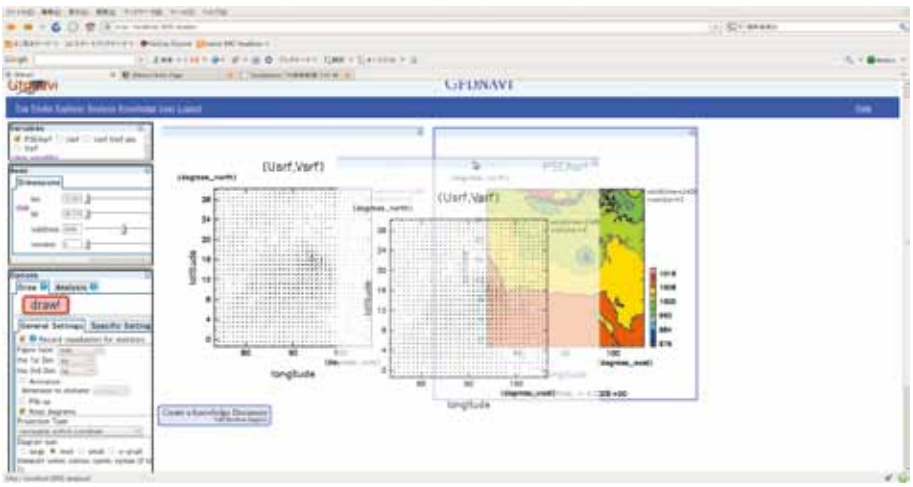

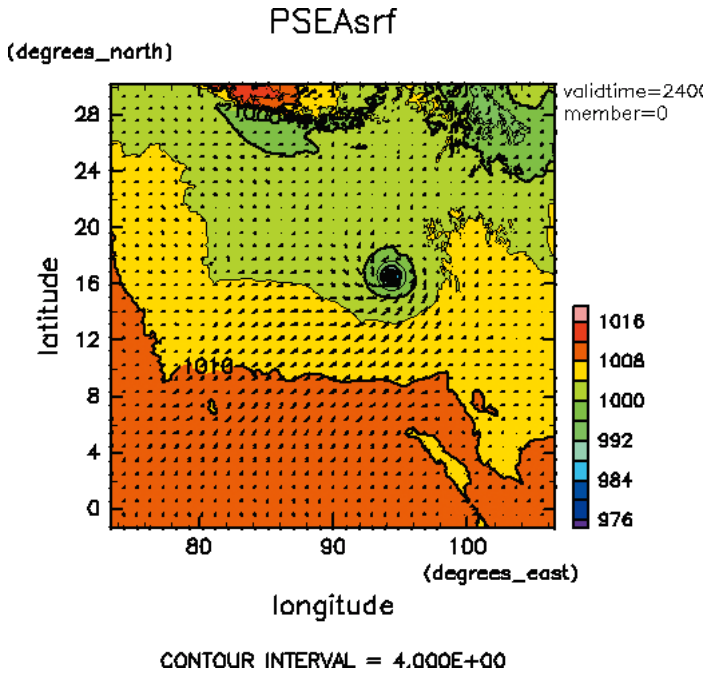

The surface pressure with the surface wind vectors.

Excercise

- Try other combinations. (Example: temperature + surface winds)

5 Basic statistical diagrams

5.1 Histogram for one quantity

Data /Nargis/NHM/UsrfVsrf.nc (*lon*, *lat*, *validtime*, *member*)

- UsrfVsrf(*lon*, *lat*)
  - lon = [73.45°E, ..., 106.54°E]
  - lat = [1.37°S, ..., 30.22°N]
  - $validtime$ = 2400 min
  - $member$ = 0

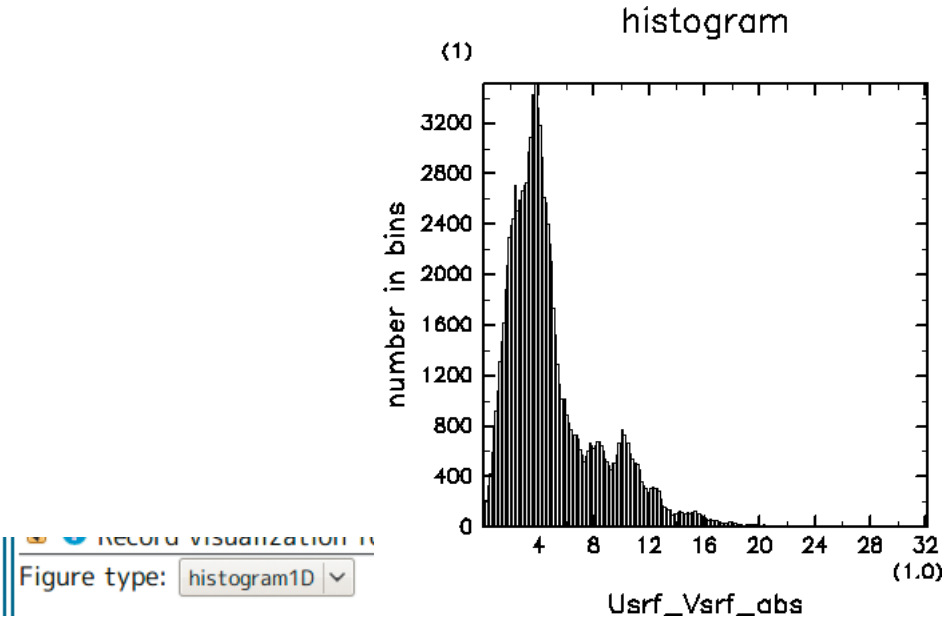

Data /Nargis/NHM/PSEAsrf.nc (*lon*, *lat*, *validtime*, *member*)

- PSEAsrf(*lon*, *lat*)
  - *lon* = 94.5°E
  - *lat* = 16.5°N
  - *validtime* = 2400 min
  - *member* = [0, ..., 20]

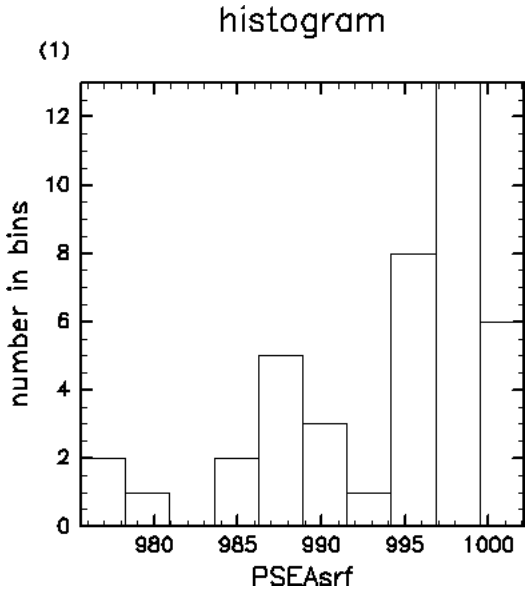

When *lon*, *lat*, *t* is fixed, the histogram shows diversity of the ensemble members.

5.2 Scatter diagram for two quantities with the same shape

Data /Nargis/NHM/PSEAsrf.nc (*lon*, *lat*, *validtime*, *member*)
/Nargis/NHM/uv_abs.nc (*lon*, *lat*, *validtime*, *member*)

- PSEAsrf(lon, lat) vs uv_abs(lon, lat)
  - lon = [73.45°E, ..., 106.54°E]
  - lat = [1.37°S, ..., 30.22°N]
  - $validtime$ = 2400 min
  - $member$ = 0

  Parameters for visualization:

  - marker type = 1

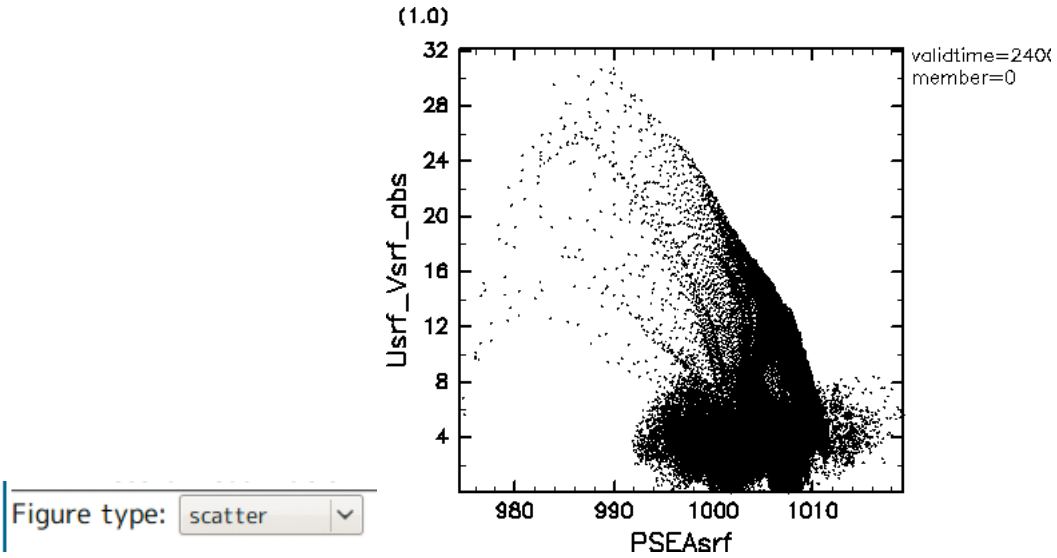

  The maximum wind speed is observed at 990 hPa (around the eyewall), whereas the wind speed is very low at the minimum pressure (center of the eye).

  You can change the marker type, the color of the markers.

Causion Do not feed too big data. Limit data size using sliders in "dimensions" tab.

Exercise

- Change the variable range along lon, lat, $time$, and $member$ to focus on the near-field of cyclone Nargis. What can you explain with this diagram?

6 Decision support tools for ensemble numerical weather prediction: I. Basic diagrams

6.1 1D line plot

Data /Nargis/NHM/POM/h.nc (lon, lat, t, $member$)

- $h_{member}(t)$ ("plume diagram")
  - lon = 95.07°E

– lat = 16.10°N
– (X) t = [0 h, ..., 71 h]
– (Ens) $member$ = 0, ..., 20

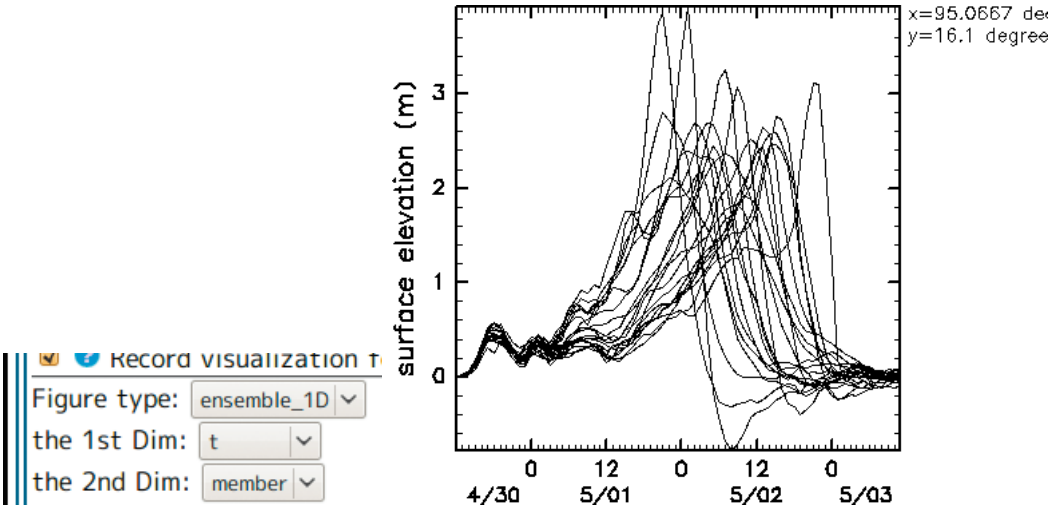

Time series of surface elevation at Irrawaddy point (95.07°E, 16.10°N) for 21 members. Some members show storm surge of more than 3 m in height.
You can highlight specific members.

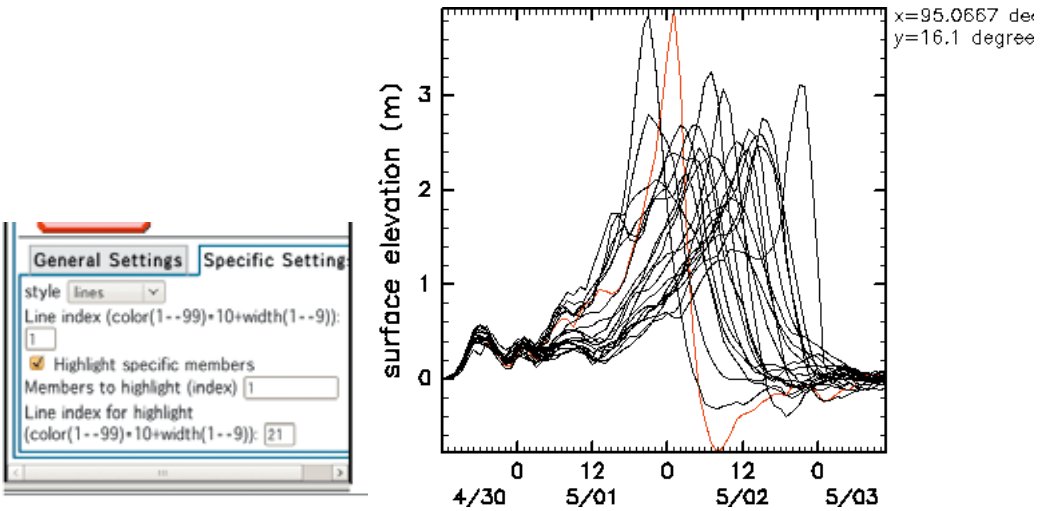

The highest storm surge is obtained by the member 1. You can go back to the 2D diagrams to further investigate the details of the member 1.

Excercise

– Check 2D diagrams of other quantities for $member$ = 1.
– Change highlighted members. Which member predicted the lowest storm surge? What is the difference between the highest and the lowest members?
– Change the location to Yangon point (96.27°E, 16.57°N).
– Try other quantities (Wind speed, hourly precipitation, accumulated precipitation, ...).

- $\mathrm{h}_{member}(lon)$ $\times t$

- (X) lon = [84°E, ..., 99°E]
- lat = 15.7°N
- (Anim) t = [0 h, ..., 71 h]
- (Ens) $member$ = 0, ..., 20

Parameters for visualization:

- Animation = true
- viewport = 0.1, 0.6, 0.2, 0.8
- max = 2.5
- min = −1

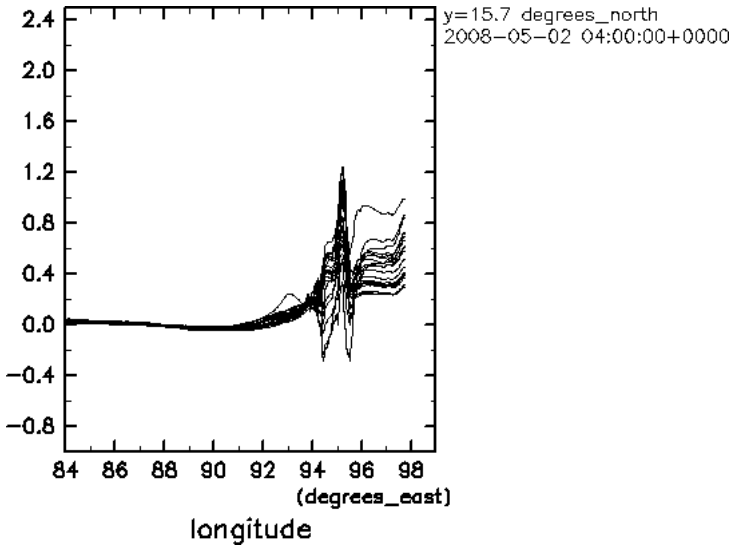

6.2 2D contour plot

Data /Nargis/NHM/PSEAsrf.nc (lon, lat, $validtime$, $member$)

- PSEAsrf$_{member}$(lon, lat) ("spaghetti diagram")

  - (X) lon = [73.45°E, ..., 106.54°E]
  - (Y) lat = [1.37°S, ..., 30.22°N]
  - $validtime$ = 2400 min
  - (Ens) $member$ = 0, ..., 20

  parameters for visualization:

  - contour level = 990 hPa

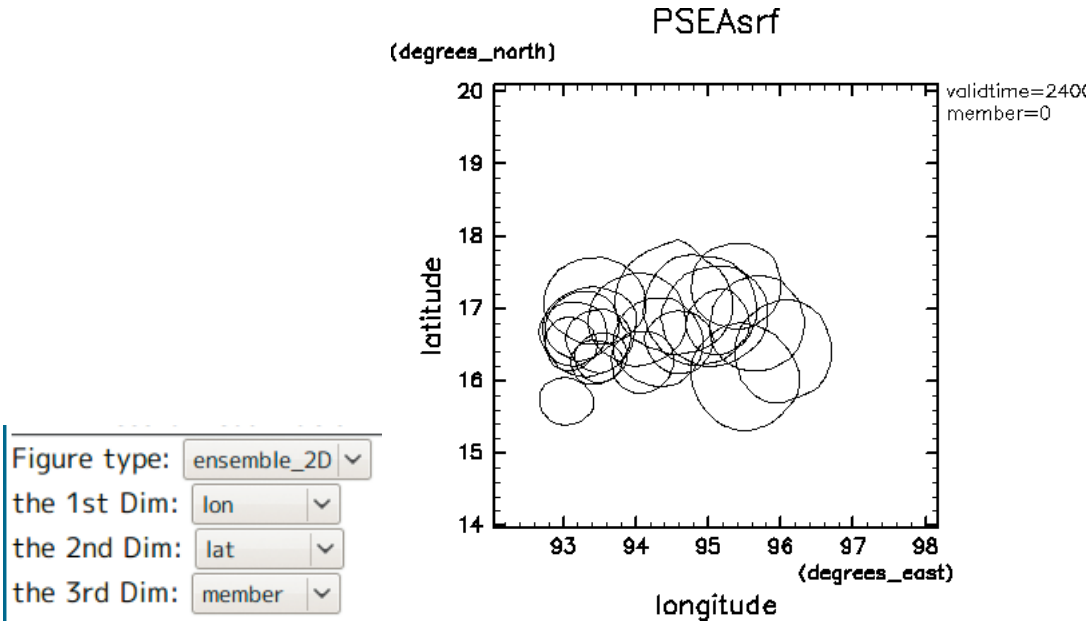

Depending on the difference of the center of Nargis, the circles widely spread. The denser the lines are, the higher the probability is.

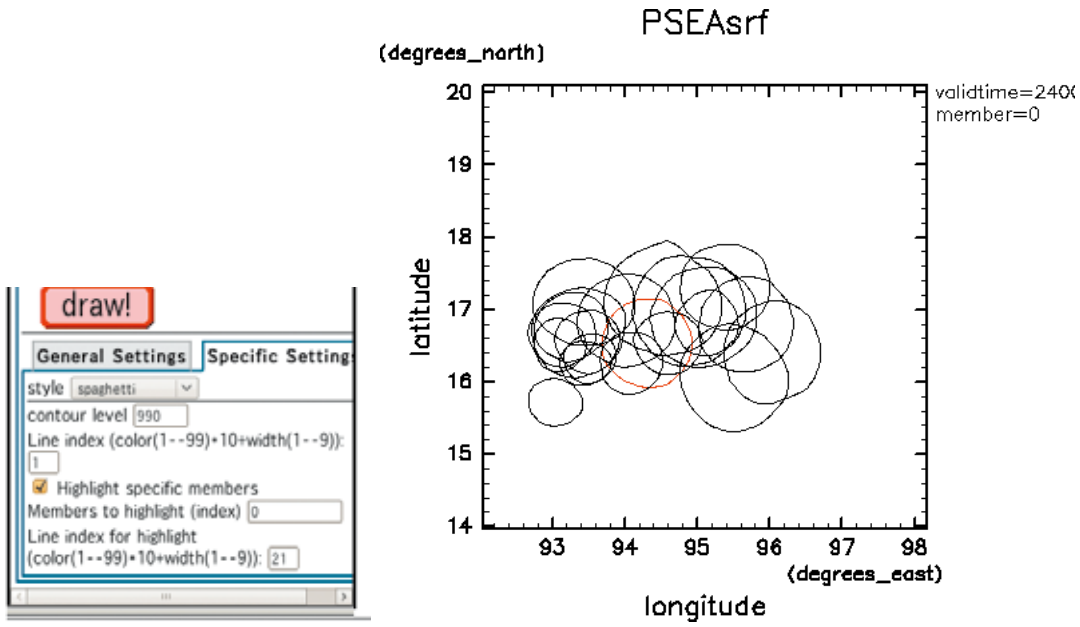

The control run ($member = 0$) is highlighted.

Excercise

- What is the best number for the contour line?

Data /Nargis/NHM/uv_abs.nc (lon, lat, $validtime$, $member$)

- $\text{uv\_abs}_{validtime}(lon, lat)$
  - (X) lon = [90°E, ..., 100°E]
  - (Y) lat = [14°N, ..., 20°N]

– (Ens) *validtime* = 0 min, ..., 4320 min
– *member* = 0

parameters for visualization:

– Projection type = equidistant cylindrical projection
– contour level = 25 m/s
– line index = 21

You can use *validtime* in place of *member*. The region swept by the contours experiences strong winds of more than 25 m/s.

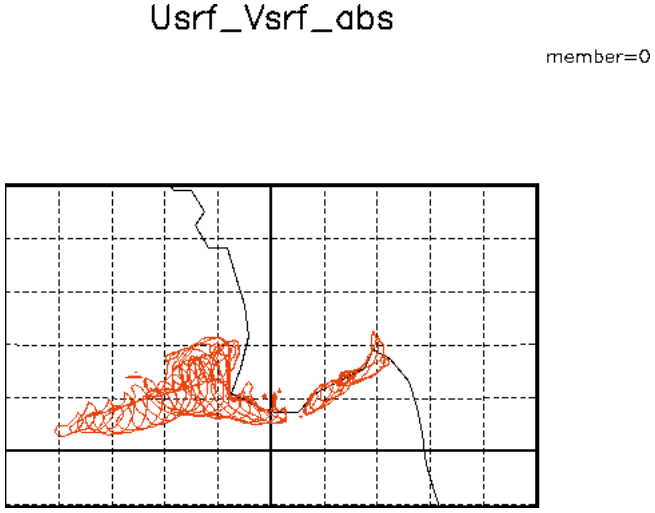

Excercise

– Change the contour level.
– Draw other ensemble members.

7 Decision support tools for ensemble numerical weather prediction: II. Advanced diagrams with mathematical operations

7.1 1D line plot

Data /Nargis/NHM/PSEAsrf.nc (*lon*, *lat*, *validtime*, *member*)

- Function = "min"

1. Compute minimum values of sea level pressure PSEAsrf(*lon*, *lat*, *validtime*, *member*) within a rectangular region around Nargis.
   – *lon* = <86°E, ..., 98°E>
   – *lat* = <12°N, ..., 22°N>
   – *validtime* = [0 min, ..., 4320 min]
   – *member* = [0, ..., 20]

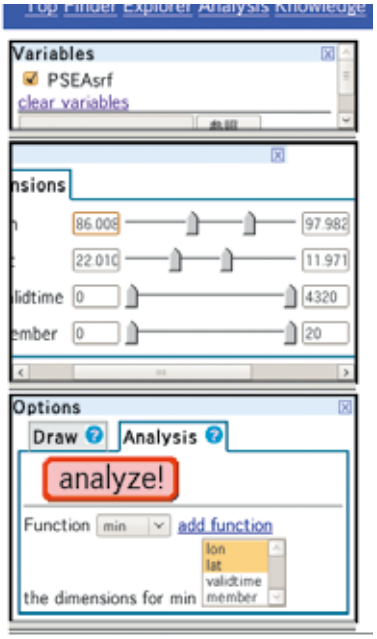

To select both *lon* and *lat*, press CTL key while clicking them. Click "analyze!". Then the result is shown in the "variables" window.

2. Draw a 1D line plot (ensemble_1D) of PSEAsrf_min$_{member}$(*validtime*).
   - (X) *validtime* = [0 min, ..., 4320 min]
   - (Ens) *member* = 0, ..., 20

   parameters for visualization:
   - highlihght specific members = true
   - members to highlihght = 0

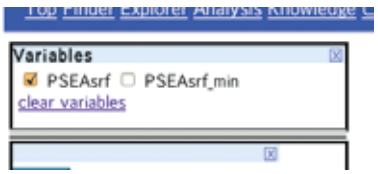

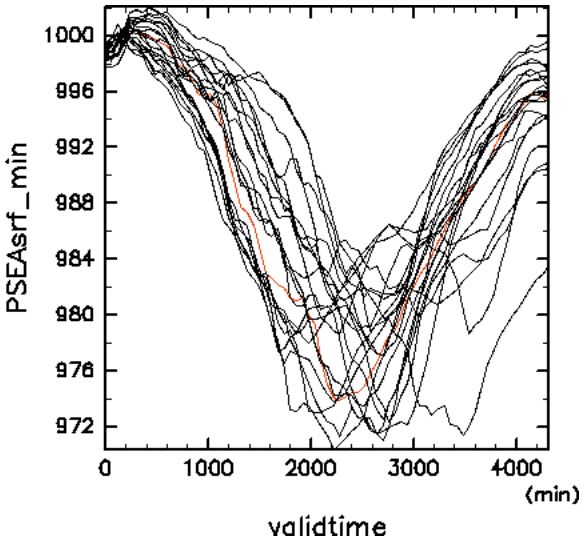

Data /Nargis/NHM/precip_hr.nc (*lon*, *lat*, *validtime*, *member*)

- Function = "mean"

1. Compute area-average of precipitation rate precip_hr(*lon*, *lat*, *validtime*, *member*):
   - *lon* = <94°E, ..., 96°E>

- lat = <16°N, ..., 18°N>
- $validtime$ = [0 min, ..., 4320 min]
- $member$ = [0, ..., 20]

2. Draw a line plot (ensemble_1D) for precip_hr_mean$_{member}$($validtime$)
   - (X) $validtime$ = [0 min, ..., 4320 min]
   - (Ens) $member$ = 0, ..., 20

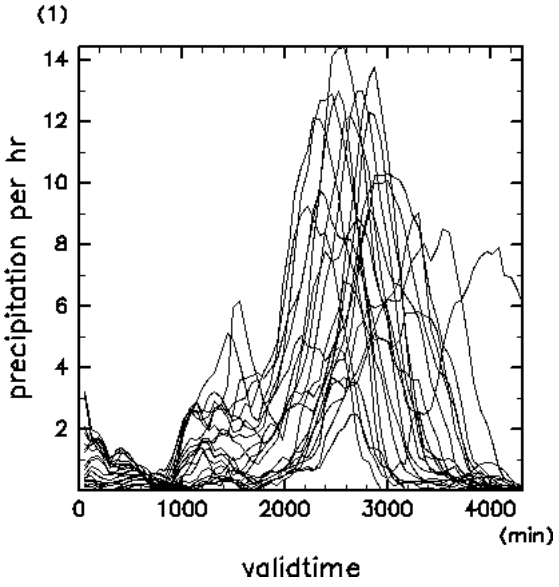

Draw methods with internal mathematical operations

Data /Nargis/NHM/POM/h.nc (lon, lat, t, $member$)

Change the style of the plume diagram shown in 6.1 to other options.

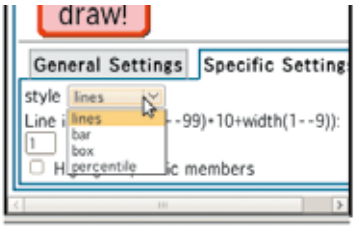

- Style = "bar"

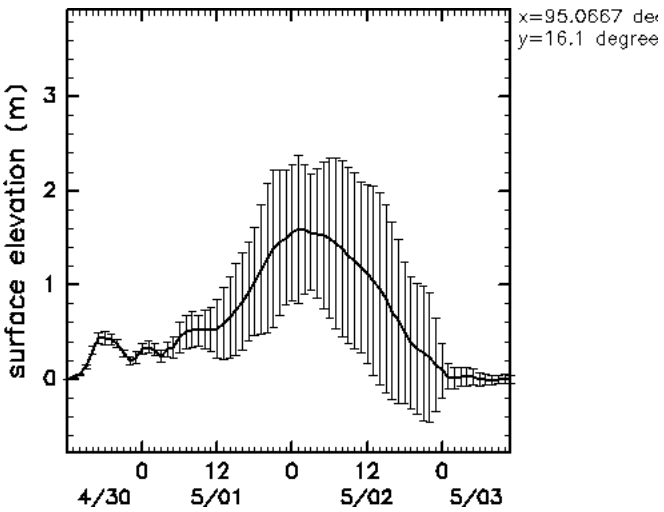

The vertical bars show the standard deviation and the thick line shows the ensemble mean.

- Style = "box"

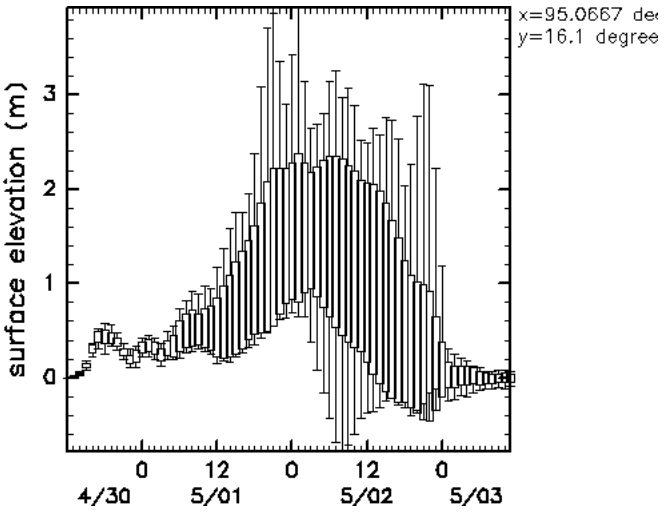

The vertical bars show the maximun and the minimum, and the boxes show the standard deviation.

- Style = "percentile"

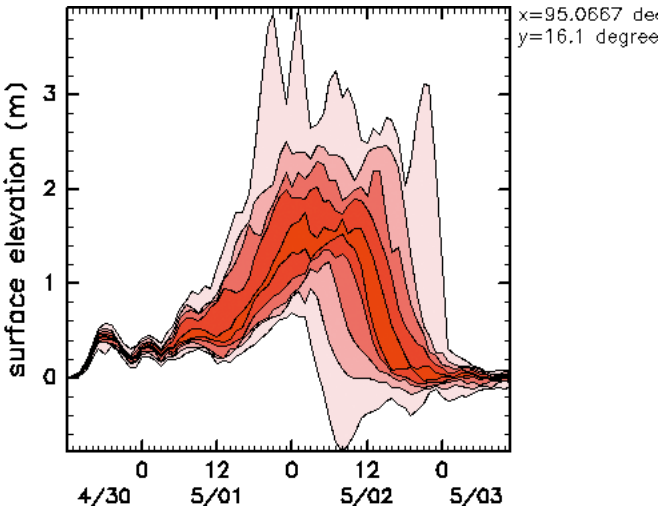

The contours show probability density.

7.2 2D tone and contour plot

Data /Nargis/NHM/PSEAsrf.nc (*lon*, *lat*, *validtime*, *member*)

- Function = "mean", "stddev"

1. Compute ensemble mean and standard deviation of PSEAsrf(*lon*, *lat*, *member*):
   - *lon* = [92°E, ..., 98°E]
   - *lat* = [14°N, ..., 20°N]
   - *validtime* = 2400 min
   - *member* = $< 0, ..., 20 >$

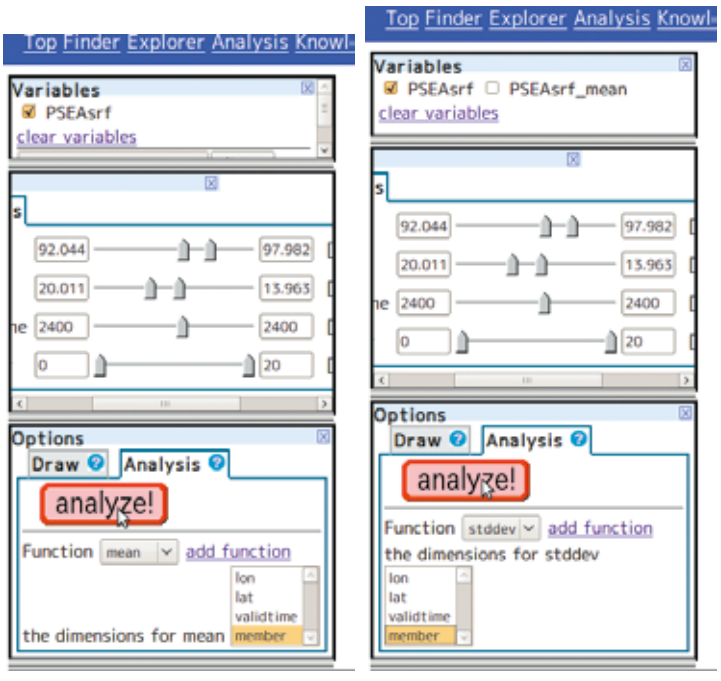

2. Draw a contour diagram of PSEAsrf_mean(*lon*, *lat*).
   - (X) *lon* = [92°E, ..., 98°E]
   - (Y) *lat* = [14°N, ..., 20°N]

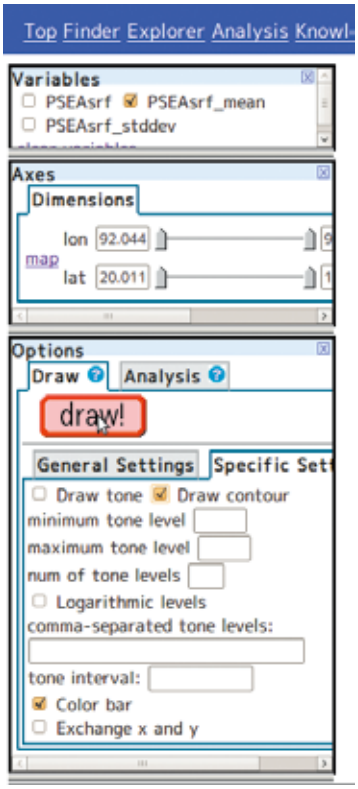

3. Check "keep diagrams" and draw a tone diagram of PSEAsrf_stddev(lon, lat).
   - (X) lon = [92°E, ..., 98°E]
   - (Y) lat = [14°N, ..., 20°N]

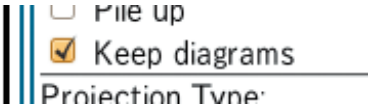

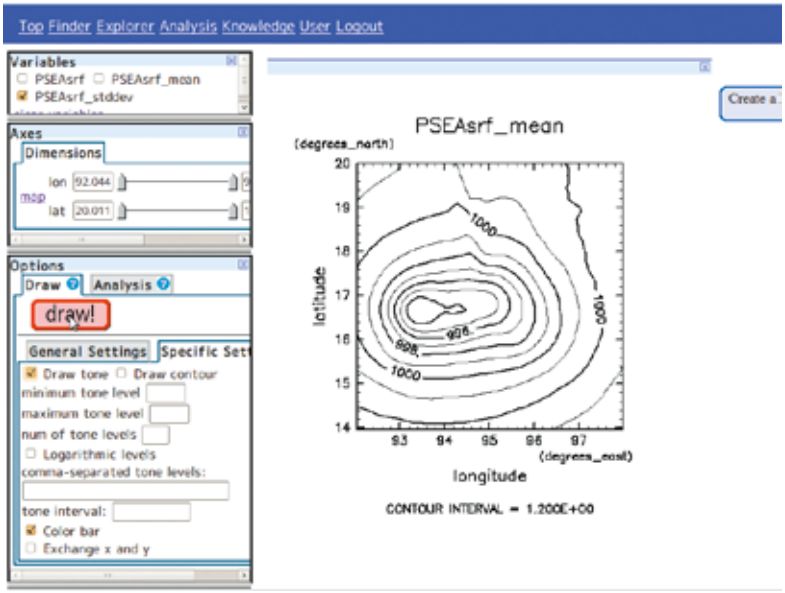

4. Pile up these two by drag and drop the left panel onto the right panel.

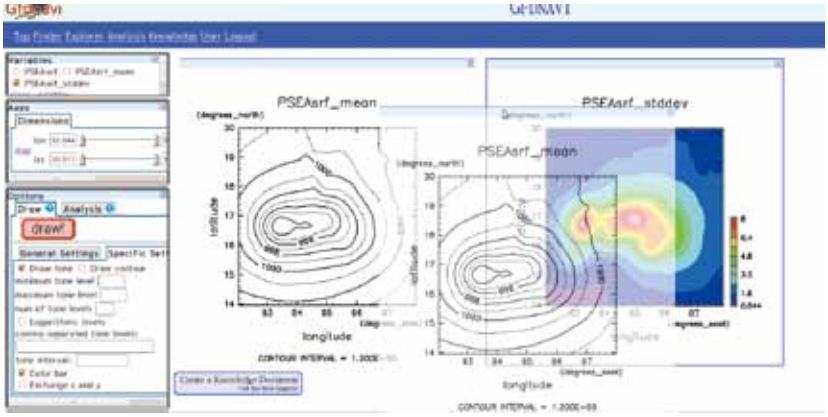

5. The final product is shown below:

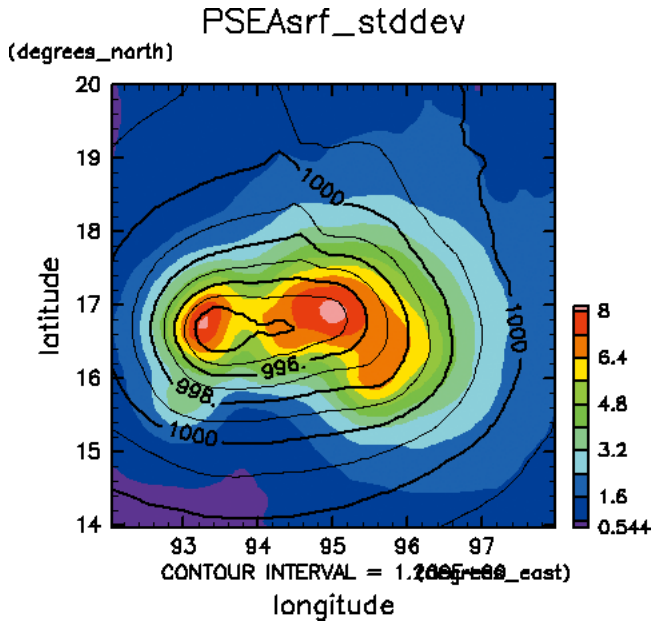

Data /Nargis/NHM/uv_abs.nc (*lon*, *lat*, *validtime*, *member*)

- Function = "max"
  1. Compute the maximum along the time of Usrf_Vsrf_abs(*lon*, *lat*, *validtime*, *member*)
     - *lon* = [90°E, ..., 100°E]
     - *lat* = [14°N, ..., 20°N]
     - *t* = <0 min, ..., 4320 min>
     - *member* = [0, ..., 20]
  2. Draw a 2D spaghetti diagram (ensemble_2D) of Usrf_Vsrf_abs_max$_{member}$(*lon*, *lat*)
     - (X) *lon* = [90°E, ..., 100°E]
     - (Y) *lat* = [14°N, ..., 20°N]
     - (Ens) *member* = 0, ..., 20

     parameters for visualization:
     - Projection type = equidistant cylindrical projection
     - line index = 21

Usrf_Vsrf_abs_max

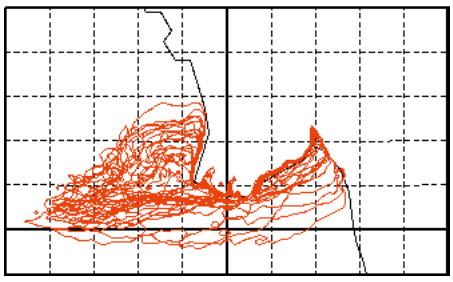

The region covered by the contours may experience strong winds of more than 25 m/s. The denser the contours are, the higher the probability is.

Excercise

– Compare this diagram with the diagram in 6.2.

Data Usrf_Vsrf_abs_max (*lon*, *lat*, *member*) (the maximum wind speed along the *time* axis, the result of the previous operation)

- Function = "mean"
  1. Compute the ensemble mean of Usrf_Vsrf_abs_max(*lon*, *lat*, *member*)
     – *lon* = [90°E, ..., 100°E]
     – *lat* = [14°N, ..., 20°N]
     – *member* = <0, ..., 20>
  2. Draw a 2D tone and contour diagram of Usrf_Vsrf_abs_max_mean(*lon*, *lat*)
     – (X) *lon* = [90°E, ..., 100°E]
     – (Y) *lat* = [14°N, ..., 20°N]

     parameters for visualization:
     – Projection type = equidistant cylindrical projection

Usrf_Vsrf_abs_max_mean

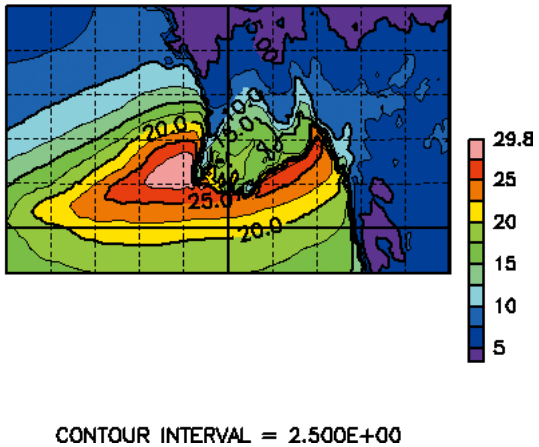

CONTOUR INTERVAL = 2.500E+00

Data /Nargis/NHM/precipitation.nc (*lon*, *lat*, *validtime*, *member*)

- Function = "mean"

  1. Compute the ensemble mean of accumulated precipitation at the end of the simulation (precipitation(*lon*, *lat*, *member*)).
     - *lon* = [90°E, ..., 100°E]
     - *lat* = [14°N, ..., 20°N]
     - *validtime* = 4320 min
     - *member* = <0, ..., 20>
  2. Draw a 2D tone and contour diagram of precipitation_mean(*lon*, *lat*)
     - (X) *lon* = [90°E, ..., 100°E]
     - (Y) *lat* = [14°N, ..., 20°N]

     parameters for visualization:
     - Projection type = equidistant cylindrical projection
     - Draw contour = false

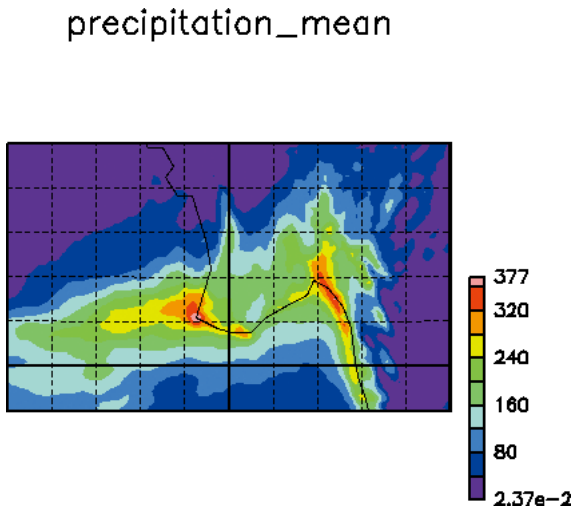

Data /Nargis/POM/h.nc (*lon*, *lat*, *t*, *member*)

- Function = "max"

  1. Compute the maximum along the *t* and *member* axes of h(*lon*, *lat*, *t*, *member*)
     - *lon* = [93.5°E, ..., 98°E]
     - *lat* = [15.5°N, ..., 17.5°N]
     - *t* = <0 min, ..., 4320 min>
     - *member* = $< 0, ..., 20 >$
  2. Draw 2D tone and contour diagram of h_max(*lon*, *lat*)
     - (X) *lon* = [93.5°E, ..., 98°E]
     - (Y) *lat* = [15.5°N, ..., 17.5°N]

     parameters for visualization:
     - Projection type = equidistant cylindrical projection

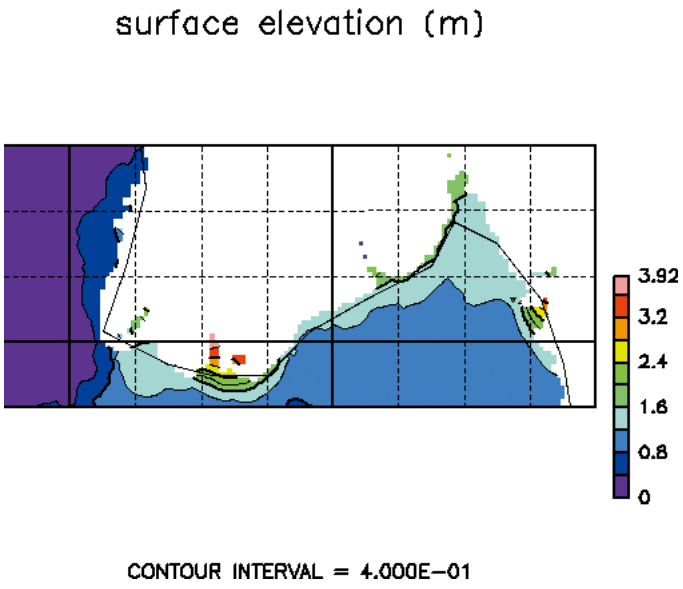

Maximum height of the storm surge can be estimated.

Excercise

- Where is the heighest point of the storm surge?
- What is the cause of the highest storm surge?
- What is the most relevant parameter?

References

Kuroda, T., K. Saito, M. Kunii, and N. Kohno, 2009: Numerical simulations of Myanmar cyclone Nargis and the associated storm surge Part I: Forecast experiment with NHM and simulation of storm surge. *J. Meteor. Soc. Japan*, submitted.

Saito, K., T. Kuroda, M. Kunii, and N. Kohno, 2009: Numerical simulations of Myanmar cyclone Nargis and the associated storm surge Part 2: Ensemble prediction. *J. Meteor. Soc. Japan*, submitted.

I-3. Links of published papers
I-3-1. Refereed Journals

C-1. Hayashi, S., K. Aranami and K. Saito, 2008: Statistical Verification of Short Term NWP by NHM and WRF-ARW with 20 km Horizontal Resolution around Japan and Southeast Asia. *SOLA*, **4**, 133-136.
<http://www.jstage.jst.go.jp/article/sola/4/0/133/_pdf>

C-3. Seko, H., S. Hayashi, M. Kunii and K. Saito, 2008: Structure of the Regional Heavy Rainfall System that Occurred in Mumbai, India, on 26 July 2005. *SOLA*, **4**, 129-132.
<http://www.jstage.jst.go.jp/article/sola/4/0/129/_pdf>

D-1. Kuroda, T., K. Saito, M. Kunii and N. Kohno, 2010: Numerical Simulations of Myanmar Cyclone Nargis and the Associated Storm Surge Part 1: Forecast Experiment with NHM and Simulation of Storm Surge. *J. Meteor. Soc. Japan*, **88**, 521-545.
<http://www.jstage.jst.go.jp/article/jmsj/88/3/521/_pdf>

D-3. Saito, K., T. Kuroda, M. Kunii and N. Kohno, 2010: Numerical Simulations of Myanmar Cyclone Nargis and the Associated Storm Surge Part 2: Ensemble prediction. *J. Meteor. Soc. Japan*. **88**, 547-570.
<http://www.jstage.jst.go.jp/article/jmsj/88/3/547/_pdf>

D-4. Kunii, M., Y. Shoji, M. Ueno and K. Saito, 2010: Mesoscale Data Assimilation of Myanmar Cyclone Nargis. *J. Meteor. Soc. Japan*, **88**, 455-474.
<http://www.jstage.jst.go.jp/article/jmsj/88/3/455/_pdf>

D-5. Shoji, Y., Kunii, M. and K. Saito, 2011: Mesoscale Data Assimilation of Myanmar Cyclone Nargis. Part 2 : Assimilation of GPS derived Precipitable Water Vapor *J. Meteor. Soc. Japan*, **89**, 67-88.
<http://www.jstage.jst.go.jp/article/jmsj/89/1/67/_pdf>

D-6. Ueno, M., and M. Kunii, 2009: Some aspects of azimuthal wavenumber-one structure of typhoons represented in the JMA operational mesoscale analyses. *J. Meteor. Soc. Japan*, **87**, 615–633.
<http://www.jstage.jst.go.jp/article/jmsj/87/4/615/_pdf>

D-9. Wong, W.K., S. Sumdin, S.T. Lai, 2010: Development of Air-Sea Bulk Transfer Coefficients and Roughness Lengths in JMA Non-hydrostatic Model and Application in Prediction of an Intense Tropical Cyclone. *SOLA*, **Vol. 6**, p.65-68.
<http://www.jstage.jst.go.jp/article/sola/6/0/65/_pdf>

E-1. Koh, T. Y. and C. K. Teo (2009), "Towards a mesoscale observation network in Southeast Asia", *Bulletin of American Meteorological Society*, **90(4)**, 481-488, doi: 10.1175/2008BAMS2561.1.
<http://journals.ametsoc.org/doi/pdf/10.1175/2008BAMS2561.1>

I-3-2. Review papers, reports and articles

Preface: Yoden, S., K. Saito, T. Takemi and S. Nishizawa, 2008: International research for prevention and mitigation of meteorological disasters in Southeast Asia. *Tenki*, **55**, 705-708. (in Japanese)
<http://www.metsoc.jp/tenki/pdf/2008/2008_08_0071.pdf>

Preface: Achievement report on International Research for Prevention and Mitigation of Meteorological Disasters in Southeast Asia. (in Japanese)
<http://scfdb.tokyo.jst.go.jp/pdf/20071440/2009/200714402009rr.pdf>

F-1. Otsuka, S. and S. Yoden, 2010: Experimental Development of Decision Support System for Prevention and Mitigation of Meteorological Disasters Based on Ensemble NWP Data. *Annuals of Dias. Prev. Res. Inst., Kyoto Univ.*, **53B**, 377-382. (in Japanese with English abstract and figure captions)
<http://www.dpri.kyoto-u.ac.jp/nenpo/no53/ronbunB/a53b0p42.pdf>

気象研究所技術報告一覧表

第１号　バックグラウンド大気汚染の測定法の開発（地球規模大気汚染特別研究班，1978）
Development of Monitoring Techniques for Global Background Air Pollution. (MRI Special Research Group on Global Atmospheric Pollution, 1978)

第２号　主要活火山の地殻変動並びに地熱状態の調査研究（地震火山研究部，1979）
Investigation of Ground Movement and Geothermal State of Main Active Volcanoes in Japan. (Seismology and Volcanology Research Division, 1979)

第３号　筑波研究学園都市に新設された気象観測用鉄塔施設（花房龍男・藤谷徳之助・伴野　登・魚津　博，1979）
On the Meteorological Tower and Its Observational System at Tsukuba Science City. (T. Hanafusa, T. Fujitani, N. Banno, and H. Uozu, 1979)

第４号　海底地震常時観測システムの開発（地震火山研究部，1980）
Permanent Ocean－Bottom Seismograph Observation System. (Seismology and Volcanology Research Division, 1980)

第５号　本州南方海域水温図－400m（又は 500m）深と 1,000m 深－（1934－1943 年及び 1954－1980 年）（海洋研究部，1981）
Horizontal Distribution of Temperature in 400m (or 500m) and 1,000m Depth in Sea South of Honshu, Japan and Western －North Pacific Ocean from 1934 to 1943 and from 1954 to 1980. (Oceanographical Research Division, 1981)

第６号　成層圏オゾンの破壊につながる大気成分及び紫外日射の観測（高層物理研究部，1982）
Observations of the Atmospheric Constituents Related to the Stratospheric ozon Depletion and the Ultraviolet Radiation. (Upper Atmosphere Physics Research Division, 1982)

第７号　83 型強震計の開発（地震火山研究部，1983）
Strong－Motion Seismograph Model 83 for the Japan Meteorological Agency Network. (Seismology and Volcanology Research Division, 1983)

第８号　大気中における雪片の融解現象に関する研究（物理気象研究部，1984）
The Study of Melting of Snowflakes in the Atmosphere. (Physical Meteorology Research Division, 1984)

第９号　御前崎南方沖における海底水圧観測（地震火山研究部・海洋研究部，1984）
Bottom Pressure Observation South off Omaezaki, Central Honsyu. (Seismology and Volcanology Research Division and Oceanographical Research Division, 1984)

第 10 号　日本付近の低気圧の統計（予報研究部，1984）
Statistics on Cyclones around Japan. (Forecast Research Division, 1984)

第 11 号　局地風と大気汚染質の輸送に関する研究（応用気象研究部，1984）
Observations and Numerical Experiments on Local Circulation and Medium－Range Transport of Air Pollutions. (Applied Meteorology Research Division, 1984)

第 12 号　火山活動監視手法に関する研究（地震火山研究部，1984）
Investigation on the Techniques for Volcanic Activity Surveillance. (Seismology and Volcanology Research Division, 1984)

第 13 号　気象研究所大気大循環モデルーⅠ（MRI・GCM－Ⅰ）（予報研究部，1984）
A Description of the MRI Atmospheric General Circulation Model (The MRI・GCM－Ⅰ). (Forecast Research Division, 1984)

第 14 号　台風の構造の変化と移動に関する研究－台風 7916 の一生－（台風研究部，1985）
A Study on the Changes of the Three - Dimensional Structure and the Movement Speed of the Typhoon through its Life Time. (Typhoon Research Division, 1985)

第 15 号　波浪推算モデル MRI と MRI－Ⅱの相互比較研究－計算結果図集－（海洋気象研究部，1985）
An Intercomparison Study between the Wave Models MRI and MRI－Ⅱ －A Compilation of Results－ (Oceanographical Research Division, 1985)

第 16 号　地震予知に関する実験的及び理論的研究（地震火山研究部，1985）
Study on Earthquake Prediction by Geophysical Method. (Seismology and Volcanology Research Division, 1985)

第 17 号　北半球地上月平均気温偏差図（予報研究部，1986）
Maps of Monthly Mean Surface Temperature Anomalies over the Northern Hemisphere for 1891－1981. (Forecast Research Division, 1986)

第 18 号　中層大気の研究（高層物理研究部・気象衛星研究部・予報研究部・地磁気観測所，1986）
Studies of the Middle Atmosphere. (Upper Atmosphere Physics Research Division, Meteorological Satellite Research Division, Forecast Research Division, MRI and the Magnetic Observatory, 1986)

第 19 号　ドップラーレーダによる気象・海象の研究（気象衛星研究部・台風研究部・予報研究部・応用気象研究部・海洋研究部，1986）
Studies on Meteorological and Sea Surface Phenomena by Doppler Radar. (Meteorological Satellite Research Division, Typhoon Research Division, Forecast Research Division, Applied Meteorology Research Division, and Oceanographical Research Division, 1986)

第 20 号　気象研究所対流圏大気大循環モデル（MRI・GCM－Ⅰ）による 12 年間分の積分（予報研究部，1986）
Mean Statistics of the Tropospheric MRI・GCM－Ⅰbased on 12－year Integration. (Forecast Research Division, 1986)

第 21 号　宇宙線中間子強度 1983－1986（高層物理研究部，1987）
Multi－Directional Cosmic Ray Meson Intensity 1983－1986. (Upper Atmosphere Physics Research Division, 1987)
第 22 号　静止気象衛星「ひまわり」画像の噴火噴煙データに基づく噴火活動の解析に関する研究（地震火山研究部，1987）
Study on Analysis of Volcanic Eruptions based on Eruption Cloud Image Data obtained by the Geostationary Meteorological satellite (GMS). (Seismology and Volcanology Research Division, 1987)
第 23 号　オホーツク海海洋気候図（篠原吉雄・四竈信行，1988）
Marine Climatological Atlas of the sea of Okhotsk. (Y. Shinohara and N. Shikama, 1988)
第 24 号　海洋大循環モデルを用いた風の応力異常に対する太平洋の応答実験（海洋研究部，1989）
Response Experiment of Pacific Ocean to Anomalous Wind Stress with Ocean General Circulation Model. (Oceanographical Research Division, 1989)
第 25 号　太平洋における海洋諸要素の季節平均分布（海洋研究部，1989）
Seasonal Mean Distribution of Sea Properties in the Pacific. (Oceanographical Research Division, 1989)
第 26 号　地震前兆現象のデータベース（地震火山研究部，1990）
Database of Earthquake Precursors. (Seismology and Volcanology Research Division, 1990)
第 27 号　沖縄地方における梅雨期の降水システムの特性（台風研究部，1991）
Characteristics of Precipitation Systems During the Baiu Season in the Okinawa Area. (Typhoon Research Division, 1991)
第 28 号　気象研究所・予報研究部で開発された非静水圧モデル（猪川元興・斉藤和雄，1991）
Description of a Nonhydrostatic Model Developed at the Forecast Research Department of the MRI. (M. Ikawa and K. Saito, 1991)
第 29 号　雲の放射過程に関する総合的研究（気候研究部・物理気象研究部・応用気象研究部・気象衛星・観測システム研究部・台風研究部，1992）
A Synthetic Study on Cloud－Radiation Processes. (Climate Research Department, Physical Meteorology Research Department, Applied Meteorology Research Department, Meteorological Satellite and Observation System Research Department, and Typhoon Research Department, 1992)
第 30 号　大気と海洋・地表とのエネルギー交換過程に関する研究（三上正男・遠藤昌宏・新野　宏・山崎孝治，1992）
Studies of Energy Exchange Processes between the Ocean－Ground Surface and Atmosphere. (M. Mikami, M. Endoh, H. Niino, and K. Yamazaki, 1992)
第 31 号　降水日の出現頻度からみた日本の季節推移－30 年間の日降水量資料に基づく統計－（秋山孝子，1993）
Seasonal Transition in Japan, as Revealed by Appearance Frequency of Precipitating-Days. －Statistics of Daily Precipitation Data During 30 Years－(T. Akiyama, 1993)
第 32 号　直下型地震予知に関する観測的研究（地震火山研究部，1994）
Observational Study on the Prediction of Disastrous Intraplate Earthquakes. (Seismology and Volcanology Research Department, 1994)
第 33 号　各種気象観測機器による比較観測（気象衛星・観測システム研究部，1994）
Intercomparisons of Meteorological Observation Instruments. (Meteorological Satellite and Observation System Research Department, 1994)
第 34 号　硫黄酸化物の長距離輸送モデルと東アジア地域への適用（応用気象研究部，1995）
The Long－Range Transport Model of Sulfur Oxides and Its Application to the East Asian Region. (Applied Meteorology Research Department, 1995)
第 35 号　ウインドプロファイラーによる気象の観測法の研究（気象衛星・観測システム研究部，1995）
Studies on Wind Profiler Techniques for the Measurements of Winds. (Meteorological Satellite and Observation System Research Department, 1995)
第 36 号　降水・落下塵中の人工放射性核種の分析法及びその地球化学的研究（地球化学研究部，1996）
Geochemical Studies and Analytical Methods of Anthropogenic Radionuclides in Fallout Samples. (Geochemical Research Department, 1996)
第 37 号　大気と海洋の地球化学的研究（1995 年及び 1996 年）（地球化学研究部，1998）
Geochemical Study of the Atmosphere and Ocean in 1995 and 1996. (Geochemical Research Department, 1998)
第 38 号　鉛直２次元非線形問題（金久博忠，1999）
Vertically 2-dmensional Nonlinear Problem (H. Kanehisa, 1999)
第 39 号　客観的予報技術の研究（予報研究部，2000）
Study on the Objective Forecasting Techniques（Forecast Research Department, 2000）
第 40 号　南関東地域における応力場と地震活動予測に関する研究（地震火山研究部，2000）
Study on Stress Field and Forecast of Seismic Activity in the Kanto Region（Seismology and Volcanology Research Department, 2000）
第 41 号　電量滴定法による海水中の全炭酸濃度の高精度分析および大気中の二酸化炭素と海水中の全炭酸の放射性炭素同位体比の測定（石井雅男・吉川久幸・松枝秀和，2000）
Coulometric Precise Analysis of Total Inorganic Carbon in Seawater and Measurements of Radiocarbon for the Carbon Dioxide in the Atmosphere and for the Total Inorganic Carbon in Seawater（I.Masao, H.Y.Inoue and H.Matsueda, 2000）
第 42 号　気象研究所／数値予報課統一非静力学モデル（斉藤和雄・加藤輝之・永戸久喜・室井ちあし，2001）
Documentation of the Meteorological Research Institute / Numerical Prediction Division Unified Nonhydrostatic Model (Kazuo Saito, Teruyuki Kato, Hisaki Eito and Chiashi Muroi，2001)

第 43 号　大気および海水中のクロロフルオロカーボン類の精密測定と気象研究所クロロフルオロカーボン類標準ガスの確立（時枝隆之・井上(吉川)久幸，2004）
Precise measurements of atmospheric and oceanic chlorofluorocarbons and MRI chlorofluorocarbons calibration scale (Takayuki Tokieda and Hisayuki Y. Inoue，2004)

第 44 号　PostScript コードを生成する描画ツール"PLOTPS"マニュアル（加藤輝之，2004）
Documentation of "PLOTPS": Outputting Tools for PostScript Code (Teruyuki Kato，2004)

第 45 号　気象庁及び気象研究所における二酸化炭素の長期観測に使用された標準ガスのスケールとその安定性の再評価に関する調査・研究（松枝秀和・須田一人・西岡佐喜子・平野礼朗・澤　庸介・坪井一寛・堤　之智・神谷ひとみ・根本和宏・長井秀樹・吉田雅司・岩野園城・山本　治・森下秀昭・鎌田匡俊・和田　晃，2004）
Re-evaluation for scale and stability of CO_2 standard gases used as long-term observations at the Japan Meteorological Agency and the Meteorological Research Institute (Hidekazu Matsueda, Kazuto Suda, Sakiko Nishioka, Toshirou Hirano, Yousuke, Sawa, Kazuhiro Tuboi, Tsutumi, Hitomi Kamiya, Kazuhiro Nemoto, Hideki Nagai, Masashi Yoshida, Sonoki Iwano, Osamu Yamamoto, Hideaki Morishita, Kamata, Akira Wada，2004)

第 46 号　地震発生過程の詳細なモデリングによる東海地震発生の推定精度向上に関する研究（地震火山研究部, 2005）
A Study to Improve Accuracy of Forecasting the Tokai Earthquake by Modeling the Generation Processes (Seismology and Volcanology Research Department, 2005)

第 47 号　気象研究所共用海洋モデル（MRI.COM）解説（海洋研究部, 2005）
Meteorological Research Institute Community Ocean Model (MRI.COM) Manual (Oceanographical Research Department, 2005)

第 48 号　日本海降雪雲の降水機構と人工調節の可能性に関する研究（物理気象研究部・予報研究部, 2005）
Study of Precipitation Mechanisms in Snow Clouds over the Sea of Japan and Feasibility of Their Modification by Seeding (Physical Meteorology Research Department, Forecast Research Department, 2005)

第 49 号　2004 年日本上陸台風の概要と環境場（台風研究部, 2006）
Summary of Landfalling Typhoons in Japan, 2004 (Typhoon Research Department, 2006)

第 50 号　栄養塩測定用海水組成標準の 2003 年国際共同実験報告（青山道夫, 2006）
2003 Intercomparison Exercise for Reference Material for Nutrients in Seawater in a Seawater Matrix (Michio Aoyama, 2006)

第 51 号　大気および海水中の超微量六フッ化硫黄(SF_6)の測定手法の高度化と SF_6 標準ガスの長期安定性の評価（時枝隆之、石井雅男、斉藤 秀、緑川 貴, 2007）
Highly developed precise analysis of atmospheric and oceanic sulfur hexafluoride (SF_6) and evaluation of SF_6 standard gas stability (Takayuki Tokieda, Masao Ishii, Shu Saito and Takashi Midorikawa, 2007)

第 52 号　地球温暖化による東北地方の気候変化に関する研究（仙台管区気象台, 環境・応用気象研究部, 2008）
Study of Climate Change over Tohoku District due to Global Warming (Sendai District Meteorological Observatory, Atmospheric Environment and Applied Meteorology Research Department, 2008)

第 53 号　火山活動評価手法の開発研究（地震火山研究部, 2008）
Studies on Evaluation Method of Volcanic Activity (Seismology and Volcanology Research Department, 2008)

第 54 号　日本における活性炭冷却捕集およびガスクロ分離による気体計数システムによる ^{85}Kr の測定システムの構築および 1995 年から 2006 年の測定結果（青山道夫, 藤井憲治, 廣瀬勝己, 五十嵐康人, 磯貝啓介, 新田 済, Hartmut Sartorius, Clemens Schlosser, Wolfgang Weiss, 2008）
Establishment of a cold charcoal trap-gas chromatography-gas counting system for ^{85}Kr measurements in Japan and results from 1995 to 2006 (Michio Aoyama, Kenji Fujii, Katsumi Hirose, Yasuhito Igarashi, Keisuke Isogai, Wataru Nitta, Hartmut Sartorius, Clemens Schlosser, Wolfgang Weiss, 2008)

第 55 号　長期係留による 4 種類の流速計観測結果の比較（中野俊也, 石崎 廣, 四竈信行, 2008）
Comparison of Data from Four Current Meters Obtained by Long-Term Deep-Sea Moorings (Toshiya Nakano, Hiroshi Ishizaki and Nobuyuki Shikama, 2008)

第 56 号　CMIP3 マルチモデルアンサンブル平均を利用した将来の海面水温・海氷分布の推定（水田 亮, 足立恭将, 行本誠史, 楠 昌司, 2008）
Estimation of the Future Distribution of Sea Surface Temperature and Sea Ice Using the CMIP3 Multi-model Ensemble Mean (Ryo Mizuta, Yukimasa Adachi, Seiji Yukimoto and Shoji Kusunoki, 2008)

第 57 号　閉流路中のフローセルを用いた分光光度法自動分析装置による海水の高精度 pH_T 測定（斉藤 秀, 石井雅男, 緑川 貴, 井上（吉川）久幸, 2008）
Precise Spectrophotometric Measurement of Seawater pH_T with an Automated Apparatus using a Flow Cell in a Closed Circuit（Shu Saito, Masao Ishii, Takashi Midorikawa and Hisayuki Y. Inoue, 2008）

第58号　栄養塩測定用海水組成標準の2006年国際共同実験報告（青山道夫,J. Barwell-Clarke, S. Becker, M. Blum, Braga E.S., S. C. Coverly, E. Czobik, I. Dahllöf, M. Dai, G. O Donnell, C. Engelke, Gwo-Ching Gong, Gi-Hoon Hong, D. J. Hydes, Ming-Ming Jin, 葛西広海, R. Kerouel, 清本容子, M. Knockaert, N. Kress, K. A. Krogslund, 熊谷正光, S. Leterme, Yarong Li, 増田真次, 宮尾 孝, T. Moutin, 村田昌彦, 永井直樹, G. Nausch, A. Nybakk, M. K. Ngirchechol, 小川浩史, J. van Ooijen, 太田秀和, J. Pan, C. Payne, O. Pierre-Duplessix, M. Pujo-Pay, T. Raabe, 齊藤一浩, 佐藤憲一郎, C. Schmidt, M. Schuett, T. M. Shammon, J. Sun, T. Tanhua, L. White, E.M.S. Woodward, P. Worsfold, P. Yeats, 芳村 毅, A. Youénou, Jia-Zhong Zhang, 2008）
2006 Inter-laboratory Comparison Study for Reference Material for Nutrients in Seawater（M. Aoyama, J. Barwell-Clarke, S. Becker, M. Blum, Braga E. S., S. C. Coverly, E. Czobik, I. Dahllöf, M. H. Dai, G. O. Donnell, C. Engelke, G. C. Gong, Gi-Hoon Hong, D. J. Hydes, M. M. Jin, H. Kasai, R. Kerouel, Y. Kiyomono, M. Knockaert, N. Kress, K. A. Krogslund, M.

Kumagai, S. Leterme, Yarong Li, S. Masuda, T. Miyao, T. Moutin, A. Murata, N. Nagai, G. Nausch, M. K. Ngirchechol, A. Nybakk, H. Ogawa, J. van Ooijen, H. Ota, J. M. Pan, C. Payne, O. Pierre-Duplessix, M. Pujo-Pay, T. Raabe, K. Saito, K. Sato, C. Schmidt, M. Schuett, T. M. Shammon, J. Sun, T. Tanhua, L. White, E.M.S. Woodward, P. Worsfold, P. Yeats, T. Yoshimura, A. Youénou, J. Z. Zhang, 2008）

第 59 号　気象研究所共用海洋モデル(MRI.COM)第 3 版解説（辻野博之, 本井達夫, 石川一郎, 平原幹俊, 中野英之, 山中吾郎, 安田珠幾, 石崎廣（気象研究所海洋研究部）, 2010）

Reference manual for the Meteorological Research Institute Community Ocean Model (MRI.COM) Version 3（Hiroyuki Tsujino, Tatsuo Motoi, Ichiro Ishikawa, Mikitoshi Hirabara, Hideyuki Nakano, Goro Yamanaka, Tamaki Yasuda, and Hiroshi Ishizaki (Oceanographic Research Department), 2010）

第 60 号　栄養塩測定用海水組成標準の 2008 年国際共同実験報告（青山道夫, Carol Anstey, Janet Barwell-Clarke, François Baurand, Susan Becker, Marguerite Blum, Stephen C. Coverly, Edward Czobik, Florence D’amico, Ingela Dahllöf, Minhan Dai, Judy Dobson, Magali Duval, Clemens Engelke, Gwo-Ching Gong, Olivier Grosso, 平山篤史, 井上博敬, 石田雄三, David J. Hydes, 葛西広海, Roger Kerouel, Marc Knockaert, Nurit Kress, Katherine A. Krogslund, 熊谷正光, Sophie C. Leterme, Claire Mahaffey, 光田均, Pascal Morin, Thierry Moutin, Dominique Munaron, 村田昌彦, Günther Nausch, 小川浩史, Jan van Ooijen, Jianming Pan, Georges Paradis, Chris Payne, Olivier Pierre-Duplessix, Gary Prove, Patrick Raimbault, Malcolm Rose, 齊藤一浩, 斉藤宏明, 佐藤憲一郎, Cristopher Schmidt, Monika Schütt, Theresa M. Shammon, Solveig Olafsdottir, Jun Sun, Toste Tanhua, Sieglinde Weigelt-Krenz, Linda White, E. Malcolm. S. Woodward, Paul Worsfold, 芳村毅, Agnès Youénou, Jia-Zhong Zhang, 2010）

2008 Inter-laboratory Comparison Study of a Reference Material for Nutrients in Seawater（青山道夫, Carol Anstey, Janet Barwell-Clarke, François Baurand, Susan Becker, Marguerite Blum, Stephen C. Coverly, Edward Czobik, Florence D’amico, Ingela Dahllöf, Minhan Dai, Judy Dobson, Magali Duval, Clemens Engelke, Gwo-Ching Gong, Olivier Grosso, 平山篤史, 井上博敬, 石田雄三, David J. Hydes, 葛西広海, Roger Kerouel, Marc Knockaert, Nurit Kress, Katherine A. Krogslund, 熊谷正光, Sophie C. Leterme, Claire Mahaffey, 光田均, Pascal Morin, Thierry Moutin, Dominique Munaron, 村田昌彦, Günther Nausch, 小川浩史, Jan van Ooijen, Jianming Pan, Georges Paradis, Chris Payne, Olivier Pierre-Duplessix, Gary Prove, Patrick Raimbault, Malcolm Rose, 齊藤一浩, 斉藤宏明, 佐藤憲一郎, Cristopher Schmidt, Monika Schütt, Theresa M. Shammon, Solveig Olafsdottir, Jun Sun, Toste Tanhua, Sieglinde Weigelt-Krenz, Linda White, E. Malcolm. S. Woodward, Paul Worsfold, 芳村毅, Agnès Youénou, Jia-Zhong Zhang, 2010）

第 61 号　強雨をもたらす線状降水帯の形成機構等の解明及び降水強度・移動速度の予測に関する研究（大阪管区気象台・彦根地方気象台・京都地方気象台・奈良地方気象台・和歌山地方気象台・神戸海洋気象台・松江地方気象台・鳥取地方気象台・舞鶴海洋気象台・広島地方気象台・徳島地方気象台・予報研究部, 2010）

Studies on formation process of line-shaped rainfall systems and predictability of rainfall intensity and moving speed（Osaka District Meteorological Observatory, Hikone Local Meteorological Observatory, Kyoto Local Meteorological Observatory, Nara Local Meteorological Observatory, Wakayama Local Meteorological Observatory, Kobe Marine Observatory, Matsue Local Meteorological Observatory, Tottori Local Meteorological Observatory, Maizuru Marine Observatory, Hiroshima Local Meteorological Observatory, Tokushima Local Meteorological Observatory AND Forecast Research Department, 2010）

第 62 号　WWRP 北京オリンピック 2008 予報実証/研究開発プロジェクト（齊藤和雄, 國井勝, 原昌弘, 瀬古弘, 原旅人, 山口宗彦, 三好建正, 黄偉健, 2010）

WWRP Beijing Olympics 2008 Forecast Demonstration/Research and Development Project (B08FDP/RDP)（Kazuo Saito, Masaru Kunii, Masahiro Hara, Hiromu Seko, Tabito Hara, Munehiko Yamaguchi, Takemasa Miyoshi and Wai-kin Wong, 2010）

第 63 号　東海地震の予測精度向上及び東南海・南海地震の発生準備過程の研究（地震火山研究部, 2011）

Improvement in prediction accuracy for the Tokai earthquake and research of the preparation process of the Tonankai and the Nankai earthquakes (Seismology and Volcanology Research Department, 2011)

第 64 号　気象研究所地球システムモデル第 1 版（MRI-ESM1）―モデルの記述―（行本誠史, 吉村裕正, 保坂征宏, 坂見智法, 辻野博之, 平原幹俊, 田中泰宙, 出牛真, 小畑淳, 中野英之, 足立恭将, 新藤永樹, 籔将吉, 尾瀬智昭, 鬼頭昭雄, 2011）

Meteorological Research Institute-Earth System Model Version 1 (MRI-ESM1) — Model Description — (Seiji Yukimoto, Hiromasa Yoshimura, Masahiro Hosaka, Tomonori Sakami, Hiroyuki Tsujino, Mikitoshi Hirabara, Taichu Y. Tanaka, Makoto Deushi, Atsushi Obata, Hideyuki Nakano, Yukimasa Adachi, Eiki Shindo, Shoukichi Yabu, Tomoaki Ose and Akio Kitoh, 2011)

気象研究所技術報告は，1978（昭和53）年の初刊以来,気象研究所が必要の都度発行する刊行物であり，気象研究所の研究計画に基づき実施した研究に関する手法、データ、結果等についてのまとめ、または、すでに公表した研究論文類をとりまとめ総合的報告としたものを掲載する。

気　象　研　究　所　技　術　報　告　　ISSN 0386-4049
第　65　号

平成23年12月　発行

編集兼
発行者　気　象　研　究　所

〒305-0052　茨城県つくば市長峰１－１
TEL(029)853-8535

印　刷　者　株式会社デジタル印刷
〒300-3262　茨城県つくば市蓮沼 1322-1